

**SYNTHESIS OF NONTRADITIONAL TETRAPYRROLE LIGAND
PLATFORM FOR SMALL MOLECULE ACTIVATION**

by
Qiuqi Cai

A dissertation submitted to the Faculty of the University of Delaware in partial fulfillment of the requirements for the degree of Doctor of Philosophy in Chemistry and Biochemistry

Fall 2020

© 2020 Qiuqi Cai
All Rights Reserved

**SYNTHESIS OF NONTRADITIONAL TETRAPYRROLE LIGAND
PLATFORM FOR SMALL MOLECULE ACTIVATION**

by

Qiuqi Cai

Approved: _____
Brian J. Bahnson, Ph.D.
Chair of the Department of Chemistry and Biochemistry

Approved: _____
John A. Pelesko, Ph.D.
Dean of the College of Arts and Sciences

Approved: _____
Louis F. Rossi, Ph.D.
Vice Provost for Graduate and Professional Education and
Dean of the Graduate College

I certify that I have read this dissertation and that in my opinion it meets the academic and professional standard required by the University as a dissertation for the degree of Doctor of Philosophy.

Signed:

Joel Rosenthal, Ph.D.
Professor in charge of dissertation

I certify that I have read this dissertation and that in my opinion it meets the academic and professional standard required by the University as a dissertation for the degree of Doctor of Philosophy.

Signed:

Mary P. Watson, Ph.D.
Member of dissertation committee

I certify that I have read this dissertation and that in my opinion it meets the academic and professional standard required by the University as a dissertation for the degree of Doctor of Philosophy.

Signed:

Klaus H. Theopold, Ph.D.
Member of dissertation committee

I certify that I have read this dissertation and that in my opinion it meets the academic and professional standard required by the University as a dissertation for the degree of Doctor of Philosophy.

Signed:

Elizabeth R. Young, Ph.D.
Member of dissertation committee

ACKNOWLEDGMENTS

I would like to express my sincere appreciation to my advisor Prof. Joel Rosenthal for his mentorship during the five-year research life in the University of Delaware. He provided me great opportunities to explore my knowledge on the chemistry, instead of just making different sorts of compounds. His passion for science and patience also taught me how to be a mature scientist. I would also like to thank my committee members, Prof. Mary Watson, Prof. Klaus Theopold and Prof. Elizabeth Young. Without your encouragements and advices, I cannot imagine how hard my research life would be.

I am also grateful for the Rosenthal research group members for both past and present. Their kindness and intelligence motivated me to grow up as a chemist. They were always ready to offer help and suggestions to go through the difficulties. I had a lot of precious and great memories in the past five years. I also want to thank to the department facilities to provide in-time helps.

In the end, I would like to thank my mon and dad for their endless love and cares for me even it has been more than five years that we cannot get together. I miss you so much!

TABLE OF CONTENTS

| | |
|-----------------------|-------|
| LIST OF TABLES | ix |
| LIST OF FIGURES | xi |
| LIST OF SCHEMES | xvi |
| ABSTRACT | xviii |

Chapter

| | | |
|-------|---|----|
| 1 | INTRODUCTION | 1 |
| 1.1 | Applications of Porphyrinoid Compounds in Catalysis Inspired by Nature | 1 |
| 1.1.1 | Porphyrins and Porphyrinoids | 1 |
| 1.1.2 | Porphyrinoids in Nature | 2 |
| 1.1.3 | Applications in Catalysis by Using Porphyrins | 3 |
| 1.2 | Oxygen Reduction Reaction and Its Important Application in Fuel Cells as Renewable Energy Sources | 5 |
| 1.2.1 | World Energy Consumptions and Production | 5 |
| 1.2.2 | Fuel Cells as Renewable Energy Sources | 7 |
| 1.3 | Cobalt Macrocycle Complexes in Nature Involving Homolytic Co–C Bond Cleavage | 9 |
| 1.4 | Photodynamic Therapy | 10 |
| 1.4.1 | Challenges of current traditional cancer treatments | 10 |
| 1.4.2 | Photodynamic therapy as an alternative cancer treatment | 11 |
| 1.4.3 | Photochemical mechanism of PDT | 12 |
| 1.4.4 | Requirements for an ideal photosensitizer for PDT | 13 |
| 2 | EXPERIMENTAL SECTION | 15 |
| 2.1 | General Procedure | 15 |
| 2.1.1 | Materials | 15 |
| 2.1.2 | Compound Characterization | 16 |

| | | |
|----------|---|-----------|
| 2.1.3 | Electrochemical Measurements..... | 16 |
| 2.1.3.1 | Cyclic voltammetry (CV) and differential pulse voltammetry (DPV)..... | 16 |
| 2.1.3.2 | Rotating ring disk electrode (RRDE) voltammetry..... | 17 |
| 2.1.4 | UV-vis Absorption Experiments..... | 17 |
| 2.1.5 | Emission Experiments..... | 18 |
| 2.1.6 | Singlet Oxygen Sensitization..... | 18 |
| 2.2 | Preparation of Biladiene Ligand Platform..... | 20 |
| 2.2.1 | Synthesis of Dipyrromethane Starting Materials..... | 20 |
| 2.2.2 | Synthesis of Diacylation Intermediates..... | 23 |
| 2.2.3 | Synthesis of Biladiene Derivatives..... | 28 |
| 2.3 | Preparation of 5-Isocorrole Ligand Platform..... | 33 |
| 2.4 | Preparation of Co(10-Isocorrole) Complexes..... | 41 |
| 2.5 | Preparation of Co(5-Isocorrole) Complexes..... | 44 |
| 2.6 | Cobalt porphyrin and Cobalt corrole Complexes..... | 47 |
| 2.7 | Preparation of Palladium Biladiene Complexes..... | 48 |
| 2.8 | Synthesis of Palladium 5,5-disubstituted Isocorrole..... | 53 |
| 2.9 | Synthesis of Zinc 5,5-disubstituted Isocorrole..... | 59 |
| 2.9.1 | Synthesis of 1-phenyloxycarbonyl cobalt 10,10-dimethyl- 5,15-bis(pentafluorophenyl) isocorrole..... | 65 |
| 2.10 | X-ray Crystallography..... | 66 |
| 2.10.1 | X-ray Structure Solution and Refinement..... | 66 |
| 2.10.1.1 | DPBil freebase..... | 67 |
| 2.10.1.2 | Pd[MPBil] and Pd[DPBil]..... | 67 |
| 2.10.1.3 | 5-DMIC, 5-MPIC and 5-DPIC..... | 67 |
| 2.10.1.4 | Co(10-MPIC) and Co(10-DPIC)..... | 68 |
| 2.10.1.5 | Co(5-DMIC), Co(5-MPIC) and Co(5-DPIC)..... | 68 |
| 2.10.1.6 | Pd(5-DMIC), Pd(5-MPIC) and Pd(5-DPIC)..... | 69 |
| 2.10.1.7 | Zn(5-DPIC)..... | 69 |
| 2.10.2 | Crystallographic Information Tables..... | 69 |
| 3 | SYNTHESIS OF NONTRADITIONAL TETRAPTRROLE PLATFORM: BILADIENE AND 5-ISOCORROLE DERIVATIVES..... | 75 |

| | | |
|-------|---|------------|
| 3.1 | Introduction | 75 |
| 3.2 | Synthesis of 10,10-disubstituted-5,15-diphenylpentafluorophenylbiladiene | 80 |
| 3.2.1 | Crystal Structures of DPBiL | 81 |
| 3.2.2 | UV-vis Spectra of Biladiene Derivatives | 82 |
| 3.3 | Synthesis of 5,5-disubstituedd Isocorrole..... | 82 |
| 3.3.1 | Crystals Structures of 5-Isocorrole Freebase..... | 83 |
| 3.4 | UV-vis Absorption Features..... | 85 |
| 3.5 | Synthesis of Zinc and Palladium 5-Isocorrole: Zn(5-IC) and Pd (5-IC) . | 85 |
| 3.5.1 | Crystal Structures of Zn(5-DPIC) and Pd(5-IC) | 86 |
| 3.5.2 | UV-vis Absorption Features..... | 88 |
| 3.6 | Electrochemical properties of Freebase, Palladium 5-Isocorrole and Zinc 5-Isocorrole Derivatives..... | 89 |
| 3.7 | Summary..... | 92 |
| 4 | OXYGEN REDUCTION REACTION CATALYZED BY TWO FAMILIES OF COBALT ISOCORROLE | 94 |
| 4.1 | Introduction | 94 |
| 4.2 | Synthesis and Characterization of Two Families of Cobalt Isocorrole Catalysts: Cobalt 5-isocorrole and Cobalt 10-isocorrole | 98 |
| 4.3 | Electrochemistry and UV-vis Absorption Spectrometry for Cobalt Isocorrole..... | 99 |
| 4.4 | Electrochemical O ₂ Reduction by Cobalt Isocorroles as Heterogeneous Catalysts | 102 |
| 4.5 | Summary..... | 106 |
| 5 | SYNTHESIS OF 1-PHENETYLOXYCARBONYL COBALT 10,10-DIMETHYL- 5,15- BIS(PENTAFLUOROPHENYL)- ISOCORROLE AND ITS Co-C BOND PHOTOCLEAVGE..... | 107 |
| 5.1 | Introduction | 107 |
| 5.2 | Synthesis of 1-phenyloxycarbonyl cobalt 10,10-dimethyl-5,15-bis(pentafluorophenyl) isocorrole | 110 |
| 5.3 | Irradiation study of 1-phenyloxycarbonyl cobalt 10,10-dimethyl-5,15-bis(pentafluorophenyl) isocorrole | 111 |
| 5.3.1 | NMR Spectroscopy Method..... | 111 |

| | | |
|-------|--|-----|
| 5.3.2 | Episodic Capture of UV-vis spectra | 114 |
| 5.4 | Summary..... | 116 |
| 6 | DEVELOPMENT OF A FAMILY OF PALLADIUM BILADIENE DERIVATIVES VARYING AT THE sp^3 HYBRIDIZED <i>meso</i> -POSITION . | 117 |
| 6.1 | Introduction | 117 |
| 6.2 | Synthesis and Characterization of Palladium Biladiene Derivatives: Pd[MPBi] and Pd]DPBi]..... | 119 |
| 6.3 | Electrochemistry and UV-Vis Study of Pd[MPBi] and Pd]DPBi] | 121 |
| 6.4 | Emission Study of Pd[MPBi] and Pd]DPBi] | 123 |
| 6.5 | Singlet Oxygen Sensitization of Pd[MPBi] and Pd]DPBi]..... | 124 |
| 6.6 | Summary..... | 125 |
| | REFERENCES | 126 |
| | Appendix | 137 |
| | A. FULLY LABELED SOLID STATE STRUCTURE WITH BOND LENGTH AND ANGLES..... | 137 |

LIST OF TABLES

| | |
|--|-----|
| Table 2.1. Crystallographic Data for DPBil freebase..... | 69 |
| Table 2.2. Crystallographic Data for Pd[MPBil] and Pd[DPBil]..... | 70 |
| Table 2.3. Crystallographic Data for 5-isocorrole derivatives: 5-DMIC, 5-MPIC and 5-DPIC | 71 |
| Table 2.4. Crystallographic Data for Co(10-MPIC) and Co(10-DPIC) | 71 |
| Table 2.5. Crystallographic Data for Co(5-isocorrole) derivatives | 72 |
| Table 2.6. Crystallographic Data for Pd(5-DMIC), Pd(5-MPIC) and Pd(5-DPIC) | 73 |
| Table 2.7. Crystallographic Data for Zn(-DPIC) with methanol binded as the fifth coordination ligand..... | 73 |
| Table 3.1 Relevant dihedral angles and atom distances measured for 5-DMIC, 5-MPIC, and 5-DPIC | 84 |
| Table 3.2. Relevant dihedral angles and atom distances measured for Pd(5-DMIC), Pd(5-MPIC), Pd(5-DPIC), and Zn(5-DPIC) | 87 |
| Table 3.3. The selected absorption maxima and its coordinated extinction coefficient | 89 |
| Table 3.4 Redox properties of 5-isocorrole freebase, Pd(5-IC) and Zn(5-IC) based on DPV | 92 |
| Table 4.1. Redox potentials for cobalt isocorrole complexes according to DPV experiment. | 101 |
| Table 4.2 Ring vs. Disk analysis results for cobalt catalysts at 1600 rpm. | 104 |
| Table 4.3 Catalytic ORR performance for Co(5-IC) and Co(10-IC) based on Koutecky-Levich analysis method. | 105 |
| Table 6.1 Relevant dihedral angles measured for Pd[MPBil] and Pd[DPBil] , including the Pd[DMBil1] for comparison. | 120 |

| | |
|---|-----|
| Table 6.2 Electrochemical and UV-vis absorption data for Pd(II) complexes..... | 122 |
| Table 6.3 Photophysical data of Pd[DMBi1], Pd[MPBi] and Pd[DPBi] | 124 |
| Table A.1. Bond Lengths (Å) and Bond angles (°) determined for DPBi | 137 |
| Table A.2 Bond Lengths (Å) and Bond angles (°) determined for Pd[MPBi] | 140 |
| Table A.3 Bond Lengths (Å) and Bond angles (°) determined for Pd[DPBi]..... | 143 |
| Table A.4 Bond Lengths (Å) and Bond angles (°) determined for Co(10-MPIC) | 147 |
| Table A.5 Bond Lengths (Å) and Bond angles (°) determined for Co(10-DPIC)..... | 150 |
| Table A.6 Bond Lengths (Å) and Bond angles (°) determined for 5-DMIC..... | 154 |
| Table A.7 Bond Lengths (Å) and Bond angles (°) determined for 5-MPIC | 157 |
| Table A.8 Bond Lengths (Å) and Bond angles (°) determined for 5-DPIC | 160 |
| Table A.9 Bond Lengths (Å) and Bond angles (°) determined for Co(5-DMIC) | 163 |
| Table A.10 Bond Lengths (Å) and Bond angles (°) determined for Co(5-MPIC)..... | 166 |
| Table A.11 Bond Lengths (Å) and Bond angles (°) determined for Co(5-DPIC)..... | 169 |
| Table A.12 Bond Lengths (Å) and Bond angles (°) determined for Pd(5-DMIC)..... | 172 |
| Table A.13 Bond Lengths (Å) and Bond angles (°) determined for Pd(5-MPIC) | 175 |
| Table A.14 Bond Lengths (Å) and Bond angles (°) determined for Pd(5-DPIC) | 178 |
| Table A.15 Bond Lengths (Å) and Bond angles (°) determined for Zn(5-DPIC)..... | 182 |

LIST OF FIGURES

| | |
|--|----|
| Figure 1.1 Examples for porphyrins (first row) and porphyrinoids (second row). | 2 |
| Figure 1.2 Chemical structures of porphyrinoids in nature: heme (left), Chlorophyll (right)..... | 3 |
| Figure 1.3 Energy consumption by sector reported by Energy Information Administration (EIA), US in 2020. | 6 |
| Figure 1.4. History and projections of energy production from Energy Information Administration (EIA), US in 2020. | 6 |
| Figure 1.5 One plausible assembly by combining solar fuel cell and solar energy for new replaceable energy sources | 7 |
| Figure 2.1 ^1H NMR and ^{13}C NMR of 5-methyl-5-phenyldipyrromethane in deuterated DMSO..... | 21 |
| Figure 2.2 ^1H NMR and ^{13}C NMR of 5, 5-diphenyldipyrromethane in CD_2Cl_2 | 23 |
| Figure 2.3 ^1H , ^{19}F and ^{13}C NMR of 5-methyl-5-phenyl-1,9-bis(pentafluorobenzoyl)dipyrromethane in CDCl_3 | 25 |
| Figure 2.4 ^1H , ^{19}F and ^{13}C NMR of 5, 5-diphenyl-1,9-bis(pentafluorobenzoyl)dipyrromethane in CDCl_3 | 28 |
| Figure 2.5 ^1H , ^{19}F and ^{13}C NMR of 10-methyl-10-phenyl-5,15-bis(pentafluorophenyl)-biladiene in CD_3CN | 30 |
| Figure 2.6 ^1H , ^{19}F and ^{13}C NMR of 10, 10-diphenyl-5,15-bis(pentafluorophenyl)-biladiene in deuterated DMSO. | 33 |
| Figure 2.7 ^1H , ^{19}F and ^{13}C NMR of 2-pentafluorobenzyl pyrrole in CDCl_3 | 35 |
| Figure 2.8 ^1H , ^{19}F and ^{13}C NMR of 5-methyl-5-phenyl-10,15-bis(pentafluorophenyl)isocorrole in deuterated DMSO. | 38 |
| Figure 2.9 ^1H , ^{19}F and ^{13}C NMR of 5,5-diphenyl-10,15-bis(pentafluorophenyl)isocorrole in deuterated DMSO. | 40 |

| | |
|--|----|
| Figure 2.10 ^1H NMR of Co(10-MPIC) in CDCl_3 | 42 |
| Figure 2.11 ^1H NMR of Co(10-MPIC) in CDCl_3 | 44 |
| Figure 2.12 ^1H NMR of Co(5-DMIC) in CDCl_3 | 45 |
| Figure 2.13 ^1H NMR of Co(5-MPIC) in CDCl_3 | 46 |
| Figure 2.14 ^1H NMR of Co(5-DPIC) in CDCl_3 | 47 |
| Figure 2.15 ^1H , ^{19}F and ^{13}C NMR of palladium 10-methyl-10-phenyl-5,15- bis(pentafluorophenyl)-biladiene, Pd[MPBil] in CD_3CN | 50 |
| Figure 2.16 ^1H , ^{19}F and ^{13}C NMR of palladium 10,10-diphenyl-5,15- bis(pentafluorophenyl)-biladiene, Pd[DPBil] in CD_3CN | 52 |
| Figure 2.17 ^1H , ^{19}F and ^{13}C NMR of Pd(5-DMIC) in CDCl_3 | 55 |
| Figure 2.18 ^1H , ^{19}F and ^{13}C NMR of Pd(5-MPIC) in CDCl_3 | 57 |
| Figure 2.19 ^1H , ^{19}F and ^{13}C NMR of Pd(5-DPIC) in CDCl_3 | 59 |
| Figure 2.20 ^1H , ^{19}F and ^{13}C NMR of Zn(5-DMIC) in CDCl_3 | 61 |
| Figure 2.21 ^1H , ^{19}F and ^{13}C NMR of Zn(5-MPIC) in C_6D_6 | 63 |
| Figure 2.22 ^1H , ^{19}F and ^{13}C NMR of Zn(5-DPIC) in C_6D_6 | 65 |
| Figure 3.1. Structures of a,c-Biladiene and Biliverdin..... | 75 |
| Figure 3.2 Two isomers of isocorrole..... | 77 |
| Figure 3.3 The crystal structure of DPBil, view from side and front. Hydrogen atoms are omitted for clarity. | 82 |
| Figure 3.4 UV-vis absorption of biladiene derivatives in DCM at room temperature. 82 | |
| Figure 3.5 Crystal structures of 5-DMIC (left), 5-MPIC (middle) and 5-DPIC (right), viewing form top and side. H atoms are omitted for clarities, except for the N–H protons. | 84 |
| Figure 3.6 UV-Vis absorption spectrometry of 5-isocorrole derivatives in methanol. 85 | |

| | |
|---|-----|
| Figure 3.7 Crystal structure of metallo 5-isocorrole viewed from top and in profile, from left to right: Pd(5-DMIC) (first column), Pd(5-MPIC) (second column), Pd(5-DPIC) (third column). | 87 |
| Figure 3.8. Crystal structure of Zn(5-DPIC) with a molecule of methanol as the fifth coordinated ligand. | 87 |
| Figure 3.9 UV-vis spectroscopy of zinc 5-isocorrole derivatives in methanol at room | 88 |
| Figure 3.10 UV-vis spectroscopy of palladium 5-isocorrole derivatives in methanol at room temperature..... | 89 |
| Figure 3.11 CV (left) and DPV (right) plots of 5-isocorrole freebase in anhydrous DCM under nitrogen..... | 90 |
| Figure 3.12 CV (left) and DPV (right) plots of Zn(5-IC) derivatives in anhydrous DCM under nitrogen..... | 90 |
| Figure 3.13 CV (left) and DPV (right) plots of Pd(5-IC) derivatives in anhydrous DCM under nitrogen..... | 90 |
| Figure 4.1. Cyclic voltammetry (left) at a scan rate of 100 mV/s and differential pulse voltammetry (right) of Co(5-DMIC), Co(5-MPIC) and Co(5-DPIC) in anhydrous acetonitrile under nitrogen. | 100 |
| Figure 4.2. Cyclic voltammetry (left) at a scan rate of 100 mV/s and differential pulse voltammetry (right) of Co(10-DMIC), Co(10-MPIC) and Co(10-DPIC) in anhydrous acetonitrile under nitrogen. | 100 |
| Figure 4.3. UV-vis absorption spectra of cobalt 5-isocorrole (left) and cobalt 10–isocorrole (right) in THF in the inert atmosphere. | 102 |
| Figure 4.4 The demonstration figure of RRDE. | 103 |
| Figure 4.5. RRDE voltammetry of Co(5-IC) (left) and Co(10-IC) (right) with modified electrodes under O ₂ -saturated conditions in 0.5 M H ₂ SO ₄ aqueous solution at 20 mV/s scan rate and 1600 rpm. | 104 |
| Figure 4.6. Koutecky-Levich plots for Co(5-IC) (left) and Co(10-IC) (right) with modified electrodes under O ₂ -saturated conditions in 0.5 M H ₂ SO ₄ (the dashed lines represent the theoretical slopes for two-electron and four-electron ORR)..... | 105 |

| | |
|--|-----|
| Figure 5.1 Time-related NMR spectroscopies during the irradiation with halogen lamp every two hours: from bottom to top is 2 hours, 4 hours and 6 hours' irradiation | 113 |
| Figure 5.2 NMR of Co(10-DMIC) in CDCl ₃ at room temperature..... | 113 |
| Figure 5.3. The episodic capture of UV-vis spectra of Co(III) complex by irradiation at wavelength of 400, 450, 500, 550, 600, 650, 700, 750 and 800 nm. | 115 |
| Figure 5.4. Left: Zoomed in episodic capture UV-vis spectra of Co(III) starting material by irradiation at 450 nm. Right: UV-vis spectra of Co(10-DMIC) (green) and the Co(III) starting material (red)..... | 116 |
| Figure 6.1 Structure of Photofrin..... | 118 |
| Figure 6.2. Second generation of porphyrinoid photosensitizers for PDT..... | 119 |
| Figure 6.3 Crystal structures of Pd[DMBil1] left, Pd[MPBil] (middle) and Pd[DPBil] (right)..... | 120 |
| Figure 6.4 CV and DPV of Pd[DMBil1], Pd[MPBil] and Pd[DPBil] in anhydrous DCM under N ₂ with ferrocene as an internal standard..... | 121 |
| Figure 6.5 UV-vis absorption spectra of Pd[DMBil1], Pd[MPBil] and Pd[DPBil] were collected in methanol at room temperature. | 122 |
| Figure 6.6 Emission spectra recorded at 298 K in methanol for Pd[MPBil] (left) and Pd[DPBil] (right)..... | 123 |
| Figure A. 1. Fully labeled solid state structure of DPBil. | 137 |
| Figure A. 2 Fully labeled solid state structure of Pd[MPBil]. All non N-H hydrogens have been omitted for clarity..... | 140 |
| Figure A. 3 Fully labeled solid state structure of Pd[DPBil]. All non N-H hydrogens have been omitted for clarity..... | 143 |
| Figure A. 4 Fully labeled solid state structure of Co(10-MPIC). All non N-H hydrogens have been omitted for clarity. | 147 |
| Figure A. 5 Fully labeled solid state structure of Co(10-DPIC) with a molecule of diethyl ether as an axial ligand. All non N-H hydrogens have been omitted for clarity..... | 150 |

| | |
|--|-----|
| Figure A. 6 Fully labeled solid state structure of 5-DMIC. All non N-H hydrogens have been omitted for clarity. | 154 |
| Figure A. 7 Fully labeled solid state structure of 5-MPIC. All non N-H hydrogens have been omitted for clarity. | 157 |
| Figure A.8 Fully labeled solid state structure of 5-DPIC. All non N-H hydrogens have been omitted for clarity. | 160 |
| Figure A. 9 Fully labeled solid state structure of Co(5-DMIC). All non N-H hydrogens have been omitted for clarity. | 163 |
| Figure A. 10 Fully labeled solid state structure of Co(5-MPIC). All non N-H hydrogens have been omitted for clarity. | 166 |
| Figure A. 11 Fully labeled solid state structure of Co(5-DPIC). All non N-H hydrogens have been omitted for clarity. | 169 |
| Figure A. 12 Fully labeled solid state structure of Pd(5-DMIC). All non N-H hydrogens have been omitted for clarity. | 172 |
| Figure A. 13 Fully labeled solid state structure of Pd(5-MPIC). All non N-H hydrogens have been omitted for clarity. | 175 |
| Figure A. 14 Fully labeled solid state structure of Pd(5-DPIC). All non N-H hydrogens have been omitted for clarity. | 178 |
| Figure A. 15 Fully labeled solid state structure of Zn(5-DPIC) with a molecule of methanol as the fifth coordination ligand. All non N-H hydrogens have been omitted for clarity. | 182 |

LIST OF SCHEMES

| | |
|---|-----|
| Scheme 1.1 The two pathways for oxygen reduction reaction to form hydrogen peroxide or water. | 8 |
| Scheme 1.2 Chemical structures of coenzyme B12 and its correlated derivatives | 9 |
| Scheme 1.3. Homolytic mechanism for coenzyme B12, the structure of coenzyme B12 is simplified. | 10 |
| Scheme 1.4 Jablonski Diagram that explains the several pathways for a photosensitizer to go through after irradiated with a certain of wavelength that it can absorb..... | 13 |
| Scheme 3.1 Oxidation from a,c-Biladiene to Corrole in the air | 76 |
| Scheme 3.2. The isocorrole-corrole conversion after the metalation | 77 |
| Scheme 3.3. Synthesis of palladium isocorrole complex and its by-products. | 79 |
| Scheme 3.4 Synthesis of 10,10-disubstitued-5,15-diphenylpentafluorophenylbiladine (MPBil and DPBil) | 81 |
| Scheme 3.5 Synthesis of 5-MPIC and 5-DPIC | 83 |
| Scheme 3.6 Synthesis of Zn(5-IC) and Pd(5-IC) | 86 |
| Scheme 4.1. From left to right: cobalt phthalocyanine (CoPc), cobalt tripentafluorophenylcorrole (Co(tpfc)) and cobalt tetrapyritylporphyrin (CoP(py) ₄)..... | 95 |
| Scheme 4.2 Examples of cofacial cobalt catalysts | 96 |
| Scheme 4.3. Examples of cobalt hangman tetrapyrrole complexes. | 97 |
| Scheme 4.4. Synthesis of cobalt 5-isocorrole derivatives. | 99 |
| Scheme 4.5. Synthesis of cobalt 10-isocorrole derivatives. | 99 |
| Scheme 5.1 Co(III) complexes with alkyl, acyl and alkoxy carbonyl groups as axial ligand and porphyrin, salen, salophen and dimethylglyoxime as ligand platforms..... | 108 |
| Scheme 5.2 Synthesis approaches for Co(III) complexes | 110 |

| | |
|--|-----|
| Scheme 5.3 Synthesis of Co(III) target complex..... | 111 |
| Scheme 5.4 The radical trap experiment | 112 |
| Scheme 6.1 Synthesis of palladium biladiene derivatives..... | 119 |

ABSTRACT

Two families of nontraditional tetrapyrrole scaffold, biladiene and isocorrole, which contain one sp^3 hybridized carbon at different *meso*-positions, were synthesized. The two series of freebases were characterized by NMR spectrometry, UV-vis spectra and X-ray diffraction experiment. Their metal complexes, cobalt and palladium derivatives, were also synthesized to investigate their applications for electrocatalytic oxygen reduction reaction, carbon monoxide activation and photodynamic therapy.

Both cobalt 5-isocorrole and cobalt 10-isocorrole derivatives, which have sp^3 hybridized carbon on the 5 or 10 position, performed extraordinary selectivity for dioxygen reduction, compared with literature reported cobalt tetrapentafluorophenylporphyrin and cobalt tripentafluorophenylcorrole. The oxygen reduction has two main product which is $2e^-$, $2H^+$ pathway to produce hydrogen peroxide and $4e^-$, $4H^+$ pathway to produce water. Each pathway has potential applications for fuel cells and energy storage. The two series of cobalt isocorrole complexes were characterized by cyclic voltammetry, UV-vis absorption and X-ray diffraction experiments. They displayed strong absorption features and rich multi-electron redox electrochemistry. Their electrocatalytic oxygen reduction performance were examined by rotating ring disk electrode technique. The cobalt 10,10-dimethyl-5,15-bis(pentafluorophenyl)-isocorrole showed the highest water production yield from O_2 , which is 85%.

Cobalt(III) macrocycles with alkyl or acetyl group as axial ligand also can serve as a radical source for polymerization reaction via irradiation or heating. The cobalt 10,10-dimethyl-5,15-bis(pentafluorophenyl)-isocorrole can be used as a cobalt precursor with phenethyl alcohol and sodium phosphate to realize the 1-phenethyloxycarbonyl cobalt 10, 10-dimethyl-5,15-bis(pentafluorophenyl)-isocorrole. It showed unique near IR absorption features and the radical dissociation process was approved by adding TEMPO as a radical trap when irradiated at 450 nm. This process is monitored by both NMR spectrometry and time related UV-vis experiment. The cobalt(II) precursor can be recycled after the irradiation. It also has potential applications for polymerization reactions or drug delivery process.

Another series of tetrapyrrole scaffold with sp^3 hybridized *meso*-carbon on the 10-position, biladiene derivatives which have methyl or phenyl substituents, were also investigated for its singlet oxygen sensitizer with palladium(II) metal center. It is interesting that even though the three complexes performed multi-electron redox electrochemistry, however, switching with one or both methyl groups to phenyl substituent didn't change the redox potential, but their absorption features did increase when introducing more phenyl groups than methyl groups. It is also interesting that the palladium 10, 10-diphenyl-5,15-bis(pentafluorophenyl)-biladiene displayed the highest fluorescent quantum yield and singlet quantum yield, as well as the lowest phosphorus quantum yield. All the three palladium biladiene derivatives can be applied as potential photodynamic therapy sensitizers.

Chapter 1

INTRODUCTION

1.1 Applications of Porphyrinoid Compounds in Catalysis Inspired by Nature

1.1.1 Porphyrins and Porphyrinoids

Porphyrins are known as a family of well-studied organic chromophores which contain tetrapyrrole macrocycle scaffolds¹. Compounds such as porphyrin, phthalocyanine and corrole² can be considered as typical porphyrins. Porphyrinoids are also considered as members of porphyrins that bearing some different structural characterizations. Thus, cyclic oligopyrroles³, heteroatom-substituted (for example, oxygen and sulfur) porphyrins⁴, N-confused porphyrins⁵ and other peripherally functionalized tetrapyrroles or core-redesigned macrocycles^{6,7} (e.g. phlorin, isocorrole) are thought of porphyrinoids (shown in **Figure 1**). The reason for arousing scientists' focus for exploring porphyrins and porphyrinoids is their extraordinary absorption features and unique electrochemical properties which have potential applications for catalysis, dye-sensing and light related applications, such as photodynamic therapy⁸.

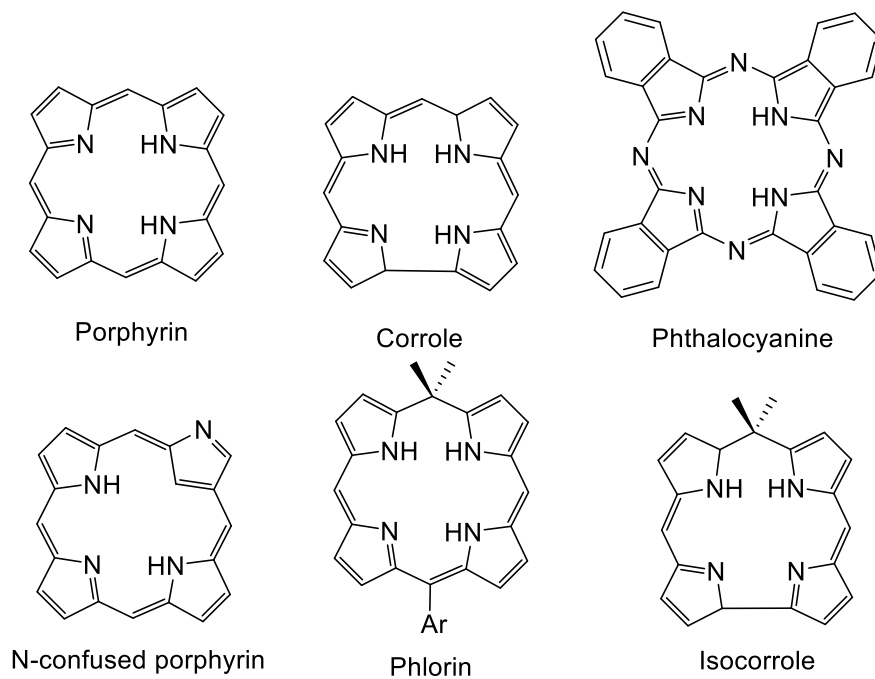


Figure 1 Examples for porphyrins (first row) and porphyrinoids (second row).

1.1.2 Porphyrinoids in Nature

There are several well-known porphyrinoid complexes that scientists have investigated for decades, such as heme⁹ and Chlorophyll^{10,11}, as shown in **Figure 2**.

Heme⁹ is one of the most famous porphyrin complexes in world perhaps because it represents the core structure, which provides dioxygen binding sites for hemoglobin and myoglobin in the circulatory system among the most non-plant multicellular organisms. Each hemoglobin is constituted by four myoglobin units, and each myoglobin unit contains one heme subunit. The Fe(II) cation in the center of heme allows a molecule of dioxygen to bind as an axial ligand at the very beginning of the oxygen transportation in the circulatory system. It also provides platforms for activation of the O–O bond by cytochrome P-450⁹, and other biological processes such as removing superoxides or peroxides through catalases and peroxidases¹².

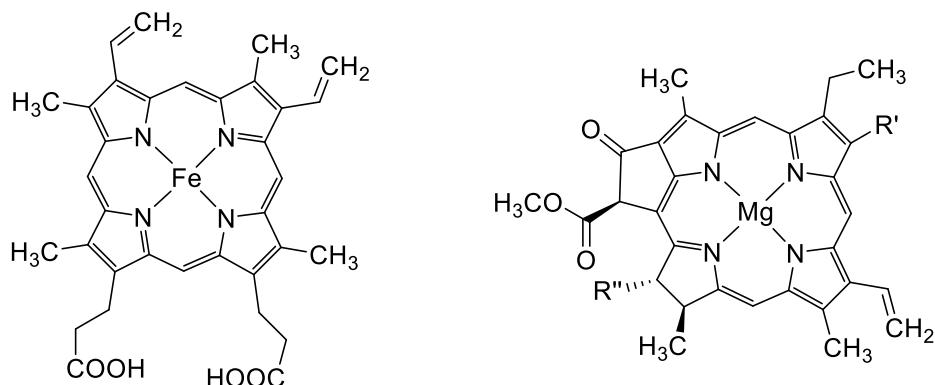


Figure 2 Chemical structures of porphyrinoids in nature: heme (left), Chlorophyll (right).

Porphyrinoids are not only applied in biological catalysis processes but also in light introduced catalytic processes like solar energy conversions, inspired by chlorophyll, which is a magnesium complex of porphyrin^{13,14}. Chlorophyll represents a group of photosynthetic pigments that primarily consume and convert photons, collected from the sunlight for example, into the chemical energy, which is required by biosynthetic processes in nature. Many studies have been carried out for long time to explain the reason why chlorophyll can realize the photochemical conversion process. The main explanation is its characteristic absorption features that allow it to harvest light from sunlight in a region of 600 – 700 nm⁸.

1.1.3 Applications in Catalysis by Using Porphyrins

Inspired by nature, several applications in catalysis by porphyrins or porphyrinoids have been explored in recent decades. Considering their light harvesting characteristics, porphyrins are potential efficient photocatalysts in different area. For example, many photosensitizers based on porphyrin skeletons have been synthesized

and characterized their performance as an anticancer drug¹⁵. Compounds such as Photofrin[®], Hemoporfin[®] and Photocyanine[®] have been approved worldwide¹⁵ as promising drugs for certain cancers and diseases like bladder cancer, early gastric cancer and colon cancer, etc.

Porphyrins can also be applied as photocatalysts in organic synthesis¹⁶, carbon dioxide reduction reaction¹⁷ and hydrogen gas formation¹⁴ reactions. Porphyrin related compounds can serve as photocatalysts because of their significant properties of single electron transfer (SET) and energy transfer (ET)¹⁶. Reactions such as alkylation/arylation of heteroarenes with aryldiazonium salts can be realized by using pentafluorophenylporphyrin (TPFPP) as photocatalyst¹⁸. On the other hand, Copper porphyrin¹⁹, Cu(II)TCPP, can generate methane and carbon monoxide irradiated by a 300 W Xenon lamp by reducing CO₂ when immobilized on TiO₂ nanoparticles. Iron porphyrins like FeTMAPP²⁰ can be used as a homogenous photocatalyst to produce pure CO gas.

Cobalt porphyrins and corroles have been shown to have great catalytic performance of dioxygen activation²¹. Cofacial porphyrins²²⁻²⁴ and correlated pacman porphyrins²³, hangman porphyrins and corroles^{25,26} have been proved their excellent oxygen reduction reaction performance.

Porphyrins can also be served as core unit of self-assembly functional materials for highly functional optoelectronic applications²⁷. Covalent organic frameworks (COFs) containing porphyrin and phthalocyanine as organic building blocks also have been attracted many attentions as a new series of highly porous materials with united pore size and various potential applications such as gas storage, electrical/photocatalytic processes and energy storage²⁸.

1.2 Oxygen Reduction Reaction and Its Important Application in Fuel Cells as Renewable Energy Sources

1.2.1 World Energy Consumptions and Production

Based on the annual energy outlook 2020 with projections to 2050²⁹ revealed by the US Department of Energy's Energy Information Administration (EIA), the need for consumption grows moderately according to the assumptions of current regulations and laws, shown in **Figure 3**. However, the energy production (shown in **Figure 4**) indicates that the production of natural gas will increase to almost 50 quadrillion Btu by 2025 and the production of crude oil and lease condensate will decrease back to 25 quadrillion Btu in 2050, which is close to the same amount of production in 2020. What is worth to be notified is that other than the hydro and nuclear energy, the prediction of the production of other renewable energy (in green trace) increases around 10 quadrillion Btu during the future, which is the second largest amount of energy production. Thus, in the next decades, there is still a lot of space for the scientists to figure out what kind of renewable energy and how to improve the usage efficiencies for the energy.

Energy consumption by sector (AEO2020 Reference case)
quadrillion British thermal units

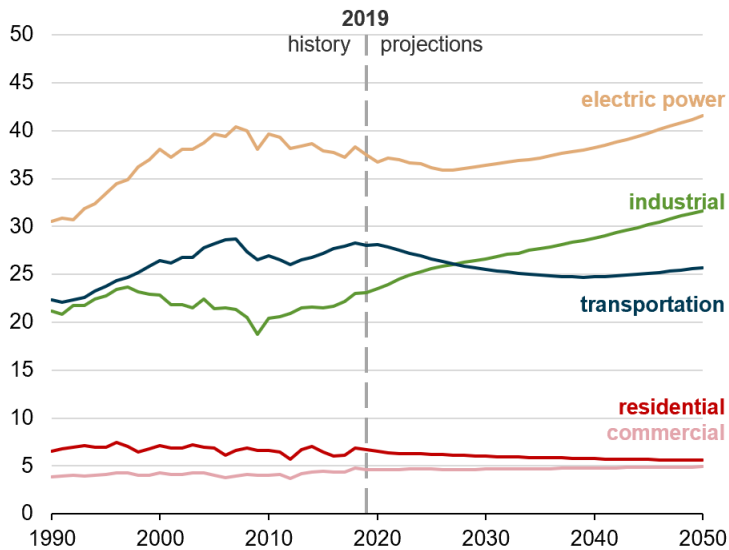


Figure 3 Energy consumption by sector reported by Energy Information Administration (EIA), US in 2020.

Energy production (AEO2020 Reference case)
quadrillion British thermal units

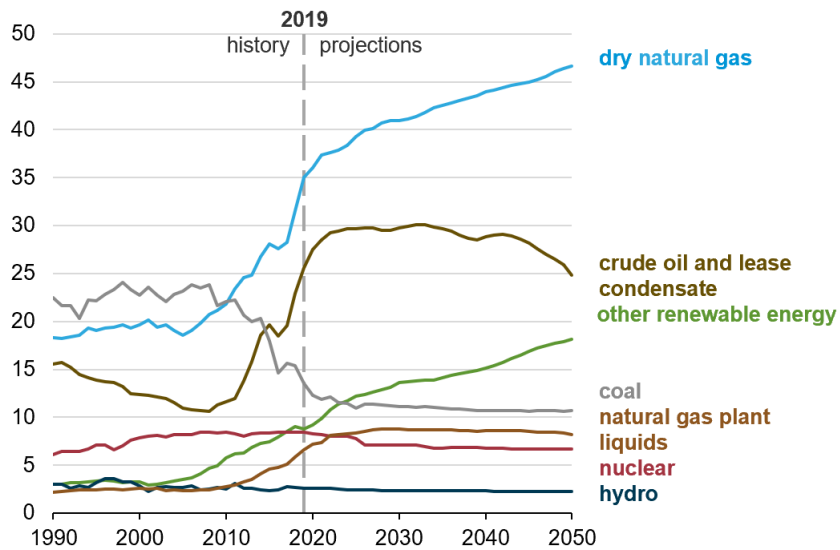


Figure 4. History and projections of energy production from Energy Information Administration (EIA), US in 2020.

1.2.2 Fuel Cells as Renewable Energy Sources

To fulfill the anticipated energy production, the storage and conversion of solar energy have aroused many interests during the decades with high efficiency and low cost. Systems that combining the solar fuel cell³⁰ and hydrogen fuel cell³¹, shown in **Figure 5**, are ideal assembly for the application for clean, renewable energy³²⁻³⁴.

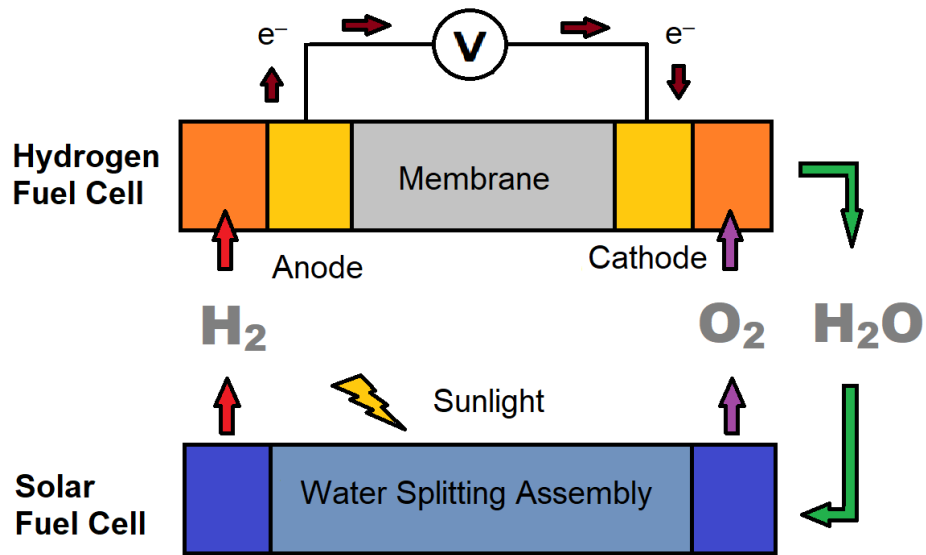


Figure 5 One plausible assembly by combining solar fuel cell and solar energy for new replaceable energy sources

For the solar fuel cell part, it imitates the photosynthetic process by green plants, which splits water to hydrogen and oxygen gas by concentrating and converting sunlight. The produced hydrogen gas and oxygen gas then can be transported to the hydrogen fuel cell units. For the hydrogen fuel cell assembly, hydrogen is combusted at the anode and oxygen is reduced to water ideally to generate electricity. Finally, the water produced on the cathode from the hydrogen fuel cell can be recycled to the solar fuel cell assembly to realize the energy converting circle.

However, several shortcomings hinder the wide spread of this replaceable energy model, mainly on the cathode of the hydrogen fuel cell assembly, which is the oxygen reduction reaction (ORR) side³⁵. Oxygen can be reduced through two main pathways: one is the $2e^-$, $2H^+$ pathway to produce hydrogen peroxide, the other is $4e^-$, $4H^+$ pathway to produce two equivalence of water, as shown in **Scheme 1.1**. Both reduction pathways are energetically favorable but producing H_2O_2 displays almost half a volt of energy, comparing with the pathway to produce water³⁶. On the other hand, the produced H_2O_2 can poison the Nafion based proton exchange membrane in the hydrogen fuel cell assembly³⁷.

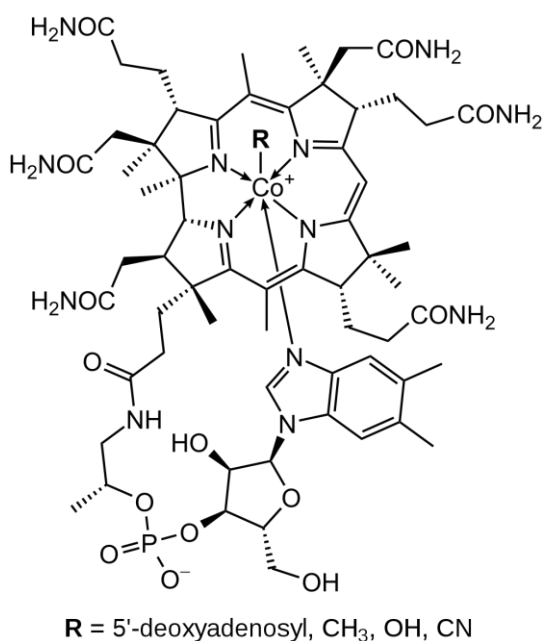


Scheme 1.1 The two pathways for oxygen reduction reaction to form hydrogen peroxide or water.

To realize the efficient oxygen reduction reaction in both high selectivity product and fast kinetic compared with the anode, huge amount of expensive platinum catalysts must be sacrificed on the cathode. So, the major challenge is to design and synthesize catalysts with efficient ORR selectivity with inexpensive costs.

1.3 Cobalt Macrocycle Complexes in Nature Involving Homolytic Co–C Bond Cleavage

Coenzyme B12 and its correlated derivatives, shown in **Scheme 1.2**, serve as necessary cofactors in a wide range of enzyme-catalyzed processes in biological systems³⁸. It is one of the most complicated organometallic cofactors in nature³⁹. The core structure of the coenzyme B12 is cobalamin, which is also called as vitamin B12, containing different axial ligand such as cyanide, methyl and hydroxyl group⁴⁰.

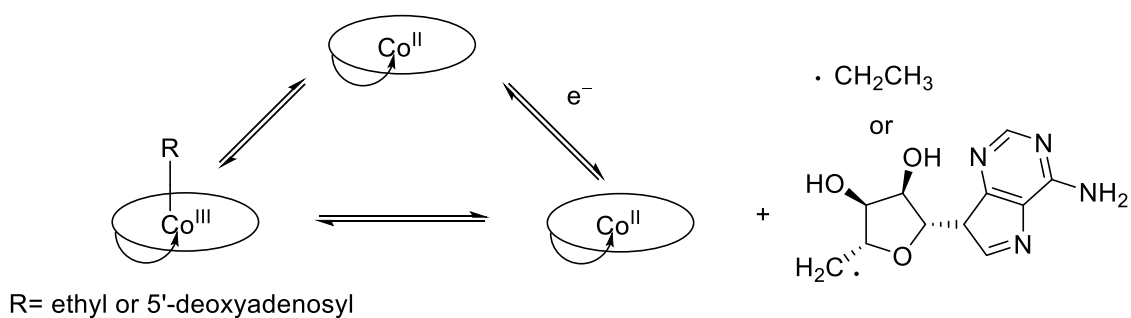


Scheme 1.2 Chemical structures of coenzyme B12 and its correlated derivatives

Vitamin B12, which is a cyanide-containing cobalt (III) corrin derivative, was isolated in red crystals and characterized as the anti-pernicious anemia factor in 1948⁴¹. Vitamin B12 is biologically inert but is an important commercially available form that provides precursors for forming related biologically active coenzyme B12.

Coenzyme B12 and its derivatives have been investigated deeply for their biological performance involving a reversible Co–C bond dissociation to for carbon

centered radical. For example, 5'-deoxyadenosyl or ethyl free radicals can be generated after the irradiation of certain wavelength, as well as forming Co(II) corrin⁴². The Co(II) corrin product can be reduced to Co(I) intermediate then be able to regenerate the Co(III) precursor to restart the catalytic cycle, shown in **Scheme 1.3**. The released 5'-deoxyadenosyl or ethyl radical can subtract a proton radical from the surroundings to go through further steps of biological catalytic cycles.



Scheme 1.3. Homolytic mechanism for coenzyme B12, the structure of coenzyme B12 is simplified.

1.4 Photodynamic Therapy

1.4.1 Challenges of current traditional cancer treatments

According to Cancer facts & figures 2020⁴³, published from American Cancer Society, more than 1.8 million new cancer cases were expected to be diagnosed in 2020. However, the number of cases did not include carcinoma in situ (noninvasive cancer) of any site except urinary bladder. Basal cell or squamous cell skin cancers did not include neither because these types of skin cancer are not required to be reported to cancer registries. It is also estimated that about 606,520 Americans were expected to die of cancer in 2020, which indicated about 1,660 deaths per day. Cancer is the second most common cause of death in the United States, that the first is heart

diseases. Most common cancer treatments^{44,45} are still focusing heavily on surgical excision, radiotherapy and chemotherapy, either as standalone treatments or in combination with each other or additional therapies.

1.4.2 Photodynamic therapy as an alternative cancer treatment

Photodynamic therapy has been arousing great interests as an alternative strategy for some types of cancers, age-related macular degeneration and skin conditions^{46, 47, 48}. PDT relies on a photosensitizer (PS) that, when activated by light of specific wavelength, generates reactive oxygen species (ROS), in particular, singlet oxygen ($^1\text{O}_2$). $^1\text{O}_2$ is toxic to cells and can kill cells directly by causing oxidative damage to cellular components, or indirectly by damaging the vasculature that supports the tumor and cutting off its supply of nutrients⁴⁸. Both apoptotic and necrotic cell death have been observed following PDT; however, numerous factors such as the light fluence and photosensitizer dose used, the intracellular location where the photosensitizer tends to accumulate, and the type of cells receiving treatment are thought to govern which of the two pathways prevails⁴⁹.

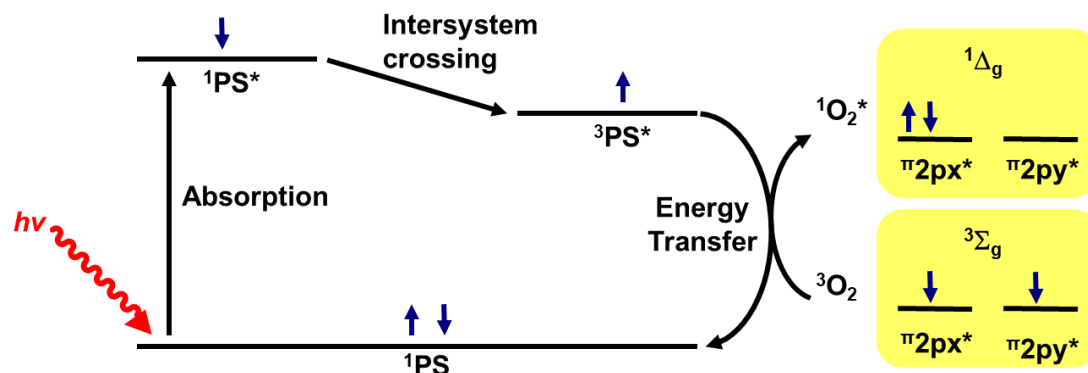
Current cancer treatments rely heavily on three strategies. One is surgery or resection, the other is radiation therapy, and chemotherapy. Each of these strategies suffers from major negative side effects: it may involve invasive surgery and increased risk of metastasis, the radiation therapy may cause radiation poisoning and increase the risk of secondary tumors, Finally, the chemotherapy may have systemic toxicity due to lack of specificity⁵⁰⁻⁵². PDT is an attractive alternative cancer treatment because of its fewer side effects and multiple advantages compared to the traditional treatment strategies. PDT can minimize the damage to healthy tissues because its light-activated mechanism allows selectively targeting the diseased tumor and controlling the

irradiation area⁵³. Furthermore, PDT provides better cosmetic outcomes than the invasive surgical excision⁵⁴. Some studies also indicate that PDT can promote an anti-tumor immune response by causing localized inflammation⁵⁵. The photosensitizers that have been approved for PDT so far do not accumulate in cell nuclei making DNA damage and its associated risks of developing secondary cancers or drug resistance minimal, and it can often be performed in an outpatient setting, which helps to lower costs⁴⁸.

1.4.3 Photochemical mechanism of PDT

An electron can be promoted by the photosensitizer ground state to the singlet excited state after this photosensitizer is irradiated at a wavelength that it can absorb by a certain light source. Then, there are several pathways available based on the Jablonski's diagram⁵⁶. As **Scheme 1.4** shows, at the beginning, the excited molecule can be fluorescent, which emits a photon of light and relax back to its original ground state. Or, it may go through a non-radiative pathway, which includes an internal conversion process from the lowest vibrational level of the first singlet excited state to an isoenergetic excited vibrational level of the singlet ground state followed by vibrational relaxation. The energy of this process is released as the form of heat to the surroundings until the molecule reaches the lowest vibrational level of the ground state. The third pathway is the intersystem crossing that happens from the lowest vibrational level of the first singlet excited state to an isoenergetic higher vibrational level of the triplet excited state with subsequent vibrational relaxation to the lowest vibrational level of the triplet excited state. A compound in the triplet excited state can also decay to emit a photon to phosphorescent and return to the ground state. Finally, if ground triplet state molecular oxygen is available around, the excited triplet

photosensitizer can engage in energy transfer with it to produce excited $^1\text{O}_2$. The energy difference between $^1\text{O}_2$ and its ground state is about 1 eV, and $^1\text{O}_2$ emits phosphorescence around 1270 nm⁵⁷.



Scheme 1.4 Jablonski Diagram that explains the several pathways for a photosensitizer to go through after irradiated with a certain of wavelength that it can absorb.

Moreover, compounds containing heavy atoms typically show higher amounts of spin-orbit coupling and more efficient intersystem crossing. Additionally, it can undergo intersystem crossing a second time to a higher singlet ground state vibrational level and return to the lowest ground state vibrational level via vibrational relaxation.

1.4.4 Requirements for an ideal photosensitizer for PDT

Firstly, the photosensitizer must be excited by light that penetrates as deeply into the tissue as possible to reach the cancerous tumors. Human tissue contains many components that absorb throughout the UV-visible region, leaving a therapeutic window of 600-900 nm⁵⁸. This absorption requirement has largely limited PDT cancer treatments to the surface of, or just under the skin, or in the lining of organs that can be reached with a light source. Secondly, the photosensitizer must efficiently undergo

intersystem crossing to generate the excited triplet state, which subsequently engages in energy transfer with the ground triplet state of molecular oxygen to generate singlet oxygen, in other word, it must have high singlet oxygen quantum yield. Finally, it is also highly desirable that photosensitizer agents be selective for tumors, as off-target PDT can result in troubling side effects, including acute skin sensitivity for patients. Also, simple synthesis steps with easy purifications, feasible large-scale preparation and aqueous solubility are another few requirement if the potent photosensitizer is trying to realize the widespread applications.

Chapter 2

EXPERIMENTAL SECTION

2.1 General Procedure

Reactions that were required an inert atmosphere were performed in the oven-dried Schlenk flasks fitted with Suba-Seal rubber septa or in a nitrogen-filled glovebox and protected under a positive pressure of N₂. Air- and moisture-sensitive reagents were transferred using standard syringe or cannula techniques.

2.1.1 Materials

Reagents and solvents were purchased from Sigma-Aldrich, Acros, Fisher, Strem, VWR, Matrix Scientific, Tokyo Chemical Industry Co. LTD or Cambridge Isotopes Laboratories. Solvents for synthesis were of reagent grade or better and were dried by passage through activated alumina and then stored over 4 Å molecular sieves prior to use. The DMBil1 ligand was prepared using published methods. Column chromatography was performed with 40–63 μm silica gel from Silicycle or neutral alumina gel from Acros.

Tetrabutylammonium hexafluorophosphate (TBAPF₆) was purchased from Tokyo Chemical Industry Co. LTD, recrystallized from ethyl alcohol, and dried under vacuum at 40 °C for at least one week prior to use. Pyrrole (reagent grade, 98%) was purchased from Acros Organics, distilled at 150 °C and stored under nitrogen at 4 °C before use. Phenethyl alcohol was also purchased from Acros Organics and distilled at 210 °C and stored in the N₂ filled glovebox.

2.1.2 Compound Characterization

^1H NMR, ^{13}C NMR and ^{19}F NMR spectra were recorded at 25 °C on a Bruker 400 MHz spectrometer with a cryogenic QNP probe or Bruker 600 MHz spectrometer with a 5-mm Bruker SMART probe. Proton spectra are referenced to the residual proton resonance of the deuterated solvent ($\text{CDCl}_3 = \delta$ 7.26, DMSO = δ 2.50, $\text{CD}_3\text{CN} = \delta$ 1.94, $\text{CD}_2\text{Cl}_2 = \delta$ 5.32) and carbon spectra are referenced to the carbon resonances of the solvent ($\text{CDCl}_3 = \delta$ 77.16, DMSO = δ 39.52, $\text{CD}_3\text{CN} = \delta$ 1.32, $\text{CD}_2\text{Cl}_2 = \delta$ 53.84)⁵⁹. All chemical shifts are reported using the standard δ notation in parts-per-million, and positive chemical shifts are to higher frequency from the given reference. High-resolution mass spectrometry analyses were performed by the University of Delaware Mass Spectrometry Laboratory in the Department of Chemistry and Biochemistry.

2.1.3 Electrochemical Measurements

2.1.3.1 Cyclic voltammetry (CV) and differential pulse voltammetry (DPV)

Experiments were performed using a CHI-620D potentiostat/galvanostat using a standard three-electrode configuration. The working electrode was a polished glassy carbon electrode (GCE, 3.0 mm diameter, CH Instruments) and the auxiliary electrode was a piece of platinum wire. Electrochemical potentials were measured against a silver wire pseudo reference, unless otherwise noted, with ferrocene as internal potential standard and calibrated to Ag/AgCl (Sat. KCl). The supporting electrolyte employed for CV and DPV experiments was 0.1 M tetrabutylammonium hexafluorophosphate (TBAPF_6), dissolved in CH_3CN or DCM. The analyte concentration was 1.0 mM, and all CV experiments were carried out using a scan rate

of 100 mV/s unless otherwise noted. All the CV and DPV experiments were performed in the inert atmosphere.

2.1.3.2 Rotating ring disk electrode (RRDE) voltammetry

Experiments were performed using a CHI-720D bipotentiostat and a modulated speed rotator from Pine Research Instrumentation. The working electrodes were a polished glassy carbon disk electrode (5.61 mm diameter) and a platinum ring electrode (6.25 mm inner diameter, 7.92 mm outer diameter) compacted in a ThinGap RRDE tip (E7R9 Series, Pine Research Instrumentation) that was attached to the rotator by a shaft (AFE6M, Pine Research Instrumentation). The auxiliary electrode for RRDE experiments was platinum mesh. Potentials were measured against a Ag/AgCl (1.0 M KCl) reference electrode. The supporting electrolyte employed for RRDE voltammetry was 0.5 M H₂SO₄ aqueous solution by using MQ-water. Linear sweep voltammetry (LSV) experiments were carried out using a scan rate of 20 mV/s unless otherwise noted. A stream of water saturated O₂ was used to saturate the electrolyte solution prior to initiating voltammetry experiments and was maintained over the headspace of the solution during RRDE experiments.

2.1.4 UV-vis Absorption Experiments

The UV-vis spectra were acquired on a Stellar Net CCD array UV-vis spectrometer using screw-cap quartz cuvettes (7Q or 6Q) of 1 cm path length from Starna. The air-sensitive samples were prepared in anhydrous solvent at concentrations of 4.0, 8.0, 12.0, 16.0, and 20.0 μ M in a nitrogen filled glovebox. All the absorbance data were collected at room temperature.

2.1.5 Emission Experiments

Emission spectra were recorded on an automated Photon Technology International (PTI) QuantaMaser 40 fluorometer equipped with a 75-W xenon arc lamp, an LPS-220B lamp power supply, and a Hamamatsu R2658 photomultiplier tube. All samples were prepared in screw cap quartz cuvettes of 1.0 cm path length from Starna Cells, Inc. Solutions of [Ru(bpy)₃][PF₆]₂ in acetonitrile and each biladiene derivative in methanol were prepared in a nitrogen-filled glove box such that the absorbance values of all samples at $\lambda = 500$ nm ranged between 0.74×10^{-1} and 5.07×10^{-1} (1 cm pathlength). The samples were excited at $\lambda_{\text{ex}} = 500$ nm, and emission was monitored from $\lambda_{\text{em}} = 515$ to 950 nm using a step size of 1 nm and an integration time of 0.25 s. Emission spectra were also taken measured for samples following 30-minute exposure to air. All reported spectra are the average of five individual acquisitions.

Emission quantum yields were calculated using a solution of [Ru(bpy)₃][PF₆]₂ in nitrogen saturated acetonitrile as reference and the expression below:

$$\Phi_S = \Phi_{\text{ref}} \left(\frac{I_S}{I_{\text{ref}}} \right) \left(\frac{A_{\text{ref}}}{A_S} \right) \left(\frac{\eta_S}{\eta_{\text{ref}}} \right)^2$$

where Φ_S and Φ_{ref} are the emission quantum yields of the sample and the reference ($\Phi_{\text{ref}} = 0.094$ for [Ru(bpy)₃][PF₆]₂ in acetonitrile) respectively, I_S and I_{ref} are the integrated emission intensities of the samples and reference, A_S and A_{ref} are the measured absorbances of the sample and reference at the excitation wavelength, and η_S and η_{ref} are the refractive indices of the solvents used for the sample and reference.

2.1.6 Singlet Oxygen Sensitization

Generation of ¹O₂ was quantified by monitoring the fluorescence of 1,3-diphenylisobenzofuran (DPBF), which is a ¹O₂ trapping reagent. The measurements of

fluorescence were carried out by an automated Photon Technology International (PTI) Quanta-Master 40 fluorometer equipped with a 150 W Xenon arc lamp, an LPS-220B lamp power supply, and a Hamamatsu R2658 photomultiplier tube using quartz cuvettes (6Q) with 1.0 cm path length.

Consumption of DPBF was monitored by observing the change in its integrated emission intensity following irradiation with light from an 150 W AmScope series haloid lamp cold-light source fitted with a 10 nm (fwhm) bandpass filter centered at 500 nm (Thor Labs, FB500-10). The cuvettes were irradiated for 10 second intervals for a total of 40 seconds. DPBF emission spectra were obtained by exciting at $\lambda_{\text{ex}} = 405$ nm and scanning from $\lambda_{\text{em}} = 400 - 600$ nm using a step size of 1 nm and an integration time of 0.25 seconds.

Calibration curves of the integrated emission intensity versus the concentration of unreacted DPBF remaining in solution were generated to correct for absorption of the photosensitizers between 400 – 600 nm. Emission spectra were collected from 10 μM solutions of Pd complexes and $[\text{Ru}(\text{bpy})_3][\text{PF}_6]_2$ containing DPBF concentrations of 10, 20, 30, 40 or 50 μM . Linear regression lines were fit to the calibration data from each solution, and the integrated emission intensity values obtained from the $^1\text{O}_2$ experiments were then used for linear regression analyses, enabling the corresponding concentrations of unreacted DPBF to be obtained. A final plot of the concentration of unreacted DPBF versus irradiation time formed a straight line with slope m , which was used with the following equation to calculate the $^1\text{O}_2$ quantum yields:

$$F_s = F_{\text{ref}} \frac{m_s}{m_{\text{ref}}} \frac{e_{\text{ref}}}{e_s}$$

Where Φ_s and Φ_{ref} are the 1O_2 sensitization quantum yields for the sample and [Ru(bpy)₃][PF₆]₂ reference ($\Phi_{ref} = 0.81$), respectively, m_s and m_{ref} are the slopes of the concentration of DPBF vs. irradiation time plots for the sample and reference, and ϵ_s and ϵ_{ref} are the extinction coefficients at the wavelength of irradiation (500 nm) for the sample and reference, respectively. Reported 1O_2 quantum yields were obtained from an average of three trials.

2.2 Preparation of Biladiene Ligand Platform

2.2.1 Synthesis of Dipyrromethane Starting Materials

5-Methyl-5-phenyldipyrromethane. Pyrrole (18 mL, 259 mmol) and acetophenone (1.5 mL, 12.5 mmol) were combined in a round bottom flask and the resulting solution was sparged with N₂ in ice bath for 5 min. To the degassed solution was added trifluoroacetic acid (350 μ L 5 mmol). The mixture was stirred for 4 h, from 0 °C to room temperature. The reaction was quenched with 2 M NaOH. The product was extracted with ethyl acetate three times. The combined organic layer was washed with water and brine, then dried over Na₂SO₄. The solvent was removed by rotary evaporation, and the crude was purified via flash chromatography on silica gel by using hexanes and ethyl acetate (10:1) as the eluent to deliver a sticky oil. This oil was then dried under vacuum at 50 °C for 3 days to deliver 3.75 g of desired compound as white solid (yield = 64%). ¹H NMR (600 MHz, DMSO, 25 °C) δ /ppm: 10.36 (s, 2H), 7.28 (m, 2H), 7.20 (m, 1H), 7.01 (d, J = 7.8 Hz, 2H), 6.67 (m, 2H), 5.92 (d, J = 2.4 Hz, 2H), 5.61 (s, 2H), 1.99 (s, 3H). ¹³C NMR (150 MHz, DMSO, 25 °C) δ /ppm: 148.86, 137.58, 127.60, 127.14, 126.87, 117.13, 106.22, 105.93, 44.26, 28.06. HR-ESI-MS [M + H]⁺ m/z: calcd for C₁₆H₁₇N₂, 237.1392; found, 237.1387.

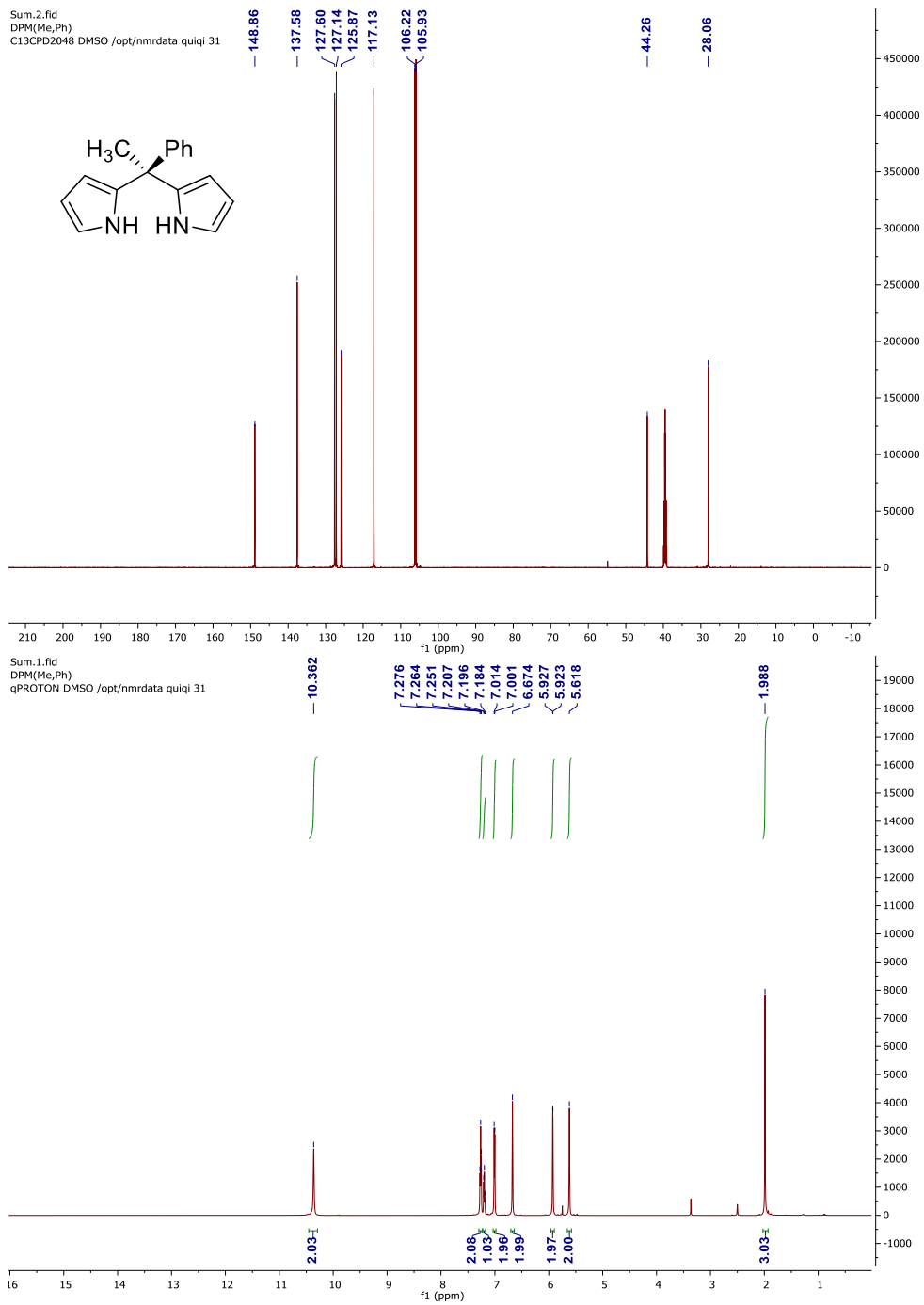
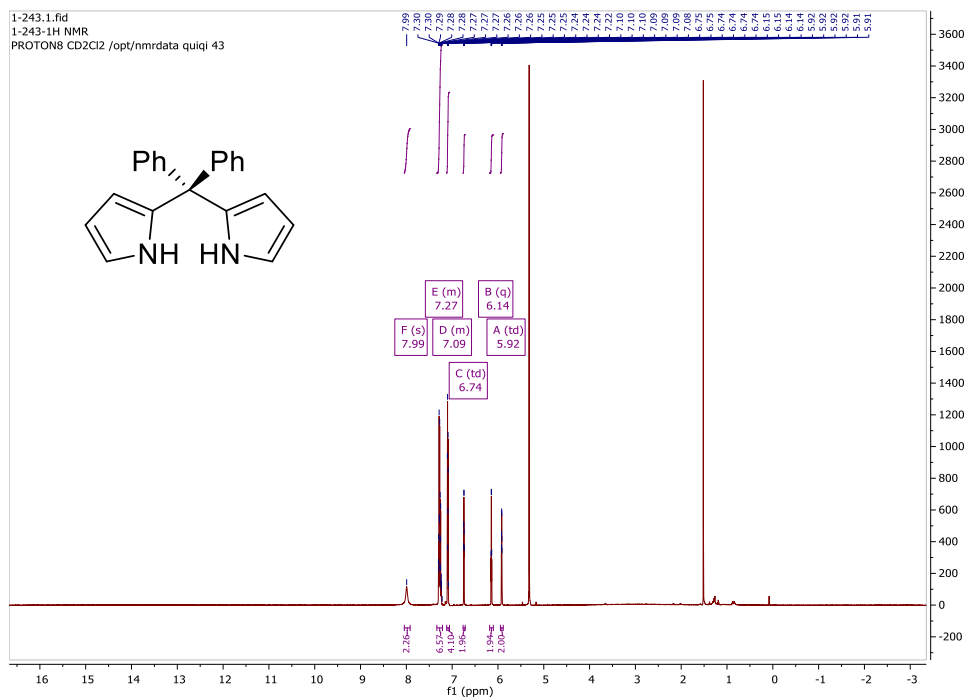


Figure 6 ^1H NMR and ^{13}C NMR of 5-methyl-5-phenyldipyrromethane in deuterated DMSO.

5,5-diphenyldipyrromethane. 10 g of benzophenone (54 mmol) was added 100 mL dry ethanol in a 200 mL Schlenk flask under an atmosphere of N₂. Fresh distilled pyrrole (10 mL, 144 mmol) and boron trifluoride etherate (10 mL, 81 mmol) was then added sequentially. The mixture was stirred for 5 d at room temperature under positive N₂ atmosphere. The crude product was separated via a simple filtration and wash with cold ethanol for three times. 6.8 g white solid was collected as product (yield = 42%). ¹H NMR (600 MHz, DMSO, 25 °C) δ/ppm: 10.28 (s, 2H), 7.25 (m, 6H), 6.94 (d, J = 6 Hz, 2H), 6.71 (s, 2H), 6.70 (m, 2H), 5.91 (s, 2H), 5.56 (s, 2H). ¹³C NMR (151 MHz, CD₂Cl₂) δ/ppm: 146.50, 135.68, 129.60, 128.24, 127.14, 117.78, 109.75, 108.24, 54.20, 54.02, 53.84, 53.66, 53.48. HR-ESI-MS [M + H]⁺ m/z: calcd for C₂₁H₁₉N₂, 299.1548; found, 299.1541.



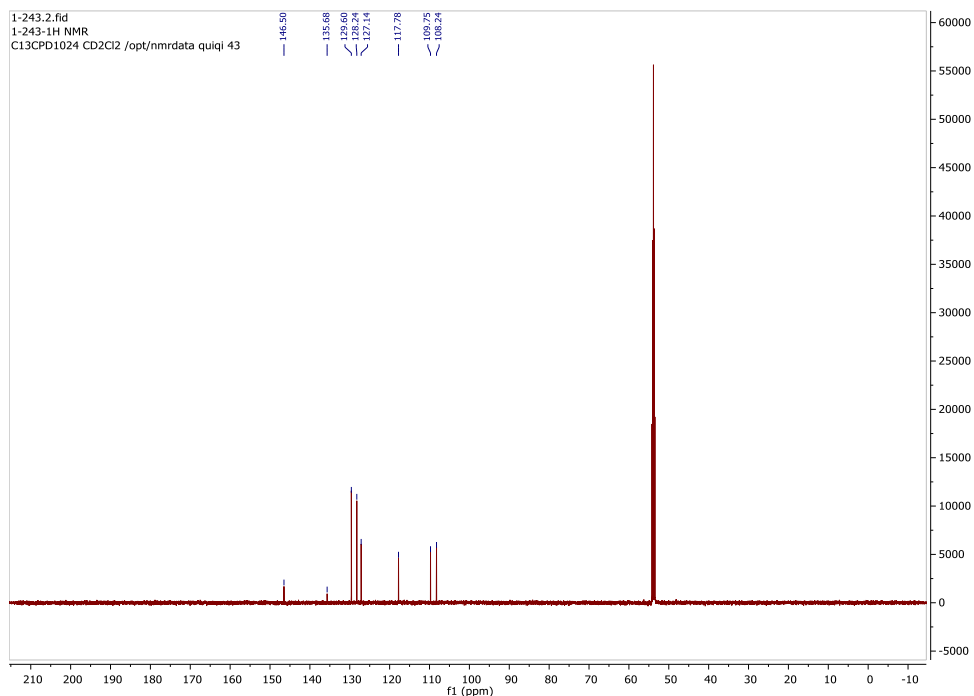
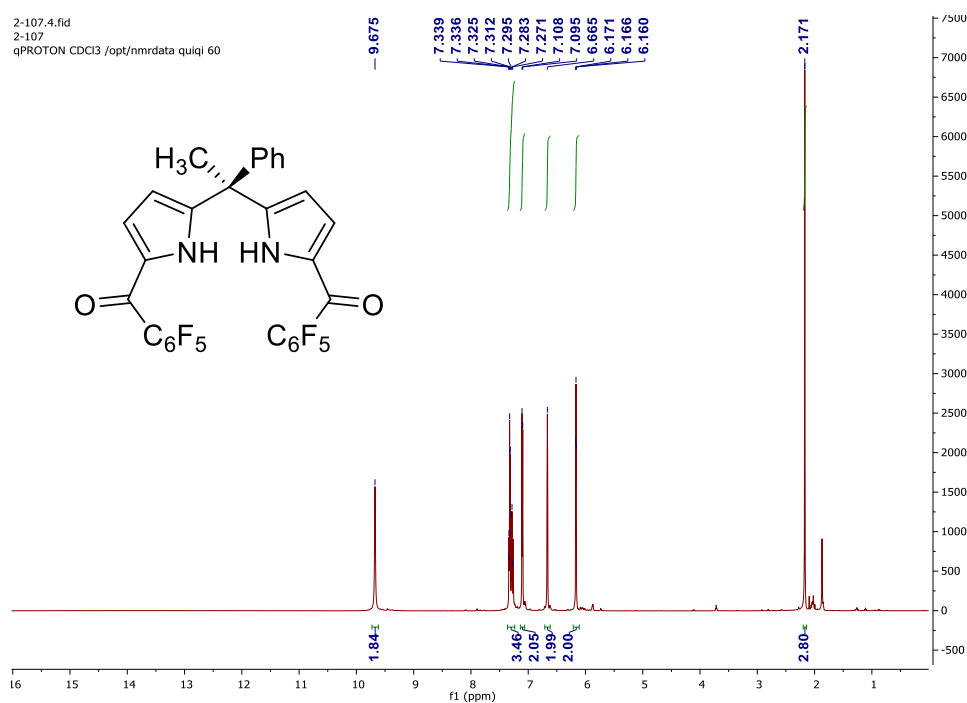


Figure 7 ^1H NMR and ^{13}C NMR of 5, 5-diphenyldipyrromethane in CD_2Cl_2 .

2.2.2 Synthesis of Diacylation Intermediates

5-Methyl-5-phenyl-1,9-bis(pentafluorobenzoyl)dipyrromethene. 5-methyl-5-phenyldipyrromethane (1.18 g, 5 mmol) was transferred to an oven baked Schlenk flask, then 100 mL of dry toluene was added under positive atmosphere of N_2 . Ethyl magnesium bromide (25 mL, 25 mmol, 1M in THF) was added dropwise into the resulting solution over 5 min. The mixture was stirred for 30 min at room temperature. A solution of 1.8 mL pentafluorobenzoyl chloride (12.5 mmol) in 12.5 mL dry toluene was then added to the stirred reaction dropwise over 5 min. The mixture was stirred for an additional 30 min at room temperature. The reaction was quenched with saturated NH_4Cl and the aqueous layer was extracted with ethyl acetate three times. The combined organic layer was washed with water and brine, and then dried over Na_2SO_4 . Following the removal of solvent via rotary evaporation, the crude product was purified via flash chromatography on silica using hexanes and ethyl acetate (5:1)

as the eluent. Recrystallization of the product at $-35\text{ }^{\circ}\text{C}$ from $\text{CH}_2\text{Cl}_2/\text{hexanes}$ delivered 2.6 g of the title compound as a white solid (yield = 43%). ^1H NMR (600 MHz, CDCl_3 , $25\text{ }^{\circ}\text{C}$) δ/ppm : 9.68 (s, 2H), 7.31 (m, 3H), 7.10 (d, $J = 7.8\text{ Hz}$, 2H), 6.67 (s, 2H), 6.17 (d, $J = 3\text{ Hz}$, 2H), 2.17 (s, 3H). ^{13}C NMR (150 MHz, CDCl_3 , $25\text{ }^{\circ}\text{C}$) δ/ppm : 172.25, 146.80, 144.89, 143.67, 143.25, 138.53, 136.84, 131.53, 129.08, 128.02, 127.20, 121.99, 111.50, 45.86, 28.29. ^{19}F NMR (565 MHz, CDCl_3 , $25\text{ }^{\circ}\text{C}$) δ/ppm : -139.74 (dd, $J = 23.7, 8.5\text{ Hz}$, 4F), -151.01 (t, $J = 20.7\text{ Hz}$, 2F), -160.22 (td, $J = 22.2, 8.2\text{ Hz}$, 4F). HR-ESI-MS $[\text{M} + \text{H}]^+$ m/z : calcd for $\text{C}_{30}\text{H}_{15}\text{F}_{10}\text{N}_2\text{O}_2$, 625.0974; found, 625.0971.



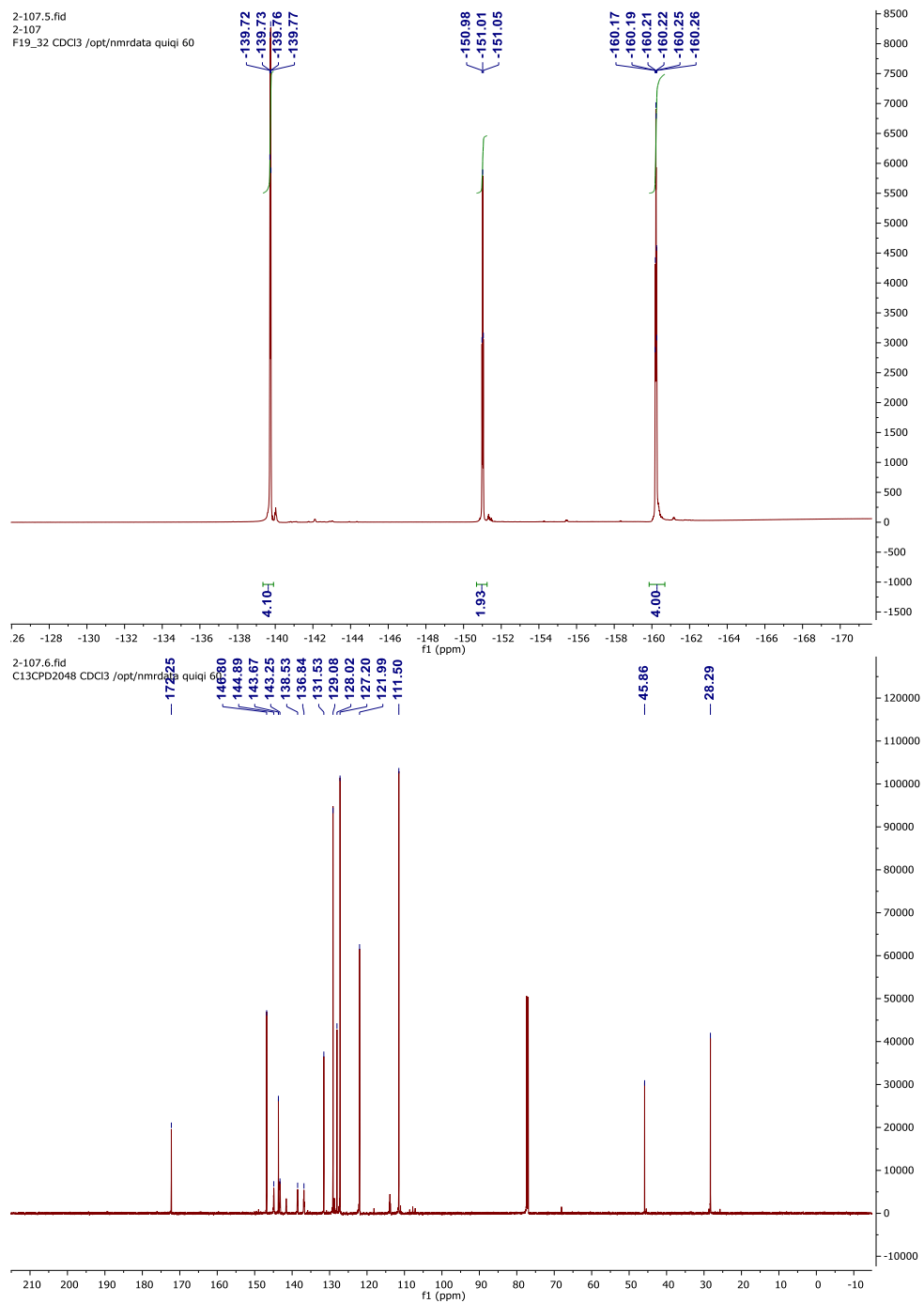
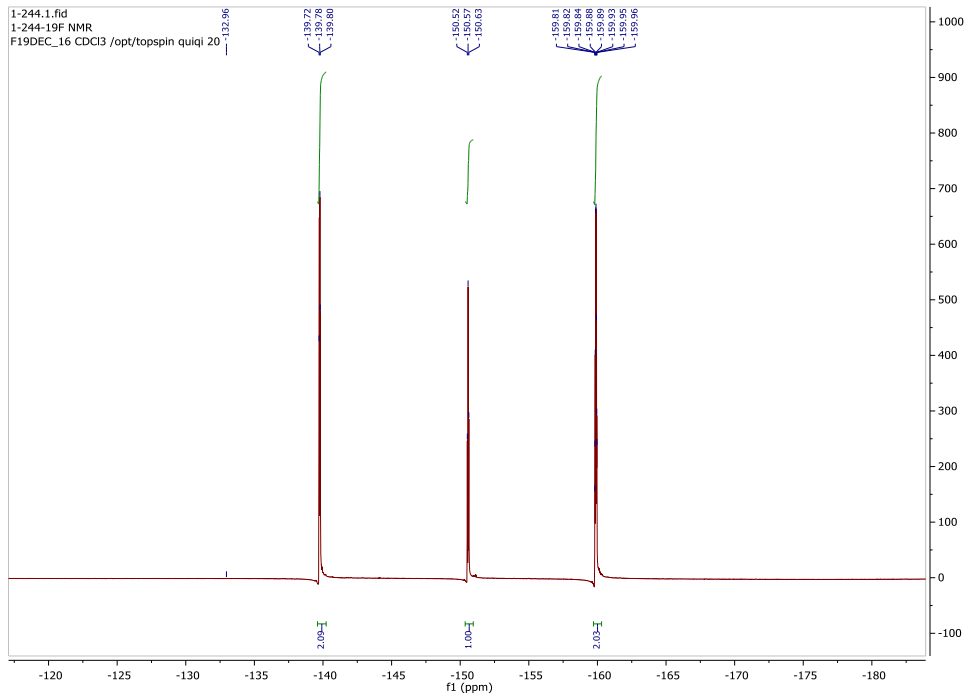
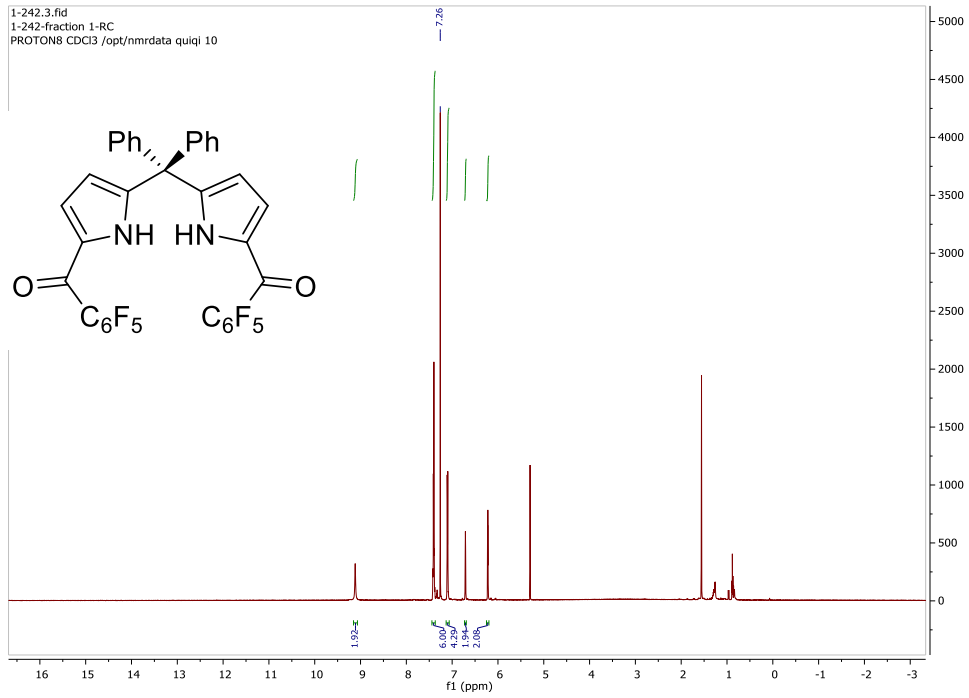


Figure 8 ^1H , ^{19}F and ^{13}C NMR of 5-methyl-5-phenyl-1,9-bis(pentafluorobenzoyl)dipyrromethene in CDCl_3 .

5,5-diphenyl-1,9-bis(pentafluorobenzoyl)dipyrromethene. 5, 5-diphenyldipyrromethane (1.5 g, 5 mmol) was transferred to an oven baked Schlenk flask and 100 mL of dry THF was added under an atmosphere of N₂. Ethyl magnesium bromide (25 mL, 25 mmol, 1M in THF) was added dropwise into the resulting solution over 5 min. The mixture was stirred for 30 min at room temperature. A solution of 1.8 mL pentafluorobenzoyl chloride (12.5 mmol) in 12.5 mL dry toluene was then added to the stirred mixture dropwise over 5 min. The mixture was stirred for an additional 30 min at room temperature. The reaction was quenched with saturated NH₄Cl and the aqueous layer was extracted with ethyl acetate three times. The combined organic layer was washed with water and brine, and then dried over Na₂SO₄. Following the removal of solvent via rotary evaporation, the crude product was purified via flash chromatography on silica using hexanes and ethyl acetate (5:1) as the eluent. Recrystallization of the product at -35 °C from CH₂Cl₂/hexanes delivered 2.9 g of the title compound as a white powder (yield = 30%). ¹H NMR (600 MHz, CDCl₃, 25 °C) δ/ppm: 9.13 (s, 2H), 7.40 (m, 6H), 7.10 (m, 4H), 6.71 (s, 2H), 6.22 (dd, J = 4.1, 2.7 Hz, 2H). ¹³C NMR (150 MHz, CDCl₃, 25 °C) δ/ppm: 172.18, 144.78, 144.35, 143.13, 142.03, 138.45, 136.76, 131.05, 129.12, 128.97, 128.40, 121.16, 113.83. ¹⁹F NMR (565 MHz, CDCl₃, 25 °C) δ/ppm: -139.78 (dd, J = 23.6, 8.3 Hz, 4F), -150.65 (t, J = 20.7 Hz, 2F), -159.96 (td, J = 29.8, 16.4 Hz, 4F). HR-ESI-MS [M + H]⁺ m/z: calcd for C₃₅H₁₇F₁₀N₂O₂, 687.1130; found, 687.1122.



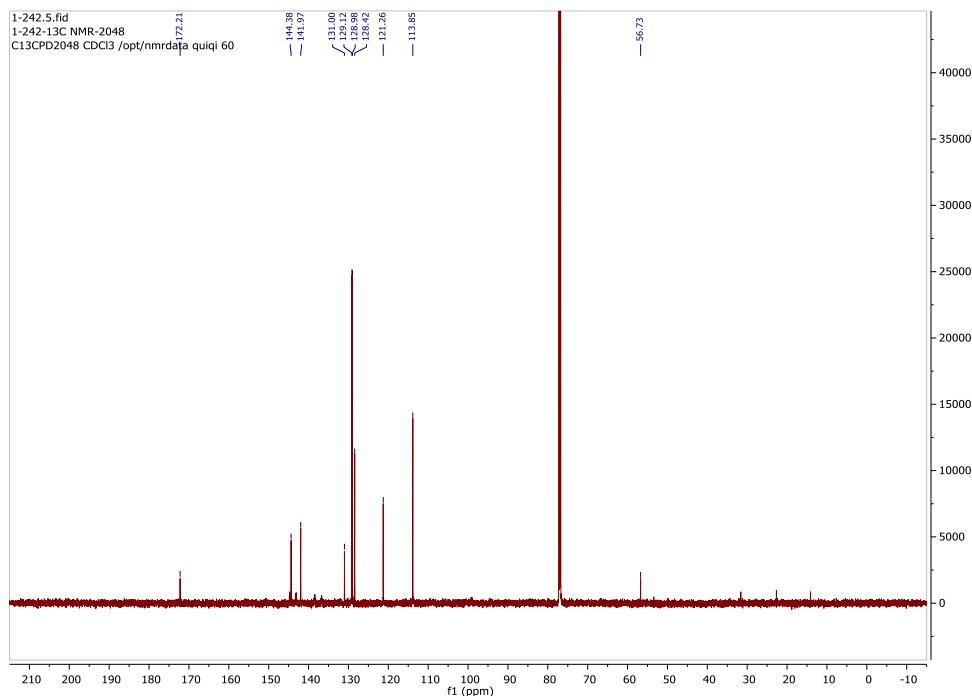
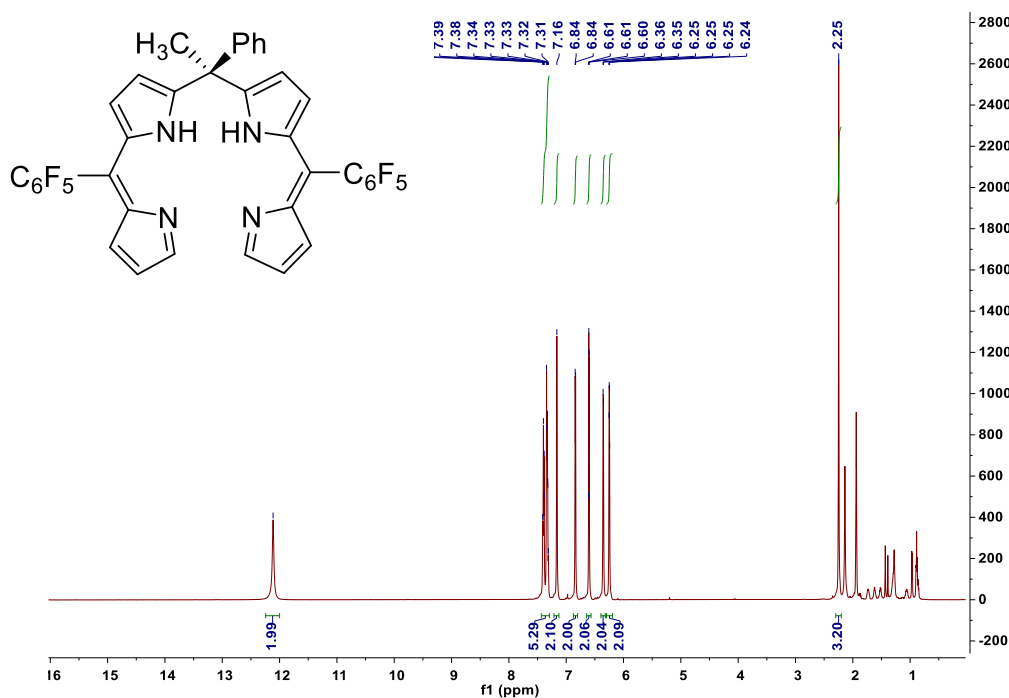


Figure 9 ^1H , ^{19}F and ^{13}C NMR of 5, 5-diphenyl-1,9-bis(pentafluorobenzoyl)dipyrromethene in CDCl_3

2.2.3 Synthesis of Biladiene Derivatives

10-Methyl-10-phenyl-5,15-bis(pentafluorophenyl)-biladiene. To a solution of 5-methyl-5-phenyl-1,9-bis(pentafluorobenzoyl)dipyrromethene (312 mg, 0.5 mmol) dissolved in 40 mL of THF and MeOH (3:1) was added 946 mg of NaBH_4 (25 mmol). The resulting mixture was stirred at room temperature for 2 h. The reaction was quenched with saturated NH_4Cl and extracted with CH_2Cl_2 . The organic layer was washed sequentially with water and brine and dried over Na_2SO_4 . Solvent was then removed via rotary evaporation and the resulting residue was dissolved in 200 mL of CH_2Cl_2 . To this solution was added InCl_3 (15 mg, 68 μmol) and pyrrole (100 μL , 1.44 mmol) and stirred at room temperature under air for 30 min. The solution turned into light pink. Then 180 mg of DDQ (0.8 mmol) was added to the stirred solution. After 5 min stirring, 14 mL of triethylamine (100 mmol) was added, and the mixture was

stirred for another 2 h. Following removal of the solvent under reduced pressure, the crude product was purified by flash chromatography on silica using a mixture of hexanes and CH₂Cl₂ (2:1) as the eluent to give 329 mg of the title compound as an orange solid (yield = 46%). ¹H NMR (600 MHz, CD₃CN, 25 °C) δ/ppm: 12.11 (s, 2H), 7.36 (m, 5H), 7.16 (s, 2H), 6.84 (d, J = 4.6 Hz, 2H), 6.60 (d, J = 4.4 Hz, 2H), 6.35 (d, J = 3.90 Hz, 2H), 6.25 (dd, J = 4.0, 2.3 Hz, 2H), 2.25 (s, 3H). ¹³C NMR (150 MHz, CD₃CN, 25 °C) δ/ppm: 177.62, 148.40, 146.29, 144.69, 143.20, 141.54, 139.30, 137.65, 133.47, 132.09, 131.32, 129.10, 128.26, 127.74, 126.70, 122.84, 121.22, 112.92, 111.66, 51.65, 24.82. ¹⁹F NMR (565 MHz, CD₃CN, 25 °C) δ/ppm: -142.08 (dd, J = 19.4, 8.5 Hz, 4F), -156.04 (t, J = 20.2 Hz, 2F), -163.51 (td, J = 20.5, 8.2 Hz, 4F). HR-ESI-MS [M + H]⁺ m/z: calcd for C₃₈H₂₁F₁₀N₄, 723.1607; found, 723.1594.



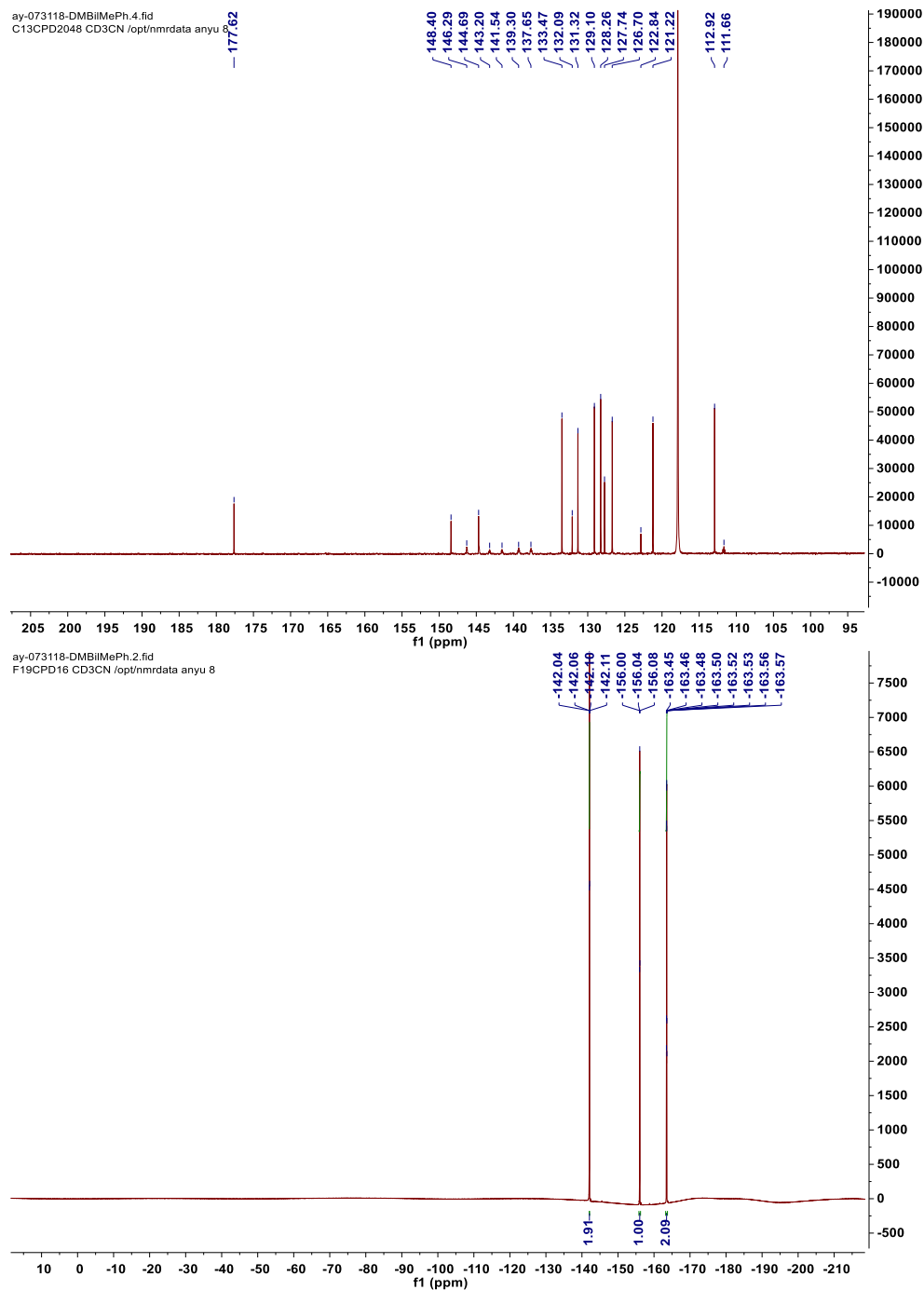
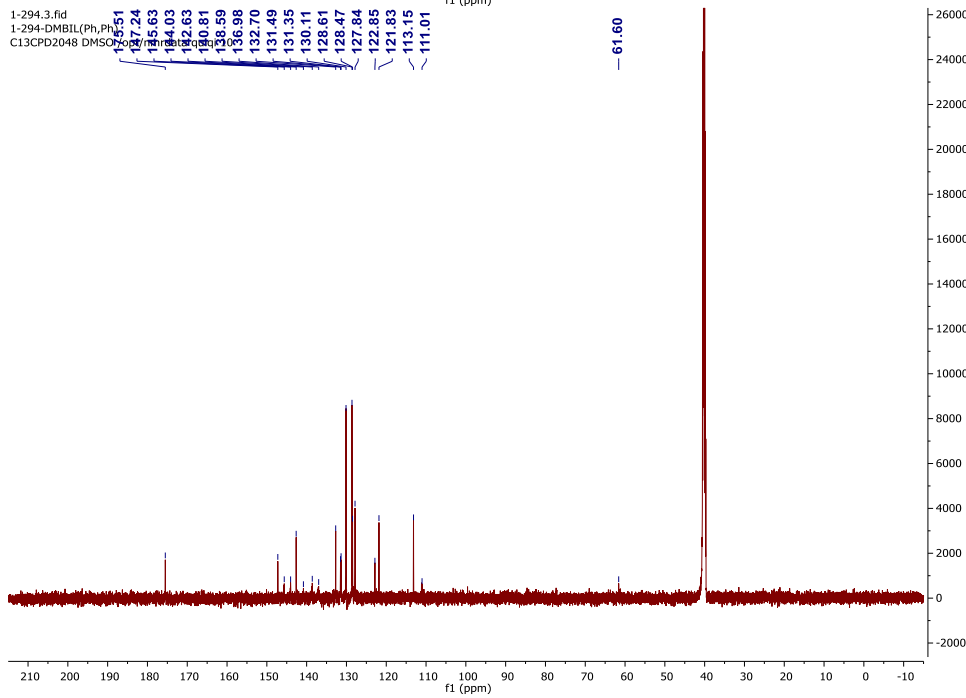
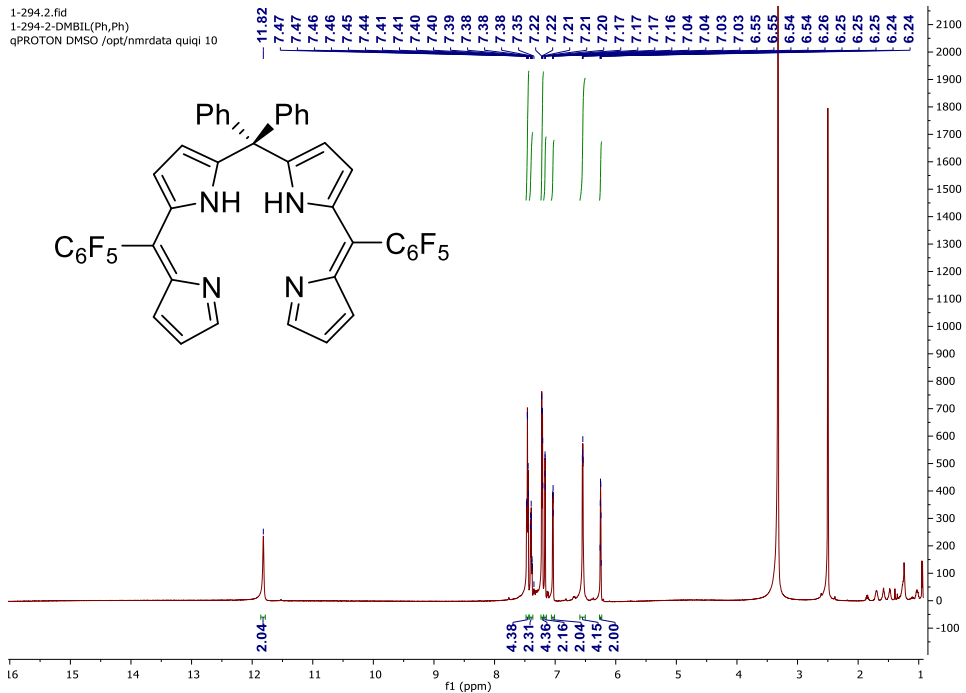


Figure 10 ^1H , ^{19}F and ^{13}C NMR of 10-methyl-10-phenyl-5,15-bis(pentafluorophenyl)-biladiene in CD_3CN .

10,10-diphenyl-5,15-bis(pentafluorophenyl)-biladiene. To a solution of 5,5-diphenyl-1,9-bis(pentafluorobenzoyl)dipyrrromethene (343 mg, 0.5 mmol) dissolved in

40 mL of THF and MeOH (3:1) was added 946 mg of NaBH₄ (25 mmol). The resulting mixture was stirred at room temperature for 2 h. The reaction was quenched with saturated NH₄Cl and extracted with CH₂Cl₂. The organic layer was washed sequentially with water and brine and dried over Na₂SO₄. Solvent was then removed via rotary evaporation and the resulting residue was dissolved in 200 mL of CH₂Cl₂. To this solution was added InCl₃ (15 mg, 68 μmol) and pyrrole (100 μL, 1.44 mmol) and stirred at room temperature under air for 30 min. The solution turned into light green/yellow. Then 180 mg of DDQ (0.8 mmol) was added to the stirred solution. After 5 min stirring, 14 mL of triethylamine (100 mmol) was added, and the mixture was stirred for another 2 h. Following removal of the solvent under reduced pressure, the crude product was purified by flash chromatography on silica using a mixture of hexanes and CH₂Cl₂ (2:1) as the eluent to give 283 mg of the title compound as an orange solid (yield = 36%). ¹H NMR (600 MHz, DMSO, 25 °C) δ/ppm: 11.82 (s, 2H), 7.46 (m, 4H), 7.40 (m, 2H), 7.21 (d, J = 6 Hz, 4H), 7.17 (s, 2H), 7.04 (d, J = 6.0 Hz, 2H), 6.55 (d, J = 6.0 Hz, 4H), 6.25 (m, 2H). ¹³C NMR (151 MHz, DMSO) δ/ppm: 175.51, 147.24, 144.03, 142.63, 132.70, 131.49, 131.35, 130.11, 128.61, 128.47, 127.84, 122.85, 121.83, 113.15, 40.54, 40.40, 40.26, 40.13, 39.99, 39.85, 39.71. ¹⁹F NMR (376 MHz, DMSO) δ/ppm: -140.81, -154.34, -161.94. HR-ESI-MS [M + H]⁺ m/z: calcd for C₄₃H₂₃F₁₀N₄, 785.1763; found, 785.1746.

1-294.2.fid
1-294-2-DMBIL(Ph,Ph)
qPROTON DMSO /opt/nmrdata quiqi 10



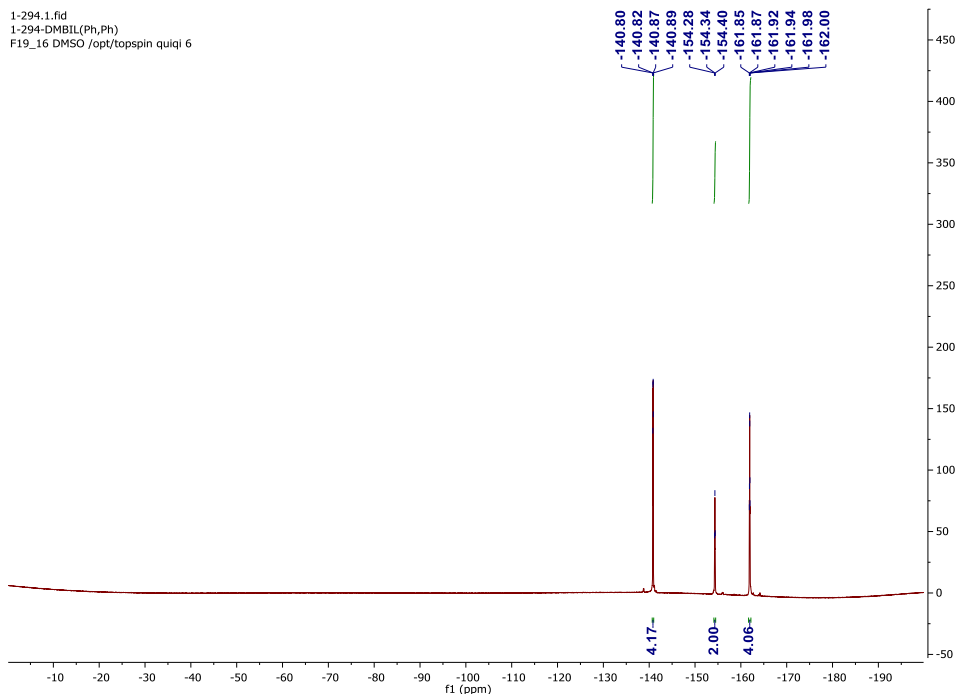
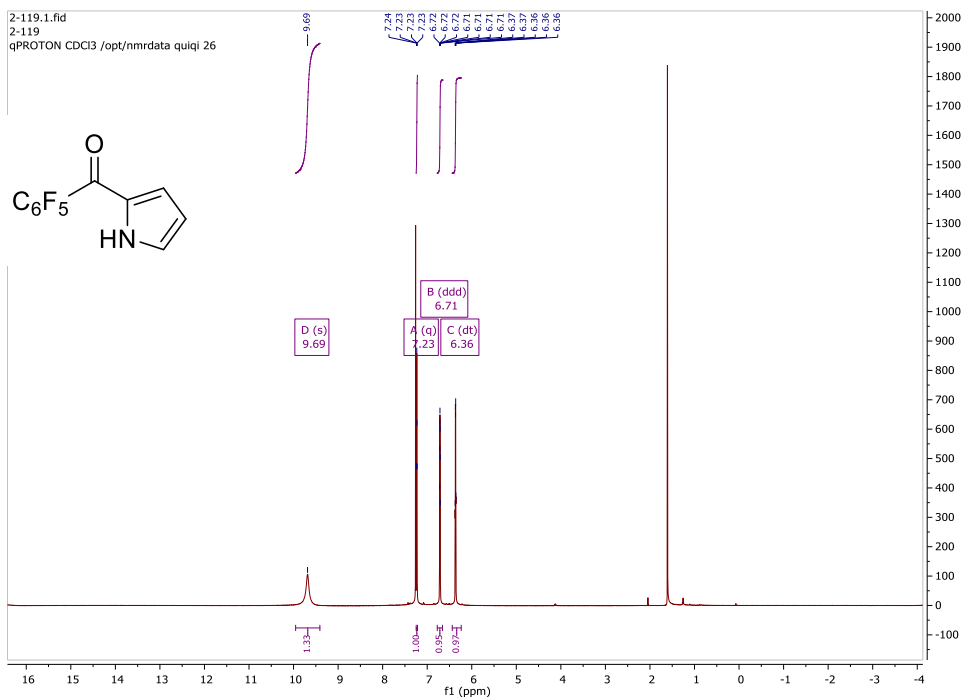


Figure 11 ^1H , ^{19}F and ^{13}C NMR of 10, 10-diphenyl-5,15-bis(pentafluorophenyl)-biladiene in deuterated DMSO.

2.3 Preparation of 5-Isocorrole Ligand Platform

2-Pentafluorobenzyl pyrrole. An oven baked Schlenk flask was charged with 200 mL dry toluene and 2 mL freshly distilled pyrrole under a positive atmosphere of N_2 . Ethyl magnesium bromide (35 mL, 1M in THF) was added dropwise to the flask over 10 min. The mixture was stirred at room temperature for 30 min. Cool the mixture to $0\text{ }^\circ\text{C}$, dropwise 2 mL pentafluorobenzyl chloride over 10 min. The mixture was stirred for 1 h, from $0\text{ }^\circ\text{C}$ to room temperature. The reaction was quenched with saturated NH_4Cl and the aqueous layer was extracted with ethyl acetate three times. The combined organic layer was washed with water and brine, and then dried over Na_2SO_4 . Following the removal of solvent via rotary evaporation, the crude product was recrystallized with CH_2Cl_2 /hexanes. 3.1 g white solid was filtered and washed with cold hexanes as desired product (42%). ^1H NMR (400 MHz, CDCl_3 , $25\text{ }^\circ\text{C}$)

δ /ppm: 9.94 (s, 1H), 7.27 – 7.22 (m, 1H), 6.72 (ddq, $J = 3.8, 2.5, 1.2$ Hz, 1H), 6.36 (dt, $J = 4.3, 2.4$ Hz, 1H). ^{19}F NMR (565 MHz, CDCl_3 , 25 °C) δ /ppm: –139.99 – –140.27 (m, 2H), –151.13 (t, $J = 20.6$ Hz, 1H), –160.05 – –160.39 (m, 2H). ^{13}C NMR (151 MHz, CDCl_3) δ /ppm: 172.58, 144.81, 144.78, 144.75, 144.73, 144.70, 143.09, 143.06, 143.03, 141.42, 138.53, 138.50, 138.42, 138.34, 138.30, 136.73, 136.62, 131.61, 128.30, 121.60, 114.16, 114.02, 112.17, 77.23, 77.02, 76.80.



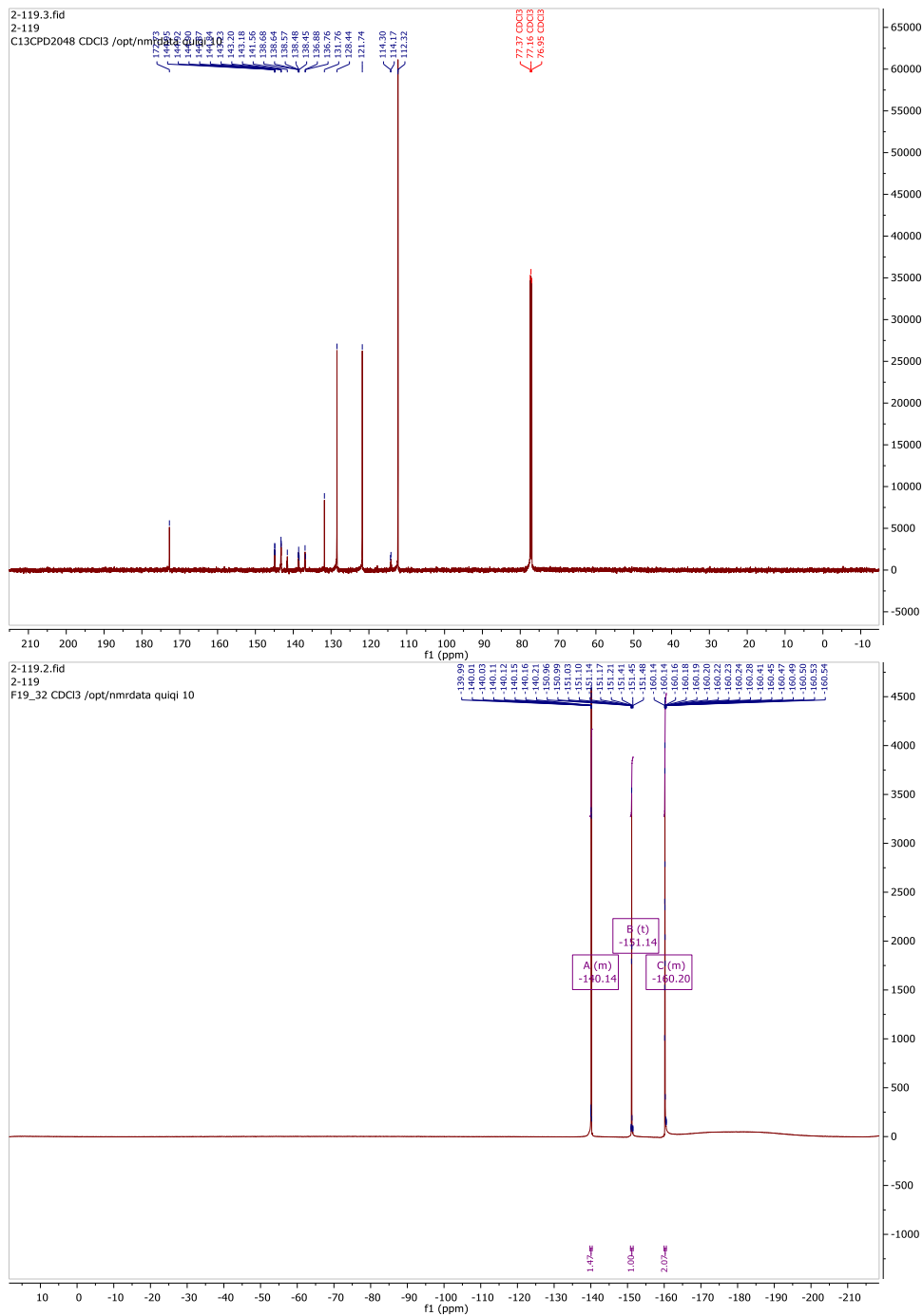
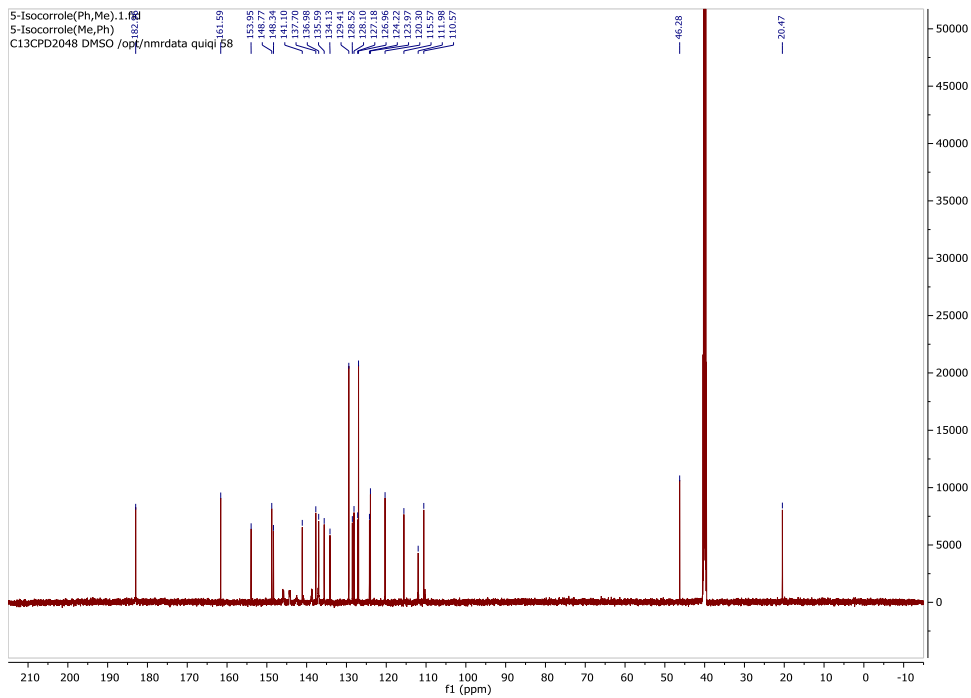
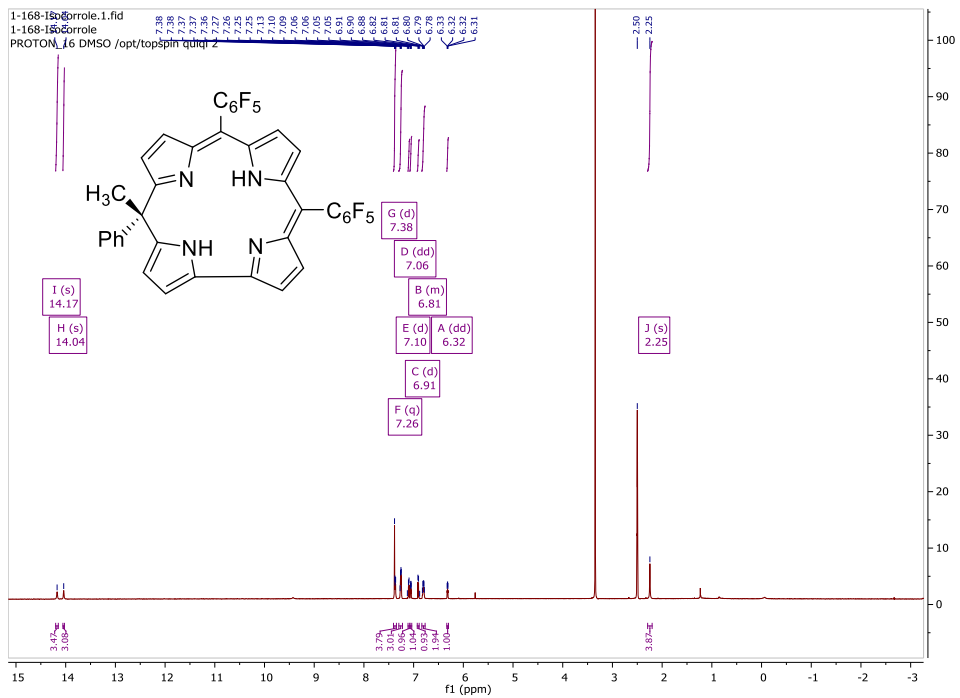


Figure 12 ^1H , ^{19}F and ^{13}C NMR of 2-pentafluorobenzyl pyrrole in CDCl_3 .

5-methyl-5-phenyl-10,15-bis(pentafluorophenyl)isocorrole 5-MPIC. 2-pentafluorobenzyl pyrrole (392 mg, 1.5 mmol) was dissolved in 40 mL MeOH/THF

(1:3) in a 200 mL round bottom flask, then NaBH₄ (946 mg, 25 mmol) was slowly added to the solution, the mixture was stirred at room temperature for 2 h. The reaction was quenched with saturated NH₄Cl and extracted with CH₂Cl₂. The organic layer was washed sequentially with water and brine and dried over Na₂SO₄. Solvent was then removed via rotary evaporation and the resulting residue was dissolved in 200 mL of CH₂Cl₂. InCl₃ (15 mg, 68 μmol) and 5-methyl-5-phenyldipyrromethane (118 mg, 0.5 mmol) were then added and stirred at room temperature under air overnight. The solution turned into dark red. Then 341 mg of DDQ (1.5 mmol) was added to the stirred solution. After 5 min stirring, 14 mL of triethylamine (100 mmol) was added, and the mixture was stirred for another 2 h. The solvent was removed under reduced pressure, and the crude was purified by column chromatography on silica using hexanes and CH₂Cl₂ (5:1) as eluent. Green eluent was collected for further purification. Usually it was combined with tetra-pentafluorophenylporphyrin as a by-product. A further purification was needed. ¹H NMR (400 MHz, DMSO-*d*₆) δ 14.17 (s, 1H), 14.04 (s, 1H), 7.38 (d, *J* = 6.5 Hz, 4H), 7.26 (q, *J* = 3.0 Hz, 3H), 7.10 (d, *J* = 4.7 Hz, 1H), 7.06 (dd, *J* = 3.8, 2.5 Hz, 1H), 6.91 (d, *J* = 4.7 Hz, 1H), 6.83 – 6.77 (m, 2H), 6.32 (dd, *J* = 3.8, 2.3 Hz, 1H), 2.25 (s, 3H). ¹³C NMR (151 MHz, DMSO) δ/ppm: 182.96, 161.59, 153.95, 148.77, 148.34, 141.10, 137.70, 136.98, 135.59, 134.13, 129.41, 128.52, 128.10, 127.18, 126.96, 124.22, 123.97, 120.30, 115.57, 111.98, 110.57, 46.28, 20.47. ¹⁹F NMR (565 MHz, DMSO-*d*₆, 25 °C) δ/ppm: -139.93 (ddd, *J* = 53.2, 25.5, 7.2 Hz), -141.27 (dd, *J* = 25.4, 6.9 Hz), -141.41 (dd, *J* = 25.3, 6.9 Hz), -154.16 (dt, *J* = 44.9, 22.3 Hz), -161.77 (td, *J* = 24.0, 7.1 Hz), -161.97 (td, *J* = 23.7, 23.1, 7.0 Hz). HR-ESI-MS [M + H]⁺ m/z: calcd for C₃₈H₁₉N₄F₁₀, 721.1450; found, 721.1431.



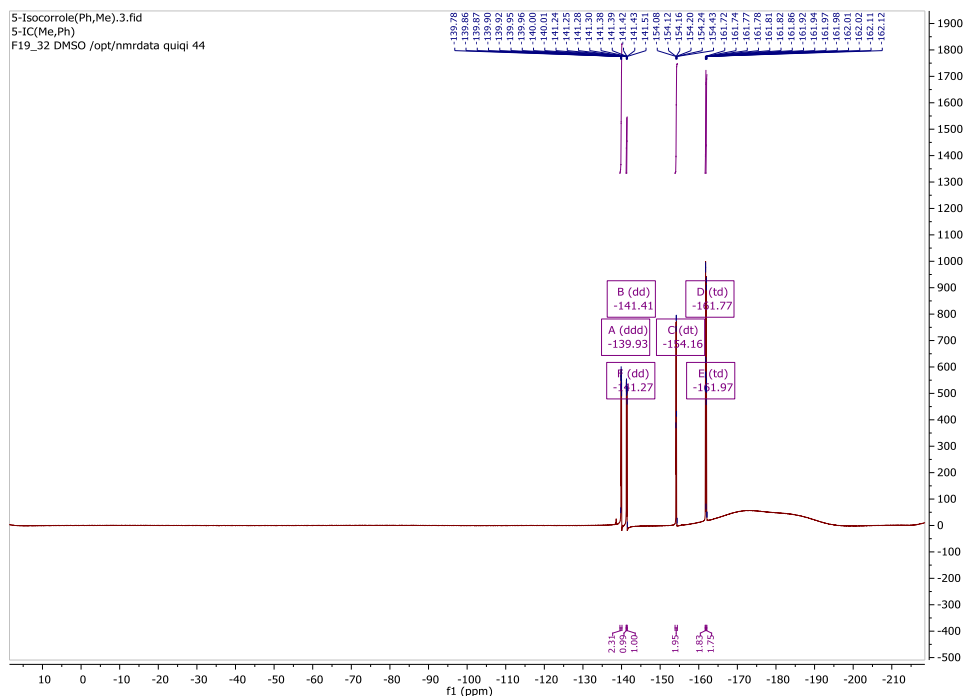
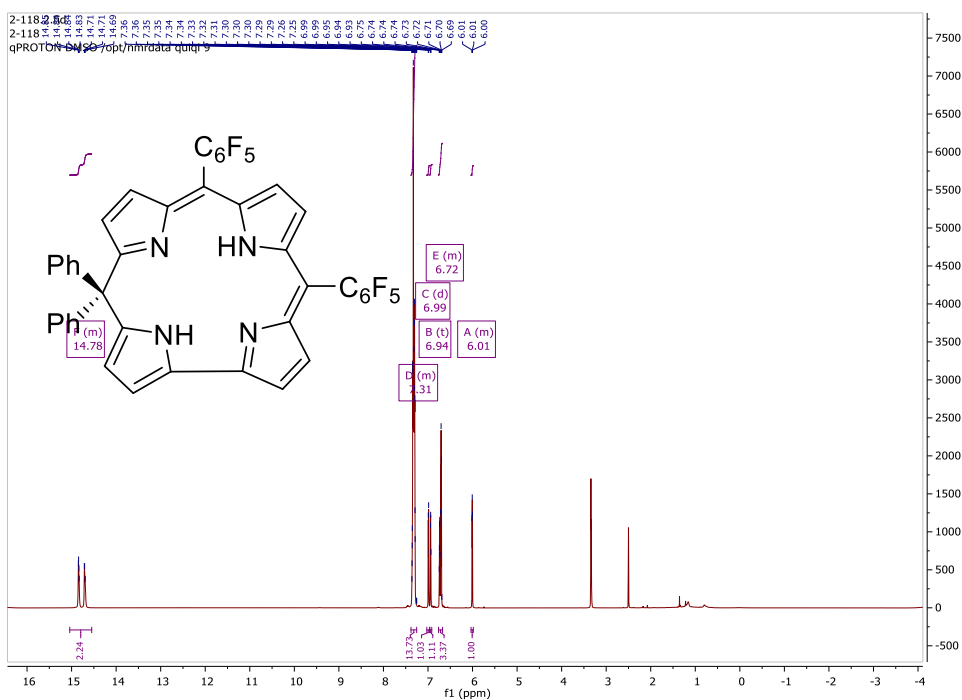


Figure 13 ^1H , ^{19}F and ^{13}C NMR of 5-methyl-5-phenyl-10,15-bis(pentafluorophenyl)isocorrole in deuterated DMSO.

5,5-diphenyl-10,15-bis(pentafluorophenyl)isocorrole 5-DPIC. 2-

pentafluorobenzyl pyrrole (392 mg, 1.5 mmol) was dissolved in 40 mL MeOH/THF (1:3) in a 200 mL round bottom flask, then NaBH_4 (946 mg, 25 mmol) was slowly added to the solution, the mixture was stirred at room temperature for 2 h. The reaction was quenched with saturated NH_4Cl and extracted with CH_2Cl_2 . The organic layer was washed sequentially with water and brine and dried over Na_2SO_4 . Solvent was then removed via rotary evaporation and the resulting residue was dissolved in 200 mL of CH_2Cl_2 . InCl_3 (15 mg, 68 μmol) and 5, 5-diphenyldipyrromethane (149 mg, 0.5 mmol) were then added and stirred at room temperature under air overnight. The solution turned into dark red. Then 341 mg of DDQ (1.5 mmol) was added to the stirred solution. After 5 min stirring, 14 mL of triethylamine (100 mmol) was added, and the mixture was stirred for another 2 h. The solvent was removed under reduced pressure, and the crude was purified by column chromatography on silica using

hexanes and CH_2Cl_2 (5:1) as eluent. Green eluent was collected for further purification. Usually it was combined with tetra-pentafluorophenylporphyrin as a by-product. A further purification was needed. ^1H NMR (600 MHz, $\text{DMSO-}d_6$, 25 °C) δ /ppm: 14.84 (s, 1H), 14.70 (s, 1H), 7.38 – 7.26 (m, 12H), 6.99 (d, $J = 4.7$ Hz, 1H), 6.96 – 6.92 (m, 1H), 6.74 (dd, $J = 4.4, 2.3$ Hz, 1H), 6.73 – 6.69 (m, 2H), 6.02 – 5.98 (m, 1H). ^{13}C NMR (151 MHz, $\text{DMSO-}d_6$, 25 °C) δ /ppm: 182.59, 161.83, 154.23, 149.11, 149.09, 148.16, 145.75, 144.14, 142.72, 142.63, 142.51, 141.66, 141.05, 140.84, 138.76, 138.67, 137.22, 137.12, 136.99, 134.75, 134.42, 129.79, 129.19, 129.16, 128.81, 128.67, 127.15, 124.53, 124.46, 121.13, 120.46, 114.84, 112.60, 112.03, 111.90, 111.77, 110.22, 110.10, 110.08, 109.96, 57.57, 40.44, 40.30, 40.16, 40.02, 39.88, 39.74, 39.60, 30.84, 29.42. ^{19}F NMR (565 MHz, $\text{DMSO-}d_6$, 25 °C) δ /ppm: -139.86 (t, $J = 18.0$ Hz), -140.95 – -141.37 (m), -153.88 – -154.36 (m), -161.65 – -161.85 (m), -161.84 – -162.10 (m). HR-ESI-MS $[\text{M} + \text{H}]^+$ m/z : calcd for $\text{C}_{43}\text{H}_{21}\text{N}_4\text{F}_{10}$, 783.1607; found, 783.1581.



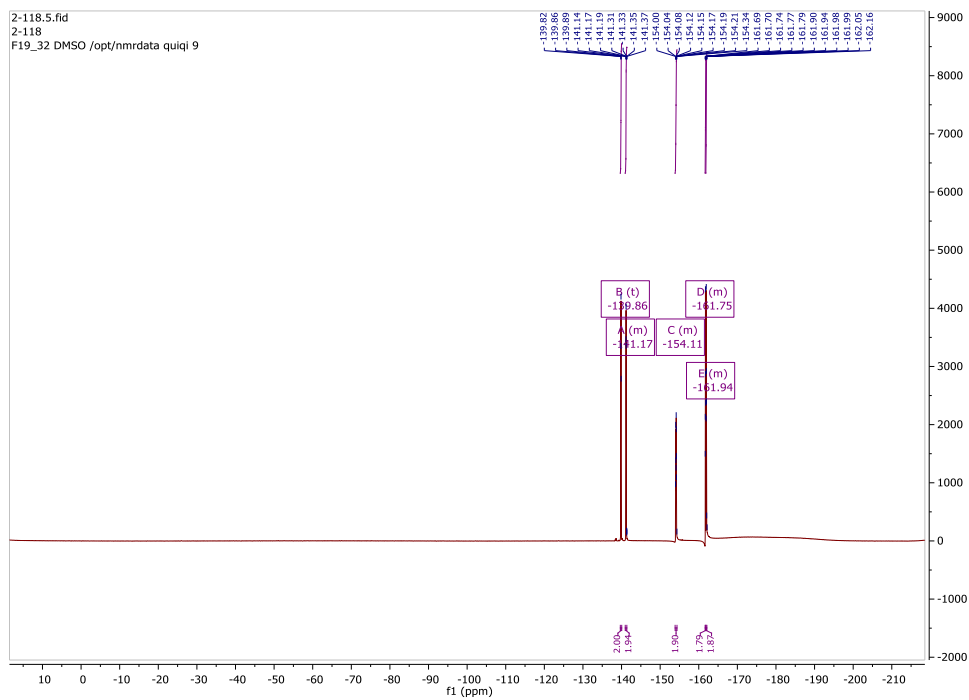
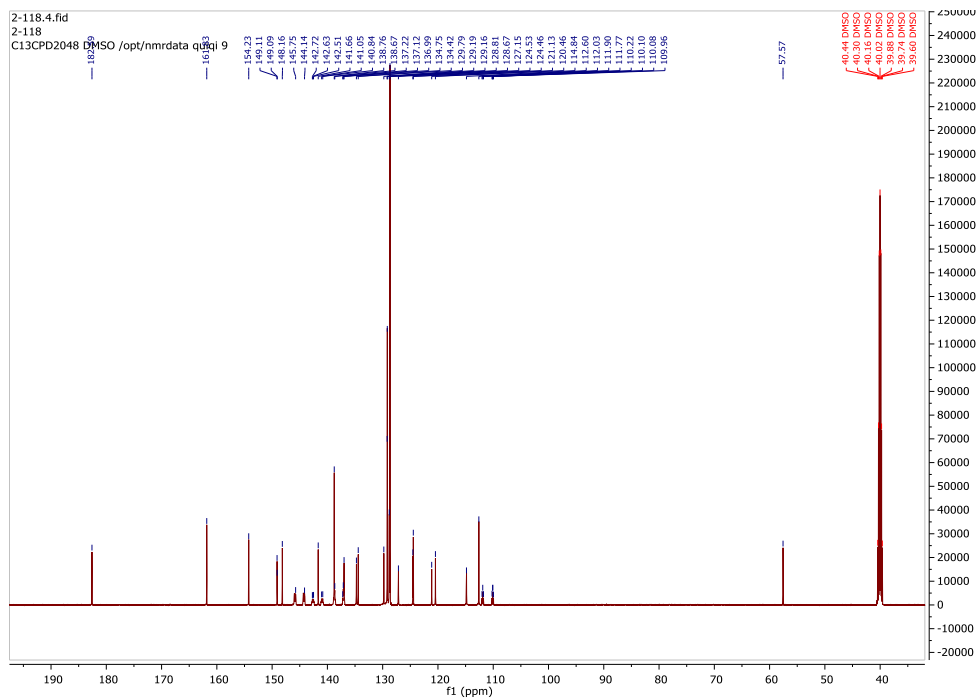


Figure 14 ^1H , ^{19}F and ^{13}C NMR of 5,5-dphenyl-10,15-bis(pentafluorophenyl)isocorrole in deuterated DMSO.

Further Purification: Dissolve the green solid and 1.5 g zinc acetate dihydrate in 50 mL acetonitrile in a 200 mL round bottom flask, then the mixture was stirred at 60 °C for 4 h. The solvent was removed under reduced pressure and the crude was purified by column chromatography on silica using hexanes and CH₂Cl₂ (20:1 to 5:1 gradually) as eluent. The green eluent was collected as the title product (31%).

2.4 Preparation of Co(10-Isocorrole) Complexes

Cobalt 10-Methyl-10-phenyl-5,15-bis(pentafluorophenyl)-isocorrole Co(10-MPIC).

Method 1: An oven baked Schlenk flask was charged with 10-Methyl-10-phenyl-5,15-bis(pentafluorophenyl)-biladiene (36 mg, 0.05 mmol), Co(OAc)₂ (18 mg) and 10 mL degassed acetonitrile in the glovebox. The mixture was stirred at 60 °C under positive N₂ atmosphere for 12 h outside of glove box. Immediately after solvent removal from the Schlenk manifold, the flask was pumped back into glovebox. The crude material was purified by column chromatography on neutral alumina using pentane and Et₂O (10:1 to 1:10 gradually) as the eluent to afford 8 mg of dark green solid (10%).

Method 2: In the glovebox, transfer 10-Methyl-10-phenyl-5,15-bis(pentafluorophenyl)-biladiene (36 mg, 0.05 mmol), Co(OAc)₂ (18 mg) and 10 mL degassed acetonitrile to a Schlenk flask. The mixture was stirred at 60 °C under positive N₂ atmosphere for 4 h outside of glove box. Then, the solvent was removed from the Schlenk manifold and the flask was pumped back into glovebox. The crude was dissolved by small amount of THF and went through a short celite bed. After removing THF, the crude and Co(OAc)₂ (18 mg) were redissolved in 10 mL

acetonitrile in a new Schlenk flask. The mixture was stirred at 60 °C under positive N₂ atmosphere for 12 h outside of glove box. The solvent was removed from the Schlenk manifold and the flask was pumped back into the glovebox. The crude was purified by flash chromatography on neutral alumina with diethyl ether as eluent to get dark green solid (75%). ¹H NMR (400 MHz, CDCl₃, 25 °C) δ/ppm: 29.48 (s, 2H), 27.58 (s, 3H), 24.97 (s, 2H), 16.55 (s, 2H), 11.68 (s, 1H), 11.50 (s, 2H), -1.98 (s, 2H), -13.93 (s, 2H). HR-LIFDI: M⁺ m/z: calcd for C₃₈H₁₆N₄F₁₀Co 777.0547; found, 777.0563.

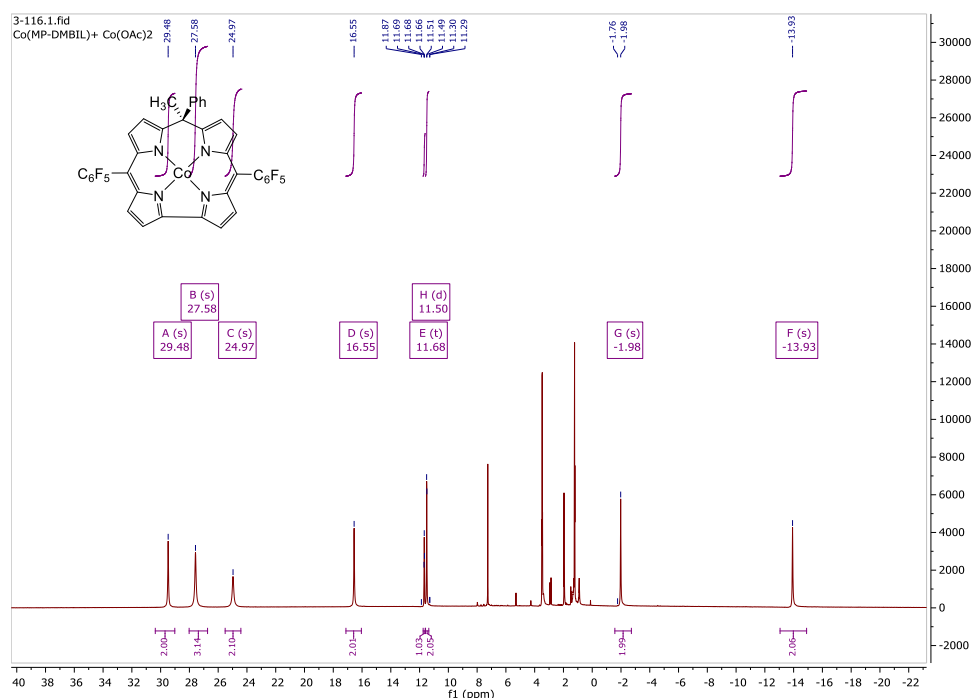


Figure 15 ¹H NMR of Co(10-MPIC) in CDCl₃.

Cobalt 10, 10-diphenyl-5,15-bis(pentafluorophenyl)-isocorrrole Co(10-DPIC).

Method 1: An oven baked Schlenk flask was charged with 10, 10-diphenyl-5,15-bis(pentafluorophenyl)-biladiene (39 mg, 0.05 mmol), Co(OAc)₂ (18 mg) and 10 mL degassed acetonitrile in the glovebox. The mixture was stirred at 60 °C under

positive N₂ atmosphere for 12 h outside of glove box. Immediately after solvent removal from the Schlenk manifold, the flask was pumped back into glovebox. The crude material was purified by column chromatography on neutral alumina using pentane and Et₂O (10:1 to 1:10 gradually) as the eluent to afford 8 mg of dark green solid (8%).

Method 2: In the glovebox, transfer 10, 10-diphenyl-5,15-bis(pentafluorophenyl)-biladiene (39 mg, 0.05 mmol), Co(OAc)₂ (18 mg) and 10 mL degassed acetonitrile to a Schlenk flask. The mixture was stirred at 60 °C under positive N₂ atmosphere for 4 h outside of glove box. Then, the solvent was removed from the Schlenk manifold and the flask was pumped back into glovebox. The crude was dissolved by small amount of THF and went through a short celite bed. After removing THF, the crude and Co(OAc)₂ (18 mg) were redissolved in 10 mL acetonitrile in a new Schlenk flask. The mixture was stirred at 60 °C under positive N₂ atmosphere for 12 h outside of glove box. The solvent was removed from the Schlenk manifold and the flask was pumped back into the glovebox. The crude was purified by flash chromatography on neutral alumina with diethyl ether as eluent to get dark green solid (50%). ¹H NMR (400 MHz, CDCl₃, 25 °C) δ 29.16 (s, 2H), 24.91 (s, 4H), 16.76 (s, 2H), 10.50 (s, 4H), 10.32 (s, 2H), -1.85 (s, 2H), -11.34 (s, 2H). HR-LIFDI: M⁺ m/z: calcd for C₄₃H₁₈N₄F₁₀Co 839.0704; found, 839.0738.

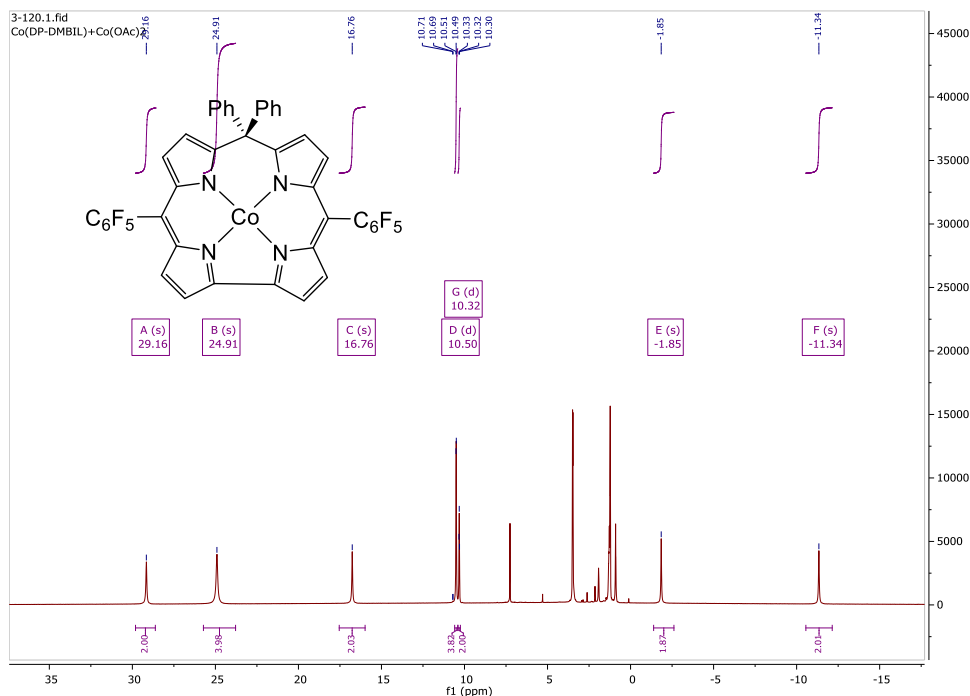


Figure 16 ¹H NMR of Co(10-MPIC) in CDCl₃.

2.5 Preparation of Co(5-Isocorrole) Complexes

In the glovebox, transfer 5,5-dimethyl-10,15-bis(pentafluorophenyl)isocorrole (33 mg, 0.05 mmol), or 5-methyl-5-phenyl-10,15-bis(pentafluorophenyl)isocorrole (36 mg, 0.05 mmol), or 5,5-diphenyl-10,15-bis(pentafluorophenyl)isocorrole (39 mg, 0.05 mmol), KOAc (70 mg, 0.7 mmol) and 15 mL acetonitrile in a 50 mL round bottom flask. The mixture was stirred at room temperature for 1 h. Then, Co(OAc)₂ (27 mg, 0.15 mmol) was added to the mixture. Then, the flask was sealed with septum, copper wire and electric tape and pumped out of the glovebox. The mixture was heated to 90 °C and stirred overnight. The solvent was removed directly by Schlenk manifold and the flask was pumped back into glovebox. The crude product was purified by column chromatography on neutral alumina using pentane and Et₂O (20:1 to 5:1 gradually) as the eluent to collect the second grass green band (35 % yield). The

first green band is the unreacted freebase. Second column chromatography could be performed if needed.

Cobalt 5,5-dimethyl-10,15-bis(pentafluorophenyl)isocorrole Co(5-DMIC):

^1H NMR (400 MHz, CDCl_3 , 25 °C) δ /ppm: 46.40 (s, 1H), 38.02 (s, 1H), 31.30 (s, 1H), 11.22 (s, 1H), -1.98 (s, 1H), -3.06 (s, 1H), -19.45 (s, 1H), -22.95 (s, 6H), -51.58 (s, 1H). HR-LIFDI: M^+ m/z : calcd for $\text{C}_{33}\text{H}_{14}\text{N}_4\text{F}_{10}\text{Co}$ 715.0391; found, 715.0419.

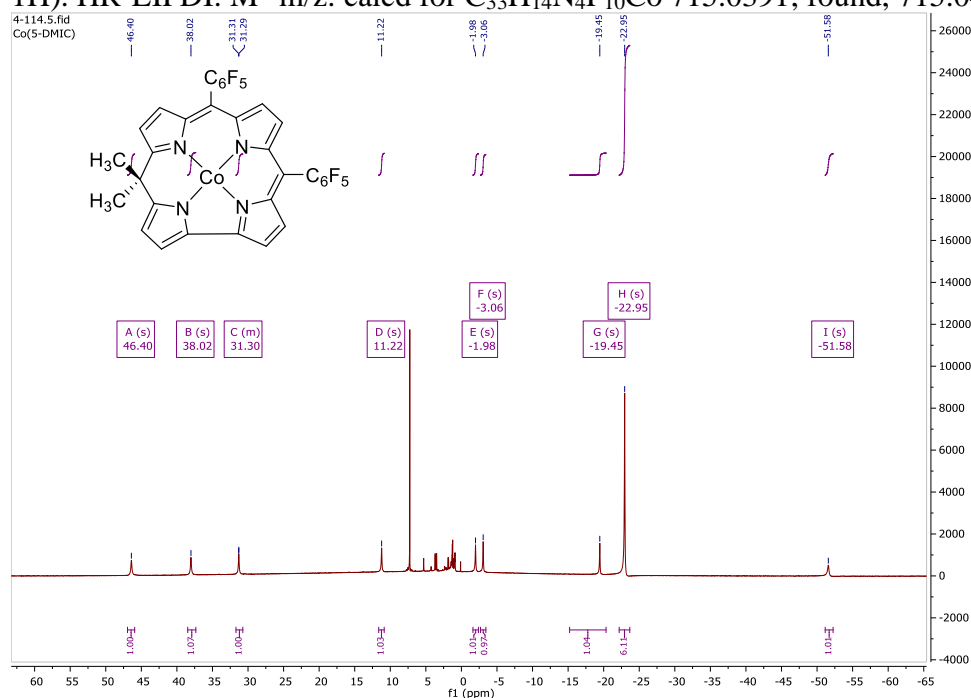


Figure 17 ^1H NMR of Co(5-DMIC) in CDCl_3 .

Cobalt 5-methyl-5-phenyl-10,15-bis(pentafluorophenyl)isocorrole Co(5-MPIC):

^1H NMR (400 MHz, CDCl_3 , 25 °C) δ /ppm: 46.21 (s, 1H), 37.69 (s, 1H), 30.72 (s, 1H), 10.36 (s, 1H), 1.76 (s, 1H), -1.55 (s, 3H), -3.32 (s, 1H), -19.82 (s, 1H), -23.70 (s, 2H), -24.18 (s, 3H), -53.84 (s, 1H). HR-LIFDI: M^+ m/z : calcd for $\text{C}_{38}\text{H}_{16}\text{N}_4\text{F}_{10}\text{Co}$ 777.0547; found, 777.0569.

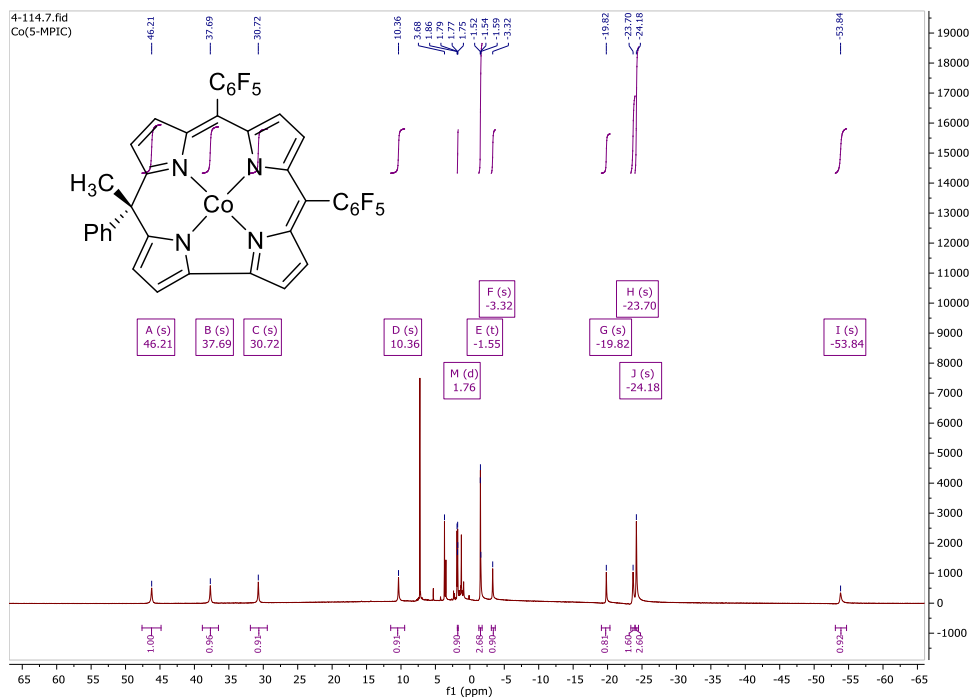


Figure 18 ^1H NMR of Co(5-MPIC) in CDCl_3 .

Cobalt 5,5-diphenyl-10,15-bis(pentafluorophenyl)isocorrole Co(5-DPIC): ^1H

NMR (400 MHz, CDCl_3 , 25 °C) δ /ppm: 46.34 (s, 1H), 37.16 (s, 1H), 31.55 (s, 1H), 11.61 (s, 1H), 3.67 (s, 2H), 1.85 (s, 1H), 0.21 (s, 1H), -0.97 (s, 4H), -2.88 (s, 1H), -14.16 (s, 4H), -19.35 (s, 1H), -50.94 (s, 1H). HR-LIFDI: M^+ m/z : calcd for $\text{C}_{43}\text{H}_{18}\text{N}_4\text{F}_{10}\text{Co}$ 839.0704; found, 839.0786.

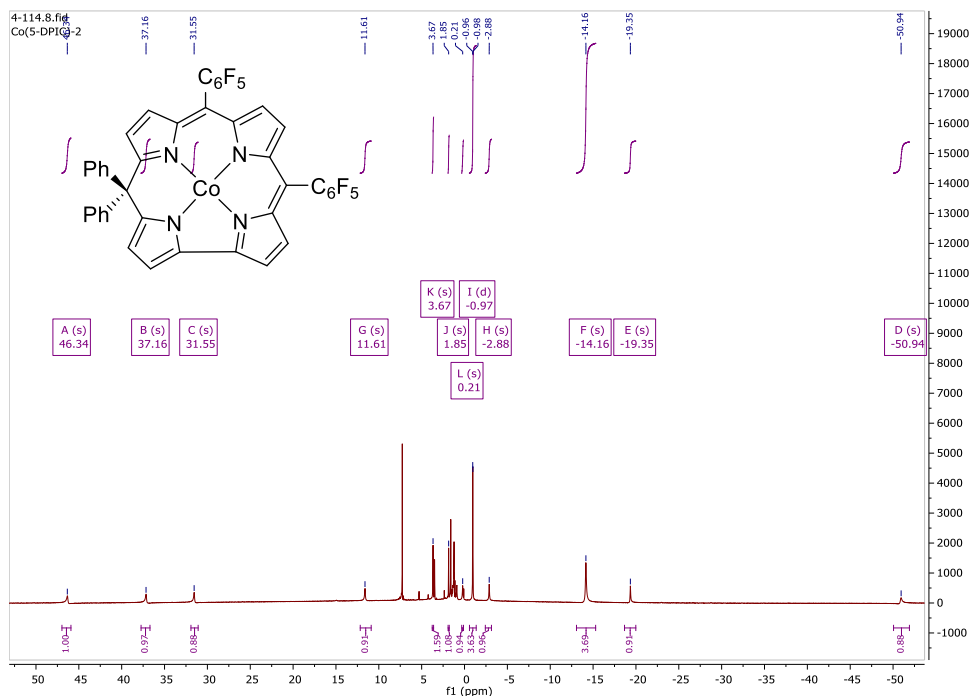


Figure 19 ^1H NMR of Co(5-DPIC) in CDCl_3

2.6 Cobalt porphyrin and Cobalt corrole Complexes

Both cobalt complexes were synthesized according to the reported method.

Cobalt 5,10,15,20-Tetrakis(pentafluorophenyl)porphyrin⁶⁰. In a 200 mL round bottom flask, 5,10,15,20-Tetrakis(pentafluorophenyl)porphyrin (0.97 g, 1 mmol) and cobalt acetate tetrahydrate (0.5 g, 2 mmol) was dissolved in 100 mL DMF. The mixture was stirred at 130 °C for 4.5 h. After cooling to room temperature, 100 mL diethyl ether was added. The mixture was washed with water three times and dry over MgSO_4 . The crude was purified by column chromatography on silica using hexanes and CH_2Cl_2 (20:1 to 5:1 gradually) as eluent to afford the target product as red solid (82%)

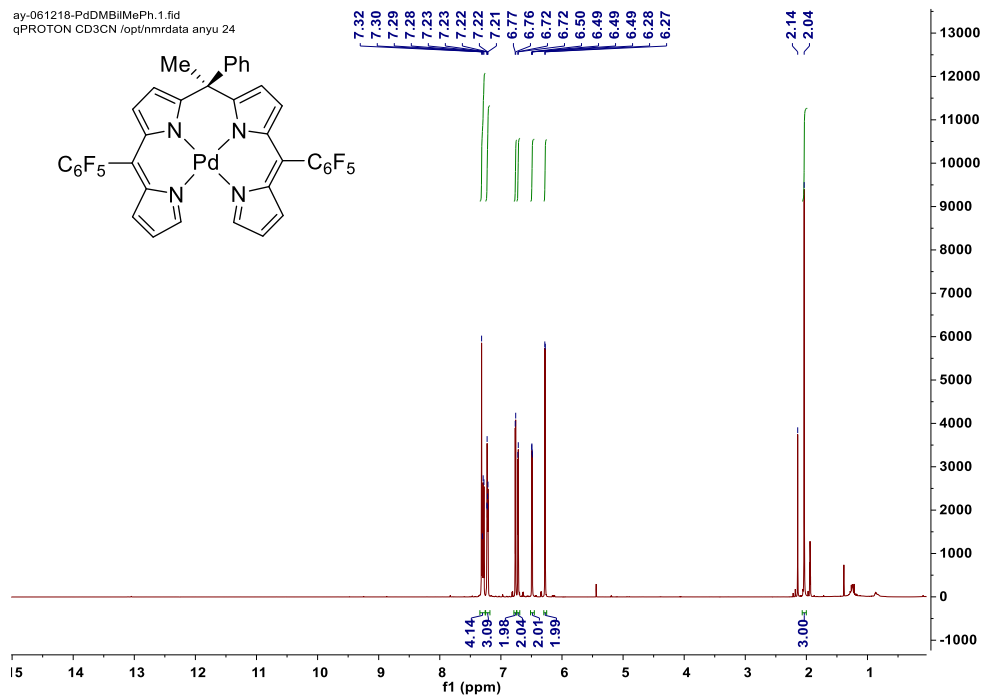
Cobalt 5,10,15-Tris(pentafluorophenyl)corrole triphenylphosphine^{61,62}. A 50 mL round bottom flask was charged with 5,10,15-Tris(pentafluorophenyl)corrole (40 mg, 0.05 mmol), NaOAc (60 mg, 0.72 mmol), cobalt acetate tetrahydrate (60 mg, 0.24 mmol),

triphenylphosphine (100 mg, 0.4 mmol) and 10 mL MeOH. The mixture was stirred at room temperature for 1.5 h. After removing the solvent under vacuo, the crude was purified by column chromatography on silica using hexanes and CH₂Cl₂ (5:1) to afford the red powder as the target product (96%) ¹H NMR (600 MHz, CDCl₃, 25 °C) δ/ppm: 8.70 (d, *J* = 4.4 Hz, 2H), 8.35 (dd, *J* = 4.7, 1.5 Hz, 2H), 8.25 (d, *J* = 4.7 Hz, 2H), 8.10 (d, *J* = 4.4 Hz, 2H), 7.02 (td, *J* = 7.7, 2.6 Hz, 3H), 6.66 (td, *J* = 7.8, 2.6 Hz, 6H), 4.62 – 4.57 (m, 6H). ¹⁹F NMR (565 MHz, CDCl₃, 25 °C) δ/ppm: –136.77 (dd, *J* = 24.2, 8.3 Hz, 2F), –137.09 (dd, *J* = 24.4, 8.2 Hz, 1F), –138.08 (dd, *J* = 24.8, 8.1 Hz, 2F), –138.42 (dd, *J* = 24.6, 8.1 Hz, 1F), –153.74 (td, *J* = 20.7, 9.4 Hz, 3F), –161.82 (td, *J* = 22.5, 7.8 Hz, 3F), –162.24 (td, *J* = 22.8, 8.2 Hz, 1F), –162.43 (td, *J* = 22.6, 8.2 Hz, 2F). ¹³C NMR (151 MHz, CDCl₃, 25 °C) δ/ppm: 146.04, 145.74, 145.55, 144.11, 143.90, 143.59, 142.29, 140.53, 138.46, 136.79, 135.84, 131.34, 131.28, 129.82, 129.80, 128.36, 127.11, 127.04, 124.79, 123.94, 122.58, 122.26, 121.36, 115.58, 105.72, 104.59, 77.22, 77.01, 76.80, 29.71.

2.7 Preparation of Palladium Biladiene Complexes

Palladium 10-Methyl-10-phenyl-5,15-bis(pentafluorophenyl)-biladiene Pd[MPBi]. To a solution of 10-methyl-10-phenyl-5,15-bis(pentafluorophenyl)-biladiene (100 mg) dissolved in 50 mL of acetonitrile was added Pd(OAc)₂. The reaction was stirred at 60 °C for 4 h. After cooling to room temperature, the solvent was removed under reduced pressure. The desired product was purified by flash chromatography on silica using a mixture of pentane and toluene (2:1) as the eluent to give of the title compound as a bright red solid. ¹H NMR (600 MHz, CD₃CN, 25 °C) δ/ppm: 7.30 (m, 4H), 7.22 (m, 3H), 6.76 (d, *J* = 4.2 Hz, 2H), 6.72 (d, *J* = 4.2 Hz, 2H), 6.49 (dd, *J* = 4.2, 1.2 Hz, 2H), 6.28 (d, *J* = 4.2 Hz, 2H), 2.03 (s, 3H). ¹³C NMR (150 MHz, CD₃CN, 25 °C) δ/ppm: 166.70, 153.15, 146.84, 146.60, 144.97, 143.70, 142.03,

139.59, 137.93, 135.25, 135.17, 132.33, 129.87, 129.67, 129.44, 128.24, 127.88,
 120.43, 119.67, 51.61, 29.49. ^{19}F NMR (565 MHz, CD_3CN , 25 °C) δ/ppm : -142.16
 (dd, $J = 19.4, 8.5$ Hz, 4F), -155.66 (t, $J = 20.0$ Hz, 2F), -163.32 (td, $J = 21.3, 10.5$ Hz,
 4F). HR-ESI-MS $[\text{M} + \text{H}]^+$ m/z : calcd for $\text{C}_{38}\text{H}_{19}\text{F}_{10}\text{N}_4\text{Pd}$, 827.0485; found, 827.0488.



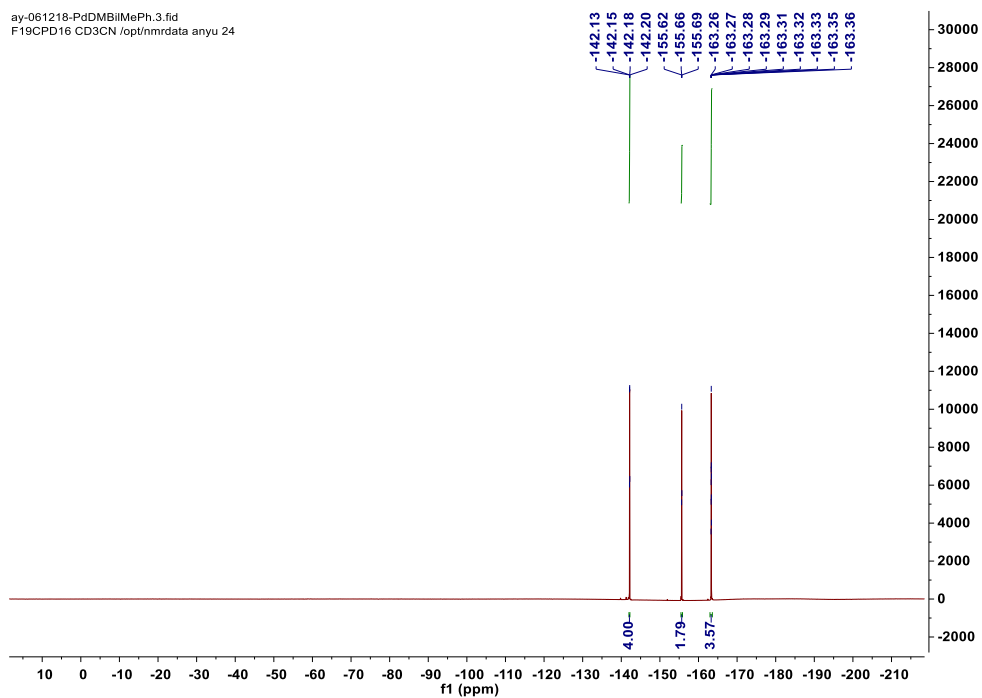
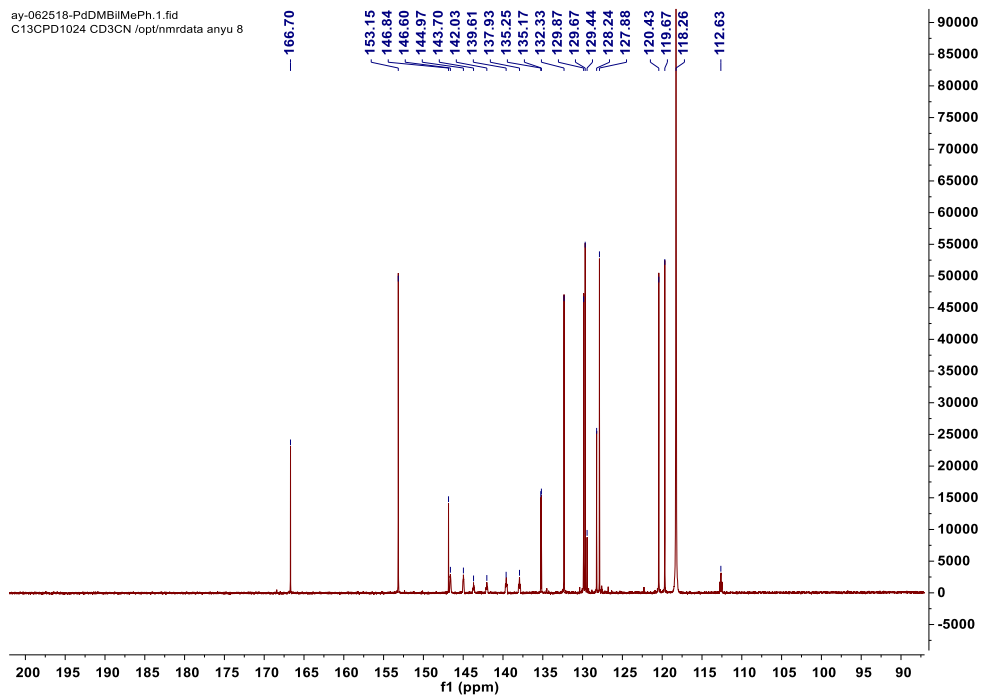
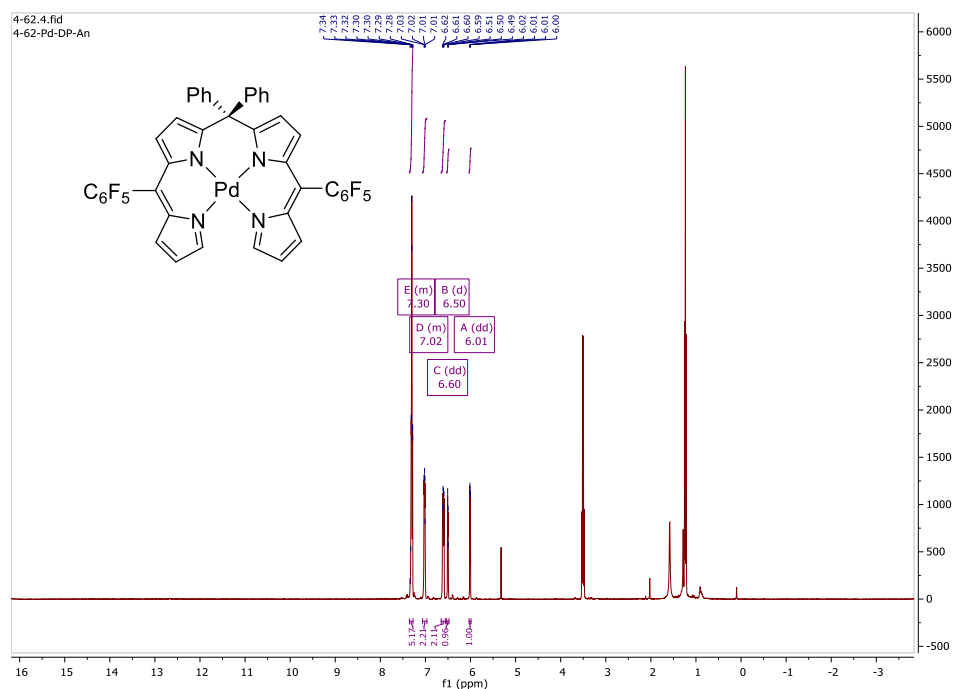


Figure 20 ^1H , ^{19}F and ^{13}C NMR of palladium 10-methyl-10-phenyl-5,15-bis(pentafluorophenyl)-biladiene, Pd[MPBi] in CD_3CN .

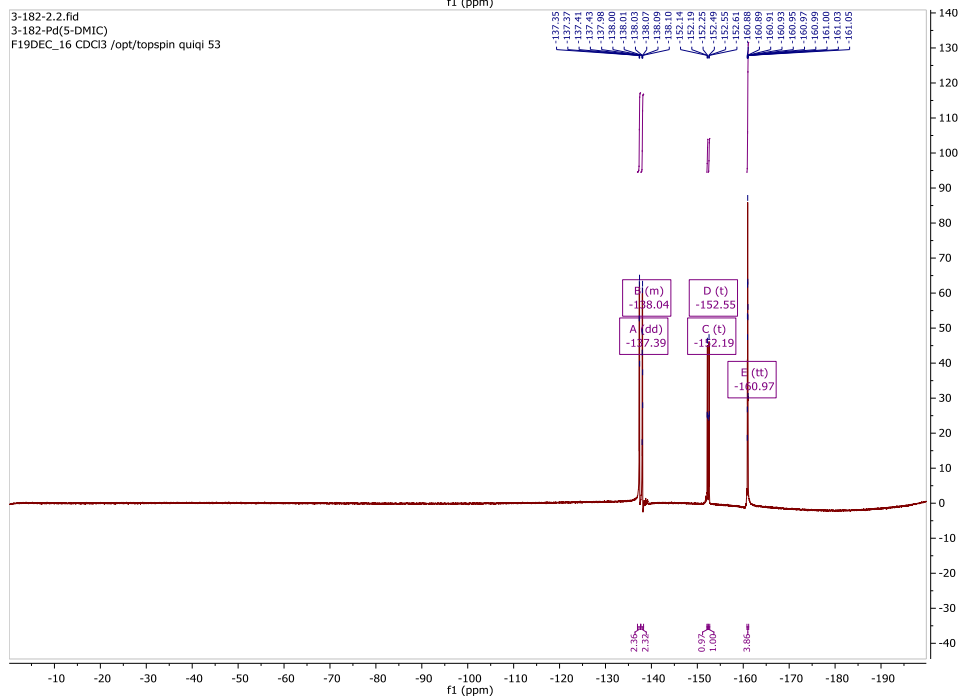
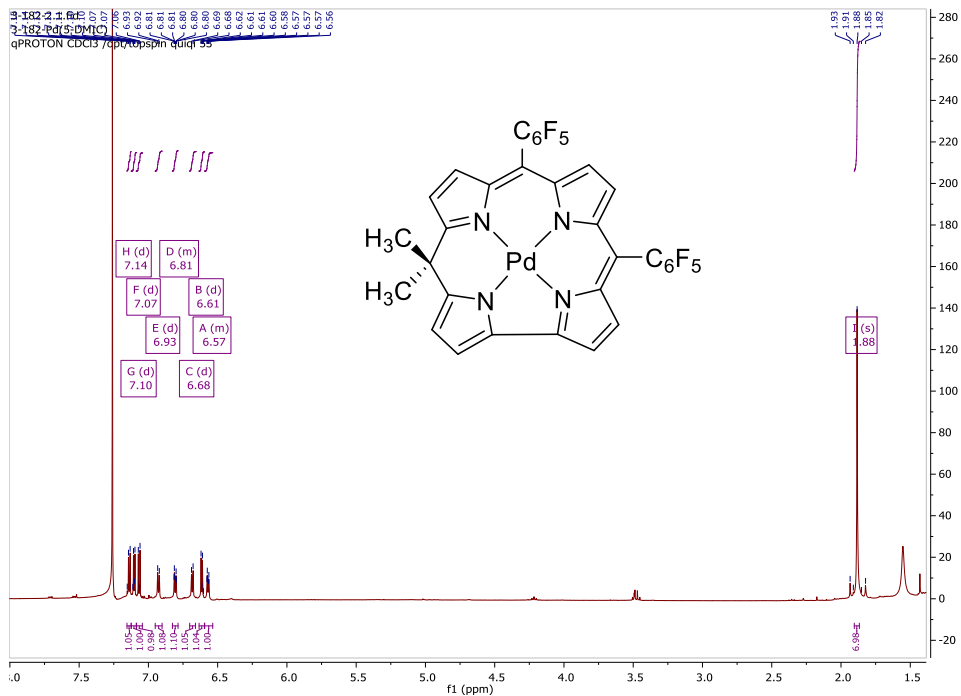
Palladium 10,10-diphenyl-5,15-bis(pentafluorophenyl)-biladiene Pd[DPBi]. To a solution of 10,10-diphenyl-5,15-bis(pentafluorophenyl)-biladiene (100 mg) dissolved in 50 mL of acetonitrile was added Pd(OAc)₂. The reaction was stirred at 60 °C for 4 h. After cooling to room temperature, the solvent was removed under reduced pressure. The desired product was purified by flash chromatography on silica using a mixture of pentane and toluene (2:1) as the eluent to give of the title compound as a bright red solid. ¹H NMR (600 MHz, CD₃CN, 25 °C) δ /ppm: 7.30 (m, 4H), 7.22 (m, 3H), 6.76 (d, J = 4.2 Hz, 2H), 6.72 (d, J = 4.2 Hz, 2H), 6.49 (dd, J = 4.2, 1.2 Hz, 2H), 6.28 (d, J = 4.2 Hz, 2H), 2.03 (s, 3H). ¹³C NMR (151 MHz, CD₃CN) δ 165.40, 154.39, 145.87, 135.67, 135.42, 131.30, 130.90, 130.24, 129.32, 128.59, 122.82, 120.16. ¹⁹F NMR (565 MHz, CD₃CN, 25 °C) δ /ppm: -142.03 – -142.42 (m, 2F), -155.57 (t, J = 20.2 Hz, 1F), -163.31 (td, J = 22.5, 8.2 Hz, 2F). HR-ESI-MS [M + H]⁺ m/z: calcd for C₄₃H₂₀F₁₀N₄Pd, 889.0641; found, 889.0652.



2.8 Synthesis of Palladium 5,5-disubstituted Isocorrolole

Transfer 5,5-dimethyl-10,15-bis(pentafluorophenyl)isocorrolole (33 mg, 0.05 mmol), or 5-methyl-5-phenyl-10,15-bis(pentafluorophenyl)isocorrolole (36 mg, 0.05 mmol), or 5,5-diphenyl-10,15-bis(pentafluorophenyl)isocorrolole (39 mg, 0.05 mmol), KOAc (70 mg, 0.7 mmol) and 15 mL acetonitrile in a 50 mL round bottom flask. The mixture was stirred at room temperature for 1 h. Then, Pd(OAc)₂ (35 mg, 0.15 mmol) was added to the mixture. The mixture was heated to reflux with a condenser and stirred overnight. The solvent was removed directly by rotary evaporation. The crude product was purified by column chromatography on silica using hexanes and diethyl ether (50:1 to 10:1 gradually) as eluent to collect the second grass green band (35 % yield). The first green band is the unreacted freebase. Second column chromatography could be performed if needed.

Pd(5-DMIC): ¹H NMR (400 MHz, CDCl₃, 25 °C) δ/ppm: 7.14 (d, *J* = 4.7 Hz, 1H), 7.10 (d, *J* = 4.1 Hz, 1H), 7.07 (d, *J* = 5.0 Hz, 1H), 6.93 (d, *J* = 4.7 Hz, 1H), 6.83 – 6.79 (m, 1H), 6.68 (d, *J* = 4.5 Hz, 1H), 6.61 (d, *J* = 4.1 Hz, 1H), 6.59 – 6.54 (m, 1H), 1.88 (s, 6H). ¹⁹F NMR (376 MHz, CDCl₃, 25 °C) δ/ppm: –137.39 (dd, *J* = 23.5, 8.1 Hz, 2F), –137.74 – –138.29 (m, 2F), –152.19 (t, *J* = 20.9 Hz, 1F), –152.55 (t, *J* = 21.0 Hz, 1F), –160.97 (tt, *J* = 23.2, 7.6 Hz, 4F). ¹³C NMR (101 MHz, CDCl₃, 25 °C) δ/ppm 167.73, 161.68, 158.13, 145.58, 141.50, 138.34, 135.60, 134.52, 134.17, 129.24, 126.92, 124.58, 124.19, 122.53, 113.56, 77.35, 77.03, 76.72, 44.47, 31.95. HR-ESI-MS [M + H]⁺ m/z: calcd for C₃₃H₁₅N₄F₁₀Pd, 763.0172; found, 763.0163.



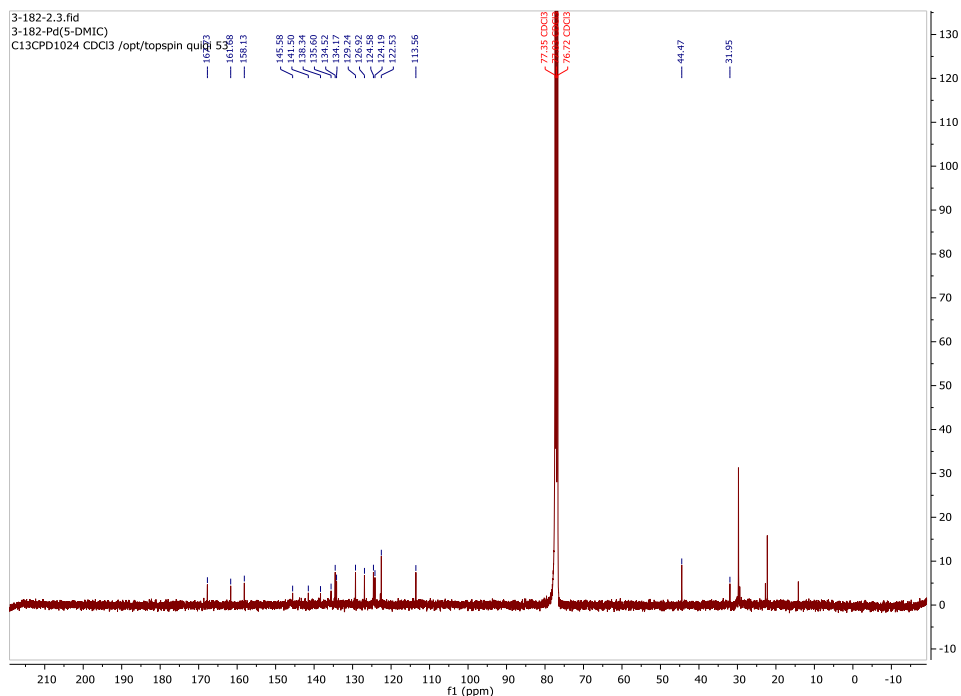
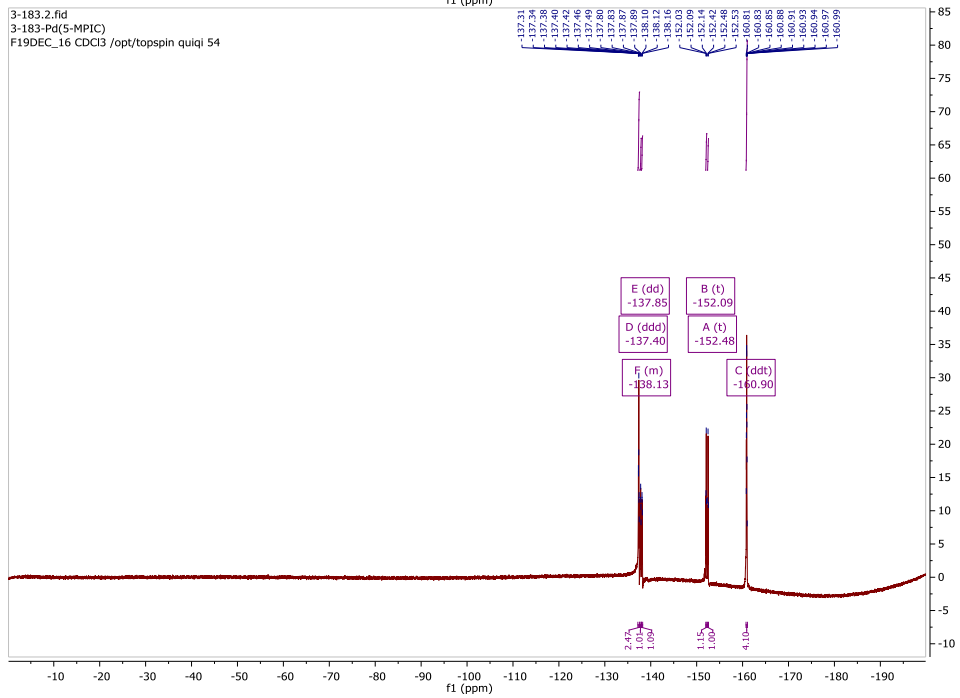
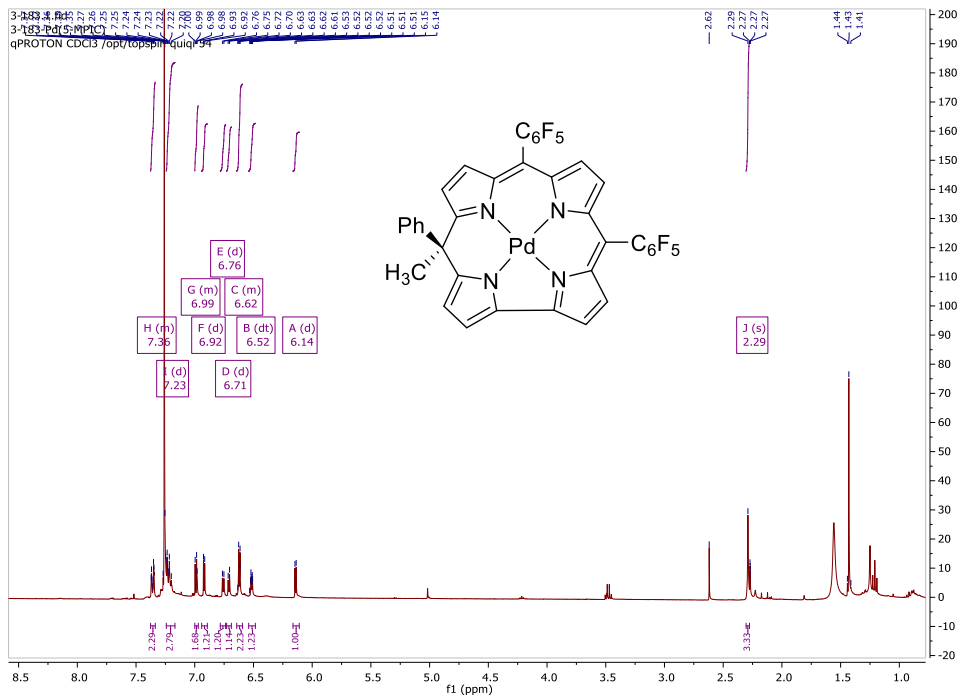


Figure 22 ^1H , ^{19}F and ^{13}C NMR of Pd(5-DMIC) in CDCl_3

Pd(5-MPIC): ^1H NMR (400 MHz, CDCl_3 , 25 °C) δ /ppm: 7.38 – 7.34 (m, 2H), 7.23 (m, 2H), 7.00 – 6.97 (m, 2H), 6.92 (d, $J = 4.1$ Hz, 1H), 6.76 (d, $J = 5.0$ Hz, 1H), 6.71 (d, $J = 4.7$ Hz, 1H), 6.64 – 6.59 (m, 2H), 6.52 (dt, $J = 4.5, 1.0$ Hz, 1H), 6.14 (d, $J = 4.2$ Hz, 1H), 2.29 (s, 3H). ^{19}F NMR (376 MHz, CDCl_3 , 25 °C) δ /ppm: –137.40 (ddd, $J = 31.4, 24.3, 9.1$ Hz, 2F), –137.85 (dd, $J = 23.9, 7.7$ Hz, 1F), –137.97 – –138.24 (m, 1F), –152.09 (t, $J = 21.2$ Hz, 1F), –152.48 (t, $J = 21.0$ Hz, 1F), –160.90 (ddt, $J = 32.2, 19.3, 8.3$ Hz, 4F). ^{13}C NMR (151 MHz, CDCl_3) δ 167.32, 162.17, 158.05, 145.96, 141.90, 138.76, 136.03, 134.75, 134.56, 133.39, 129.39, 129.28, 128.28, 127.08, 126.41, 124.76, 124.31, 124.21, 122.92, 52.28, 30.48. (C-F splitting peaks are not presented). HR-ESI-MS $[\text{M} + \text{H}]^+$ m/z : calcd for $\text{C}_{38}\text{H}_{17}\text{N}_4\text{F}_{10}\text{Pd}$, 825.0328; found, 824.0308.



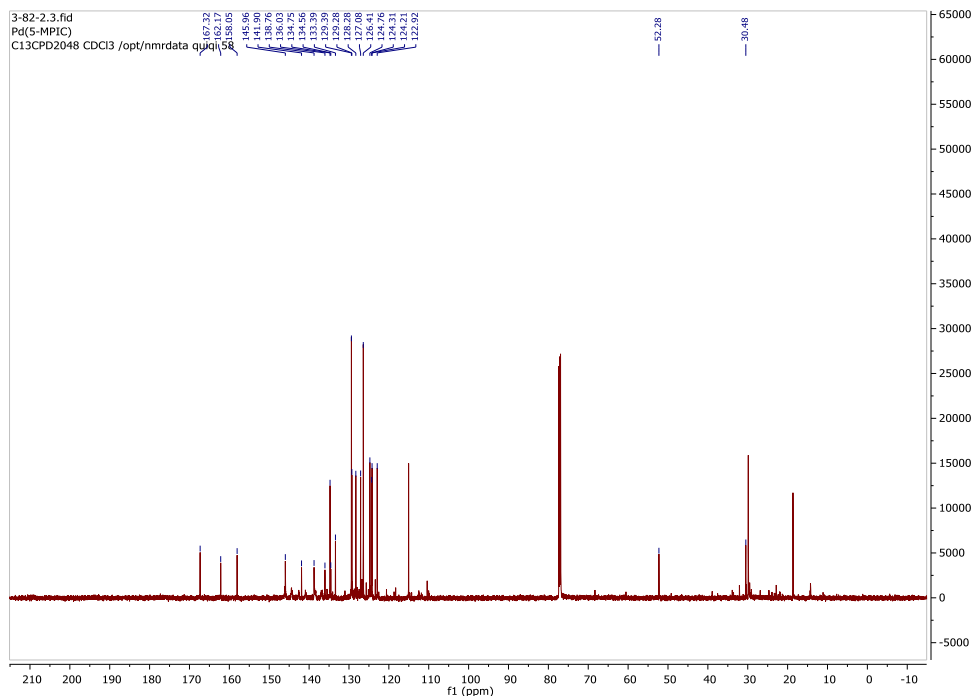


Figure 23 ^1H , ^{19}F and ^{13}C NMR of Pd(5-MPIC) in CDCl_3

Pd(5-DPIC): ^1H NMR (400 MHz, CDCl_3 , 25 °C) δ /ppm: 7.48 – 7.43 (m, 4H), 7.38 – 7.30 (m, 4H), 7.24 (d, $J = 1.3$ Hz, 2H), 6.89 (d, $J = 5.1$ Hz, 1H), 6.80 (d, $J = 4.2$ Hz, 1H), 6.67 (d, $J = 5.0$ Hz, 1H), 6.62 – 6.57 (m, 2H), 6.53 (d, $J = 4.5$ Hz, 1H), 6.41 (d, $J = 4.6$ Hz, 1H), 6.06 (d, $J = 4.2$ Hz, 1H). ^{19}F NMR (376 MHz, CDCl_3 , 25 °C) δ /ppm: –137.42 (dd, $J = 23.6$, 8.2 Hz, 2F), –137.87 (dd, $J = 23.0$, 7.8 Hz, 2F), –152.02 (t, $J = 21.0$ Hz, 1F), –152.42 (t, $J = 21.0$ Hz, 1F), –160.84 (tdd, $J = 22.6$, 17.0, 7.6 Hz, 4F). ^{13}C NMR (151 MHz, CDCl_3) δ 167.38, 162.54, 159.11, 146.40, 142.22, 139.04, 136.37, 135.29, 135.19, 134.90, 128.91, 128.80, 128.71, 128.53, 128.47, 127.26, 125.92, 124.76, 124.38, 122.38, 116.95, 30.47. (C-F splitting peaks are not presented). HR-ESI-MS $[\text{M} + \text{H}]^+$ m/z : calcd for $\text{C}_{43}\text{H}_{19}\text{N}_4\text{F}_{10}\text{Pd}$, 887.0485; found, 887.04898.

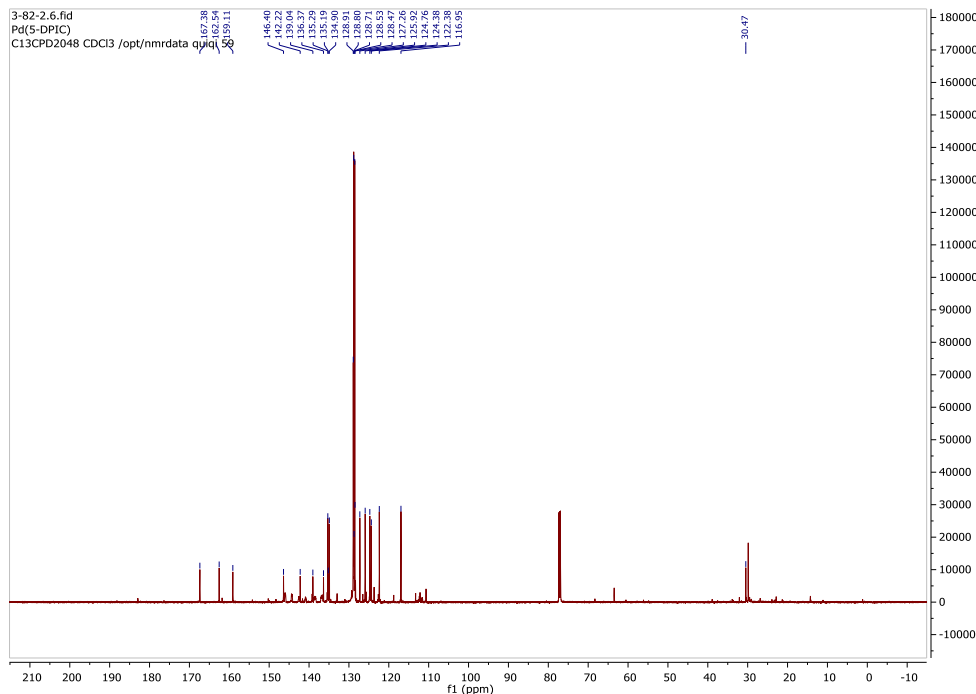


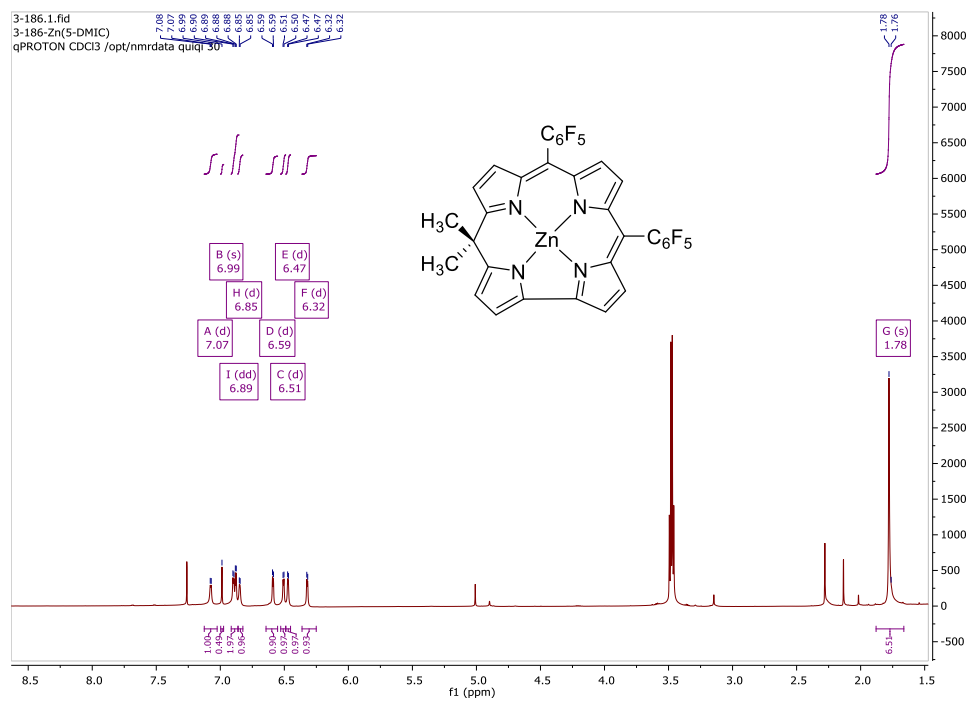
Figure 24 ^1H , ^{19}F and ^{13}C NMR of Pd(5-DPIC) in CDCl_3

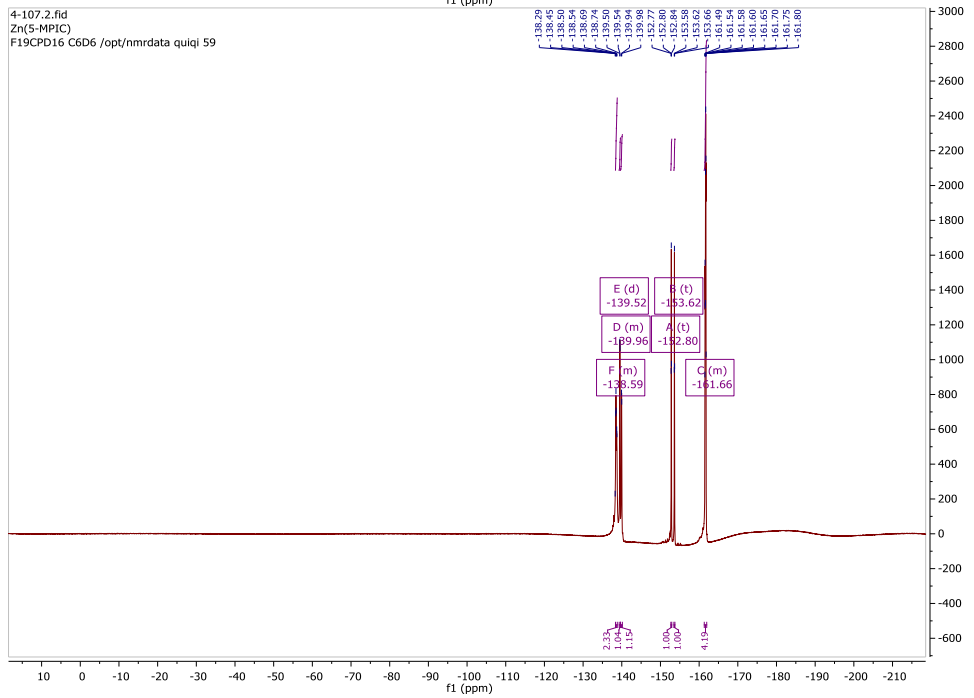
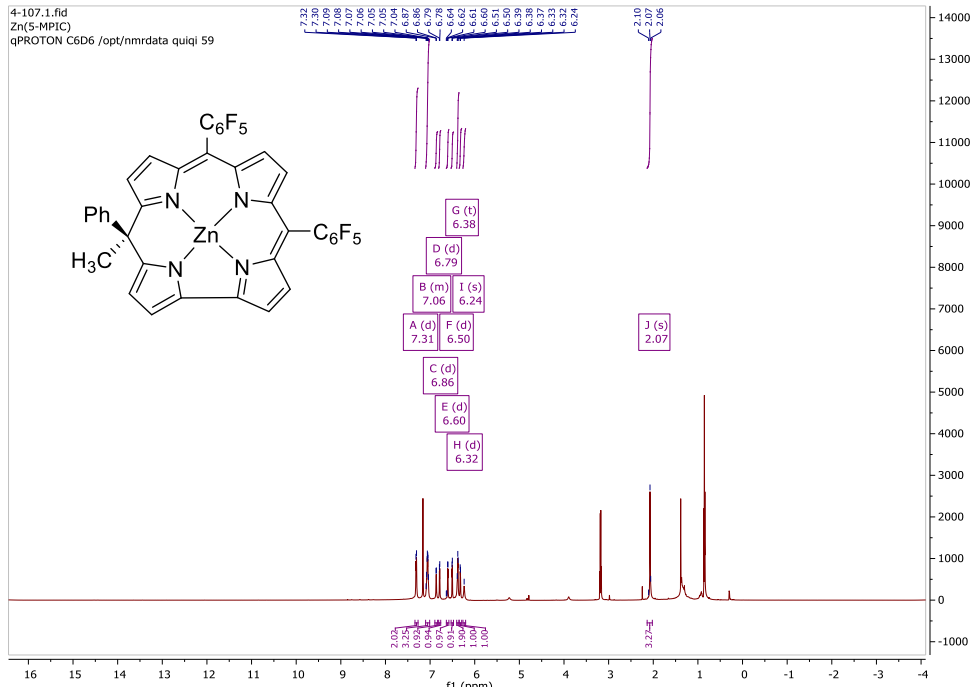
2.9 Synthesis of Zinc 5,5-disubstituted Isocorrole

5,5-dimethyl-10,15-bis(pentafluorophenyl)isocorrole (33 mg, 0.05 mmol), or 5-methyl-5-phenyl-10,15-bis(pentafluorophenyl)isocorrole (36 mg, 0.05 mmol), or 5,5-diphenyl-10,15-bis(pentafluorophenyl)isocorrole (39 mg, 0.05 mmol) and KOAc (17 mg) were dissolved in 10 mL acetonitrile. The mixture was stirred at room temperature for one hour. Then, Zinc acetate dihydrate (50 mg) was added to the mixture. The flask was wrapped with aluminum foil. The mixture was heated to reflux and stirred overnight in the dark. Then, the mixture was cooled to room temperature and the solvent was removed under vacuum. The crude was purified by going through a celite bed twice in DCM to give the brown solid (91% yield).

Zn(5-DMIC): ^1H NMR (600 MHz, CDCl_3 , 25 °C) δ /ppm: 7.07 (d, $J = 4.6$ Hz, 1H), 6.89 (m, 2H), 6.85 (d, $J = 3.7$ Hz, 1H), 6.59 (d, $J = 4.3$ Hz, 1H), 6.51 (d, $J = 4.2$ Hz, 1H), 6.47 (d, $J = 3.7$ Hz, 1H), 6.32 (d, $J = 4.2$ Hz, 1H), 1.78 (s, 6H). ^{19}F NMR (565 MHz, CDCl_3 , 25 °C)

δ /ppm: -138.13 (d, $J = 23.9$ Hz, 2F), -139.19 (d, $J = 23.0$ Hz, 2F), -153.35 (t, $J = 21.0$ Hz, 1F), -153.85 (t, $J = 21.7$ Hz, 1F), -161.66 (dt, $J = 72.9, 23.0$ Hz, 4F). HR-ESI-MS $[M + H]^+$ m/z : calcd for $C_{33}H_{15}N_4F_{10}Zn$, 721.0429; found, 721.0409.





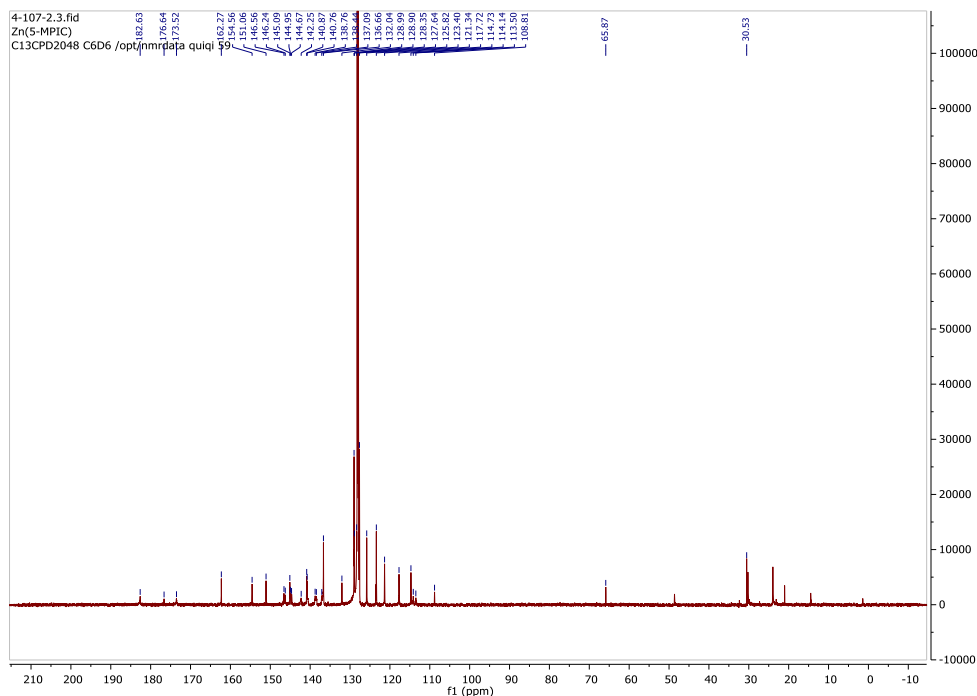
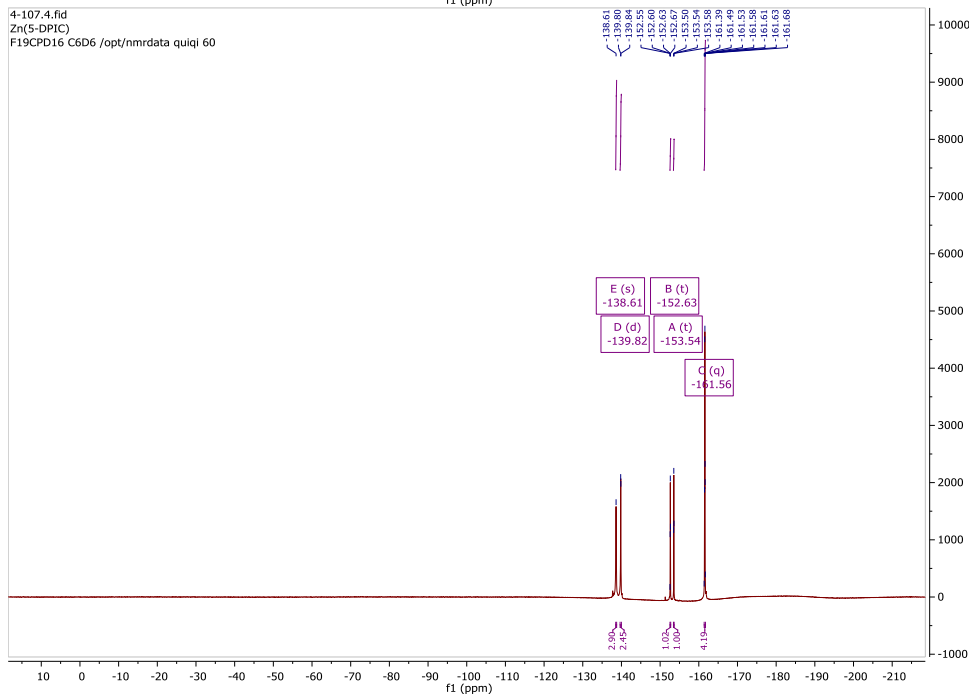
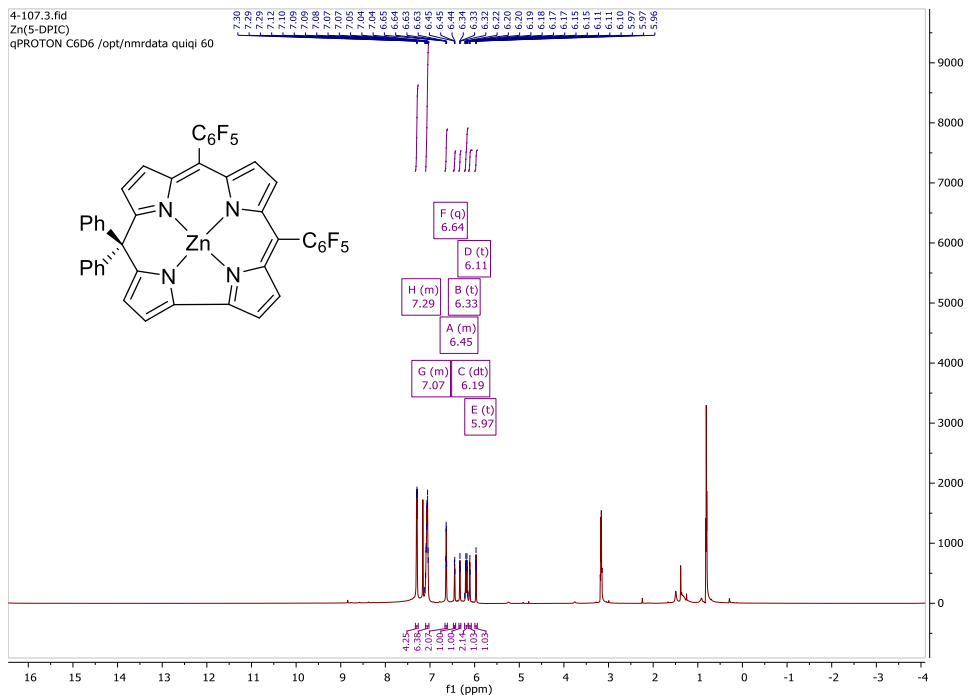


Figure 26 ^1H , ^{19}F and ^{13}C NMR of Zn(5-MPIC) in C_6D_6 .

Zn(5-DPIC): ^1H NMR (600 MHz, C_6D_6 , 25 $^\circ\text{C}$) δ/ppm : 7.33 – 7.26 (m, 4H), 7.10 – 7.02 (m, 6H), 6.64 (q, $J = 3.9, 3.2$ Hz, 2H), 6.47 – 6.43 (m, 1H), 6.33 (t, $J = 3.3$ Hz, 1H), 6.19 (dt, $J = 15.1, 3.4$ Hz, 2H), 6.11 (t, $J = 3.3$ Hz, 1H), 5.97 (t, $J = 3.0$ Hz, 1H). ^{19}F NMR (565 MHz, C_6D_6 , 25 $^\circ\text{C}$) δ/ppm : -138.61, -139.82 (d, $J = 23.0$ Hz), -152.63 (t, $J = 21.9$ Hz), -153.54 (t, $J = 21.8$ Hz), -161.56 (q, $J = 29.4, 26.8$ Hz). ^{13}C NMR (151 MHz, C_6D_6 , 25 $^\circ\text{C}$) δ/ppm : 186.98, 180.63, 162.59, 155.90, 151.59, 146.48, 146.15, 145.65, 144.82, 144.55, 142.59, 142.35, 140.55, 138.72, 138.44, 136.99, 131.57, 129.78, 128.86, 128.69, 126.75, 126.22, 124.34, 123.52, 123.17, 116.80, 115.72, 113.81, 113.03, 109.44, 66.26, 59.96, 30.54. HR-ESI-MS $[\text{M} + \text{H}]^+$ m/z : calcd for $\text{C}_{43}\text{H}_{19}\text{N}_4\text{F}_{10}\text{Zn}$, 845.0742; found, 845.0709.



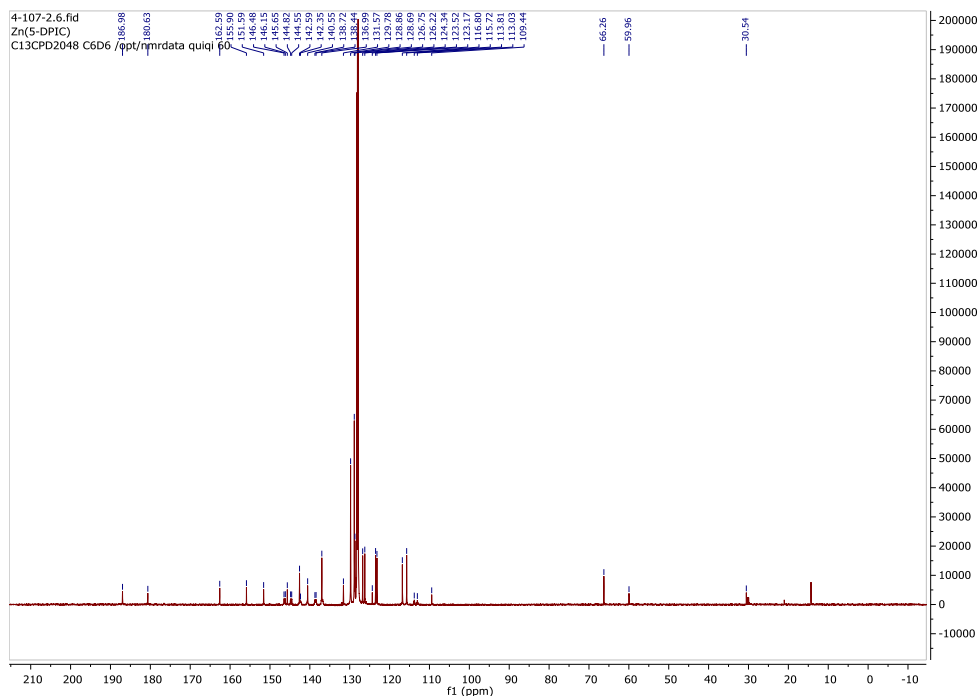


Figure 27 ^1H , ^{19}F and ^{13}C NMR of Zn(5-DPIC) in C_6D_6

2.9.1 Synthesis of 1-phenyloxycarbonyl cobalt 10,10-dimethyl-5,15-bis(pentafluorophenyl) isocorrole

Transfer $\text{Co}^{\text{III}}(10\text{-DMIC})(\text{PF}_6)$ (30 mg, 0.05 mmol), Na_2HPO_4 (15 mg), Benzenemethanol (0.1 mL, excess) in an oven dried round bottom flask in the glove box, dissolve the mixture by 3 mL dry toluene and 1 mL dry acetonitrile. Then, the sealed flask was pumped out and wrapped with aluminum foil to keep it away from light. The mixture was sparged by CO gas for 10 min, then charged with 1 atm CO (CO balloon), the mixture was stirred for 24 h at rt, in the dark. After that, the solvent was removed by schlenck line and the flask was pumped back to the glove box, also the crude was worked up in the dark. The crude was recrystallized by DCM and pentane. The filtrate solution was concentrated. The crude was purified by prep-TLC technique by using DCM/pentane (1:5, v/v) to get a green solid (42% yield). ^1H NMR (600 MHz, CD_3CN , 25 °C) δ /ppm: 7.90 (d, $J = 7.6$ Hz, 2H), 7.55 (t, $J = 7.3$ Hz, 1H),

7.45 (t, $J = 7.5$ Hz, 2H), 7.01 (dt, $J = 14.2, 7.0$ Hz, 4H), 6.94 (d, $J = 4.0$ Hz, 1H), 6.91 (d, $J = 4.0$ Hz, 1H), 6.84 (d, $J = 3.6$ Hz, 1H), 6.81 (d, $J = 3.6$ Hz, 1H), 6.52 (d, $J = 7.1$ Hz, 2H), 5.19 (q, $J = 6.6$ Hz, 1H), 2.55 (s, 3H), 1.78 (d, $J = 5.9$ Hz, 3H), 0.74 (d, $J = 6.6$ Hz, 2H). ^{19}F NMR (376 MHz, CD_3CN , 25 °C) δ/ppm : -140.87 (dddd, $J = 57.2, 23.4, 8.3, 3.3$ Hz), -142.00 (dtd, $J = 21.7, 8.7, 3.0$ Hz), -156.59 (t, $J = 20.0$ Hz), -163.70 – -164.17 (m). HR-LIFDI-MS M^+ m/z : calcd for $\text{C}_{42}\text{H}_{23}\text{N}_4\text{O}_2\text{F}_{10}\text{Co}$, 864.0993; found, 864.0988.

2.10 X-ray Crystallography

2.10.1 X-ray Structure Solution and Refinement

Crystals were mounted onto a plastic mesh using viscous oil and cooled to the data collection temperature. Data were collected on a Bruker-AXS APEX II DUO CCD diffractometer with Cu $\text{K}\alpha$ radiation ($\lambda = 1.5418$ Å) or Mo- $\text{K}\alpha$ radiation ($\lambda = 0.7107$ Å). Unit cell parameters were obtained from 48 data frames, $0.5^\circ \omega$, from three different sections of the Ewald sphere⁶³. The data sets were treated with multi-scan absorption corrections (Apex3 software suite, Madison, WI, 2015) or with SADABS absorption corrections based on redundant multi-scan data (Sheldrick, G., Bruker-AXS, 2001). The structures were solved using intrinsic phasing methods and refined with full-matrix, least-squares procedures on F^2 .^{64,65} All non-hydrogen atoms were refined with anisotropic displacement parameters. H-atoms were constrained in idealized positions with isotropic parameters based on their attached atoms. The penultimate difference maps were treated with Squeeze to model disordered solvent molecules as diffused contributions⁶⁶. Atomic scattering factors are contained in the SHELXTL program library. Crystallographic data were collected by Maxwell Martin

and Dr. Glenn P. A. Yap, Department of Chemistry and Biochemistry, University of Delaware.

2.10.1.1 DPBil freebase

Crystals of DPBil were obtained through slow evaporation of a concentrated solution of dichloromethane and hexanes at room temperature. A suitable crystal was selected and coated with Paratone® oil and mounted onto a Nylon loop. The data collection temperature for the crystals was 200K. The systematic absences in the diffraction data are consistent with the asymmetric monoclinic space group, $P2_1/n$. The compound co-crystallized with a molecule of dichloromethane. Hydrogen atoms were treated as idealized contributions. The detailed data collection and refinement parameter were listed in Table 2.1.

2.10.1.2 Pd[MPBil] and Pd[DPBil]

Crystals of Pd[MPBil] and Pd[DPBil] were obtained via slow evaporation of a concentrated solution of dichloromethane and hexanes at room temperature. The data collection temperature for the crystals was 200K for Pd[MPBil] and 105K for Pd[DPBil]. The systematic absences in the diffraction data are consistent with the asymmetric monoclinic space group, $P2_1/c$ for Pd[MPBil] and $P-1$ for Pd[DPBil], respectively. Hydrogen atoms were treated as idealized contributions. The detailed data collection and refinement parameter were listed in Table 2.2.

2.10.1.3 5-DMIC, 5-MPIC and 5-DPIC

Crystals of 5-DMIC, 5-MPIC and 5-DPIC were obtained through slow evaporation of a concentrated solution of dichloromethane and hexanes at room temperature. A suitable crystal was selected and coated with Paratone® oil and

mounted onto a Nylon loop. The data collection temperature for the crystals was 150K for 5-DMIC and 200K for both 5-MPIC and 5-DPIC. The systematic absences in the diffraction data are consistent with the asymmetric monoclinic space group, $P21/n$ for 5-DMIC and 5-DPIC. The space group for 5-MPIC is $C2/c$. Hydrogen atoms were treated as idealized contributions. The detailed data collection and refinement parameter were listed in Table 2.3.

2.10.1.4 Co(10-MPIC) and Co(10-DPIC)

Crystals of Co(10-MPIC) and Co(10-DPIC) were obtained through slow evaporation of a mixed solution of anhydrous dichloromethane, diethyl ether and pentane in the N_2 filled glove box at room temperature. A suitable crystal was selected and coated with Paratone® oil and mounted onto a Nylon loop. The data collection temperature for the crystals was 200K. The systematic absences in the diffraction data are consistent with the asymmetric monoclinic space group, $P21/n$ for Co(10-MPIC) and $C2/c$ for Co(10-DPIC). Hydrogen atoms were treated as idealized contributions. The detailed data collection and refinement parameter were listed in Table 2.4.

2.10.1.5 Co(5-DMIC), Co(5-MPIC) and Co(5-DPIC)

Crystals of Co(5-DMIC), Co(5-MPIC) and Co(5-DPIC) were obtained through slow evaporation of a mixed solution of anhydrous dichloromethane, diethyl ether and pentane in the N_2 filled glove box at room temperature. A suitable crystal was selected and coated with Paratone® oil and mounted onto a Nylon loop. The data collection temperature for the crystals was 150, 200 and 120K, respectively. The systematic absences in the diffraction data are consistent with the orthorhombic, monoclinic and triclinic space group. The compound co-crystallized with a molecule of

dichloromethane. Hydrogen atoms were treated as idealized contributions. The detailed data collection and refinement parameter were listed in Table 2.5.

2.10.1.6 Pd(5-DMIC), Pd(5-MPIC) and Pd(5-DPIC)

The crystals of Pd(5-DMIC), Pd(5-MPIC) and Pd(5-DPIC) were obtained through slow evaporation of a mixed solution of anhydrous dichloromethane and hexanes at room temperature. A suitable crystal was selected and coated with Paratone® oil and mounted onto a Nylon loop. The data collection temperature for the crystals was 200K. The systematic absences in the diffraction data are consistent with the asymmetric monoclinic space group, $C 2/c$ for Pd(5-MPIC) and $P21/n$ for Pd(5-DMIC) and Pd(5-DPIC). Hydrogen atoms were treated as idealized contributions. The detailed data collection and refinement parameter were listed in Table 2.6.

2.10.1.7 Zn(5-DPIC)

Crystals of Zn(5-DPIC) were obtained through slow evaporation of a concentrated solution of methanol and chloroform at room temperature. A suitable crystal was selected and coated with Paratone® oil and mounted onto a Nylon loop. The data collection temperature for the crystals was 200K. The systematic absences in the diffraction data are consistent with the asymmetric monoclinic space group, $P c$. The compound co-crystallized with two molecules of methanol. Hydrogen atoms were treated as idealized contributions. The detailed data collection and refinement parameter were listed in Table 2.7.

2.10.2 Crystallographic Information Tables

Table 2.1. Crystallographic Data for DPBil freebase

| | DPBil freebase |
|--------------------|--|
| Empirical Formula | C ₄₄ H ₂₄ C ₁₂ F ₁₀ N ₄ |
| Formula Weight | 869.57 |
| Crystal System | monoclinic |
| Space Group | P2 ₁ /n |
| <i>a</i> | 8.2507(2) Å |
| <i>b</i> | 22.1150(6) Å |
| <i>c</i> | 21.0697(6) Å |
| α | 90° |
| β | 96.4860(10)° |
| γ | 90° |
| Volume | 3819.86(18) Å ³ |
| Z | 4 |
| Temperature | 200(2) K |
| D _{calcd} | 1.512 g/cm ⁻³ |
| 2 θ range | 2.906° – 75.137° |
| μ | 2.317 mm ⁻¹ (Mo K α) |
| Reflections | 72428 |
| Unique | 7858 |
| R(int) | 0.0487 |
| R ₁ | 0.0579 |
| wR ₂ | 0.1634 |

Table 2.2. Crystallographic Data for Pd[MPBil] and Pd[DPBil]

| | Pd[MPBil] | Pd[DPBil] |
|--------------------|---|---|
| Empirical Formula | C ₃₈ H ₁₈ F ₁₀ N ₄ Pd | C ₄₃ H ₂₀ F ₁₀ N ₄ Pd |
| Formula Weight | 826.96 | 889.03 |
| Crystal System | Monoclinic | Triclinic |
| Space Group | P2 ₁ /c | P-1 |
| <i>a</i> | 15.1965(6) Å | 9.2976(3) Å |
| <i>b</i> | 10.3049(4) Å | 14.3221(5) Å |
| <i>c</i> | 26.695(1) Å | 14.5571(5) Å |
| α | 90° | 92.171(2)° |
| β | 103.936(2)° | 100.234(2)° |
| γ | 90° | 90.638(3)° |
| Volume | 4057.4(3) Å ³ | 1905.9(11) Å ³ |
| Z | 4 | 2 |
| Temperature | 200(2) K | 105(2) K |
| D _{calcd} | 1.354 g/cm ⁻³ | 1.549 g/cm ⁻³ |
| 2 θ range | 2.996° – 75.717° | 3.09° – 75.14° |

| | | |
|-----------------|---|---|
| μ | 4.367 mm ⁻¹ (Cu K α) | 4.696 mm ⁻¹ (Mo K α) |
| Reflections | 66763 | 51319 |
| Unique | 8341 | 7559 |
| $R(\text{int})$ | 0.0475 | 0.1231 |
| R_1 | 0.0317 | 0.0548 |
| wR_2 | 0.0815 | 0.1552 |

Table 2.3. Crystallographic Data for 5-isocorrole derivatives: 5-DMIC, 5-MPIC and 5-DPIC

| | 5-DMIC | 5-MPIC | 5-DPIC |
|--------------------|--|--|--|
| Empirical Formula | C ₃₃ H ₁₆ F ₁₀ N ₄ | C ₃₈ H ₁₈ F ₁₀ N ₄ | C ₄₃ H ₂₀ F ₁₀ N ₄ |
| Formula Weight | 658.50 | 720.56 | 782.63 |
| Crystal System | Monoclinic | Monoclinic | Monoclinic |
| Space Group | $P 2_1/n$ | $C 2/c$ | $P 2_1/n$ |
| a | 9.3323(19) | 28.0197(8) Å | 17.7426(6) Å |
| b | 11.006(2) | 11.4314(3) Å | 13.4012(4) Å |
| c | 26.806(6) | 22.5090(7) Å | 18.6609(6) Å |
| α | 90° | 90° | 90° |
| β | 92.337(12)° | 105.107(2)° | 116.283(2)° |
| γ | 90° | 90° | 90° |
| Volume | 2751.0(10) Å ³ | 6960.6(4) Å ³ | 3978.3(2) Å ³ |
| Z | 4 | 8 | 4 |
| Temperature | 150(2) K | 200(2) K | 200(2) K |
| D_{calcd} | 1.590 g/cm ⁻³ | 1.375 g/cm ⁻³ | 1.307 g/cm ⁻³ |
| 2θ range | 3.300° – 83.576° | 3.267° – 75.158° | 2.862° – 75.590° |
| μ | 1.258 mm ⁻¹ (Cu K α) | 1.046 mm ⁻¹ (Cu K α) | 0.960 mm ⁻¹ (Cu K α) |
| Reflections | 41444 | 66377 | 62138 |
| Unique | 5713 | 7029 | 7972 |
| $R(\text{int})$ | 0.1201 | 0.0914 | 0.0964 |
| R_1 | 0.0767 | 0.0555 | 0.0569 |
| wR_2 | 0.1863 | 0.1526 | 0.1897 |

Table 2.4. Crystallographic Data for Co(10-MPIC) and Co(10-DPIC)

| | Co(10-MPIC) | Co(10-DPIC) |
|-------------------|--|--|
| Empirical Formula | C ₃₈ H ₁₆ CoF ₁₀ N ₄ | C ₄₇ H ₂₈ CoF ₁₀ N ₄ O |
| Formula Weight | 777.48 | 913.66 |
| Crystal System | monoclinic | monoclinic |
| Space Group | $P2_1/n$ | $C 2/c$ |
| a | 14.6124(5) Å | 31.3050(14) Å |

| | | |
|--------------------|---|---|
| <i>b</i> | 9.9800(3) Å | 18.7780(8) Å |
| <i>c</i> | 44.7134(15) Å | 15.4314(7) Å |
| α | 90° | 90° |
| β | 92.404(2)° | 118.738(2)° |
| γ | 90° | 90° |
| Volume | 6514.9(4) Å ³ | 7953.9(6) Å ³ |
| Z | 8 | 8 |
| Temperature | 200(2) K | 200(2) K |
| D_{calcd} | 1.585 g/cm ⁻³ (Block) | 1.526 g/cm ⁻³ (Block) |
| 2θ range | 1.978° – 75.815° | 2.851° – 75.755° |
| μ | 4.973 mm ⁻¹ (Cu K α) | 2.317 mm ⁻¹ (Cu K α) |
| Reflections | 90145 | 68774 |
| Unique | 13104 | 7994 |
| $R(\text{int})$ | 0.2497 | 0.0932 |
| R_1 | 0.1063 | 0.0564 |
| wR_2 | 0.2613 | 0.1545 |

Table 2.5. Crystallographic Data for Co(5-isocorrole) derivatives

| | Co(5-DMIC) | Co(5-MPIC) | Co(5-DPIC) |
|--------------------|--|--|--|
| Empirical Formula | C ₃₃ H ₁₄ CoF ₁₀ N ₄ | C ₃₈ H ₁₆ CoF ₁₀ N ₄ | C ₄₃ H ₁₈ CoF ₁₀ N ₄ |
| Formula Weight | 715.41 | 777.48 | 987.78 |
| Crystal System | orthorhombic | monoclinic | triclinic |
| Space Group | Pbca | C 2/c | P-1 |
| <i>a</i> | 17.2066(3) Å | 27.981(4) Å | 15.3754(7) Å |
| <i>b</i> | 11.8365(3) Å | 11.4618(16) Å | 17.7025(9) Å |
| <i>c</i> | 27.1385(6) Å | 22.519(4) Å | 18.4983(9) Å |
| α | 90° | 90° | 87.774(4)° |
| β | 90° | 106.586(9)° | 72.136(4)° |
| γ | 90° | 90° | 68.312(3)° |
| Volume | 5527.2(2) Å ³ | 6921.5(18) Å ³ | 4437.1(4) Å ³ |
| Z | 8 | 8 | 4 |
| Temperature | 150(2) K | 150(2) K | 120(2) K |
| D_{calcd} | 1.719 g/cm ⁻³ | 1.492 g/cm ⁻³ | 1.479 g/cm ⁻³ (Block) |
| 2θ range | 3.257° – 75.377° | 3.296° – 75.656° | 2.518° – 68.537° |
| μ | 5.796 mm ⁻¹ (Cu K α) | 4.681 mm ⁻¹ (Cu K α) | 3.812 mm ⁻¹ (Cu K α) |
| Reflections | 58758 | 32529 | 62261 |
| Unique | 5703 | 7014 | 15669 |

| | | | |
|-----------------|--------|--------|--------|
| $R(\text{int})$ | 0.1412 | 0.1100 | 0.1028 |
| R_1 | 0.0620 | 0.0938 | 0.0830 |
| wR_2 | 0.1444 | 0.2622 | 0.2081 |

Table 2.6. Crystallographic Data for Pd(5-DMIC), Pd(5-MPIC) and Pd(5-DPIC)

| | Pd(5-DMIC) | Pd(5-MPIC) | Pd(5-DPIC) |
|--------------------|---|---|---|
| Empirical Formula | C ₃₃ H ₁₄ F ₁₀ N ₄ Pd | C ₃₈ H ₁₆ F ₁₀ N ₄ Pd | C ₄₃ H ₁₈ F ₁₀ N ₄ Pd |
| Formula Weight | 762.88 | 824.95 | 887.01 |
| Crystal System | Monoclinic | Monoclinic | Monoclinic |
| Space Group | <i>P</i> 2 ₁ / <i>n</i> | <i>C</i> 2/ <i>c</i> | <i>P</i> 2 ₁ / <i>n</i> |
| <i>a</i> | 9.4214(8) | 27.625(2) | 17.5646(14) |
| <i>b</i> | 11.0516(10) | 11.5442(9) | 13.5785(11) |
| <i>c</i> | 26.825(2) | 23.1776(19) | 18.1709(15) |
| α | 90° | 90° | 90° |
| β | 93.430(2)° | 104.6690(10)° | 116.1420(10)° |
| γ | 90° | 90° | 90° |
| Volume | 2788.0(4) Å ³ | 7150.7(10) Å ³ | 3890.5(5) Å ³ |
| Z | 4 | 8 | 4 |
| Temperature | 200(2) K | 200(2) K | 200(2) K |
| D _{calcd} | 1.817 g/cm ⁻³ | 1.533 g/cm ⁻³ | 1.514 g/cm ⁻³ |
| 2 θ range | 1.994° – 27.723° | 1.816° – 27.820° | 1.951° – 27.663° |
| μ | 0.766 mm ⁻¹ (Mo K α) | 0.604 mm ⁻¹ (Mo K α) | 0.561 mm ⁻¹ (Mo K α) |
| Reflections | 31038 | 26711 | 44415 |
| Unique | 6545 | 8358 | 9067 |
| $R(\text{int})$ | 0.0597 | 0.0624 | 0.1308 |
| R_1 | 0.0522 | 0.0628 | 0.0658 |
| wR_2 | 0.1165 | 0.1624 | 0.1523 |

Table 2.7. Crystallographic Data for Zn(-DPIC) with methanol binded as the fifth coordination ligand.

| | Zn(5-DPIC)(MeOH) |
|-------------------|--|
| Empirical Formula | C ₄₅ H ₂₆ F ₁₀ N ₄ O ₂ Zn |
| Formula Weight | 910.07 |
| Crystal System | Monoclinic |
| Space Group | <i>P</i> <i>c</i> |
| <i>a</i> | 13.4671(14) |
| <i>b</i> | 14.9524(15) |
| <i>c</i> | 9.3797(9) |

| | |
|--------------------|---|
| α | 90° |
| β | 101.9200(10)° |
| γ | 90° |
| Volume | 1848.0(3) Å ³ |
| Z | 2 |
| Temperature | 200(2) K |
| D _{calcd} | 1.635 g/cm ⁻³ |
| 2 θ range | 2.060° – 31.346° |
| μ | 0.763 mm ⁻¹ (Mo K α) |
| Reflections | 35881 |
| Unique | 11993 |
| R(int) | 0.0377 |
| R ₁ | 0.0387 |
| wR ₂ | 0.0788 |

Chapter 3

SYNTHESIS OF NONTRADITIONAL TETRAPYRROLE PLATFORM: BILADIENE AND 5-ISOCORROLE DERIVATIVES

3.1 Introduction

Nonmacrocyclic linear tetrapyrroles such as biladienes and biliverdins⁶⁷ (**Figure 28**), which have been synthesized and studied in recent decade of years, have been proved to perform unique photophysical properties. On the other hand, the metalation products of these nonmacrocyclic linear tetrapyrroles⁶⁸ still remain a huge blank space to explore. Recent coordination products of nonmacrocyclic linear tetrapyrroles⁶⁹ are mostly with copper^{70,71}, nickel⁷² and cobalt^{73,74}, which are the common transition metals. As a result, the coordination chemistry of nonmacrocyclic oligopyrrole constructs has been much more limited than that which is known for porphyrins, corroles, phthalocyanines and other polypyrrole macrocycles.

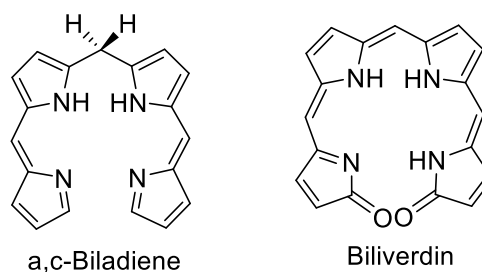
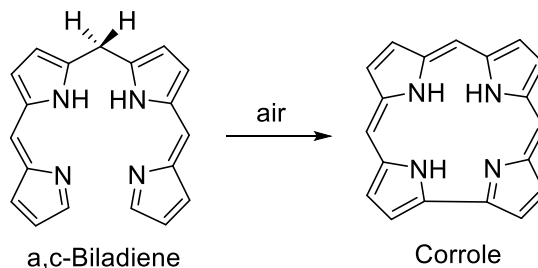


Figure 28. Structures of a,c-Biladiene and Biliverdin

One of the drawbacks that hinders the exploration of coordination chemistry of nonmacrocyclic linear tetrapyrroles is the instability of such frameworks caused by their nonaromaticity, unlike the traditional aromatic tetrapyrroles. For example, a,c-biladienes, where the two protons on the 10 *meso*-carbon interrupt the aromaticity by forming an sp^3 -hybridized *meso*-carbon, are not stable in the presence of air (**Scheme 3.1**). In addition, if there is no functional modification at the tetrapyrrole termini, such as the 1 and 19-position, the a,c-biladiene can decompose back to the corresponding aromatic corrole architecture^{75,76}.



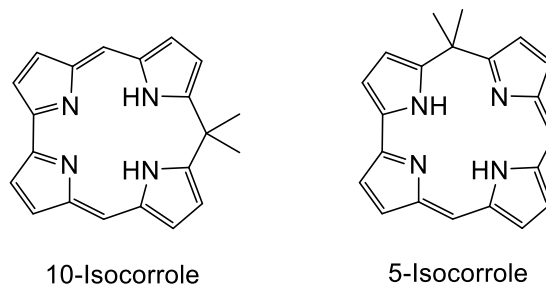
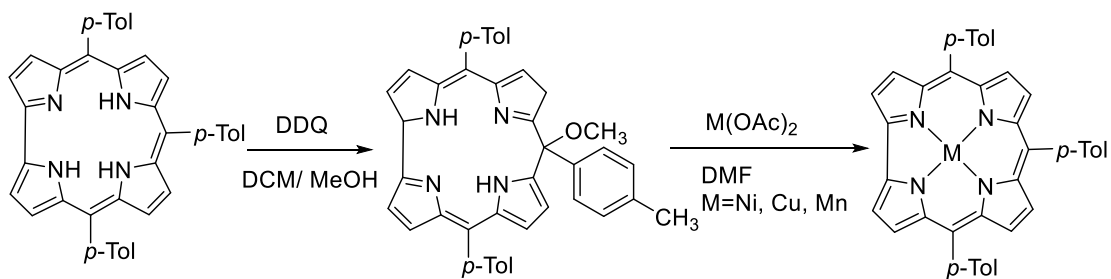


Figure 29 Two isomers of isocorrole

However, most of the reported metallated isocorrole complexes' synthetic routes are based on available *meso*-triaryl corrole as the precursor. This type of synthetic route includes an oxidation of the sp^2 hybridized *meso*-carbon by 2,3-dichloro-5,6-dicyano-1,4-benzoquinone (DDQ) with a nucleophile, usually methanol or ethanol^{79,80}.

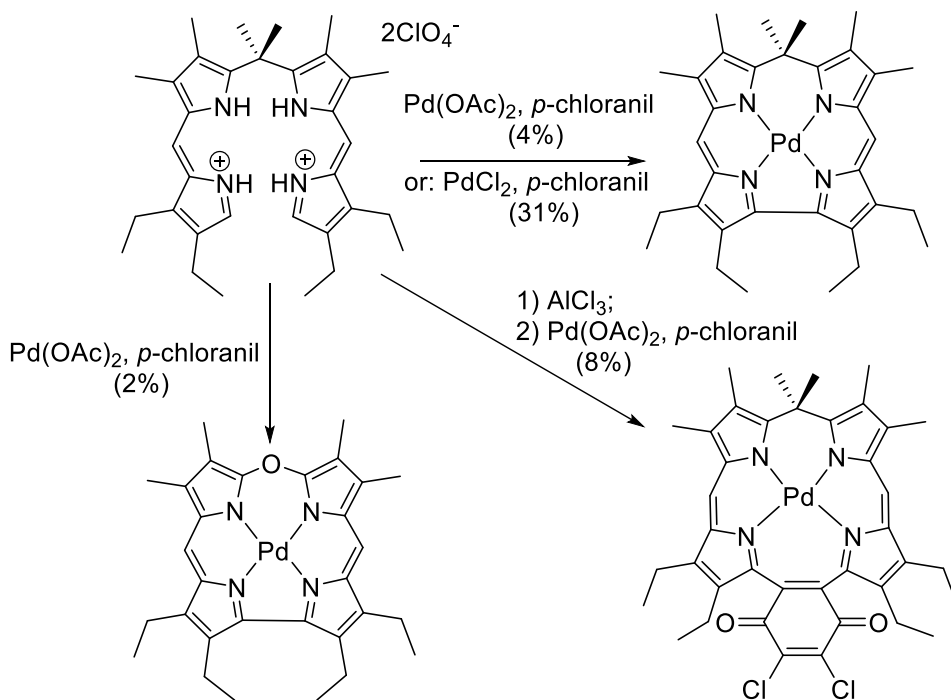


Scheme 3.2. The isocorrole-corrole conversion after the metalation

Although the presence of the methoxy or the hydroxy substituent group on the *meso*-carbon can stabilize the free base isocorrole, there was an isocorrole-corrole conversion during the metalation step⁷⁹, as shown in **Scheme 3.2** the methoxy or the hydroxy group interrupted the reaction as a leaving group with the coordination chemistry of nickel, copper and manganese was attempted.

Another synthetic method was discovered as a by-product that can be separated during the demetalation of metallocorrole complexes by using concentrated sulfuric acid⁸¹. The formation of 10/5-hydroxy-isocorrole was rationalized that the target molecule, corrole freebase, could be easily oxidized, then attacked by a molecule of water, which was observed in the preparation of isocorrole by oxidation of corrole with DDQ⁷⁹. With this approach, nickel/ cobalt b-octabromo-meso-triphenylisocorrole derivatives were prepared from the demetallation reaction of copper b-octabromo-meso- triphenylcorrole with concentrated H₂SO₄ in chloroform⁸².

It is also worth mentioned that isocorrole could be a key intermediate in the process of the functionalization of corrole⁸³. Bröring's group reported another isocorrole synthesis method in 2016, including copper, palladium, platinum and nickel metalation product⁸⁴. One of the synthesis methods is shown in **Scheme 3.3**. However, they failed to use the direct isocorrole ligand metalation method, instead, they synthesized biladiene derivatives as the starting material, in the presence of oxidant, such as *p*-chloranil, and metal source salt in chloroform. This method displayed many unwanted by-products, which would lower the yield of the target products.



Scheme 3.3. Synthesis of palladium isocorrrole complex and its by-products.

In 2009, Naho Okazaki's group reported a synthesis method of 10-isocorrrole freebase from 5,5-dipyrrrolemethane and bisazafulvene under neutral conditions followed by DDQ oxidation giving rise to 27% yield⁸⁵. They also successfully metallated the freebase with nickel, copper, iron, manganese and rhodium. They provided a new isocorrrole platform that can be a potential ligand for four-, five-, and six-coordinate metal complexes. However, the zinc isocorrrole is not stable in their system.

A year later, meso-alkyl substituted 5/10-isocorrroles was prepared by addition of Grignard reagent, ethyl magnesium bromide, to 5,10,15-tritolyllorrole before the DDQ oxidation step in satisfying yield⁸⁶. This work expanded the properties of the isocorrroles for use in real applications, instead of the limitations on the sp^3 -hybridized meso-position only with alcohol or alkyl ether groups. Instead of using Grignard

reagent or alcohol, pyrrole was also applied in the formation of isocorroles from the corrole platform⁸⁷.

Richard Geier, III's group did an in-depth investigation of the formation of 5,5-dimethyl-isocorrole through two different reaction routes with decent yields, which is the most recent reported method⁸⁸. Metalation products of copper and zinc was also characterized by X-ray and UV-vis experiments⁸⁹.

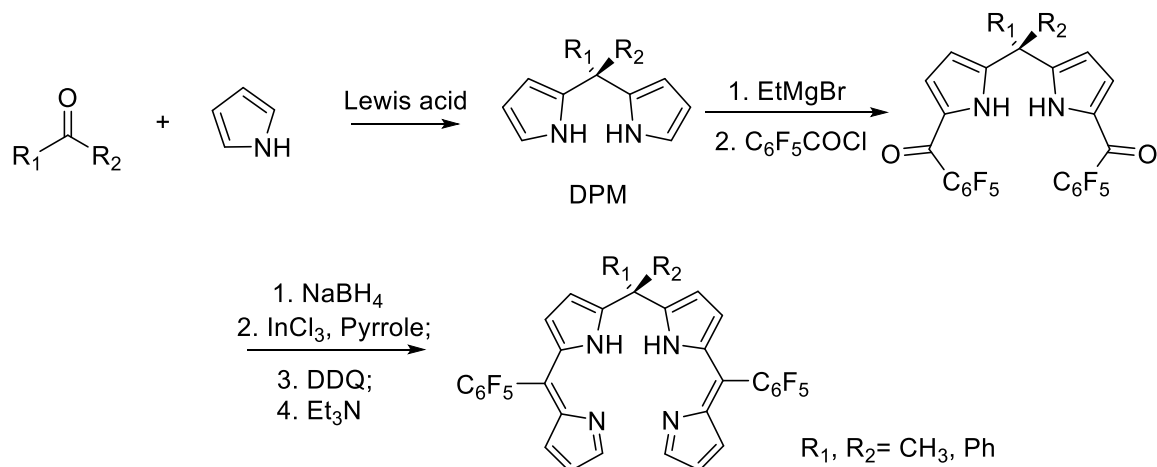
Therefore, it is a great challenge to design a new method to synthesize the isocorrole free base to utilize it as a potential tetrapyrrole ligand with different metal sources. In this chapter, the synthesis of 10,10-disubstituted biladiene and 5,5-disubstituted isocorrole will be shown. The use of 5-isocorrole as a ligand platform for transition metals, such as palladium and zinc will be characterized by solid-state structures, NMR spectroscopy and UV-Vis absorptions.

3.2 Synthesis of 10,10-disubstituted-5,15-diphenylpentafluorophenylbiladiene

The detailed synthesis procedure of 10,10-disubstituted-5,15-diphenylpentafluorophenylbiladiene (DMBil1, MPBil and DPBil) were presented in Chapter 2. It started with the coordinated 5,5-disubstituted dipyrromethene, which was prepared from the condensation reaction with ketone and different Lewis acids. Then, the dipyrromethene was treated with ethyl magnesium bromide (EtMgBr) and pentafluorobenzyl chloride (C₆F₅COCl) to realize the diacylation reaction. The diacylated product was then reduced with NaBH₄ in THF and methanol (3/1: v/v). The reaction was quenched by saturated NH₄Cl aqueous solution and extracted with DCM. After that, the concentrated reduced diol crude product was dissolved in DCM and stirred with InCl₃ and pyrrole at room temperature for 2 hours. The following oxidation process was realized by adding DDQ and triethylamine. The product was

purified by column chromatography with hexanes and DCM as eluent, shown in

Scheme 3.4.



Scheme 3.4 Synthesis of 10,10-disubstitued-5,15-diphenylpentafluorophenylbiladine (MPBil and DPBil)

3.2.1 Crystal Structures of DPBil

The solid-state crystal structure of DPBil is shown in **Figure 30**. The dipyrromethane unit next to the sp^3 -hybridized *meso* carbon is distorted significantly, that the dihedral angle is 73.77° , which is larger than the reported DMBil1 ligand (66.08°). The two pentafluorophenyl groups are canted with the coordinated dipyrromethane moieties with the angle of 80.50° and 69.98° respectively which is also larger than the same angles in DMBil1.

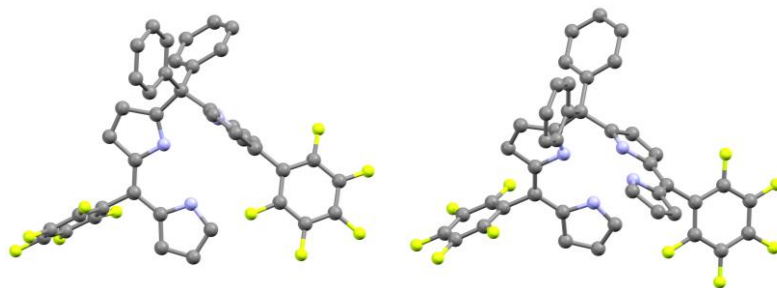


Figure 30 The crystal structure of DPBil, view from side and front. Hydrogen atoms are omitted for clarity.

3.2.2 UV-vis Spectra of Biladiene Derivatives

The UV-vis experiment were carried out in dichloromethane at room temperature, shown in **Figure 31**. The MPBil and DPBil displayed very distinct absorption features comparing with the dimethyl derivative, they displayed one broad absorption peak from 350 – 550 nm, instead of presenting two broad peaks in the same region. More phenyl substituents, the higher extinction coefficient it had.

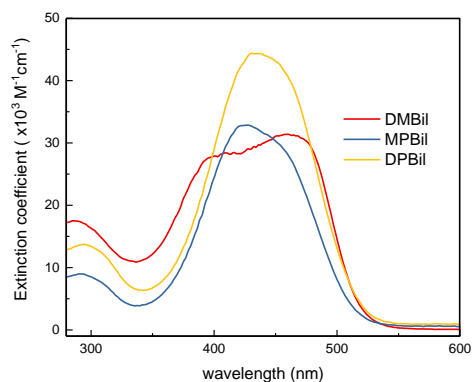
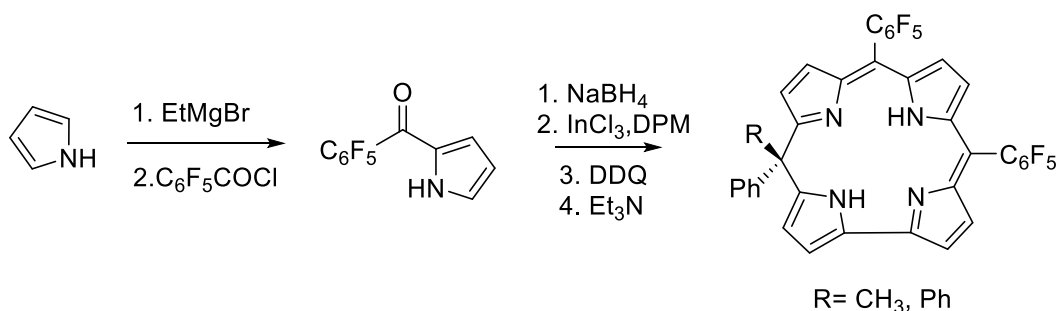


Figure 31 UV-vis absorption of biladiene derivatives in DCM at room temperature

3.3 Synthesis of 5,5-disubstituedd Isocorrole

The 5,5-dimethyl-10,15-diphenylpentafluorophenylisocorrole (5-DMIC) was prepared by the reported literature procedure. The detailed synthesis and characterization of 5-MPIC and 5-DPIC were presented in Chapter 2. The freebase of

5-MPIC and 5-DPIC began with an acylation reaction of pyrrole, then, the pentafluorobenzyl pyrrole was reduced by NaBH₄ in THF/MeOH (v/v: 3:1). The reaction was quenched by saturated NH₄Cl aqueous solution. The reduced intermediate was dissolved again together with InCl₃ and 5,5-disubstituted dipyrromethene in DCM without purification. The mixture was stirred at room temperature overnight and oxidized by adding DDQ and triethylamine. The crude product was purified by column chromatography, as shown in Scheme 3.5.



Scheme 3.5 Synthesis of 5-MPIC and 5-DPIC

3.3.1 Crystals Structures of 5-Isocorrole Freebase

The solid-state structures of 5-isocorrole freebases are shown in Figure 32. For all the freebases, there are two N–H protons in the core of the ring: one of the proton is located in the pyrrole ring that is in between the two perfluorophenyl groups, the other proton is located in the pyrrole ring that is in the unit of bipyrrrole. These two asymmetric protons are consistent with the analysis of proton NMR (shown in **Figure 13** and **Figure 14**), which displays two broad peaks in the down field. By measuring the N–N separations (Table 3.1), the shortest separate N–N distance (~2.50 Å) is the bottom two pyrrole units without *meso* carbon in between, the longest N–N distance (~3.00 Å) is the rest two pyrrole units opposite the pyrrole rings mentioned before.

The huge difference of the N–N distance is also an indication of the asymmetry for the structure of freebases. What can be notified is that the sp^3 *meso*-carbon is not in the plane of the core ring for the 5-DPIC, the angle between the core ring and the sp^3 *meso*-carbon is 16.29° . The C–C bond distance for the bipyrrrole unit is 1.416 Å, 1.424 Å and 1.429 Å respectively, which is also similar as the C–C bond distance in traditional corroles⁹⁰.

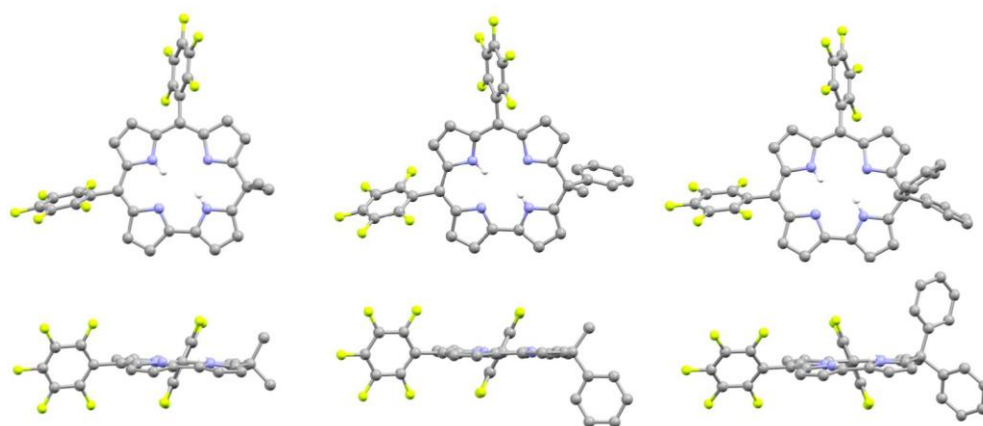


Figure 32 Crystal structures of 5-DMIC (left), 5-MPIC (middle) and 5-DPIC (right), viewing form top and side. H atoms are omitted for clarities, except for the N–H protons.

Table 3.1 Relevant dihedral angles and atom distances measured for 5-DMIC, 5-MPIC, and 5-DPIC

| | 5-DMIC | 5-MPIC | 5-DPIC |
|---|---|---|---|
| Dipyrrromethane units and meso C ₆ F ₅ groups | 68.80° (close to sp^3 <i>meso</i> carbon) | 65.06° (close to sp^3 <i>meso</i> carbon) | 69.24° (close to sp^3 <i>meso</i> carbon) |
| N–N separations (Å) | 68.80° | 74.98° | 57.06° |
| | 2.625(5) | 2.627(2) | 2.996(4) |
| | 2.565(5) | 2.558(2) | 2.605(4) |
| | 2.976(4) | 2.611(2) | 2.574(4) |
| | 2.635(4) | 2.988(2) | 2.619(4) |
| C–C bond distance for the bipyrrrole unit (Å) | 1.416 | 1.424 | 1.429 |

3.4 UV-vis Absorption Features

The UV-vis absorption experiments were carried out in methanol at room temperature. The UV-vis plot is presented in **Figure 33**. All three freebases displayed strong traditional porphyrin type Soret absorption features around 400 nm and two weak absorption features between 600 – 800 nm.

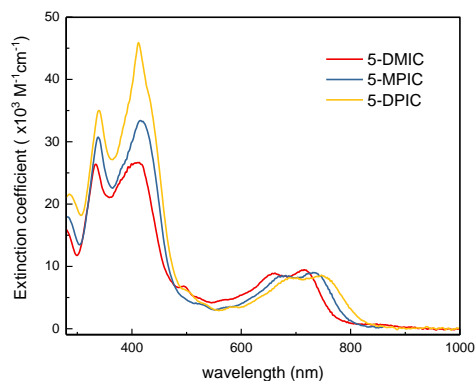
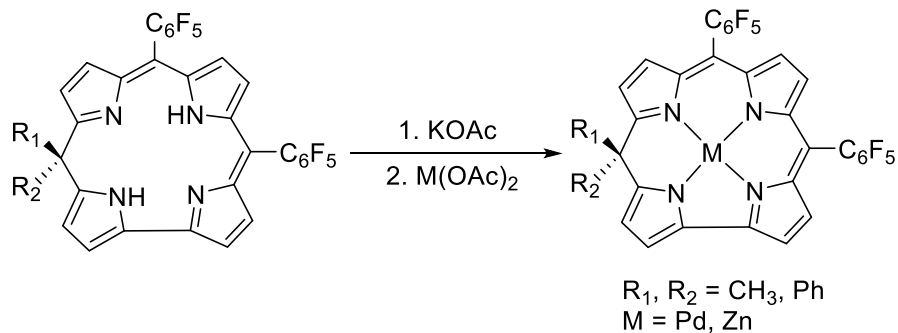


Figure 33 UV-Vis absorption spectrometry of 5-isocorrole derivatives in methanol

3.5 Synthesis of Zinc and Palladium 5-Isocorrole: Zn(5-IC) and Pd(5-IC)

Pd(5-IC)s were synthesized with adding excess KOAc and Pd(OAc)₂ to the 5-isocorrole freebase in acetonitrile. The mixture was refluxed in the dark overnight and purified by column chromatography.

The zinc 5-isocorrole derivatives were also prepared by a similar method as the palladium products by refluxing with excess KOAc and Zn(OAc)₂ · 2H₂O, both shown in **Scheme 3.6**. It should be notified that the zinc complexes were not stable on the silica, the metal center would be removed on the silica column chromatography. As a result, the work up for Zn(5-IC) derivatives was let it go through the celite bed twice in DCM.



Scheme 3.6 Synthesis of Zn(5-IC) and Pd(5-IC)

3.5.1 Crystal Structures of Zn(5-DPIC) and Pd(5-IC)

The Pd(5-IC) derivatives are the first examples in palladium 5-isocorrole complexes, shown in **Figure 34**. All palladium derivatives exhibit square planar or pseudo geometry with quite equal Pd–N bond distances ($\sim 1.95 \text{ \AA}$), which is slightly shorter than the traditional palladium tetrapentafluorophenyl porphyrin⁹¹, ranging from 2.010(4) \AA to 2.050(4) \AA . The Zn(5-DPIC), **shown in Figure 35**, has a fifth coordination with a molecule of methanol, which is consistent with the crystal structure of Zn1⁸⁹ reported by Geier's group. The zinc cation is hanging above the core ring of 5-DPIC, making the puckered geometry, which shows the larger angle between the core ring and the sp^3 meso-carbon (27.35°) than the 5-DPIC freebase and Pd[5-DPIC]. The Zn–N bonds, ranging from 2.007(3) \AA to 2.031(3) \AA , are longer than the Pd–N bonds and Zn1 complex, however, the Zn–O bond is 2.067(3) \AA , which is in the range of Zn–O bond reported for the Zn1 complex. The other bond distance and dihedral angle information is summarized in Table 3.2 below.

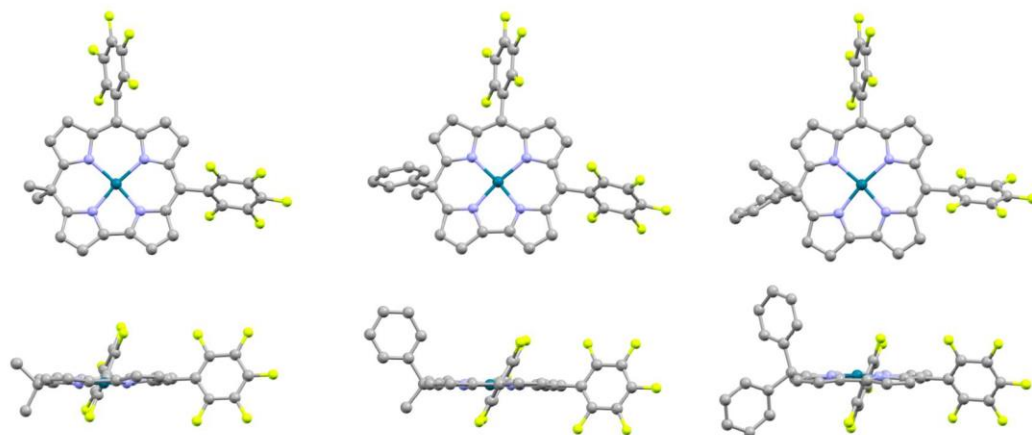


Figure 34 Crystal structure of metallo 5-isocorrole viewed from top and in profile, from left to right: Pd(5-DMIC) (first column), Pd(5-MPIC) (second column), Pd(5-DPIC) (third column).

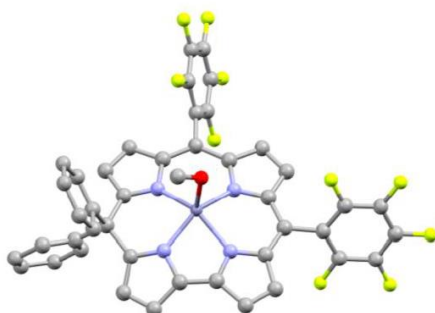


Figure 35. Crystal structure of Zn(5-DPIC) with a molecule of methanol as the fifth coordinated ligand.

Table 3.2. Relevant dihedral angles and atom distances measured for Pd(5-DMIC), Pd(5-MPIC), Pd(5-DPIC), and Zn(5-DPIC)

| | Pd[5-DMIC] | Pd[5-MPIC] | Pd[5-DPIC] | Zn[5-DPIC] |
|--|--|--|--|--|
| Dipyrromethane units and meso C₆F₅ groups | 68.15° (close to <i>sp</i> ³ meso carbon) | 63.85° (close to <i>sp</i> ³ meso carbon) | 66.47° (close to <i>sp</i> ³ meso carbon) | 78.81° (close to <i>sp</i> ³ meso carbon) |
| N–N separations(Å) | 69.73° | 73.42° | 68.94° | 67.03° |
| | 2.787(5) | 2.494(5) | 2.783(8) | 2.924(4) |
| | 2.496(5) | 2.784(5) | 2.502(7) | 2.793(4) |
| | 2.800(5) | 2.907(5) | 2.789(8) | 2.556(3) |
| | 2.895(5) | 2.784(5) | 2.913(7) | 2.723(4) |

| | | | | |
|---------------------|----------|----------|----------|----------|
| M–N distance | 1.920(4) | 1.934(4) | 1.964(6) | 2.013(3) |
| (Å) | 1.936(3) | 1.910(4) | 1.928(4) | 2.007(3) |
| | 1.968(3) | 1.967(4) | 1.931(6) | 2.012(2) |
| | 1.947(4) | 1.952(4) | 1.956(4) | 2.031(3) |

3.5.2 UV-vis Absorption Features

The absorption profiles of the two series of zinc 5-isocorrole (**Figure 36**) and palladium 5-isocorrole (**Figure 37**) were collected in methanol at room temperature under air. Their maximum absorption wavelength and extinction coefficient were summarized in **Table 3.3**.

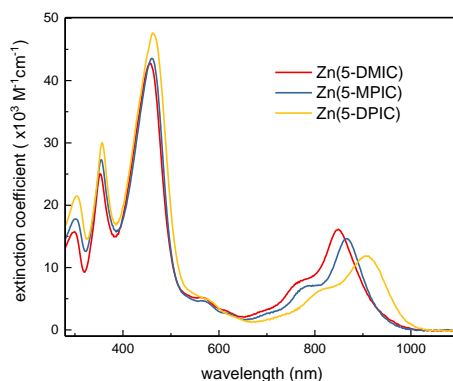


Figure 36 UV-vis spectroscopy of zinc 5-isocorrole derivatives in methanol at room temperature.

Comparing with the freebases, the metalation products displayed farther weak absorption from 800 – 1000 nm. Both absorption features for Zn(5-DPIC) and Pd(5-IC) tailed off at 1000 nm.

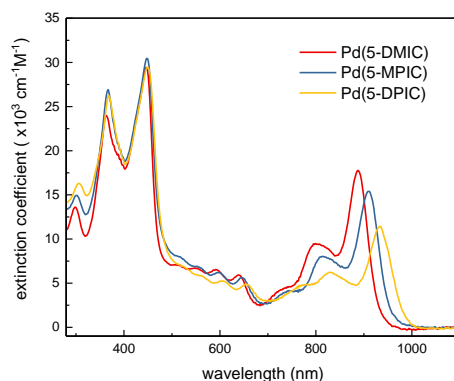


Figure 37 UV-vis spectroscopy of palladium 5-isocorrole derivatives in methanol at room temperature.

Table 3.3. The selected absorption maxima and its coordinated extinction coefficient

| Complexes | $\lambda_{\text{abs}}/\text{nm}$ ($\epsilon \times 10^3/\text{M}^{-1}\text{cm}^{-1}$) | $\lambda_{\text{abs}}/\text{nm}$ ($\epsilon \times 10^3/\text{M}^{-1}\text{cm}^{-1}$) |
|-------------------|--|--|
| Pd(5-DMIC) | 363 (24.0), 446.5 (29.4), 888 (17.8) | Zn(5-DMIC) 457 (42.8), 849 (16.1) |
| Pd(5-MPIC) | 367 (26.9), 448 (30.4), 910.5 (15.4) | Zn(5-MPIC) 460.5 (43.5), 868 (14.6) |
| Pd(5-DPIC) | 368 (26.3), 449.5 (29.4), 934.5 (11.5) | Zn(5-DPIC) 462 (47.6), 907 (11.8) |

3.6 Electrochemical properties of Freebase, Palladium 5-Isocorrole and Zinc 5-Isocorrole Derivatives

The cyclic voltammetry (CV) and differential pulse voltammetry (DPV) experiments of the 5-isocorrole freebase, Pd(5-IC) and Zn(5-IC) were carried out in anhydrous DCM under N₂ atmosphere with ferrocene as internal standard and TBAPF₆ as supporting electrolyte. Their CV and DPV plots are shown in **Figure 38**, **Figure 39** and **Figure 40** and the parent redox performances based on DPV are summarized in **Table 3.4**.

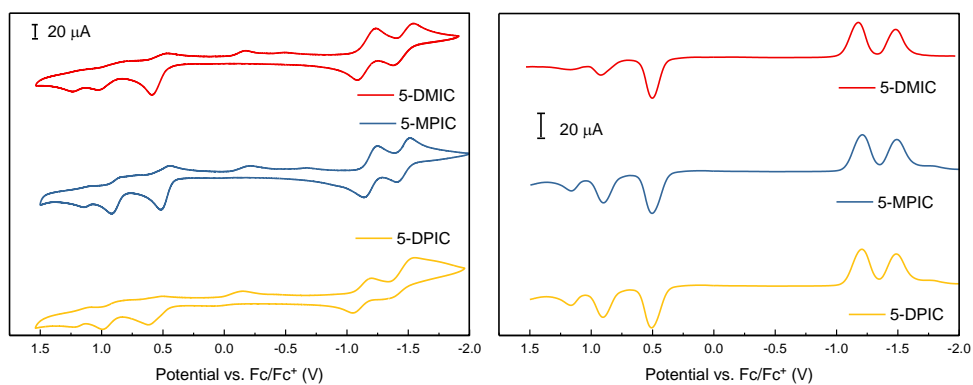


Figure 38 CV (left) and DPV (right) plots of 5-isocorrole freebase in anhydrous DCM under nitrogen.

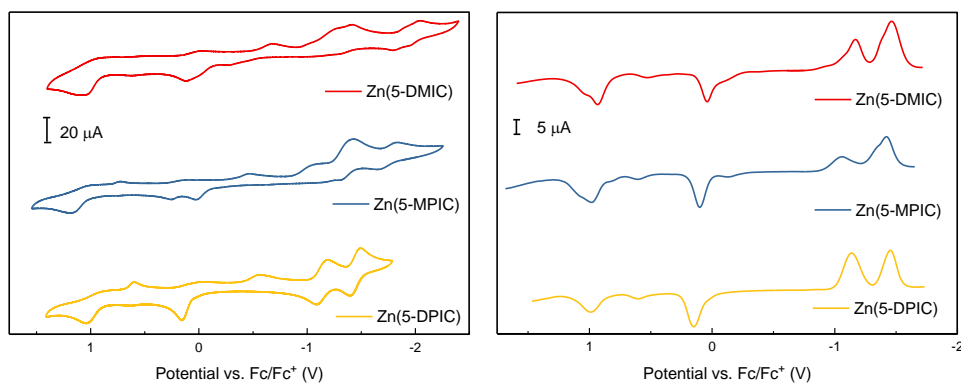


Figure 39 CV (left) and DPV (right) plots of Zn(5-IC) derivatives in anhydrous DCM under nitrogen.

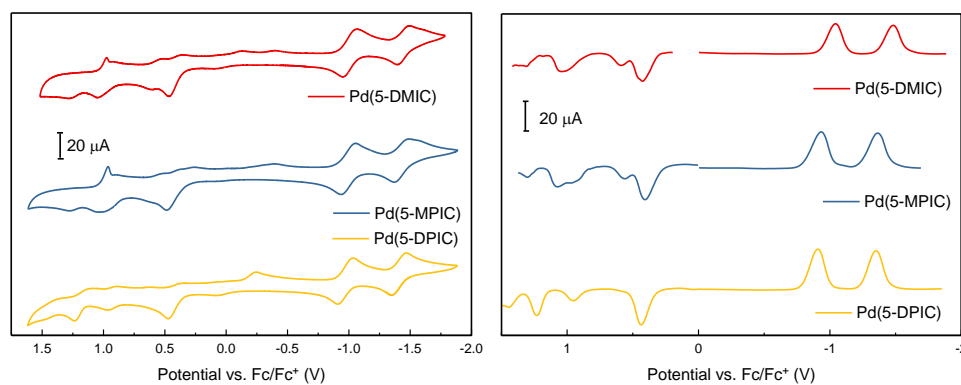


Figure 40 CV (left) and DPV (right) plots of Pd(5-IC) derivatives in anhydrous DCM under nitrogen.

For the 5-isocorrole freebases, they all displayed two reversible reduction peaks and three irreversible oxidation peaks. The redox window for the 5-DMIC was narrower than the one for 5-MPIC and 5-DPIC. The redox potentials for both 5-MPIC and 5-DPIC didn't show much difference. On the other hand, based on DPV plots, the third oxidation peak of 5-DMIC was much broader than the rest of two, so the potential for the third oxidation peak was omitted in **Table 3.4**.

However, after the metalation of Pd(II) cation, it displayed obvious potential shifts for all three palladium derivatives. Their redox performance windows are much narrower than the one for the freebase. Similar as the freebase, the palladium derivatives displayed two reversible reduction peaks, but more oxidation peaks than the freebase based on the DPV. It is interesting that in the oxidation region, Pd(5-DMIC) and Pd(5-MPIC) showed another weak oxidation property just following the first oxidation performance, which was 0.588 V and 0.560 V respectively. However, this performance disappeared for the Pd(5-DPIC).

The zinc derivatives also performed two $1e^-$ reductions and two $1e^-$ oxidations. Assume Zn(II) is electrochemically inactive, the two reduction peaks are ligand based reductions. The reduction potentials for the zinc derivatives are similar as the reduction potentials for the freebases, which prove the reduction performance are triggered by the ligand center. The zinc derivatives displayed one less oxidation peak compared with the freebases, which is probably caused by the insertion of Zn(II) cation.

Table 3.4 Redox properties of 5-isocorrole freebase, Pd(5-IC) and Zn(5-IC) based on DPV

| | E_{ox} (vs. Fc/Fc ⁺) (V) | E_{red} (vs. Fc/Fc ⁺) (V) |
|-------------------|---|--|
| 5-DMIC | 0.504, 0.920 | -1.176, -1.484 |
| 5-MPIC | 0.504, 0.900, 1.160 | -1.212, -1.492 |
| 5-DPIC | 0.508, 0.904, 1.164 | -1.208, -1.488 |
| Pd(5-DMIC) | 0.424, 0.588, 1.036 | -1.044, -1.480 |
| Pd(5-MPIC) | 0.408, 0.560, 1.068 | -0.936, -1.364 |
| Pd(5-DPIC) | 0.436, 0.952, 1.270 | -0.908, -1.352 |
| Zn(5-DMIC) | 0.044, 0.932 | -1.172, -1.464 |
| Zn(5-MPIC) | 0.100, 0.984 | -1.064, -1.420 |
| Zn(5-DPIC) | 0.156, 0.992 | -1.132, -1.456 |

3.7 Summary

In conclusion, in this chapter, the synthesis of 10,10-disubstituted biladiene, 5,5-disubstituted isocorrole and its zinc and palladium complexes were reported. The crystal structures of zinc and palladium derivatives of 5-isocorroles proved that both 10,10-disubstituted and 5,5-disubstituted isocorrole could serve as ligand platforms for metals such as zinc and palladium. The cyclic voltammetry plots displayed not only the freebase of 5-isocorrole had multi-redox electrochemistry, both zinc and palladium 5-isocorrole derivatives can also display multi-redox electrochemistry, which had narrower redox windows. The UV-vis spectra of 5-isocorrole freebase displayed weak absorption in the 600 – 800 region and this absorption features displayed red shift after metalation with Zn(II) and Pd(II) metal cation, which was 800 – 1000 nm. Furthermore, the more phenyl substituents, the higher extinction coefficient it had.

These near IR absorption features provide potential applications for light harvest study such as photodynamic therapy.

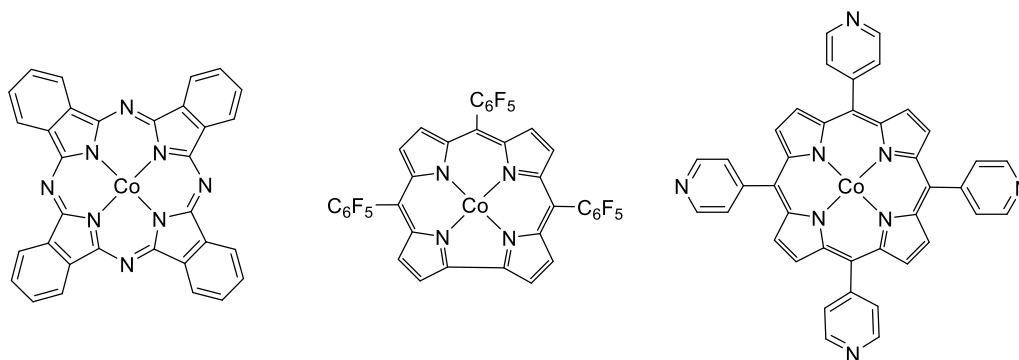
Chapter 4

OXYGEN REDUCTION REACTION CATALYZED BY TWO FAMILIES OF COBALT ISOCORROLE

4.1 Introduction

Platinum based catalysts are still considered as the most common cathode catalyst because it can reduce dioxygen through $4e^-$, $4H^+$ pathway to produce 100% H_2O ⁹². However, because of the durability and high cost of manufacturing, it is necessary for scientists to develop an efficient cathode catalyst with non-precious metal source^{25,37,93}. During the last few decades, cobalt catalysts have been investigated as inexpensive catalysts to enhance the oxygen reduction on the cathode of the fuel cells instead of platinum containing catalysts. Besides, cobalt complexes can form the relatively stable Co–O₂ adduct⁹⁴.

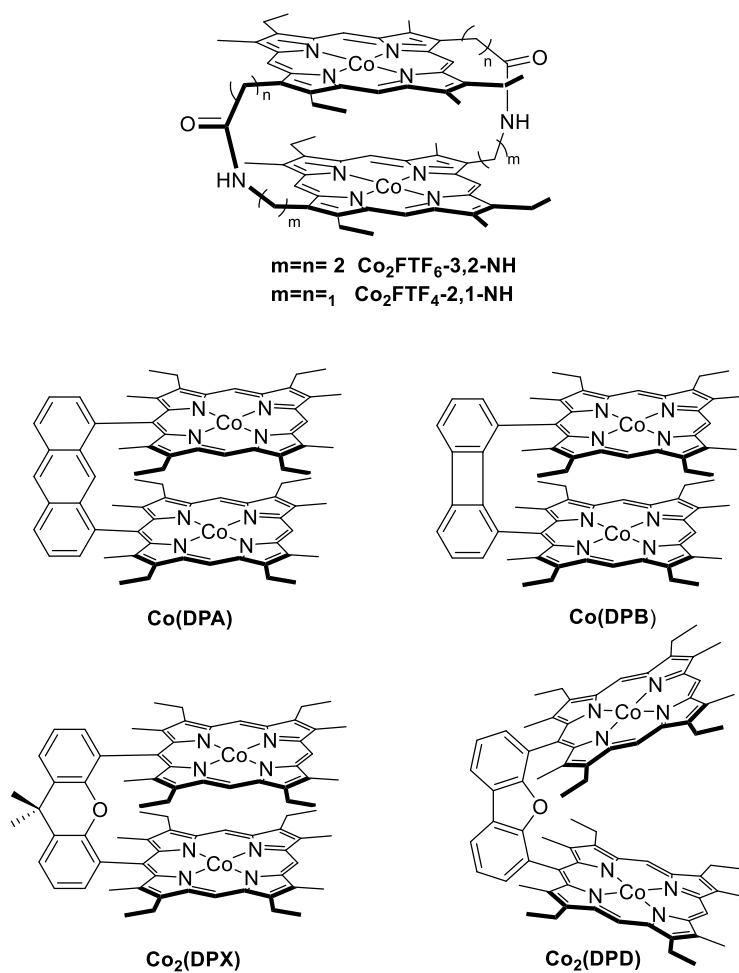
The first cobalt tetrapyrrole complex that showed ORR performance is cobalt phthalocyanine (CoPc)⁹⁵, as shown in **Scheme 4.1**, which was reported by Jasinski's group in 1964. It was immobilized on the surface of a nickel electrode and activated O₂ at -0.21 V vs. NHE. However, it just performed 100% H₂O₂ oxygen reduction product, which went through the $2e^-$, $2H^+$ pathway. Other cobalt catalysts, such as cobalt triphenylfluorophenylcorrole⁹⁶ (Co(tpfc)) and cobalt tetrapyrrolylporphyrin⁹⁷ (CoP(py)₄) (**Scheme 4.1**) also displayed the $2e^-$, $2H^+$ pathway for ORR.



Scheme 4.1. From left to right: cobalt phthalocyanine (CoPc), cobalt tri(pentafluorophenyl)corrole (Co(tpfc)) and cobalt tetrapyrrolylporphyrin (CoP(py)₄)

As time went, in order to enhance the O₂ reduction selectivity to water, designing catalysts with multilayers⁹⁸ is one of the efficient strategies. For example, many cofacial bis(cobalt) diporphyrins⁹⁹ with various linkages were prepared and quantified their ORR performance, shown in **Scheme 4.2**. This work was initially pioneered by Collman^{100,101}: cobalt porphyrins were connected through flexible amide linkages forming a “face to face” structure ([Co₂(FTF)]¹⁰². It was immobilized on edge plane graphite (EPG) electrode and performed high selectivity reduction of oxygen, from two to four electrons. However, the distance of the porphyrins had a strong impact on the selectivity for O₂ reduction. For instance, the Co₂FTF6-3,2-NH complex with five-atom linkages only performed 50% H₂O production at 0.5 V vs NHE, but the Co₂FTF4-2,1-NH complex with three-atom linkages could reduce O₂ completely to H₂O at more positive potential (0.7 V vs NHE). Other types of linkages²² have been synthesized to have a deeper understand of the distance, such as Co(DPA) and Co(DPB), they perform excellent 4e⁻, 4H⁺ pathway O₂ reduction to water around 0.4 V vs. NHE. To explore more cofacial cobalt catalyst, “Pacman” cobalt porphyrins^{22,101,103} were designed. Co₂(DPX) and Co₂(DPD) delivered 80% water production at 0.38 V vs. Ag/AgCl and 90% water production at 0.33 V vs.

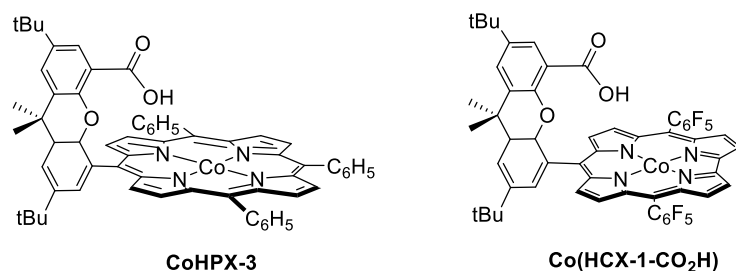
Ag/AgCl. The most recent cofacial cobalt catalyst for ORR was reported by Timothy Cook's group in 2017²⁴, which is a self-assembled cofacial cobalt porphyrin prism. It performed produce over 50% water at speed of 2500 rpm by using the RRDE technique with an onset potential at 0.0 V vs. Ag/AgNO₃. Later, he was able to increase the water production to 97% yield by switching to a shorter ruthenium containing linkage¹⁰⁴.



Scheme 4.2 Examples of cofacial cobalt catalysts

However, not all Pacman cobalt catalysts displayed high ORR selectivity product as water because the distance between the cofacial layer might hinder the protonation process and release of two-electron peroxo-type intermediates, resulting H_2O_2 as the major product. As a result, it was realized that the pK_a of the dioxygen adduct played an important role on the formation of water. Processes such as proton-coupled multi-electron transfer reactions (PCmET) were favored³⁶, which can facilitate the cleavage of dioxygen bond, instead of forming hydrogen peroxide.

Therefore, “Hangman” cobalt tetrapyrrole complexes^{25,26,105–107} as monomeric catalysts were also designed to investigate the ORR performance instead of the bimetallic systems, shown in **Scheme 4.3**. It is a kind of cobalt tetrapyrrolic complexes that poise an acid or base group over the face of the porphyrin macrocycle containing a cobalt metal center. It can adjust the pK_a of dioxygen intermediate and go through the proton-coupled multi-electron transfer process to promote the O–O bond cleavage. The CoHPX-3 yielded 71% water production at 0.8 V vs. NHE. Similar complexes as “hangman” corroles showed similar catalytic ORR selectivity.



Scheme 4.3. Examples of cobalt hangman tetrapyrrole complexes.

Furthermore, there are other type of cobalt tetrapyrrole catalysts that can promote the 4e^- , 4H^+ pathway reduction of O_2 , which imitated the natural cytochrome

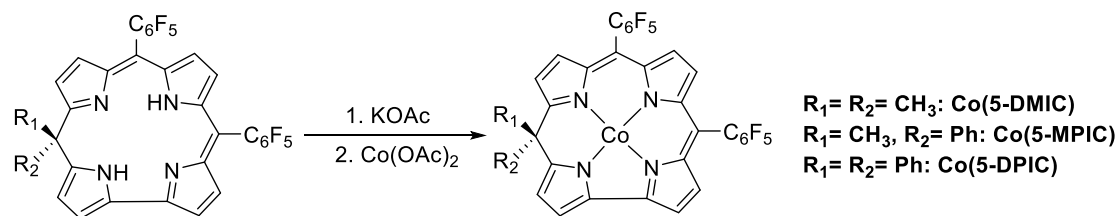
c oxidase model. One example of such cobalt catalysts was synthesized by Collman in 1997¹⁰⁸ that produced almost 95% water at around 0.2 V vs. NHE.

So far, tremendous progresses have been made for the development of cobalt tetrapyrrole catalysts for ORR, however, the fatal weakness of the cobalt catalysts above is the complicated synthesis and they cannot be prepared in large scales with high yield. For example, the $[\text{Co}_2(\text{DPX})]^{22,36,101}$ took 18 synthesis steps to prepare, yielding less than 1%. Also, to synthesize the CoHPX-3²⁶, it involved 9 steps of synthesis, which increased the cost for purification procedures and labors. The catalyst that Collman¹⁰⁸ designs in 1997, even though they did not report the total yield, but it is believed that the high cost purification techniques were needed, and the yield was low.

So, the challenge for the era of designing the new cobalt monomeric ORR catalysts is to synthesize the catalyst with large scale, low cost and simple purification processes, which perform high selectivity for O₂ reduction. As mentioned in Chapter 3, several tetrapyrrole ligand platforms have been prepared, so it is beneficial for us to take advantage of the existed ligand to synthesize the new series of cobalt catalysts using biladiene and 5-isocorrole freebases.

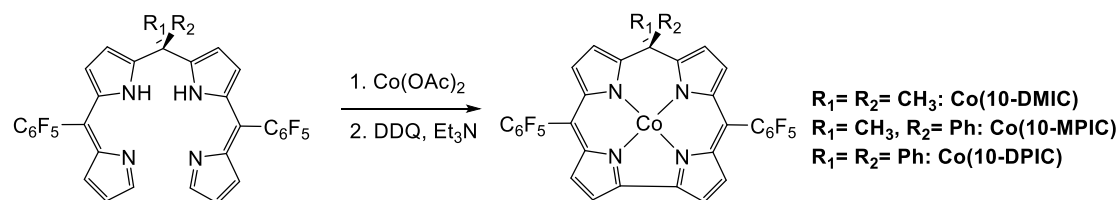
4.2 Synthesis and Characterization of Two Families of Cobalt Isocorrole Catalysts: Cobalt 5-isocorrole and Cobalt 10-isocorrole

As mentioned in Chapter 2, cobalt 5-isocorrole can be prepared through the metalation reaction with potassium acetate and cobalt acetate anhydrous reflux in anhydrous acetonitrile overnight in the inert atmosphere, shown in **Scheme 4.4**.



Scheme 4.4. Synthesis of cobalt 5-isocorrrole derivatives.

Cobalt 10-isocorrrole can be prepared through an oxidation reaction with DDQ and triethylamine after a direct metalation reaction with coordinated biladiene freebase and cobalt acetate anhydrous in CH₃CN (**Scheme 4.5**).



Scheme 4.5. Synthesis of cobalt 10-isocorrrole derivatives.

The detailed synthesis and characterization were provided in Chapter 2. Cobalt tetrapentafluorophenylporphyrin (Co(TPFPP)) and cobalt tripentafluorophenylcorrole (Co(TPFPC)) were also prepared according to the reported method as the control standard catalysts for RRDE experiments.

4.3 Electrochemistry and UV-vis Absorption Spectrometry for Cobalt Isocorrrole

Cyclic voltammetry and differential pulse voltammetry measurements for the both series of cobalt isocorrrole complexes were carried out in anhydrous CH₃CN under nitrogen, shown in **Figure 41** and **Figure 42**.

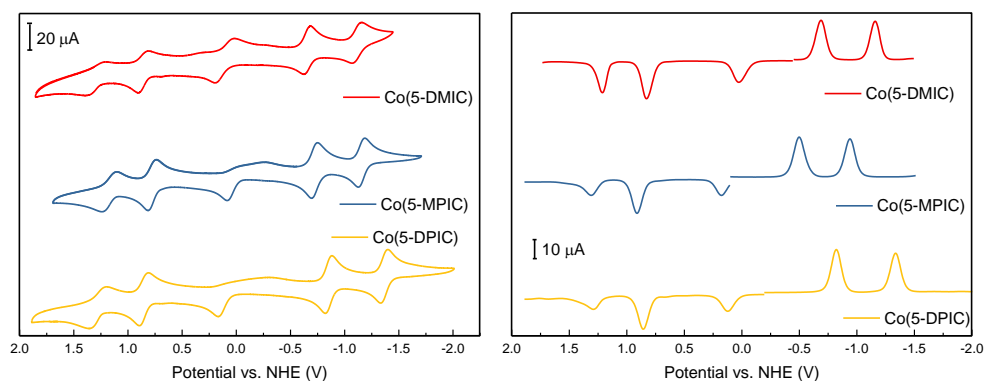


Figure 41. Cyclic voltammetry (left) at a scan rate of 100 mV/s and differential pulse voltammetry (right) of Co(5-DMIC), Co(5-MPIC) and Co(5-DPIC) in anhydrous acetonitrile under nitrogen.

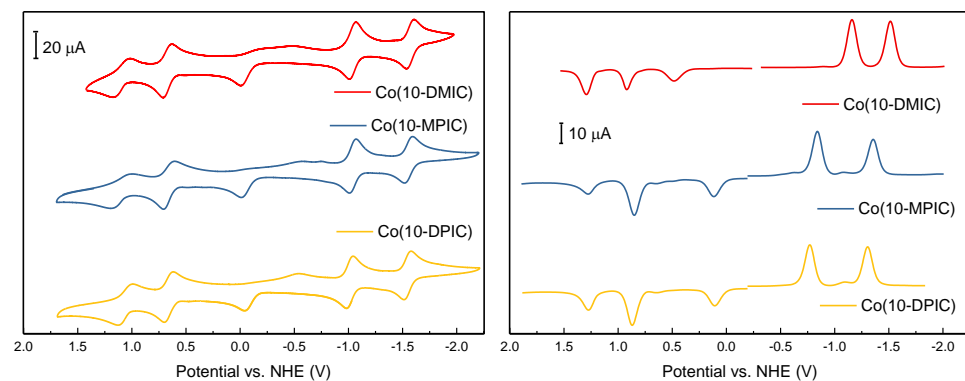


Figure 42. Cyclic voltammetry (left) at a scan rate of 100 mV/s and differential pulse voltammetry (right) of Co(10-DMIC), Co(10-MPIC) and Co(10-DPIC) in anhydrous acetonitrile under nitrogen.

All cobalt catalysts displayed two reversible reduction peaks and one irreversible oxidation peak, one reversible oxidation peak and a pseudo reversible oxidation peak, except Co(5-DMIC), which has two reversible oxidation peak and one pseudo reversible oxidation peak. The potentials were summarized according to the DPV spectrometry in **Table 4.1**. Both series of cobalt complexes performed multi-electron redox electrochemistry. In general, cobalt 5-isocorrole complexes had less

negative reduction potentials than cobalt 10-isocorrole complexes, but the difference of the reduction potentials was not significant.

Table 4.1. Redox potentials for cobalt isocorrole complexes according to DPV experiment.

| | Red. vs. NHE (V) | Ox. vs. NHE (V) |
|--------------------|------------------|---------------------|
| Co(5-DMIC) | - 0.686, - 1.158 | 1.214, 0.825, 0.025 |
| Co(5-MPIC) | - 0.495, - 0.939 | 1.313, 0.913, 0.181 |
| Co(5-DPIC) | - 0.819, - 1.335 | 1.293, 0.853, 0.121 |
| Co(10-DMIC) | - 1.158, - 1.514 | 1.294, 0.918, 0.482 |
| Co(10-MPIC) | - 0.839, - 1.355 | 1.277, 0.853, 0.113 |
| Co(10-DPIC) | - 0.771, - 1.307 | 1.277, 0.865, 0.133 |

The absorption profiles (**Figure 43**) for cobalt 5-isocorrole and cobalt 10-isocorrole differ a lot at the near IR region even though they were dark green after dissolving in the anhydrous THF. They all displayed strong Soret absorption around 450 nm and weak near IR absorption features farther than 700 nm. It is interesting that Co(5-DPIC) performed farthest near IR absorption and the λ_{\max} difference for Co(5-IC)s' near IR region is larger than the one for Co(10-IC)s.

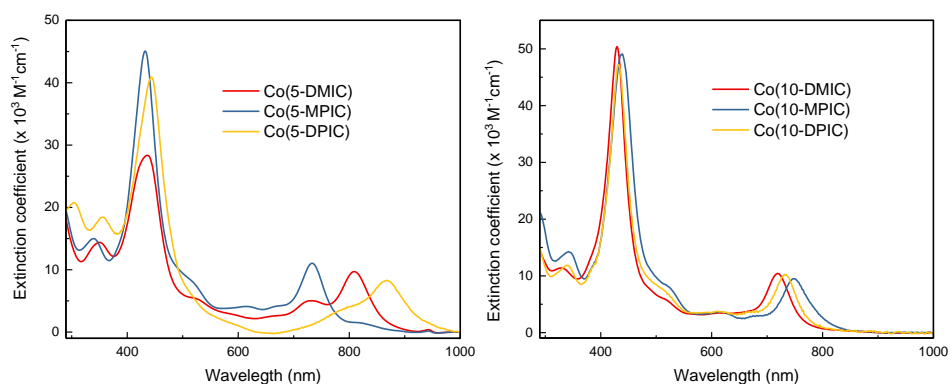


Figure 43. UV-vis absorption spectra of cobalt 5-isocorrole (left) and cobalt 10-isocorrole (right) in THF in the inert atmosphere.

4.4 Electrochemical O₂ Reduction by Cobalt Isocorroles as Heterogeneous Catalysts

The O₂ reduction reactivity of three cobalt catalysts was performed through rotating ring disc electrode (**RRDE**) technique. The illustration figure of the RRDE is shown in **Figure 44**. The most common electrochemical measurement method to quantify the catalytic performance of ORR for the catalysts is the RRDE technique^{109,110}. As the demonstrated figure shows, one RRDE is usually made up of a glassy carbon disk electrode and a platinum ring electrode, the materials for both electrodes can be exchanged to gold, copper or platinum, which depend on the requirements for the experiments¹¹¹. On the disk electrode, the catalyst ink is immobilized on the surface with Nafion. As the RRDE is rotating, the flow of the electrolyte which contains O₂ is moving constantly to the surface of the electrode. The O₂ reduction reaction happens at the disk electrode: the oxygen can be reduced to water through 4H⁺/4e⁻ pathway or to hydrogen peroxide through 2H⁺/2e⁻ pathway. Then, the formed H₂O₂ is forced to diffuse to the surface of the Pt ring electrode by the electrolyte flow. At the ring electrode, the H₂O₂ is reoxidized back to oxygen at a specific overpotential. So that, the catalytic performance of ORR for the catalysts can be analyzed by the current from both disk electrode (I_d) and ring electrode (I_r)¹¹².

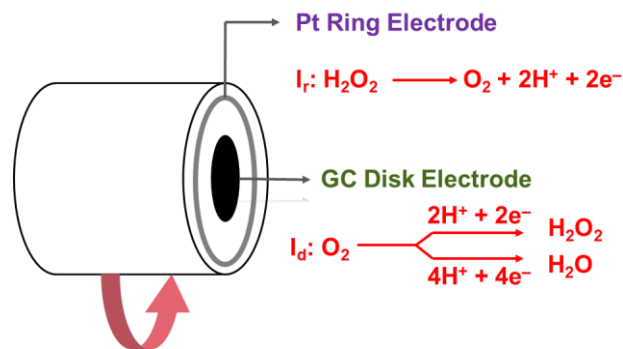


Figure 44 The demonstration figure of RRDE.

The catalyst ink is immobilized on the glassy carbon electrode (GCE), which the catalyst ink consists of multi-wall carbon nanotube (MWCNT) and 5% Nafion in THF. In an O₂-saturated 0.5 M H₂SO₄ electrolyte solution, the linear sweep voltammograms (LSVs) were recorded at 0, 100, 400, 900, and 1600 rpm rotation rates with the disk potential scanning cathodically at 20 mV/s¹⁰⁵. The oxidation potential for the platinum ring electrode was fixed at 1.23V (vs. Ag/AgCl). The number of electrons (n) transferred during the ORR process at 1600 rpm (**Figure 45**) and percentage yield for H₂O (H₂O%) and H₂O₂ (H₂O₂%) were calculated using both the disk and ring current density according to **Equation 4.4.1** and **Equation 4.4.2** and summarized in **Table 4.2**. Co(10-DMIC) showed highest water production at 1600 rpm around 85%, and it is interesting that as the number of phenyl groups increased for the Co(10-IC)s, we can switch the O₂ reduction selectivity from the 4-electron pathway to 2-electron pathway.

$$n = 4I_d / (I_d + I_r/N) \quad \text{Equation 4.4.1}$$

$$\% \text{ H}_2\text{O} = 100 \times (I_d - I_r/N) / (I_d + I_r/N) \quad \text{Equation 4.4.2}$$

where I_d is the disk current density, I_r is the ring current density, N is the collection coefficient which was determined to be 0.51 using the reversible [Fe(CN)₆]^{2-/3-} redox couple according to the manufacturer's instruction^{113,114}.

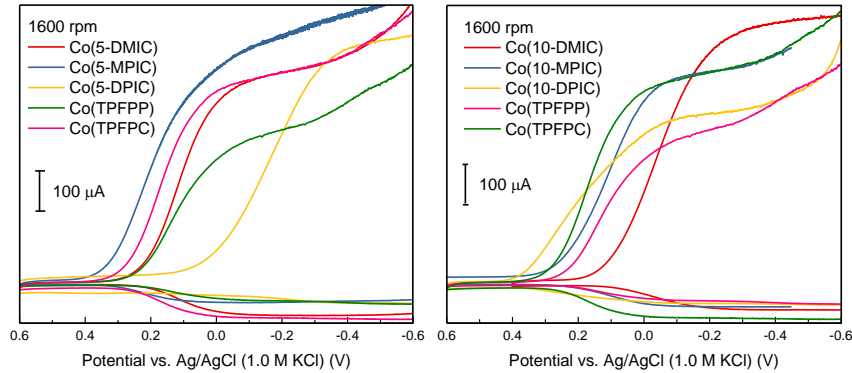


Figure 45. RRDE voltammetry of Co(5-IC) (left) and Co(10-IC) (right) with modified electrodes under O₂-saturated conditions in 0.5 M H₂SO₄ aqueous solution at 20 mV/s scan rate and 1600 rpm.

Table 4.2 Ring vs. Disk analysis results for cobalt catalysts at 1600 rpm.

| Ring vs Disk | n | H ₂ O% | H ₂ O ₂ % |
|--------------------|------------|-------------------|---------------------------------|
| Co(10-DMIC) | 3.5 ± 0.1 | 75.6 ± 4.6 | 24.4 ± 4.6 |
| Co(10-MPIC) | 3.0 ± 0.06 | 47.2 ± 3.3 | 52.7 ± 3.3 |
| Co(10-DPIC) | 2.5 ± 0.02 | 25.3 ± 1.2 | 74.7 ± 1.2 |
| Co(5-DMIC) | 3.1 ± 0.14 | 50.6 ± 7.2 | 49.4 ± 7.2 |
| Co(5-MPIC) | 3.3 ± 0.08 | 65.0 ± 4.1 | 35.0 ± 4.1 |
| Co(5-DPIC) | 3.2 ± 0.18 | 62.5 ± 8.0 | 37.6 ± 8.0 |
| Co(TPFPP) | 2.3 ± 0.04 | 15.5 ± 2.2 | 84.4 ± 2.2 |
| Co(TPFPC) | 2.2 ± 0.01 | 10.0 ± 0.6 | 90.0 ± 0.5 |

The Koutecky-Levich¹¹⁵ (KL) plots of reciprocal measured current density (j^{-1}) vs reciprocal square root of rotation rate ($\omega^{-1/2}$) were obtained (**Figure 41**) using the current density at the glassy carbon disc electrode of the RDE voltammograms. From the KL plots, the number of electrons for oxygen reduction and the kinetic current density (summarized in **Table 4.3**) can be determined on the basis of **Equation 4.4.3**.

Equation 4.4.3
$$\frac{1}{j} = \frac{1}{j_k} + \frac{1}{j_l} = j_k^{-1} + \frac{1}{0.62nFD_O^{2/3} \nu^{-1/6} C_O^*} \cdot \omega^{-1/2}$$

where j_k is kinetic current density, j_l is limiting current density, n is the number of electrons transferred, F is Faraday's constant (96485 C/mol), A is the electrode area (0.2475 cm²), D_o is the diffusion coefficient of O₂ (1.15 x 10⁻⁵ mol/cm³), ν is the kinematic viscosity of electrolyte (1.0 x 10⁻² V s⁻¹), C_o is concentration of O₂ (1.4 x 10⁻⁶ M), and ω is the angular rotation rate of the electrode (2 π f, f is revolutions per second).

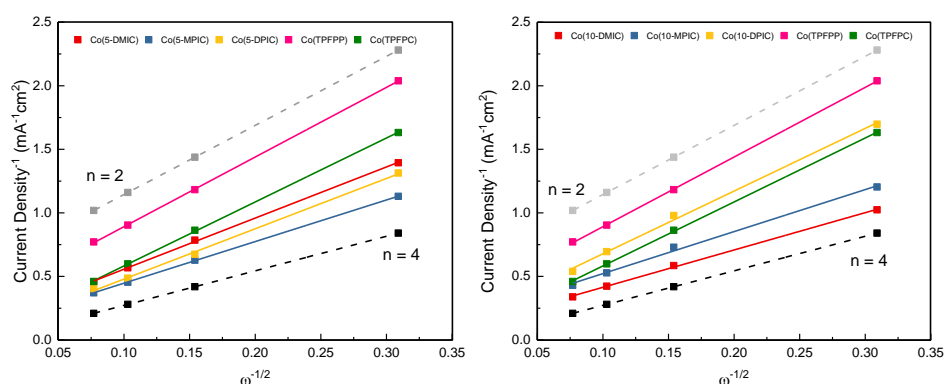


Figure 46. Koutecky-Levich plots for Co(5-IC) (left) and Co(10-IC) (right) with modified electrodes under O₂-saturated conditions in 0.5 M H₂SO₄ (the dashed lines represent the theoretical slopes for two-electron and four-electron ORR).

Table 4.3 Catalytic ORR performance for Co(5-IC) and Co(10-IC) based on Koutecky-Levich analysis method.

| KL analysis | n | H ₂ O% | J _k (mA/cm ²) | V _{onset} (vs. Ag/AgCl) |
|--------------------|------------|-------------------|--------------------------------------|----------------------------------|
| Co(10-DMIC) | 3.7 ± 0.19 | 85 ± 10 | 8.7 ± 2.5 | 200 mV |
| Co(10-MPIC) | 3.0 ± 0.18 | 48 ± 8 | 4.4 ± 1.0 | 350 mV |
| Co(10-DPIC) | 2.2 ± 0.11 | 8 ± 6 | 6.4 ± 0.9 | 420 mV |
| Co(5-DMIC) | 2.7 ± 0.18 | 30 ± 8 | 5.7 ± 1.3 | 320 mV |
| Co(5-MPIC) | 3.3 ± 0.16 | 65 ± 8 | 7.8 ± 1.5 | 450 mV |
| Co(5-DPIC) | 2.8 ± 0.18 | 40 ± 9 | 8.2 ± 1.8 | 150 mV |
| Co(TPFPP) | 2.3 ± 0.3 | 15 ± 15 | 2.4 ± 0.5 | 250 mV |
| Co(TPFPC) | 2.0 ± 0.04 | 0 ± 2 | 5.5 ± 1 | 350 mV |

4.5 Summary

In summary, two series of cobalt monomeric isocorrole catalysts had been prepared. They were basically characterized by high-resolution mass spectroscopy, NMR spectroscopy and X-ray crystallography. They displayed extraordinary multi-redox electrochemistry and rich photophysical properties according to cyclic voltammetry and UV-vis spectroscopy experiments. Their performance toward oxygen reduction reaction were quantified by rotating ring disk electrode technique. Co(10-DMIC) displayed best ORR catalytic performance, based on both KL and Ring vs. Disk analysis methods. Co(10-DMIC) facilitated the reduce of O₂ to H₂O by 3.7 ± 0.2 electrons, with the most significant kinetic performance, which is 8.7 ± 2.5 mA/cm². The Ring vs. Disk analysis at 1600 rpm data also confirmed Co(10-DMIC) produced highest yield of water production, which is around 80%. For the cobalt 10-isocorrole series, we can turn the oxygen reduction reaction product form water to 100% hydrogen peroxide by substituting the two methyl groups on the *sp*³ hybridized *meso*-position to one/ two phenyl groups. However, the cobalt 5-isocorrole series showed closer all around 3-electron ORR products, which are 50% water and 50% hydrogen peroxide.

Chapter 5

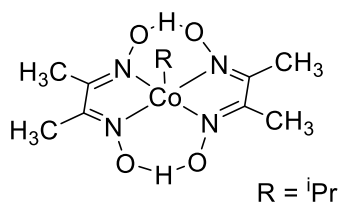
SYNTHESIS OF 1-PHENETHYLOXYCARBONYL COBALT 10,10-DIMETHYL-5,15-BIS(PENTAFLUOROPHENYL)-ISOCORROLE AND ITS Co-C BOND PHOTOCLEAVAGE

5.1 Introduction

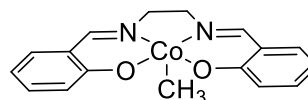
Coenzyme B12 and its correlated analogues (e.g. adenosylcobalamin, methylcobalamin, etc.) have been studied extensively because they are regarded as one of the most complicated cobalt complexes that can be found in nature. Cobalt corrinoid is the core structure of these coenzyme B12 and its derivatives. Vitamin B12, which is a commercially available nutrition supplement for human beings, is an inactivated form of coenzyme B12 containing axial ligands such as methyl, 5'-deoxyadenosyl and hydroxyl groups. The cobalt corrinoid works as a key center for the important biological catalytic cycles among the nature. These processes can be classified to four main groups⁴⁰: B12-dependent methyl transfers, isomerases and ribonucleotide reductases, dehalogenases and others. The mechanisms for the B12-dependent biocatalytic processes have been investigated in very detailed. It has been proved that these reactions are started with a homolytic Co-C bond cleavage process to generate a carbon centered radical and cobalt(II) corrinoid. The Co(II) corrinoid intermediate can be then reduced to Co(I) species and rebinding the coordinated alkyl precursor to regenerate the radicals. Many cobalt complexes systems with different ligand platforms such as salen, salophen, dimethylglyoxime and porphyrin have been developed to imitate the homolysis procedure through irradiation or heating to realize

the carbon centered radical release. Systems like alkyl Co(III) complexes, acyl Co(III) complexes and Co(III) alkoxy carbonyl complexes, shown in **Scheme 5.1**, have been studied widely.

Alkyl Co(III) Complex

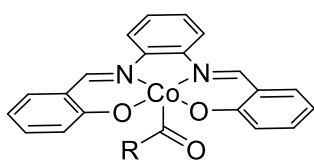


Co dimethylglyoxime



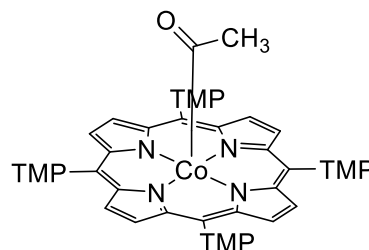
Co salen

Acyl Co(III) Complex



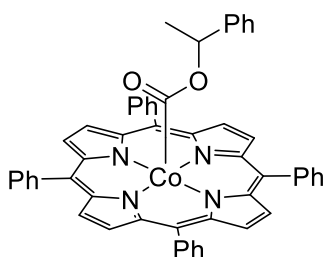
R = Et, CH₂^tBu

Co salophen

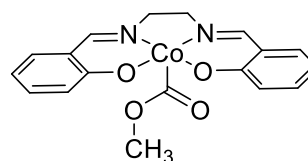


Co porphyrin

Alkoxy carbonyl Co(III) Complex



Co porphyrin



Co salen

Scheme 5.1 Co(III) complexes with alkyl, acyl and alkoxy carbonyl groups as axial ligand and porphyrin, salen, salophen and dimethylglyoxime as ligand platforms.

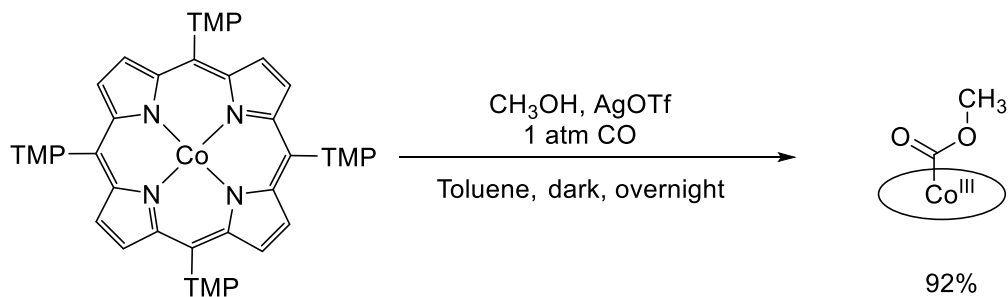
The alkyl Co(III) complexes, as well as the acyl Co(III) complexes have been applied as a radical initiator for organic synthesis and polymerization chemistry. For

example, acyl radical from the cobalt salen complex can be released after irradiation and then get involved in the Michael addition type C–C bond formation with alkenes reaction¹¹⁶. Cobalt-mediated intramolecular radical cyclization reactions is also reported by using sodium Co(I) salen complex and iodo/bromoarylallyl compounds as precursors to form Co(III) intermediates, then this Co(III) intermediates can go through the light introduced radical formation and go back to Co(II) product¹¹⁷. Another intramolecular Heck-type cross coupling reaction between olefins and alkyl iodides with irradiation at 465 nm is catalyzed by cobalt dimethylglyoxime complex, with triphenyl tin or isopropyl groups as axial binding ligand¹¹⁸. Acrylate polymerization reactions can be controlled by acyl cobalt porphyrin¹¹⁹. Several new alkoxy carbonyl Co(III) porphyrins have been synthesized and examined to release alkyl radicals and a molecule of carbon monoxide with absorption of green/blue light¹²⁰. So we are interested in if we can utilize the Co(10-DMIC) reported in Chapter 2 and Chapter 4, which displays unique electrochemical (multi-redox) and strong absorption in both Soret and near IR regions features to realize the photo-introduced Co–C bond cleavage, especially from the Co(III) alkoxy carbonyl complexes.

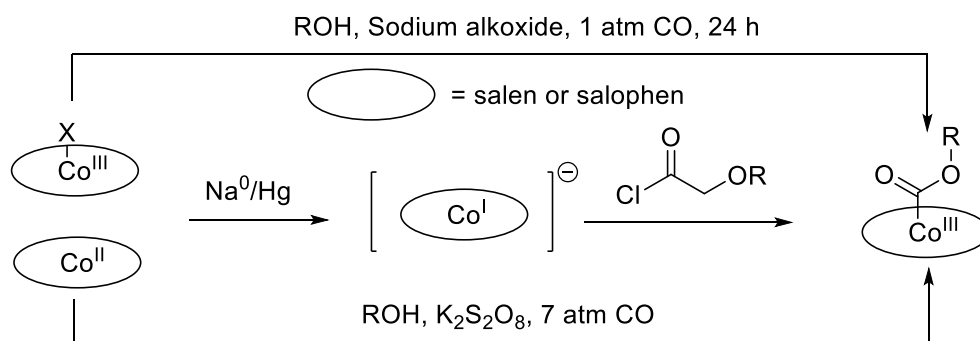
Even though many cobalt complexes mentioned before have been synthesized and characterized, the synthetic approaches for these complexes are still limited. There are three main strategies, shown in **Scheme 5.2**. The first method that reported by Xuefeng Fu's group only tolerated the methyl group¹¹⁹. For the second strategy, it is usually started with Co(II) or Co(III) halide complexes and reduced by toxic sodium amalgam followed by adding expensive acid chloride or chloroformate reagents. Or it is oxidized by potassium persulfate with alcohol and high pressure of CO gas¹²¹. The most recent reported method by David B. C. Martin's group is that the Co(III)

porphyrin product can be synthesized with DDQ, different sorts of alcohols and 7 atm CO gas¹²⁰. As a result, there are still space for us to explore the synthetic methods.

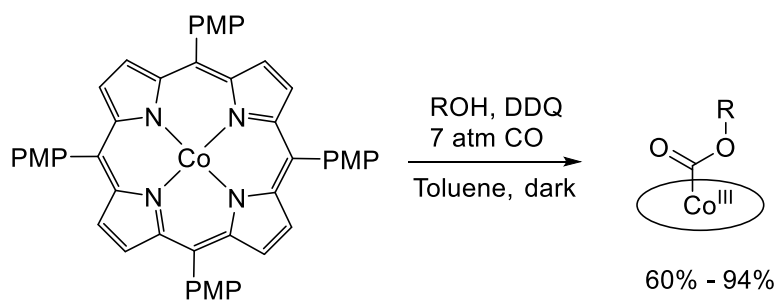
1.



2.



3.

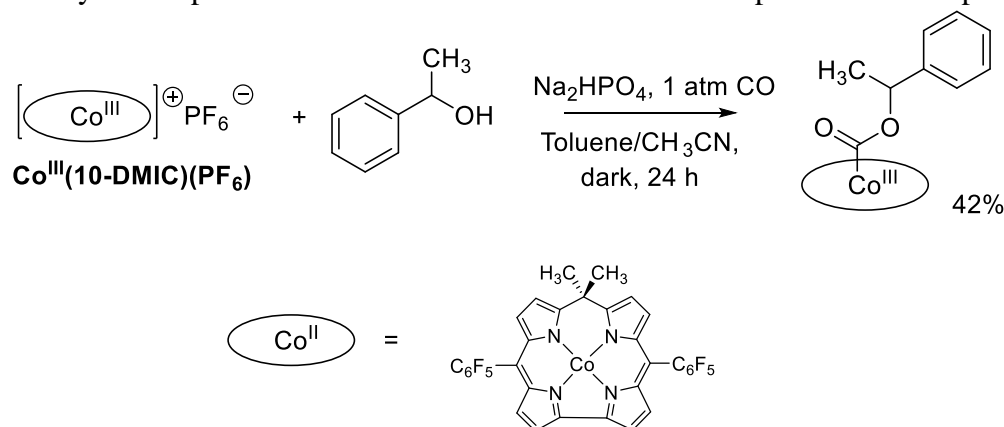


Scheme 5.2 Synthesis approaches for Co(III) complexes

5.2 Synthesis of 1-phenyloxycarbonyl cobalt 10,10-dimethyl-5,15-bis(pentafluorophenyl) isocorrole

To test if our Co(10-DMIC) can be activated by carbon monoxide and alcohols with an oxidant, the first trial was carried out by dissolving 33 mg (0.05 mmol)

Co(10-DMIC), 7 mg DDQ, 0.1 mL distilled benzenemethanol in a sealed round bottom flask and charged with 1 atm CO. The mixture was stirred for 1 day under CO atmosphere at room temperature. The reaction was monitored by NMR spectroscopy, no desired product was found by crude NMR. Several trials had been carried out also, and finally, the synthesis method was determined by stirring the mixture of Co(III)(10-DMIC), sodium phosphate and benzenemethanol under 1 atm CO atmosphere in anhydrous toluene/acetonitrile at room temperature for 24 hours, as shown in **Scheme 5.3**. The synthesis procedure and characterization details were provided in Chapter 2.



Scheme 5.3 Synthesis of Co(III) target complex

5.3 Irradiation study of 1-phenyloxycarbonyl cobalt 10,10-dimethyl-5,15-bis(pentafluorophenyl) isocorrole

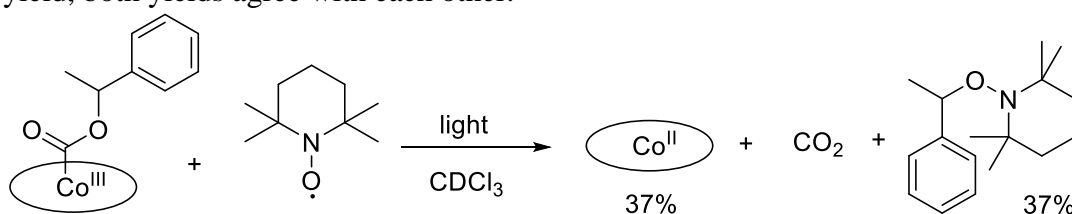
The irradiation study was monitored by both NMR spectroscopy and UV-vis spectroscopy methods.

5.3.1 NMR Spectroscopy Method

The primary irradiation study was carried out by using a halogen lamp as light source. Around 5 mg of Co(III) product was dissolved in CDCl_3 in a J-Young tube.

The J-Young tube was placed in a water filled beaker so that heat could be avoided as an extra energy source during the irradiation. The crude NMRs were collected every two hours before and after the irradiation. **Figure 47** is showing how the crude NMRs look like after the irradiation: after the 2-hour irradiation, the signals for the diamagnetic Co(10-DMIC) (**Figure 48**) showed up and after the 4-hour irradiation, the signals for Co(10-DMIC) increased and the intensity of the signals no longer increased after the 6-hour irradiation. So that we can conclude that 6-hour is long enough to realize the Co–C bond dissociation chemistry. However, from the crude NMR, the other product ethylbenzene was hard to find. To confirm that it was a radical dissociation mechanism in the period of irradiation process, (2,2,6,6-Tetramethylpiperidin-1-yl)oxyl (TEMPO) was added as a radical trap to examine the proposed mechanism.

In an oven dried J-Young tube, around 5 mg of Co(III) product, 2 mg (2.5 equiv) TEMPO and 0.5 mg of 1,3,5-trimethoxybenzene (TMB) as internal NMR yield standard were dissolved in CDCl₃. The similar experimental procedure was carried out to get the NMR results. Fortunately, the trap product (**Scheme 5.4**) could be quantified by the internal standard of TMB, which is 37%. The Co(10-DMIC) also had 37% yield, both yields agree with each other.



Scheme 5.4 The radical trap experiment

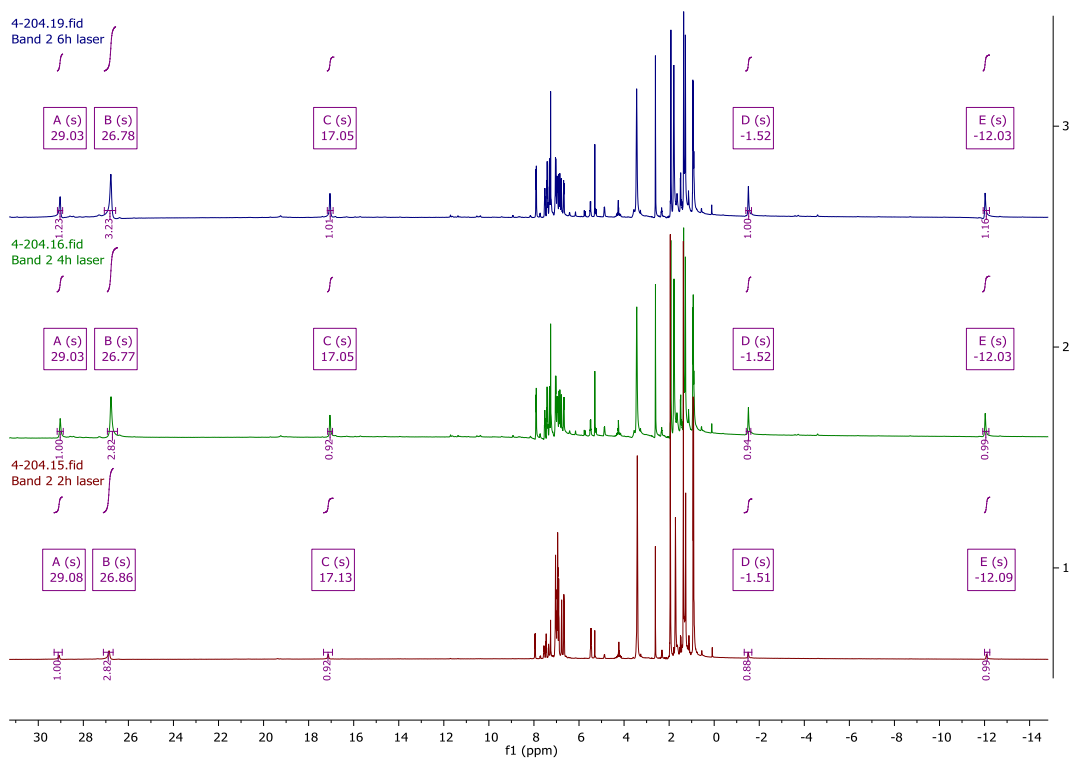


Figure 47 Time-related NMR spectroscopies during the irradiation with halogen lamp every two hours: from bottom to top is 2 hours, 4 hours and 6 hours' irradiation

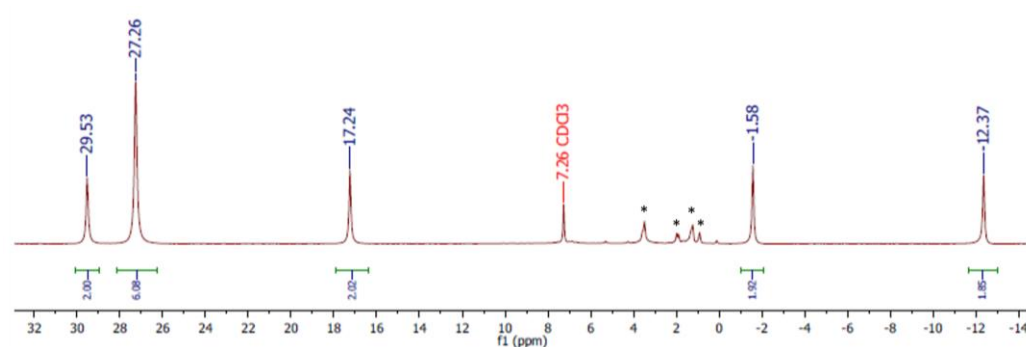
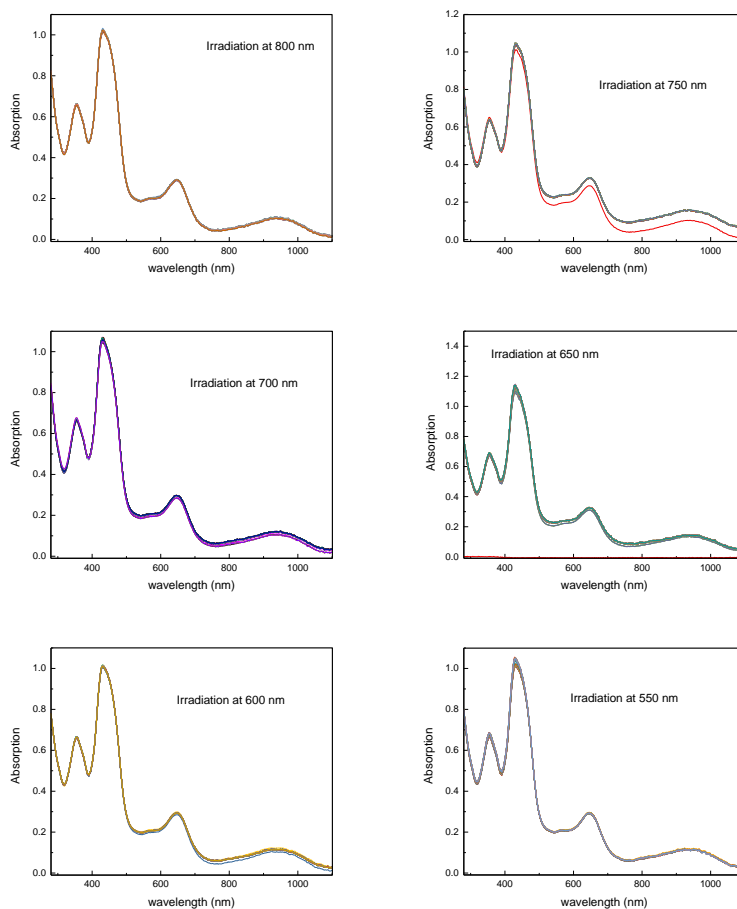


Figure 48 NMR of Co(10-DMIC) in CDCl₃ at room temperature.

5.3.2 Episodic Capture of UV-vis spectra

Because we are interested in exploring the which region of the light triggered this bond cleavage process, UV-vis absorption experiments were carried out as a more efficient monitor method instead of NMR spectroscopy. The UV-vis spectra were collected every 5 minutes. In a sealed 7Q UV-vis cuvette, 20 mM of Co(III) complex and 45 mM TEMPO in anhydrous DCM were prepared. The cuvette was then irradiated by the halogen lamp with different light filters at 800, 750, 700, 650, 600, 550, 500 and 450 nm. The UV-vis data were plotted below, as shown in **Figure 49**.



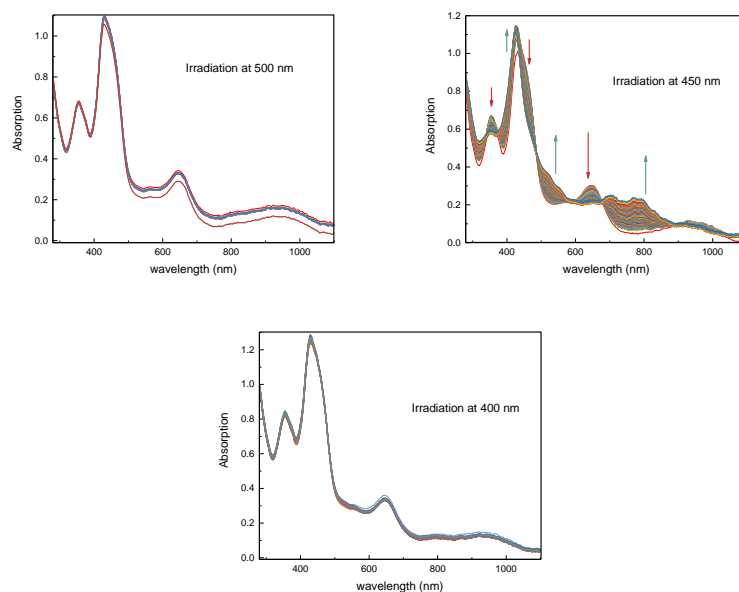


Figure 49. The episodic capture of UV-vis spectra of Co(III) complex by irradiation at wavelength of 400, 450, 500, 550, 600, 650, 700, 750 and 800 nm.

Unfortunately, absorption features only changed by irradiation at 450nm (Figure). To determine if the product is Co(10-DMIC) after the irradiation, beer's law experiment was performed and for comparison, the absorption features of Co(III) precursor was also collected, as shown in **Figure 50**. For the Co(10-DMIC), it displayed unique near IR absorption characterizations at 700.5 nm ($9.43 \times 10^3 \text{ M}^{-1}\text{cm}^{-1}$) and 780 nm ($5.67 \times 10^3 \text{ M}^{-1}\text{cm}^{-1}$), which agreed with the episodic UV-vis spectra on the left. What is interesting that by adding the fifth axial ligand to Co(10-DMIC), the soret absorption decreased a lot from $50.32 \times 10^3 \text{ M}^{-1}\text{cm}^{-1}$ (425.5 nm) to $24.83 \times 10^3 \text{ M}^{-1}\text{cm}^{-1}$ (430.5 nm). As a result the conversion yield was calculated by measuring the first and last absorption intensities of Co(III) starting material and Co(II) product, which is 39%, the yield for the trap product was calculated by NMR spectroscopy, which is 37%. The two numbers agreed with each other.

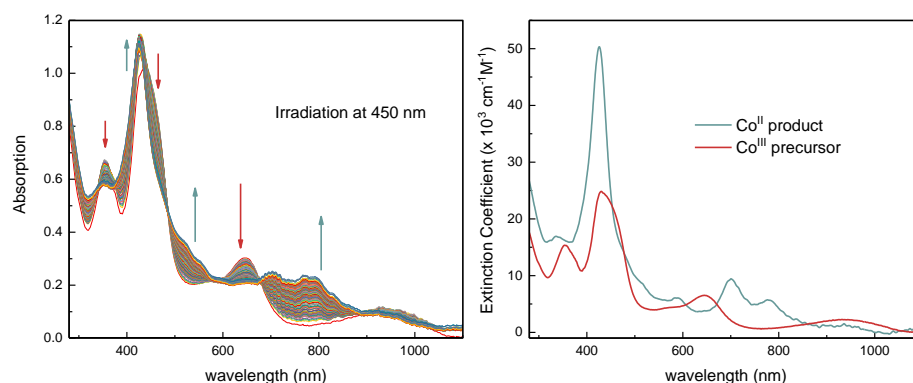


Figure 50. Left: Zoomed in episodic capture UV-vis spectra of Co(III) starting material by irradiation at 450 nm. Right: UV-vis spectra of Co(10-DMIC) (green) and the Co(III) starting material (red).

5.4 Summary

A new cobalt(III) 1-phenyloxycarbonyl complexes with 10,10-dimethyl isocorrole as the ligand platform has been synthesized and characterized by NMR spectroscopy, high resolution LIFDI mass spectrometry and UV-vis absorption experiments. It displays extraordinary absorption features from 800 – 1100 nm, however, this Co(III) product can only perform the Co–C bond cleavage reaction with the irradiation at 450 nm, which doesn't make use of the unique absorption features in the near IR region. Further studies can be carried out to understand why the longer wavelength absorption does not trigger the photocatalytic radical production process. The Co–C bond cleavage is proved to be a radical process which was confirmed by TEMPO as the radical trap. This approach also provides a new method by utilizing the abundant alcohol source to produce deoxygenation products.

Chapter 6

DEVELOPMENT OF A FAMILY OF PALLADIUM BILADIENE DERIVATIVES VARYING AT THE sp^3 HYBRIDIZED *meso*-POSITION

6.1 Introduction

Current FDA-approved PDT agents are chlorin and bacteriochlorin like tetrapyrrole structures which is based on porphyrin. The most widely used around the world is a haematoporphyrin derivative called Photofrin^{50,52}, as shown in **Figure 51**. Photofrin was the first photosensitizer that approved by FDA for photodynamic therapy: it is a mixture of monomers, dimers and oligomers that hematoporphyrin is treated with acetic acid and sulfuric acid with partial purification to get rid of the most monomers^{122,123}. This preparation method hampers the wide use of it because its reproducibility varies batch by batch¹²⁴, meaning that it is hard for the industries to control the qualities of the drug products. In addition, Photofrin performs a low extinction coefficient at longer wavelengths and only absorbs out to 630 nm where the tissue penetration depth is 2 to 3 mm¹²⁵. It also takes Photofrin about 6 to 10 weeks to metabolize it completely, which means that the patients must avoid light exposure during the metabolism process.

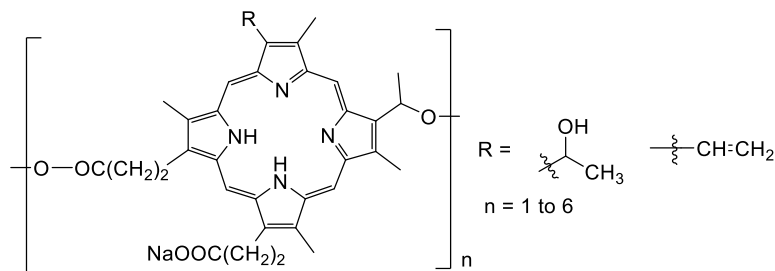


Figure 51 Structure of Photofrin

A large amount of second generation of photosensitizers^{15,53,125} have been synthesized and studied to cover the shortcomings of Photofrin, shown in **Figure 52**. Even though these compounds are monomers with high ¹O₂ quantum yields, they still have various drawbacks. For example, Purlytin and Foscan can cause skin photosensitivity after treatment; Protoporphyrin does not absorb well within the therapeutic window; Silicon and Tookad Phthalocyanine's poor water solubility; complicated synthetic procedure and poor stability of Verteporfin, Lutrin and Photochlor. Consequently, research aimed at identifying improved photosensitizers is ongoing.

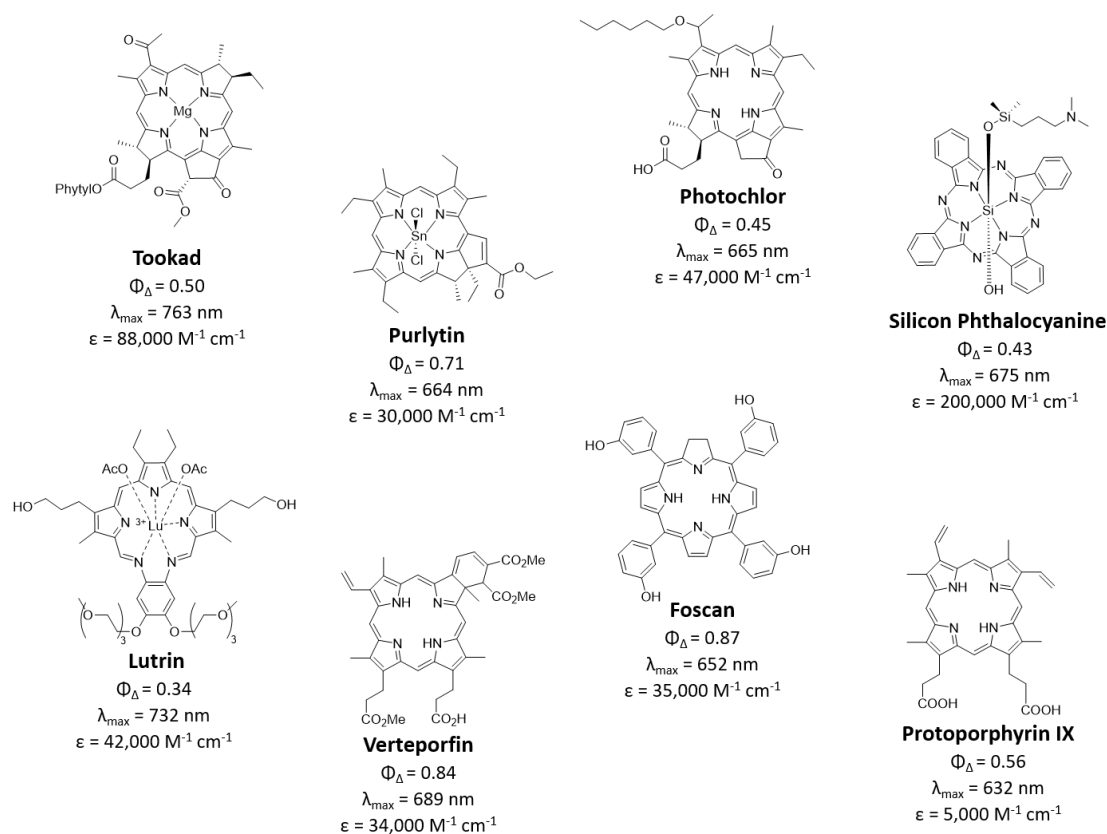
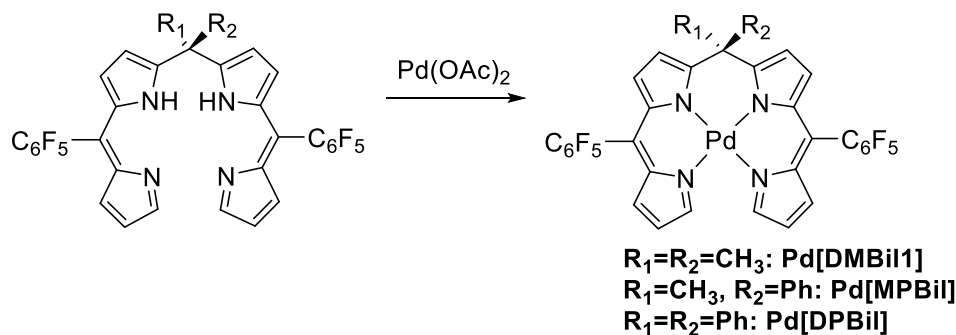


Figure 52. Second generation of porphyrinoid photosensitizers for PDT

6.2 Synthesis and Characterization of Palladium Biladiene Derivatives: Pd[MPBiI] and Pd[DPBiI]

The palladium biladiene derivatives were synthesized by stirring biladiene freebase with excess Pd(OAc)₂ in acetonitrile at 60°C for 4 hours (**Scheme 6.1**). The crude product was purified by silica column chromatography with DCM/hexanes as eluent to get the red solid product. The detailed synthesis and characterizations including NMR spectroscopy and high-resolution mass spectroscopy were presented in Chapter 2.



Scheme 6.1 Synthesis of palladium biladiene derivatives

The crystal structures of Pd[MPBiI] and Pd[DPBiI] are shown in

Figure 53 from a profile and above view, combining the crystal structures of Pd[DMBiI] we reported before¹²⁶. Pd(II) metal cations show similar coordination to the four nitrogen atoms on the pyrrole units as the previous reported Pd[DMBiI]. Based on all the crystal structures, they do not satisfy the square planar geometry of d⁸ metal species which is commonly displayed in the traditional palladium tetrapyrrole complexes¹²⁷. This is probably due to the steric interaction between the protons on C1 and C19 of the biladiene ligand scaffolds. Similar as the Pd[DMBiI], the meso-

pentafluorophenyl rings are almost perpendicular for both Pd[MPBil] and Pd[DPBil], **Table 6.1** summarizes these and other significant dihedral angles for both species. The Pd-N bonds for Pd[MPBil] range from 2.009–2.015 Å and 2.005–2.031 Å for Pd[DPBil], both within previously published palladium tetrapyrroles including Pd[DMBil1]’s 2.000–2.043 Å. These characteristics are important to indicate that the core structures of palladium tetrapyrrole for each complex do not change significantly from one another, signifying that any other physical variations are due to the electronic effects of the substitution of the phenyl rings.

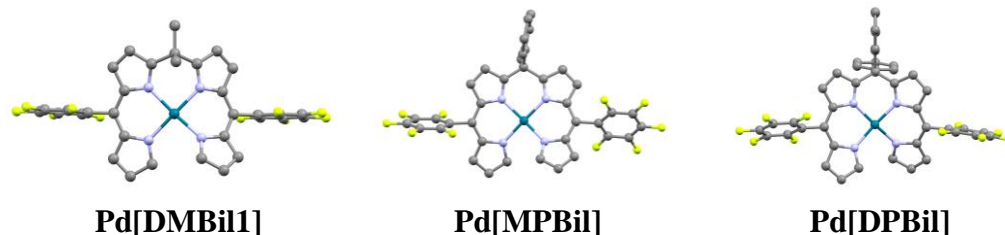


Figure 53 Crystal structures of Pd[DMBil1] left, Pd[MPBil] (middle) and Pd[DPBil] (right)

Table 6.1 Relevant dihedral angles measured for **Pd[MPBil]** and **Pd[DPBil]**, including the **Pd[DMBil1]** for comparison.

| Dihedral angles between | Pd[DMBil1] | Pd[MPBil] | Pd[DPBil] |
|---|------------|-----------|-----------|
| Interior pyrroles^a | 44.73° | 16.92° | 31.84° |
| Terminal pyrroles^b | 52.74° | 49.58° | 51.50° |
| Dipyrromethane units | 83.02° | 81.64° | 70.62° |
| and meso C₆F₅ groups | 83.80° | 69.75° | 70.41° |

^aThe DMBil1 interior pyrroles are the pyrroles connected to the sp³-hybridized meso carbon.

^bThe DMBil1 terminal pyrroles are the pyrroles on the open end of the tetrapyrrole scaffold.

6.3 Electrochemistry and UV-Vis Study of Pd[MPBil] and Pd[DPBil]

The electrochemical experiments were carried out by using a method of cyclic voltammetry (CV) and differential pulse voltammetry (DPV) in anhydrous dichloromethane with 0.1 M TBAPF₆ as supporting electrolyte under N₂ atmosphere. The CV and DPV plots for the three Pd(II) complexes are shown in **Figure 54**, and their parent redox potentials were summarized in the **Table 3**.

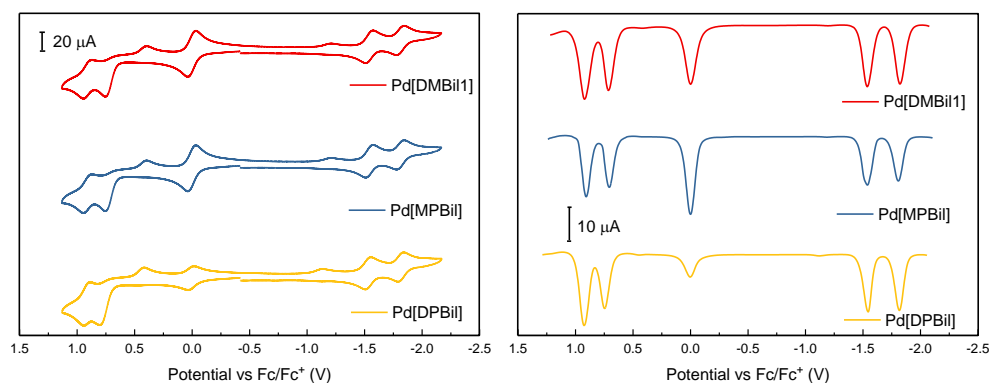


Figure 54 CV and DPV of Pd[DMBil1], Pd[MPBil] and Pd[DPBil] in anhydrous DCM under N₂ with ferrocene as an internal standard.

Comparing with the Pd[DMBil1], the other two palladium biladiene derivatives performed similar electrochemical redox performance of two 1e⁻ reductions and two 1e⁻ oxidations versus Fc/Fc⁺. Based on both CV and DPV plots (**Figure 54**), the first reduction potential for Pd[DMBil1] is -1.536 V (vs Fc/Fc⁺). The first reduction potential for Pd[MPBil] and Pd[DPBil] are -1.536 V and -1.540 V respectively. The second reduction potential is -1.822 V, -1.808 V and -1.816 V for each of the Pd(II) complexes. The two oxidation potentials for each Pd(II) for Pd[DMBil1] was 0.922 V and 0.712 V; Pd[MPBil] was 0.908 V and 0.708 V and Pd[DPBil] was 0.924 V and 0.746 V. According to the electrochemical performance

of three Pd(II) complexes, incorporating one or two phenyl groups on the sp^3 -hybridized *meso*-position doesn't change the electronic properties.

The UV-vis absorption spectra of Pd[DMBi1], Pd[MPBi1] and Pd[DPBi1] in MeOH are displayed in **Figure 55**. It is interesting that as the number of phenyl substituents increases, the extinction coefficient increased. Specifically, at 482 nm, the extinction coefficient of Pd[DPBi1] almost doubled comparing with Pd[DMBi1].

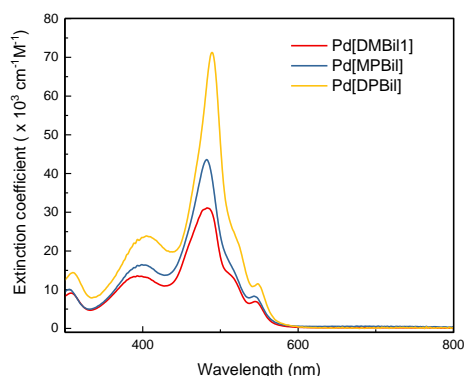


Figure 55 UV-vis absorption spectra of Pd[DMBi1], Pd[MPBi1] and Pd[DPBi1] were collected in methanol at room temperature.

Table 6.2 Electrochemical and UV-vis absorption data for Pd(II) complexes

| | $E_{ox1, 2}$ (V) | $E_{red1, 2}$ (V) | λ_{abs}/nm ($\epsilon \times 10^3/M^{-1}cm^{-1}$) |
|------------------|------------------|-------------------|--|
| Pd[DMBi1] | 0.922, 0.712 | 1.536, 1.822 | 393 (13.6), 482 (31.0), 544 (6.9) |
| Pd[MPBi1] | 0.908, 0.708 | 1.536, 1.808 | 396 (16.2), 482 (43.6), 543 (8.3) |
| Pd[DPBi1] | 0.924, 0.746 | 1.540, 1.816 | 405 (23.9), 489 (71.2), 548 (11.5) |

All redox potentials reported are collected from DPVs (vs Fc/Fc⁺) in CH₂Cl₂. All spectroscopic data recorded in MeOH.

6.4 Emission Study of Pd[MPBiI] and Pd[DPBiI]

The emission study suggested that both Pd[MPBiI] and Pd[DPBiI] also performed weak luminescent as Pd[DMBiI1], as **Figure 56** showed. Pd[MPBiI] produced two emission features with maximum emission intensity at 559 nm and 804 nm in a solution of N₂ saturated methanol when irradiated at 500 nm. Under the same condition, Pd[DPBiI] displayed a broad emission spectrum with maxima at 538 and 801 nm. On the other hand, both Pd[MPBiI] and Pd[DPBiI] both displayed phosphorescence, indicated by the longer emission wavelength. Furthermore, the solutions of Pd(II) complexes were exposed to air for 20 minutes, the new-take emission spectra displayed the disappearance of their longer wavelength emission profiles, meaning that introducing phenyl substituents to the *sp*³-hybridized *meso*-carbon would still produce ¹O₂, indicated by the quenched phosphorescence of Pd[MPBiI] and Pd[DPBiI]. However, the shorter wavelength emissions do not change upon exposure to air.

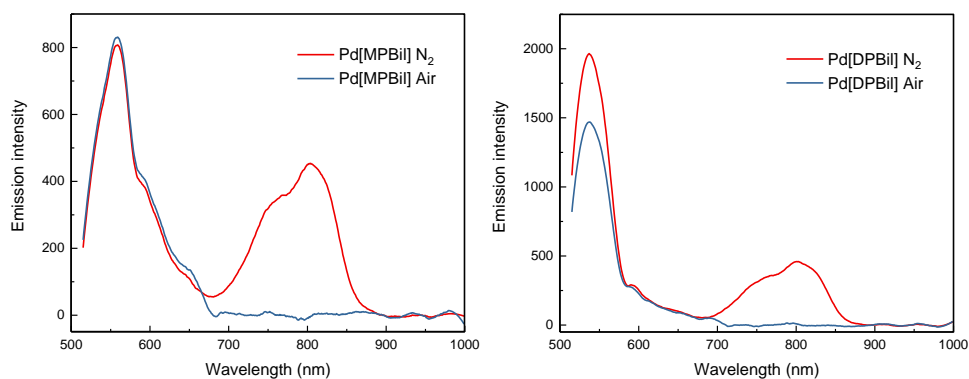


Figure 56 Emission spectra recorded at 298 K in methanol for Pd[MPBiI] (left) and Pd[DPBiI] (right).

The fluorescence and phosphorescence quantum yields were summarized in **Table 6.3**. The fluorescence quantum yields decreased in the following sequence: Pd[DPBiI] > Pd[DMBiI1] > Pd[MPBiI], which were not in consistent with the number

of phenyl substituents introduced. However, the phosphorescence quantum yield decreased in the opposite order as the increase number of phenyl groups: Pd[DMBil1] displayed the highest phosphorescence quantum yield, followed by Pd[MPBil] and Pd[DPBil].

Table 6.3 Photophysical data of Pd[DMBil1], Pd[MPBil] and Pd[DPBil]

| | $\lambda_n/\text{nm} (\Phi_n)$ | $\lambda_{ph}/\text{nm} (\Phi_{ph})$ | Φ_Δ |
|-------------------|---------------------------------|--------------------------------------|-----------------|
| Pd[DMBil1] | 537 (1.6×10^{-4}) | 805 (1.8×10^{-4}) | 0.81 ± 0.04 |
| Pd[MPBil] | 559 (1.4×10^{-4}) | 804 (1.5×10^{-4}) | 0.86 ± 0.07 |
| Pd[DPBil] | 538 (2.3×10^{-4}) | 801 (1.4×10^{-4}) | 0.76 ± 0.03 |

6.5 Singlet Oxygen Sensitization of Pd[MPBil] and Pd[DPBil]

Singlet oxygen studies were quantified by monitoring the fluorescence of 1,3-diphenylisobenzofuran (DPBF), which is a $^1\text{O}_2$ trapping reagent in methanol.

[Ru(bpy)₃]₂[PF₆]₂ was used as an actinometer ($\Phi_{\text{ref}} = 0.81$ in methanol). The quantum yields of $^1\text{O}_2$ of Pd[DMBil1], Pd[MPBil] and Pd[DPBil] were calculated to be $\Phi_\Delta = 81\%$, 86% and 78% respectively where irradiated with light of at $\lambda_{\text{ex}} = 500$ nm, the detailed procedure for the experimental set ups and procedures were presented in Chapter 2. It needs to be notified that, Pd[MPBil] has the highest $^1\text{O}_2$ sensitization quantum yields among the three complexed, as well as Pd[DPBil] has the lowest singlet oxygen quantum yield. However, they still display the higher $^1\text{O}_2$ production compared with the current FDA approved drugs for PDT¹²⁵.

6.6 Summary

Palladium biladiene bearing geminal methyl or phenyl substituents on the sp^3 -hybridized *meso*-position were synthesized and characterized by NMR, X-ray crystallography, UV-vis and emission spectra. All three derivatives showed similar electrochemical characteristics based on CV and DPV experiments. Substituting the two methyl groups on the parent Pd[DMBi1] with one or two phenyl functional groups does not influence the isolation yield and stability of the two new Pd(II) biladienes whose synthetic routes are the typical preparation steps for the palladium biladiene. However, incorporating one or two phenyl substituents results in a drastic enhancement in absorption capabilities. These two new Pd[MPBi] and Pd[DPBi] also maintain significant 1O_2 production, even though both show lower phosphorescence emission quantum yields than Pd[DMBi1] under the same concentration in methanol. If the absorption performance is taken into considerations, Pd[MPBi] and Pd[DPBi] actually are the better candidates for the photodynamic therapy because the intake dose can be lowered to half to keep the similar 1O_2 production yield.

REFERENCES

- (1) Smith, R. A. The Colours of Life: An Introduction to the Chemistry of Porphyrins and Related Compounds (Milgrom, Lionel R.). *J. Chem. Educ.* **1998**, *75* (4), 420. <https://doi.org/10.1021/ed075p420.1>.
- (2) Paolesse, R. Corrole: The Little Big Porphyrinoid. *Synlett* **2008**, No. 15, 2215–2230. <https://doi.org/10.1055/s-2008-1078687>.
- (3) Misra, R.; Chandrashekar, T. K. Structural Diversity in Expanded Porphyrins. *Acc. Chem. Res.* **2008**, *41* (2), 265–279. <https://doi.org/10.1021/ar700091k>.
- (4) Pushpan, S. K.; Chandrashekar, T. K. Aromatic Core-Modified Expanded Porphyrinoids with Meso-Aryl Substituents. *Pure Appl. Chem.* **2003**, *74* (11), 2045–2055. <https://doi.org/10.1351/pac200274112045>.
- (5) Furuta, H.; Maeda, H.; Osuka, A. Confusion, Inversion, and Creation - A New Spring from Porphyrin Chemistry. *Chem. Commun.* **2002**, No. 17, 1795–1804. <https://doi.org/10.1039/b200525p>.
- (6) Pistner, A. J.; Lutterman, D. A.; Ghidui, M. J.; Ma, Y. Z.; Rosenthal, J. Synthesis, Electrochemistry, and Photophysics of a Family of Phlorin Macrocycles That Display Cooperative Fluoride Binding. *J. Am. Chem. Soc.* **2013**, *135* (17), 6601–6607. <https://doi.org/10.1021/ja401391z>.
- (7) Bruce, A. M.; Weyburne, E. S.; Engle, J. T.; Ziegler, C. J.; Geier, G. R. Phlorins Bearing Different Substituents at the Sp³-Hybridized Meso-Position. *J. Org. Chem.* **2014**, *79* (12), 5664–5672. <https://doi.org/10.1021/jo5008256>.
- (8) Hill, J. P.; D'Souza, F.; Ariga, K. Porphyrinoids: Highly Versatile, Redox-Active Scaffolds for Supramolecular Design and Biomimetic Applications. *Supramol. Chem.* **2012**. <https://doi.org/10.1002/9780470661345.smc171>.
- (9) Sono, M.; Roach, M. P.; Coulter, E. D.; Dawson, J. H. Heme-Containing Oxygenases. *Chem. Rev.* **1996**, *96* (7), 2841–2887. <https://doi.org/10.1021/cr9500500>.
- (10) Green, B. R.; Durnford, D. G. The Chlorophyll-Carotenoid Proteins of Oxygenic Photosynthesis. *Annu. Rev. Plant Physiol. Plant Mol. Biol.* **1996**, *47* (1), 685–714. <https://doi.org/10.1146/annurev.arplant.47.1.685>.
- (11) Ben-Shem, A.; Frolow, F.; Nelson, N. Light-Harvesting Features Revealed by the Structure of Plant Photosystem I. *Photosynth. Res.* **2004**, *81* (3), 239–250. <https://doi.org/10.1023/B:PRES.0000036881.23512.42>.
- (12) Branchaud, B. P. Heme Peroxidases By H. Brian Dunford (University of Alberta). Wiley-VCH, John Wiley and Sons: New York. 1999. Xi + 507 Pp. \$195.00. ISBN 0-471-24244-6. *J. Am. Chem. Soc.* **2000**, *122* (30), 7434–7434. <https://doi.org/10.1021/ja995730p>.

- (13) Otori, H.; Hiroto, S.; Shinokubo, H. 10-Silacorroles Exhibiting Near-Infrared Absorption and Emission. *Chem. - A Eur. J.* **2017**, *23* (33), 7866–7870. <https://doi.org/10.1002/chem.201701474>.
- (14) Min Park, J.; Lee, J. H.; Jang, W. D. Applications of Porphyrins in Emerging Energy Conversion Technologies. *Coord. Chem. Rev.* **2020**, *407*, 213157. <https://doi.org/10.1016/j.ccr.2019.213157>.
- (15) Zhang, Q.; He, J.; Yu, W.; Li, Y.; Liu, Z.; Zhou, B.; Liu, Y. A Promising Anticancer Drug: A Photosensitizer Based on the Porphyrin Skeleton. *RSC Med. Chem.* **2020**, *11* (4), 427–437. <https://doi.org/10.1039/c9md00558g>.
- (16) Costa e Silva, R.; da Silva, L. O.; de Andrade Bartolomeu, A.; Brocksom, T. J.; de Oliveira, K. T. Recent Applications of Porphyrins as Photocatalysts in Organic Synthesis: Batch and Continuous Flow Approaches. *Beilstein J. Org. Chem.* **2020**, *16*, 917–955. <https://doi.org/10.3762/bjoc.16.83>.
- (17) Shen, J.; Kolb, M. J.; G?ttle, A. J.; Koper, M. T. M. DFT Study on the Mechanism of the Electrochemical Reduction of CO₂ Catalyzed by Cobalt Porphyrins. *J. Phys. Chem. C* **2016**, *120* (29), 15714–15721. <https://doi.org/10.1021/acs.jpcc.5b10763>.
- (18) De Souza, A. A. N.; Silva, N. S.; Müller, A. V.; Polo, A. S.; Brocksom, T. J.; De Oliveira, K. T. Porphyrins as Photoredox Catalysts in Csp²-H Arylations: Batch and Continuous Flow Approaches. *J. Org. Chem.* **2018**, *83* (24), 15077–15086. <https://doi.org/10.1021/acs.joc.8b02355>.
- (19) Wang, L.; Duan, S.; Jin, P.; She, H.; Huang, J.; Lei, Z.; Zhang, T.; Wang, Q. Anchored Cu(II) Tetra(4-Carboxylphenyl)Porphyrin to P25 (TiO₂) for Efficient Photocatalytic Ability in CO₂ Reduction. *Appl. Catal. B Environ.* **2018**, *239* (June), 599–608. <https://doi.org/10.1016/j.apcatb.2018.08.007>.
- (20) Rao, H.; Bonin, J.; Robert, M. Non-Sensitized Selective Photochemical Reduction of CO₂ to CO under Visible Light with an Iron Molecular Catalyst. *Chem. Commun.* **2017**, *53* (19), 2830–2833. <https://doi.org/10.1039/c6cc09967j>.
- (21) Zhang, W.; Lai, W.; Cao, R. Energy-Related Small Molecule Activation Reactions: Oxygen Reduction and Hydrogen and Oxygen Evolution Reactions Catalyzed by Porphyrin- and Corrole-Based Systems. *Chem. Rev.* **2017**, *117* (4), acs.chemrev.6b00299. <https://doi.org/10.1021/acs.chemrev.6b00299>.
- (22) Fukuzumi, S.; Okamoto, K.; Gros, C. P.; Guillard, R. Mechanism of Four-Electron Reduction of Dioxygen to Water by Ferrocene Derivatives in the Presence of Perchloric Acid in Benzonitrile, Catalyzed by Cofacial Dicobalt Porphyrins. *J. Am. Chem. Soc.* **2004**, *126* (33), 10441–10449. <https://doi.org/10.1021/ja048403c>.
- (23) Kadish, K. M.; Frémond, L.; Shen, J.; Chen, P.; Ohkubo, K.; Fukuzumi, S.; El Ojaimi, M.; Gros, C. P.; Barbe, J. M.; Guillard, R. Catalytic Activity of Biscobalt Porphyrin-Corrole Dyads toward the Reduction of Dioxygen. *Inorg.*

- Chem.* **2009**, *48* (6), 2571–2582. <https://doi.org/10.1021/ic802092n>.
- (24) Oldacre, A. N.; Friedman, A. E.; Cook, T. R. A Self-Assembled Cofacial Cobalt Porphyrin Prism for Oxygen Reduction Catalysis. *J. Am. Chem. Soc.* **2017**, *139* (4), 1424–1427. <https://doi.org/10.1021/jacs.6b12404>.
- (25) Bashyam, R.; Zelenay, P. A Class of Non-Precious Metal Composite Catalysts for Fuel Cells. *Nature* **2006**, *443* (7107), 63–66. <https://doi.org/10.1038/nature05118>.
- (26) Dogutan, D. K.; Stoian, S. A.; McGuire, R.; Schwalbe, M.; Teets, T. S.; Nocera, D. G. Hangman Corroles: Efficient Synthesis and Oxygen Reaction Chemistry. *J. Am. Chem. Soc.* **2011**, *133* (1), 131–140. <https://doi.org/10.1021/ja108904s>.
- (27) Jiang, Y. B.; Sun, Z. Self-Assembled Porphyrin and Macrocyclic Derivatives: From Synthesis to Function. *MRS Bull.* **2019**, *44* (3), 167–171. <https://doi.org/10.1557/mrs.2019.44>.
- (28) Liu, Q. Y.; Li, J. F.; Wang, J. W. Research of Covalent Organic Framework Materials Based on Porphyrin Units. *J. Incl. Phenom. Macrocycl. Chem.* **2019**, *95* (1–2), 1–15. <https://doi.org/10.1007/s10847-019-00924-8>.
- (29) Sugawara, E.; Nikaido, H. EIA Energy Outlook 2020. *Antimicrob. Agents Chemother.* **2019**, *58* (12), 7250–7257. <https://doi.org/10.1128/AAC.03728-14>.
- (30) Minh, N. Q.; Shirley Meng, Y. Future Energy, Fuel Cells, and Solid-Oxide Fuel-Cell Technology. *MRS Bull.* **2019**, *44* (09), 682–683. <https://doi.org/10.1557/mrs.2019.209>.
- (31) Cheng, X.; Shi, Z.; Glass, N.; Zhang, L.; Zhang, J.; Song, D.; Liu, Z. S.; Wang, H.; Shen, J. A Review of PEM Hydrogen Fuel Cell Contamination: Impacts, Mechanisms, and Mitigation. *J. Power Sources* **2007**, *165* (2), 739–756. <https://doi.org/10.1016/j.jpowsour.2006.12.012>.
- (32) Fuel, H.; Engines, C. *Solar Hydrogen*; 2012. <https://doi.org/10.1039/9781849733175>.
- (33) Yilanci, A.; Dincer, I.; Ozturk, H. K. A Review on Solar-Hydrogen/Fuel Cell Hybrid Energy Systems for Stationary Applications. *Prog. Energy Combust. Sci.* **2009**, *35* (3), 231–244. <https://doi.org/10.1016/j.pecs.2008.07.004>.
- (34) Lewis, N. S.; Nocera, D. G. Powering the Planet: Chemical Challenges in Solar Energy Utilization. *Proc. Natl. Acad. Sci.* **2006**, *103* (43), 15729–15735. <https://doi.org/10.1073/pnas.0603395103>.
- (35) Stacy, J.; Regmi, Y. N.; Leonard, B.; Fan, M. The Recent Progress and Future of Oxygen Reduction Reaction Catalysis: A Review. *Renew. Sustain. Energy Rev.* **2017**, *69* (September 2016), 401–414. <https://doi.org/10.1016/j.rser.2016.09.135>.
- (36) Rosenthal, J.; Nocera, D. G. Role of Proton-Coupled Electron Transfer in O-O Bond Activation. *Acc. Chem. Res.* **2007**, *40* (7), 543–553. <https://doi.org/10.1021/ar7000638>.
- (37) Gewirth, A. A.; Thorum, M. S. Electroreduction of Dioxygen for Fuel-Cell Applications: Materials and Challenges. *Inorg. Chem.* **2010**, *49* (8), 3557–3566.

- <https://doi.org/10.1021/ic9022486>.
- (38) He, M.; Dowd, P. Mechanism of Action of Vitamin B12. Ultrafast Radical Clocks Provide No Evidence for Radical Intermediates in Cyclopropane Models for the Methylmalonyl-Coa to Succinyl-Coa Carbon Skeleton Rearrangement. *J. Am. Chem. Soc.* **1998**, *120* (6), 1133–1137. <https://doi.org/10.1021/ja971415w>.
- (39) Linck, R. C.; Rauchfuss, T. B. Synthetic Models for Bioorganometallic Reaction Centers. In *Bioorganometallics*; John Wiley & Sons, Ltd, 2006; pp 403–435. <https://doi.org/10.1002/3527607692.ch12>.
- (40) Stanger, O. *Water Soluble Vitamins*; Stanger, O., Ed.; Subcellular Biochemistry; Springer Netherlands: Dordrecht, 2012; Vol. 56. <https://doi.org/10.1007/978-94-007-2199-9>.
- (41) Stich, T. A.; Yamanishi, M.; Banerjee, R.; Brunold, T. C. Spectroscopic Evidence for the Formation of a Four-Coordinate Co²⁺-cobalamin Species upon Binding to the Human ATP:Cobalamin Adenosyltransferase. *J. Am. Chem. Soc.* **2005**, *127* (21), 7660–7661. <https://doi.org/10.1021/ja050546r>.
- (42) Joblin, K. N.; Johnson, A. W.; Lappert, M. F.; Nicholson, B. K. Light-Induced Anaerobic Co^{III}-C Homolysis of Aqueous Vitamin B₁₂ Coenzyme or of Ethylcobalamin; Spin-Trapping of the 5'-Deoxyadenosyl or Et Radical. *J. Chem. Soc., Chem. Commun.* **1975**, No. 11, 441–442. <https://doi.org/10.1039/C39750000441>.
- (43) Institute, N. N. C. Cancer Facts & Figures 2020. **2020**.
- (44) Arruebo, M.; Vilaboa, N.; Sáez-Gutiérrez, B.; Lambea, J.; Tres, A.; Valladares, M.; González-Fernández, Á. Assessment of the Evolution of Cancer Treatment Therapies. *Cancers (Basel)*. **2011**, *3* (3), 3279–3330. <https://doi.org/10.3390/cancers3033279>.
- (45) Miller, K. D.; Nogueira, L.; Mariotto, A. B.; Rowland, J. H.; Yabroff, K. R.; Alfano, C. M.; Jemal, A.; Kramer, J. L.; Siegel, R. L. Cancer Treatment and Survivorship Statistics, 2019. *CA. Cancer J. Clin.* **2019**, *69* (5), 363–385. <https://doi.org/10.3322/caac.21565>.
- (46) Ozog, D. M.; Rkein, A. M.; Fabi, S. G.; Gold, M. H.; Goldman, M. P.; Lowe, N. J.; Martin, G. M.; Munavalli, G. S. Photodynamic Therapy: A Clinical Consensus Guide. *Dermatologic Surg.* **2016**, *42* (7), 804–827. <https://doi.org/10.1097/DSS.0000000000000800>.
- (47) Detty, M. R.; Gibson, S. L.; Wagner, S. J. Current Clinical and Preclinical Photosensitizers for Use in Photodynamic Therapy. *J. Med. Chem.* **2004**, *47* (16), 3897–3915. <https://doi.org/10.1021/jm040074b>.
- (48) Agostinis P, Berg K, Cengel K., et al. Republic of Yemen Ministry of Public Health and Population Nutrition and Mortality Survey Report Ibb Governorate, Yemen. *Ca Cancer J Clin* **2017**, *61* (April), 250–281. <https://doi.org/10.3322/caac.20114>. Available.
- (49) Mroz, P.; Yaroslavsky, A.; Kharkwal, G. B.; Hamblin, M. R. Cell Death Pathways in Photodynamic Therapy of Cancer. *Cancers (Basel)*. **2011**, *3* (2),

- 2516–2539. <https://doi.org/10.3390/cancers3022516>.
- (50) Abrahamse, H.; Hamblin, M. R. New Photosensitizers for Photodynamic Therapy. *Biochem. J.* **2016**, *473* (4), 347–364. <https://doi.org/10.1042/BJ20150942>.
- (51) Abrahamse, H.; Hamblin, M. R.; Dąbrowski, J. M.; Pucelik, B.; Regiel-Futyr, A.; Brindell, M.; Mazuryk, O.; Kyzioł, A.; Stochel, G.; Macyk, W.; Arnaut, L. G.; Knoll, J. D.; Turro, C. Control and Utilization of Ruthenium and Rhodium Metal Complex Excited States for Photoactivated Cancer Therapy. *Coord. Chem. Rev.* **2016**, *282–283* (4), 347–364. <https://doi.org/10.1042/BJ20150942>.
- (52) Dąbrowski, J. M.; Pucelik, B.; Regiel-Futyr, A.; Brindell, M.; Mazuryk, O.; Kyzioł, A.; Stochel, G.; Macyk, W.; Arnaut, L. G. *Engineering of Relevant Photodynamic Processes through Structural Modifications of Metallotetrapyrrolic Photosensitizers*; 2016; Vol. 325. <https://doi.org/10.1016/j.ccr.2016.06.007>.
- (53) Calin, M. A.; Parasca, S. V. Photodynamic Therapy in Oncology. *J. Optoelectron. Adv. Mater.* **2006**, *8* (3), 1173–1179. <https://doi.org/10.1634/theoncologist.11-9-1034>.
- (54) Wang, H.; Xu, Y.; Shi, J.; Gao, X.; Geng, L. Photodynamic Therapy in the Treatment of Basal Cell Carcinoma: A Systematic Review and Meta-Analysis. *Photodermatol. Photoimmunol. Photomed.* **2015**, *31* (1), 44–53. <https://doi.org/10.1111/phpp.12148>.
- (55) Castano, A. P.; Mroz, P.; Hamblin, M. R. Photodynamic Therapy and Anti-Tumour Immunity. *Nat. Rev. Cancer* **2006**, *6* (7), 535–545. <https://doi.org/10.1038/nrc1894>.
- (56) Jablonski, A. Efficiency of Anti-Stokes Fluorescence in Dyes. *Nature* **1933**, *131* (3319), 839–840. <https://doi.org/10.1038/131839b0>.
- (57) DeRosa, M. C.; Crutchley, R. J. Photosensitized Singlet Oxygen and Its Applications. *Coord. Chem. Rev.* **2002**, *233–234*, 351–371. [https://doi.org/10.1016/S0010-8545\(02\)00034-6](https://doi.org/10.1016/S0010-8545(02)00034-6).
- (58) Plaetzer, K.; Krammer, B.; Berlanda, J.; Berr, F.; Kiesslich, T. Photophysics and Photochemistry of Photodynamic Therapy: Fundamental Aspects. *Lasers Med. Sci.* **2009**, *24* (2), 259–268. <https://doi.org/10.1007/s10103-008-0539-1>.
- (59) Fulmer, G. R.; Miller, A. J. M.; Sherden, N. H.; Gottlieb, H. E.; Nudelman, A.; Stoltz, B. M.; Bercaw, J. E.; Goldberg, K. I. NMR Chemical Shifts of Trace Impurities: Common Laboratory Solvents, Organics, and Gases in Deuterated Solvents Relevant to the Organometallic Chemist. *Organometallics* **2010**, *29* (9), 2176–2179. <https://doi.org/10.1021/om100106e>.
- (60) Peters, M. K.; Röhricht, F.; Näther, C.; Herges, R. One-Pot Approach to Chlorins, Isobacteriochlorins, Bacteriochlorins, and Pyrrocorphins. *Org. Lett.* **2018**, *20* (24), 7879–7883. <https://doi.org/10.1021/acs.orglett.8b03433>.
- (61) Reith, L. M.; Stiftinger, M.; Monkowius, U.; Knör, G.; Schoefberger, W. Synthesis and Characterization of a Stable Bismuth(III) A 3-Corrole. *Inorg. Chem.* **2011**, *50* (14), 6788–6797. <https://doi.org/10.1021/ic200840m>.

- (62) Meng, J.; Lei, H.; Li, X.; Qi, J.; Zhang, W.; Cao, R. Attaching Cobalt Corroles onto Carbon Nanotubes: Verification of Four-Electron Oxygen Reduction by Mononuclear Cobalt Complexes with Significantly Improved Efficiency. *ACS Catal.* **2019**, *9* (5), 4551–4560. <https://doi.org/10.1021/acscatal.9b00213>.
- (63) Analysis, A.; Manual, U. User Manual User Manual. **2012**, *3304* (January), 1–148.
- (64) Sheldrick, G. M. SHELXT - Integrated Space-Group and Crystal-Structure Determination. *Acta Crystallogr. Sect. A Found. Crystallogr.* **2015**, *71* (1), 3–8. <https://doi.org/10.1107/S2053273314026370>.
- (65) Sheldrick, G. M. Crystal Structure Refinement with SHELXL. *Acta Crystallogr. Sect. C Struct. Chem.* **2015**, *71* (Md), 3–8. <https://doi.org/10.1107/S2053229614024218>.
- (66) Spek, A. L. PLATON SQUEEZE: A Tool for the Calculation of the Disordered Solvent Contribution to the Calculated Structure Factors. *Acta Crystallogr. Sect. C Struct. Chem.* **2015**, *71*, 9–18. <https://doi.org/10.1107/S2053229614024929>.
- (67) Braslavsky, S. E.; Holzwarth, A. R.; Schaffner, K. Solution Conformations, Photophysics, and Photochemistry of Bile Pigments; Bilirubin and Biliverdin, Dimethyl Esters and Related Linear Tetrapyrroles. *Angew. Chemie Int. Ed. English* **1983**, *22* (9), 656–674. <https://doi.org/10.1002/anie.198306561>.
- (68) Mizutani, T.; Yagi, S. Linear Tetrapyrroles as Functional Pigments in Chemistry and Biology. *J. Porphyr. Phthalocyanines* **2004**, *8* (1–3), 226–237. <https://doi.org/10.1142/s1088424604000210>.
- (69) Bonfiglio, J. V.; Bonnett, R.; Buckley, D. G.; Hamzesh, D.; Hursthouse, M. B.; Malik, K. M. A.; McDonagh, A. F.; Trotter, J. Linear Tetrapyrroles as Ligands. Syntheses and x-Ray Analyses of Boron and Nickel Complexes of Octaethyl-21H,24H-Bilin-1,19-Dione. *Tetrahedron* **1983**, *39* (11), 1865–1874. [https://doi.org/10.1016/S0040-4020\(01\)88700-7](https://doi.org/10.1016/S0040-4020(01)88700-7).
- (70) Balch, A. L.; Mazzanti, M.; Noll, B. C.; Olmstead, M. M. Geometric and Electronic Structure and Dioxygen Sensitivity of the Copper Complex of Octaethylbilindione, a Biliverdin Analog. *J. Am. Chem. Soc.* **1993**, *115* (25), 12206–12207. <https://doi.org/10.1021/ja00078a086>.
- (71) Koerner, R.; Olmstead, M. M.; Ozarowski, A.; Balch, A. L. A Linear Tetrapyrrole as a Binucleating Ligand with Copper(II). Coordination beyond the Usual M–N 4 Bonding. *Inorg. Chem.* **1999**, *38* (14), 3262–3263. <https://doi.org/10.1021/ic9901113>.
- (72) Koerner, R.; Olmstead, M. M.; Ozarowski, A.; Phillips, S. L.; Van Calcar, P. M.; Winkler, K.; Balch, A. L.; Lord, P. A.; Olmstead, M. M.; Balch, A. L. Possible Intermediates in Biological Metalloporphyrin Oxidative Degradation. Nickel, Copper, and Cobalt Complexes of Octaethylformylbiliverdin and Their Conversion to a Verdoheme. *Inorg. Chem.* **2000**, *39* (6), 1128–1134. <https://doi.org/10.1021/ja973088y>.
- (73) Attar, S.; Balch, A. L.; Van Calcar, P. M.; Winkler, K. Electron Transfer

- Behavior and Solid State Structures of the Helical Cobalt Complexes of the Open-Chain Tetrapyrrole Ligand, Octaethylbilindione. *J. Am. Chem. Soc.* **1997**, *119* (14), 3317–3323. <https://doi.org/10.1021/ja9628718>.
- (74) Koerner, R.; Olmstead, M. M.; Van Calcar, P. M.; Winkler, K.; Balch, A. L. Carbon Monoxide Production during the Oxygenation of Cobalt Complexes of Linear Tetrapyrroles. Formation and Characterization of Co II (Tetraethylpropentdyopent Anion) 2. *Inorg. Chem.* **1998**, *37* (5), 982–988. <https://doi.org/10.1021/ic971265q>.
- (75) Paolesse, R.; Froiio, A.; Nardis, S.; Mastroianni, M.; Russo, M.; Nurco, D. J.; Smith, K. M. Novel Aspects of the Chemistry of 1,19-Diunsubstituted a,c-Biladienes. *J. Porphyr. Phthalocyanines* **2003**, *7* (8), 585–592. <https://doi.org/10.1142/S1088424603000744>.
- (76) Pandey, R. K.; Zhou, H.; Gerzevske, K.; Smith, K. M. Stepwise Synthesis of 1,19-Dibromo-a,c-Biladienes and Their Conversion into Biliverdins, Corroles and Azaporphyrins. *J. Chem. Soc. Chem. Commun.* **1992**, No. 2, 183. <https://doi.org/10.1039/c39920000183>.
- (77) Hohlneicher, G.; Bremm, D.; Wytko, J.; Bley-Esrich, J.; Gisselbrecht, J. P.; Gross, M.; Michels, M.; Lex, J.; Vogel, E. Spiroconjugation in Spirocorrolato-Dinickel(II). *Chem. - A Eur. J.* **2003**, *9* (22), 5636–5642. <https://doi.org/10.1002/chem.200305094>.
- (78) Setsune, J. I.; Tsukajima, A.; Watanabe, J. Synthesis of Isocorrole and the Higher Homologues. *Tetrahedron Lett.* **2006**, *47* (11), 1817–1820. <https://doi.org/10.1016/j.tetlet.2006.01.013>.
- (79) Nardis, S.; Pomarico, G.; Fronczek, F. R.; Vicente, M. G. H.; Paolesse, R. One-Step Synthesis of Isocorroles. *Tetrahedron Lett.* **2007**, *48* (49), 8643–8646. <https://doi.org/10.1016/j.tetlet.2007.10.033>.
- (80) Pomarico, G.; Xiao, X.; Nardis, S.; Paolesse, R.; Fronczek, F. R.; Smith, K. M.; Fang, Y.; Ou, Z.; Kadish, K. M. Synthesis and Characterization of Free-Base, Copper, and Nickel Isocorroles. *Inorg. Chem.* **2010**, *49* (12), 5766–5774. <https://doi.org/10.1021/ic100730j>.
- (81) Mandoj, F.; Nardis, S.; Pomarico, G.; Paolesse, R. Demetalation of Corrole Complexes: An Old Dream Turning into Reality. *J. Porphyr. Phthalocyanines* **2008**, *12* (1), 19–26. <https://doi.org/10.1142/S1088424608000042>.
- (82) Thomas, K. E.; Beavers, C. M.; Gagnon, K. J.; Ghosh, A. β -Octabromo- and β -Octakis(Trifluoromethyl)Isocorroles: New Sterically Constrained Macrocyclic Ligands. *ChemistryOpen* **2017**, *6* (3), 402–409. <https://doi.org/10.1002/open.201700035>.
- (83) Tortora, L.; Nardis, S.; Fronczek, F. R.; Smith, K. M.; Paolesse, R. Functionalization of the Corrole Ring: The Role of Isocorrole Intermediates. *Chem. Commun.* **2011**, *47* (14), 4243–4245. <https://doi.org/10.1039/c0cc05837h>.
- (84) Hoffmann, M.; Cordes, B.; Kleeberg, C.; Schweyen, P.; Wolfram, B.; Bröring, M. Template Synthesis of Alkyl-Substituted Metal Isocorroles. *Eur. J. Inorg.*

- Chem.* **2016**, *2016* (19), 3043. <https://doi.org/10.1002/ejic.201600718>.
- (85) Setsune, J.; Tsukajima, A.; Okazaki, N. Synthesis and Structure of Isocorrole Metal Complexes. *J. Porphyr. Phthalocyanines* **2009**, *13* (02), 256–265. <https://doi.org/10.1142/S1088424609000334>.
- (86) Nardis, S.; Pomarico, G.; Mandoj, F.; Fronczek, F. R.; Smith, K. M.; Paolesse, R. One-Pot Synthesis of Meso-Alkyl Substituted Isocorroles: The Reaction of a Triarylcorrole with Grignard Reagent. *J. Porphyr. Phthalocyanines* **2010**, *14* (8), 752–757. <https://doi.org/10.1142/S1088424610002513>.
- (87) Larsen, S.; McCormick, L. J.; Ghosh, A. Rapid One-Pot Synthesis of Pyrrole-Appended Isocorroles. *Org. Biomol. Chem.* **2019**, *17* (12), 3159–3166. <https://doi.org/10.1039/c9ob00168a>.
- (88) Flint, D. L.; Fowler, R. L.; LeSaulnier, T. D.; Long, A. C.; O'Brien, A. Y.; Geier, G. R. Investigation of Complementary Reactions of a Dipyrromethane with a Dipyrromethanemonocarbinol Leading to a 5-Isocorrole. *J. Org. Chem.* **2010**, *75* (3), 553–563. <https://doi.org/10.1021/jo902452c>.
- (89) Costa, R.; Geier, G. R.; Ziegler, C. J. Structure and Spectroscopic Characterization of Free Base and Metal Complexes of 5,5-Dimethyl-10,15-Bis(Pentafluorophenyl)Isocorrole. *Dalton Trans.* **2011**, *40*, 4384–4386. <https://doi.org/7>.
- (90) Ghosh, A.; Jynge, K. Molecular Structures and Energetics of Corrole Isomers: A Comprehensive Local Density Functional Theoretical Study. *Chem. - A Eur. J.* **1997**, *3* (5), 823–833. <https://doi.org/10.1002/chem.19970030523>.
- (91) Obata, M.; Hirohara, S.; Tanaka, R.; Kinoshita, I.; Ohkubo, K.; Fukuzumi, S.; Tanihara, M.; Yano, S. In Vitro Heavy-Atom Effect of Palladium(II) and Platinum(II) Complexes of Pyrrolidine-Fused Chlorin in Photodynamic Therapy. *J. Med. Chem.* **2009**, *52* (9), 2747–2753. <https://doi.org/10.1021/jm8015427>.
- (92) Gasteiger, H. A.; Marković, N. M. Just a Dream—or Future Reality? *Science* (80-.). **2009**, *324* (5923), 48–49. <https://doi.org/10.1126/science.1172083>.
- (93) Kim, J.; Gewirth, A. A. Electrocatalysis of Peroxide Reduction by Au-Stabilized, Fe-Containing Poly(Vinylpyridine) Films. *J. Phys. Chem. B* **2005**, *109* (19), 9684–9690. <https://doi.org/10.1021/jp050672h>.
- (94) Sherry, A. E.; Wayland, B. B. Metalloradical Activation of Methane. *J. Am. Chem. Soc.* **1990**, *112*, 1259–1261. <https://doi.org/10.1021/ja00159a064>.
- (95) JASINSKI, R. A New Fuel Cell Cathode Catalyst. *Nature* **1964**, *201* (4925), 1212–1213. <https://doi.org/10.1038/2011212a0>.
- (96) Collman, J. P.; Kaplun, M.; Decréau, R. A. Metal Corroles as Electrocatalysts for Oxygen Reduction. *Dalt. Trans.* **2006**, No. 4, 554–559. <https://doi.org/10.1039/b512982f>.
- (97) Shi, C.; Anson, F. C. Electrocatalysis of the Reduction of O₂ to H₂O by Tetraruthenated Cobalt /Neso-Tetrakis(4-Pyridyl)Porphyrin Adsorbed on Graphite Electrodes. *Inorg. Chem.* **1992**, *31* (24), 5078–5083. <https://doi.org/10.1021/ic00050a029>.

- (98) Hijazi, I.; Bourgeteau, T.; Cornut, R.; Morozan, A.; Filoramo, A.; Leroy, J.; Derycke, V.; Joussetme, B.; Campidelli, S. Carbon Nanotube-Templated Synthesis of Covalent Porphyrin Network for Oxygen Reduction Reaction. *J. Am. Chem. Soc.* **2014**, *136* (17), 6348–6354. <https://doi.org/10.1021/ja500984k>.
- (99) Collman, J. P.; Wagenknecht, P. S.; Hutchison, J. E. Molecular Catalysts for Multielectron Redox Reactions of Small Molecules: The “Cofacial Metallodiporphyrin” Approach. *Angew. Chemie Int. Ed. English* **1994**, *33* (1516), 1537–1554. <https://doi.org/10.1002/anie.199415371>.
- (100) Chang, C. K.; Liu, H. Y.; Abdalmuhdi, I.; Liu, H. Y. Electroreduction of Oxygen by Pillared Cobalt Cofacial Diporphyrin Catalysts. *J. Am. Chem. Soc.* **1984**, *106* (9), 2725–2726. <https://doi.org/10.1021/ja00321a055>.
- (101) Chang, C. J.; Deng, Y.; Shi, C.; Chang, C. K.; Anson, F. C.; Nocera, D. G. Electrocatalytic Four-Electron Reduction of Oxygen to Water by a Highly Flexible Cofacial Cobalt Bisporphyrin. *Chem. Commun.* **2000**, No. 15, 1355–1356. <https://doi.org/10.1039/b001620i>.
- (102) Coliman, J. P.; Barnes, C. E.; Bencosme, C. S.; Evitt, E. R.; Kreh, R. P.; Meier, K.; Pettman, R. B.; Anson, F. C.; Geiger, T. Further Studies of the Dimeric β -Linked “Face-to-Face Four” Porphyrin: FTF 4. *J. Am. Chem. Soc.* **1983**, *105* (9), 2694–2699. <https://doi.org/10.1021/ja00347a029>.
- (103) Chang, C. J.; Loh, Z. H.; Shi, C.; Anson, F. C.; Nocera, D. G. Targeted Proton Delivery in the Catalyzed Reduction of Oxygen to Water by Bimetallic Pacman Porphyrins. *J. Am. Chem. Soc.* **2004**, *126* (32), 10013–10020. <https://doi.org/10.1021/ja049115j>.
- (104) Oldacre, A. N.; Crawley, M. R.; Friedman, A. E.; Cook, T. R. Tuning the Activity of Heterogeneous Cofacial Cobalt Porphyrins for Oxygen Reduction Electrocatalysis through Self-Assembly. *Chem. - A Eur. J.* **2018**, *24* (43), 10984–10987. <https://doi.org/10.1002/chem.201802585>.
- (105) McGuire Jr., R.; Dogutan, D. K.; Teets, T. S.; Suntivich, J.; Shao-Horn, Y.; Nocera, D. G. Oxygen Reduction Reactivity of Cobalt(Ii) Hangman Porphyrins. *Chem. Sci.* **2010**, *1* (3), 411. <https://doi.org/10.1039/c0sc00281j>.
- (106) Solis, B. H.; Maher, A. G.; Honda, T.; Powers, D. C.; Nocera, D. G.; Hammes-Schiffer, S. Theoretical Analysis of Cobalt Hangman Porphyrins: Ligand Dearomatization and Mechanistic Implications for Hydrogen Evolution. *ACS Catal.* **2014**, *4* (12), 4516–4526. <https://doi.org/10.1021/cs501454y>.
- (107) Graham, D. J.; Zheng, S. L.; Nocera, D. G. Post-Synthetic Modification of Hangman Porphyrins Synthesized on the Gram Scale. *ChemSusChem* **2014**, *7* (9), 2449–2452. <https://doi.org/10.1002/cssc.201402242>.
- (108) Collman, J. P.; Fu, L.; Herrmann, P. C.; Zhang, X. A Functional Model Related to Cytochrome c Oxidase and Its Electrocatalytic Four-Electron Reduction of O₂. *Science (80-.)*. **1997**, *275* (5302), 949–951. <https://doi.org/10.1126/science.275.5302.949>.
- (109) Albery, W. J. Ring-Disc Electrodes. Part 1.—A New Approach to the Theory. *Trans. Faraday Soc.* **1966**, *62*, 1915–1919.

- <https://doi.org/10.1039/TF9666201915>.
- (110) Alberly, W. J.; Bruckenstein, S. Ring-Disc Electrodes. Part 2.—Theoretical and Experimental Collection Efficiencies. *Trans. Faraday Soc.* **1966**, *62*, 1920–1931. <https://doi.org/10.1039/TF9666201920>.
- (111) Buck, R. P. Expanding Technology for Sensor Design and Fabrication. *Electrochim. Acta* **1991**, *36* (2), 243–251. [https://doi.org/10.1016/0013-4686\(91\)85245-3](https://doi.org/10.1016/0013-4686(91)85245-3).
- (112) Lee, S.-J.; Pyun, S.-I.; Lee, S.-K.; Kang, S.-J. L. Fundamentals of Rotating Disc and Ring-Disc Electrode Techniques and Their Applications to Study of the Oxygen Reduction Mechanism at Pt/C Electrode for Fuel Cells. *Isr. J. Chem.* **2008**, *48* (3–4), 215–228. <https://doi.org/10.1560/IJC.48.3-4.215>.
- (113) Alberly, W. J.; Bruckenstein, S. Ring-Disc Electrodes. Part 5.—First-Order Kinetic Collection Efficiencies at the Ring Electrode. *Trans. Faraday Soc.* **1966**, *62*, 1946–1954. <https://doi.org/10.1039/TF9666201946>.
- (114) Zoski, C. G.; Leddy, J.; Bard, A. J.; Faulkner, L. R. *Student solutions manual to accompany Electrochemical methods - fundamentals and applications by Allen J. Bard, Larry R. Faulkner* LK - <https://delcat.on.worldcat.org/oclc/746928220>, 2nd ed.; Wiley: New York SE - 145 pages : illustrations ; 26 cm, 2002.
- (115) Treimer, S.; Tang, A.; Johnson, D. C. A Consideration of the Application of Koutecký-Levich Plots in the Diagnoses of Charge-Transfer Mechanisms at Rotated Disk Electrodes. *Electroanalysis* **2002**, *14* (3), 165–171. [https://doi.org/10.1002/1521-4109\(200202\)14:3<165::AID-ELAN165>3.0.CO;2-6](https://doi.org/10.1002/1521-4109(200202)14:3<165::AID-ELAN165>3.0.CO;2-6).
- (116) Coveney, D. J.; Patel, V. F.; Pattenden, G.; Thompson, D. M. Acylcobalt Salophen Reagents. Precursors to Acyl Radical Intermediates for Use in Carbon-to-Carbon Bond-Forming Reactions to Alkenes. *J. Chem. Soc. Perkin Trans. 1* **1990**, No. 10, 2721–2728. <https://doi.org/10.1039/p19900002721>.
- (117) Patel, V. F.; Pattenden, G. Free Radical Reactions in Synthesis. Homolysis of Alkylcobalt Complexes in the Presence of Radical-Trapping Agents. *J. Chem. Soc. Perkin Trans. 1* **1990**, No. 10, 2703. <https://doi.org/10.1039/p19900002703>.
- (118) Weiss, M. E.; Kreis, L. M.; Lauber, A.; Carreira, E. M. Cobalt-Catalyzed Coupling of Alkyl Iodides with Alkenes: Deprotonation of Hydridocobalt Enables Turnover. *Angew. Chemie - Int. Ed.* **2011**, *50* (47), 11125–11128. <https://doi.org/10.1002/anie.201105235>.
- (119) Zhao, Y.; Yu, M.; Zhang, S.; Liu, Y.; Fu, X. Visible Light Induced Living/Controlled Radical Polymerization of Acrylates Catalyzed by Cobalt Porphyrins. *Macromolecules* **2014**, *47* (18), 6238–6245. <https://doi.org/10.1021/ma5014385>.
- (120) Chambers, D. R.; Juneau, A.; Ludwig, C. T.; Frenette, M.; Martin, D. B. C. C-O Bond Cleavage of Alcohols via Visible Light Activation of Cobalt Alkoxy-carbonyls. *Organometallics* **2019**, *38* (24), 4570–4577.

- <https://doi.org/10.1021/acs.organomet.9b00552>.
- (121) Chambers, D. R.; Sullivan, R. E.; Martin, D. B. C. Synthesis and Characterization of Alkoxy carbonyl Cobalt Complexes via Direct Carbonylation Methods. *Organometallics* **2017**, *36* (8), 1630–1639. <https://doi.org/10.1021/acs.organomet.7b00186>.
- (122) Moan, J.; Peng, Q. An Outline of the Hundred-Year History of PDT. *Anticancer Res.* **2003**, *23* (5 A), 3591–3600.
- (123) Stapleton, M.; Rhodes, L. E. Photosensitizers for Photodynamic Therapy of Cutaneous Disease. *J. Dermatolog. Treat.* **2003**, *14* (2), 107–112. <https://doi.org/10.1080/09546630310012127>.
- (124) Kessel, D.; Musselman, B.; Thompson, P.; Chang, C. K. Probing the Structure and Stability of the Tumor-Localizing Derivative of Hematoporphyrin by Reductive Cleavage with LiAlH₄. *Cancer Res.* **1987**, *47* (17), 4642–4645.
- (125) Ormond, A. B.; Freeman, H. S. Dye Sensitizers for Photodynamic Therapy. *Materials (Basel)*. **2013**, *6* (3), 817–840. <https://doi.org/10.3390/ma6030817>.
- (126) Potocny, A. M.; Pistner, A. J.; Yap, G. P. A. A.; Rosenthal, J. Electrochemical, Spectroscopic, and 1 O 2 Sensitization Characteristics of Synthetically Accessible Linear Tetrapyrrole Complexes of Palladium and Platinum. *Inorg. Chem.* **2017**, *56* (21), 12703–12711. <https://doi.org/10.1021/acs.inorgchem.7b00796>.
- (127) Fleischer, E. B.; Miller, C. K.; Webb, L. E. Crystal and Molecular Structures of Some Metal Tetraphenylporphines. *J. Am. Chem. Soc.* **1964**, *86* (12), 2342–2347. <https://doi.org/10.1021/ja01066a009>.

Appendix

A. FULLY LABELED SOLID STATE STRUCTURE WITH BOND LENGTH AND ANGLES

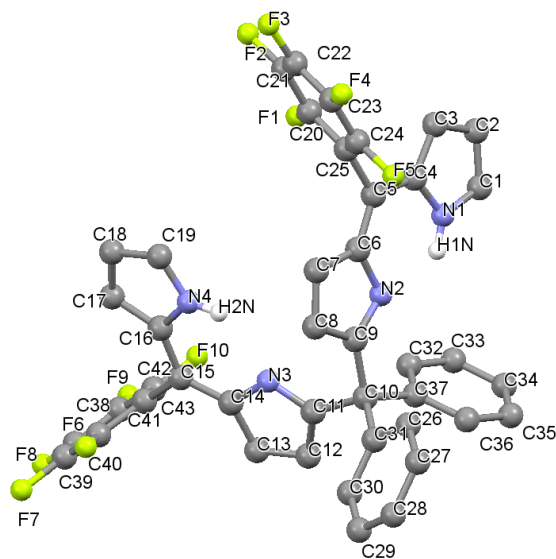


Figure A. 1. Fully labeled solid state structure of DPBil.

Table A. 1. Bond Lengths (Å) and Bond angles (°) determined for DPBil

| Bond | Length | Bond | Length |
|------------|----------|-------------|----------|
| C(1)-N(1) | 1.346(3) | C(22)-F(3) | 1.337(2) |
| C(1)-C(2) | 1.377(3) | C(22)-C(23) | 1.372(3) |
| C(1)-H(1) | 0.95 | C(23)-F(4) | 1.335(2) |
| C(2)-C(3) | 1.396(3) | C(23)-C(24) | 1.381(3) |
| C(2)-H(2) | 0.95 | C(24)-F(5) | 1.333(2) |
| C(3)-C(4) | 1.397(3) | C(24)-C(25) | 1.389(3) |
| C(3)-H(3) | 0.95 | C(26)-C(27) | 1.386(3) |
| C(4)-N(1) | 1.379(2) | C(26)-C(31) | 1.392(3) |
| C(4)-C(5) | 1.426(3) | C(26)-H(26) | 0.95 |
| C(5)-C(6) | 1.371(2) | C(27)-C(28) | 1.382(3) |
| C(5)-C(25) | 1.494(2) | C(27)-H(27) | 0.95 |
| C(6)-N(2) | 1.410(2) | C(28)-C(29) | 1.384(3) |
| C(6)-C(7) | 1.449(3) | C(28)-H(28) | 0.95 |
| C(7)-C(8) | 1.350(3) | C(29)-C(30) | 1.388(3) |
| C(7)-H(7) | 0.95 | C(29)-H(29) | 0.95 |
| C(8)-C(9) | 1.461(3) | C(30)-C(31) | 1.390(2) |
| C(8)-H(8) | 0.95 | C(30)-H(30) | 0.95 |

| | | | |
|-------------|----------|--------------|----------|
| C(9)-N(2) | 1.304(2) | C(32)-C(33) | 1.390(3) |
| C(9)-C(10) | 1.527(2) | C(32)-C(37) | 1.395(3) |
| C(10)-C(11) | 1.532(2) | C(32)-H(32) | 0.95 |
| C(10)-C(31) | 1.538(2) | C(33)-C(34) | 1.381(3) |
| C(10)-C(37) | 1.543(2) | C(33)-H(33) | 0.95 |
| C(11)-N(3) | 1.302(2) | C(34)-C(35) | 1.376(4) |
| C(11)-C(12) | 1.460(2) | C(34)-H(34) | 0.95 |
| C(12)-C(13) | 1.347(3) | C(35)-C(36) | 1.391(3) |
| C(12)-H(12) | 0.95 | C(35)-H(35) | 0.95 |
| C(13)-C(14) | 1.448(3) | C(36)-C(37) | 1.391(3) |
| C(13)-H(13) | 0.95 | C(36)-H(36) | 0.95 |
| C(14)-C(15) | 1.365(3) | C(38)-F(6) | 1.344(2) |
| C(14)-N(3) | 1.405(2) | C(38)-C(43) | 1.384(3) |
| C(15)-C(16) | 1.428(3) | C(38)-C(39) | 1.386(3) |
| C(15)-C(43) | 1.499(3) | C(39)-F(7) | 1.337(3) |
| C(16)-N(4) | 1.377(3) | C(39)-C(40) | 1.369(3) |
| C(16)-C(17) | 1.394(3) | C(40)-F(8) | 1.334(2) |
| C(17)-C(18) | 1.395(3) | C(40)-C(41) | 1.369(3) |
| C(17)-H(17) | 0.95 | C(41)-F(9) | 1.331(2) |
| C(18)-C(19) | 1.376(3) | C(41)-C(42) | 1.386(3) |
| C(18)-H(18) | 0.95 | C(42)-F(10) | 1.337(2) |
| C(19)-N(4) | 1.348(3) | C(42)-C(43) | 1.386(3) |
| C(19)-H(19) | 0.95 | N(1)-H(1N) | 0.86(3) |
| C(20)-F(1) | 1.338(2) | N(4)-H(2N) | 0.81(3) |
| C(20)-C(21) | 1.383(3) | C(44)-Cl(2) | 1.706(3) |
| C(20)-C(25) | 1.386(3) | C(44)-Cl(1) | 1.751(3) |
| C(21)-F(2) | 1.337(2) | C(44)-H(44A) | 0.99 |
| C(21)-C(22) | 1.376(3) | C(44)-H(44B) | 0.99 |

| Bond | Angle | Bond | Angle |
|----------------|------------|-------------------|------------|
| N(1)-C(1)-C(2) | 108.84(19) | F(5)-C(24)-C(25) | 119.88(16) |
| N(1)-C(1)-H(1) | 125.6 | C(23)-C(24)-C(25) | 121.76(17) |
| C(2)-C(1)-H(1) | 125.6 | C(20)-C(25)-C(24) | 116.95(16) |
| C(1)-C(2)-C(3) | 107.04(19) | C(20)-C(25)-C(5) | 121.62(16) |
| C(1)-C(2)-H(2) | 126.5 | C(24)-C(25)-C(5) | 121.43(16) |
| C(3)-C(2)-H(2) | 126.5 | C(27)-C(26)-C(31) | 121.0(2) |
| C(4)-C(3)-C(2) | 107.93(18) | C(27)-C(26)-H(26) | 119.5 |
| C(4)-C(3)-H(3) | 126 | C(31)-C(26)-H(26) | 119.5 |
| C(2)-C(3)-H(3) | 126 | C(28)-C(27)-C(26) | 120.5(2) |
| N(1)-C(4)-C(3) | 106.33(17) | C(28)-C(27)-H(27) | 119.8 |
| N(1)-C(4)-C(5) | 123.20(17) | C(26)-C(27)-H(27) | 119.8 |
| C(3)-C(4)-C(5) | 130.45(17) | C(27)-C(28)-C(29) | 119.2(2) |
| C(6)-C(5)-C(4) | 125.50(16) | C(27)-C(28)-H(28) | 120.4 |

| | | | |
|-------------------|------------|-------------------|------------|
| C(6)-C(5)-C(25) | 118.31(16) | C(29)-C(28)-H(28) | 120.4 |
| C(4)-C(5)-C(25) | 116.19(15) | C(28)-C(29)-C(30) | 120.31(19) |
| C(5)-C(6)-N(2) | 121.01(16) | C(28)-C(29)-H(29) | 119.8 |
| C(5)-C(6)-C(7) | 129.40(16) | C(30)-C(29)-H(29) | 119.8 |
| N(2)-C(6)-C(7) | 109.53(15) | C(31)-C(30)-C(29) | 121.04(18) |
| C(8)-C(7)-C(6) | 106.15(16) | C(31)-C(30)-H(30) | 119.5 |
| C(8)-C(7)-H(7) | 126.9 | C(29)-C(30)-H(30) | 119.5 |
| C(6)-C(7)-H(7) | 126.9 | C(30)-C(31)-C(26) | 118.02(18) |
| C(7)-C(8)-C(9) | 106.37(16) | C(30)-C(31)-C(10) | 122.69(16) |
| C(7)-C(8)-H(8) | 126.8 | C(26)-C(31)-C(10) | 119.29(16) |
| C(9)-C(8)-H(8) | 126.8 | C(33)-C(32)-C(37) | 121.26(19) |
| N(2)-C(9)-C(8) | 112.13(15) | C(33)-C(32)-H(32) | 119.4 |
| N(2)-C(9)-C(10) | 122.24(16) | C(37)-C(32)-H(32) | 119.4 |
| C(8)-C(9)-C(10) | 125.59(15) | C(34)-C(33)-C(32) | 120.0(2) |
| C(9)-C(10)-C(11) | 106.76(13) | C(34)-C(33)-H(33) | 120 |
| C(9)-C(10)-C(31) | 108.40(14) | C(32)-C(33)-H(33) | 120 |
| C(11)-C(10)-C(31) | 111.91(14) | C(35)-C(34)-C(33) | 119.6(2) |
| C(9)-C(10)-C(37) | 109.76(14) | C(35)-C(34)-H(34) | 120.2 |
| C(11)-C(10)-C(37) | 106.85(14) | C(33)-C(34)-H(34) | 120.2 |
| C(31)-C(10)-C(37) | 112.98(14) | C(34)-C(35)-C(36) | 120.6(2) |
| N(3)-C(11)-C(12) | 111.68(15) | C(34)-C(35)-H(35) | 119.7 |
| N(3)-C(11)-C(10) | 121.23(15) | C(36)-C(35)-H(35) | 119.7 |
| C(12)-C(11)-C(10) | 126.92(16) | C(35)-C(36)-C(37) | 120.8(2) |
| C(13)-C(12)-C(11) | 106.43(16) | C(35)-C(36)-H(36) | 119.6 |
| C(13)-C(12)-H(12) | 126.8 | C(37)-C(36)-H(36) | 119.6 |
| C(11)-C(12)-H(12) | 126.8 | C(36)-C(37)-C(32) | 117.83(18) |
| C(12)-C(13)-C(14) | 106.42(17) | C(36)-C(37)-C(10) | 123.11(17) |
| C(12)-C(13)-H(13) | 126.8 | C(32)-C(37)-C(10) | 119.06(16) |
| C(14)-C(13)-H(13) | 126.8 | F(6)-C(38)-C(43) | 119.63(18) |
| C(15)-C(14)-N(3) | 121.77(16) | F(6)-C(38)-C(39) | 117.85(19) |
| C(15)-C(14)-C(13) | 129.03(17) | C(43)-C(38)-C(39) | 122.53(19) |
| N(3)-C(14)-C(13) | 109.03(15) | F(7)-C(39)-C(40) | 120.3(2) |
| C(14)-C(15)-C(16) | 124.82(17) | F(7)-C(39)-C(38) | 120.2(2) |
| C(14)-C(15)-C(43) | 119.23(17) | C(40)-C(39)-C(38) | 119.5(2) |
| C(16)-C(15)-C(43) | 115.93(16) | F(8)-C(40)-C(39) | 119.9(2) |
| N(4)-C(16)-C(17) | 106.60(18) | F(8)-C(40)-C(41) | 120.1(2) |
| N(4)-C(16)-C(15) | 123.16(17) | C(39)-C(40)-C(41) | 119.96(19) |
| C(17)-C(16)-C(15) | 130.22(19) | F(9)-C(41)-C(40) | 119.50(19) |
| C(18)-C(17)-C(16) | 107.6(2) | F(9)-C(41)-C(42) | 120.8(2) |
| C(18)-C(17)-H(17) | 126.2 | C(40)-C(41)-C(42) | 119.68(19) |
| C(16)-C(17)-H(17) | 126.2 | F(10)-C(42)-C(41) | 118.00(19) |
| C(19)-C(18)-C(17) | 107.54(18) | F(10)-C(42)-C(43) | 119.73(18) |
| C(19)-C(18)-H(18) | 126.2 | C(41)-C(42)-C(43) | 122.26(19) |

| | | | |
|-------------------|------------|---------------------|------------|
| C(17)-C(18)-H(18) | 126.2 | C(38)-C(43)-C(42) | 116.05(18) |
| N(4)-C(19)-C(18) | 108.4(2) | C(38)-C(43)-C(15) | 122.09(17) |
| N(4)-C(19)-H(19) | 125.8 | C(42)-C(43)-C(15) | 121.84(17) |
| C(18)-C(19)-H(19) | 125.8 | C(1)-N(1)-C(4) | 109.84(18) |
| F(1)-C(20)-C(21) | 117.96(17) | C(1)-N(1)-H(1N) | 128.2(18) |
| F(1)-C(20)-C(25) | 120.03(16) | C(4)-N(1)-H(1N) | 122.0(18) |
| C(21)-C(20)-C(25) | 122.01(18) | C(9)-N(2)-C(6) | 105.78(15) |
| F(2)-C(21)-C(22) | 120.11(18) | C(11)-N(3)-C(14) | 106.43(14) |
| F(2)-C(21)-C(20) | 120.54(19) | C(19)-N(4)-C(16) | 109.89(18) |
| C(22)-C(21)-C(20) | 119.33(18) | C(19)-N(4)-H(2N) | 128.3(18) |
| F(3)-C(22)-C(23) | 119.60(19) | C(16)-N(4)-H(2N) | 121.7(18) |
| F(3)-C(22)-C(21) | 120.12(19) | Cl(2)-C(44)-Cl(1) | 114.56(18) |
| C(23)-C(22)-C(21) | 120.24(17) | Cl(2)-C(44)-H(44A) | 108.6 |
| F(4)-C(23)-C(22) | 119.27(17) | Cl(1)-C(44)-H(44A) | 108.6 |
| F(4)-C(23)-C(24) | 121.02(18) | Cl(2)-C(44)-H(44B) | 108.6 |
| C(22)-C(23)-C(24) | 119.70(18) | Cl(1)-C(44)-H(44B) | 108.6 |
| F(5)-C(24)-C(23) | 118.36(17) | H(44A)-C(44)-H(44B) | 107.6 |

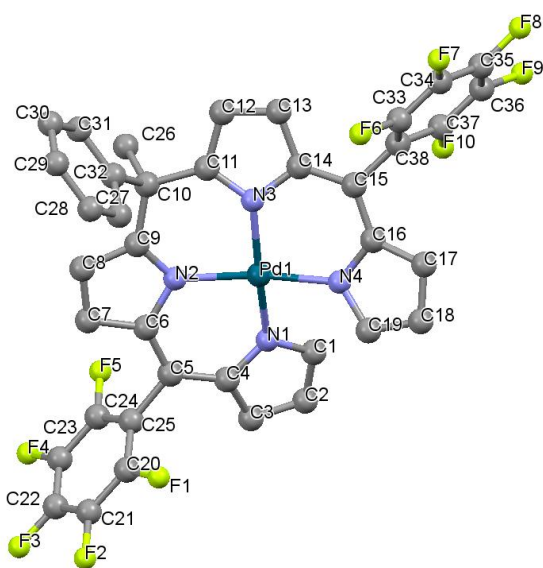


Figure A. 2 Fully labeled solid state structure of Pd[MPBil]. All non N-H hydrogens have been omitted for clarity.

Table A. 2 Bond Lengths (Å) and Bond angles (°) determined for Pd[MPBil]

| Bond | Length | Bond | Length |
|------------|------------|-------------|----------|
| Pd(1)-N(1) | 2.0093(17) | C(11)-C(12) | 1.428(3) |
| Pd(1)-N(2) | 2.0109(15) | C(12)-C(13) | 1.356(3) |
| Pd(1)-N(4) | 2.0127(16) | C(12)-H(12) | 0.95 |

| | | | |
|-------------|------------|--------------|----------|
| Pd(1)-N(3) | 2.0150(16) | C(13)-C(14) | 1.424(3) |
| F(1)-C(20) | 1.337(3) | C(13)-H(13) | 0.95 |
| F(2)-C(21) | 1.342(3) | C(14)-C(15) | 1.381(3) |
| F(3)-C(22) | 1.334(3) | C(15)-C(16) | 1.397(3) |
| F(4)-C(23) | 1.332(3) | C(15)-C(38) | 1.500(3) |
| F(5)-C(24) | 1.330(3) | C(16)-C(17) | 1.415(3) |
| F(6)-C(33) | 1.339(3) | C(17)-C(18) | 1.372(4) |
| F(7)-C(34) | 1.337(3) | C(17)-H(17) | 0.95 |
| F(8)-C(35) | 1.343(3) | C(18)-C(19) | 1.401(3) |
| F(9)-C(36) | 1.336(3) | C(18)-H(18) | 0.95 |
| F(10)-C(37) | 1.338(3) | C(19)-H(19) | 0.95 |
| N(1)-C(1) | 1.342(3) | C(20)-C(25) | 1.381(3) |
| N(1)-C(4) | 1.385(3) | C(20)-C(21) | 1.385(3) |
| N(2)-C(9) | 1.328(3) | C(21)-C(22) | 1.371(4) |
| N(2)-C(6) | 1.407(2) | C(22)-C(23) | 1.371(4) |
| N(3)-C(11) | 1.333(3) | C(23)-C(24) | 1.387(3) |
| N(3)-C(14) | 1.410(2) | C(24)-C(25) | 1.384(3) |
| N(4)-C(19) | 1.343(3) | C(26)-H(26A) | 0.98 |
| N(4)-C(16) | 1.387(3) | C(26)-H(26B) | 0.98 |
| C(1)-C(2) | 1.403(3) | C(26)-H(26C) | 0.98 |
| C(1)-H(1) | 0.95 | C(27)-C(28) | 1.387(4) |
| C(2)-C(3) | 1.375(4) | C(27)-C(32) | 1.394(4) |
| C(2)-H(2) | 0.95 | C(27)-H(27) | 0.95 |
| C(3)-C(4) | 1.411(3) | C(28)-C(29) | 1.362(6) |
| C(3)-H(3) | 0.95 | C(28)-H(28) | 0.95 |
| C(4)-C(5) | 1.398(3) | C(29)-C(30) | 1.369(7) |
| C(5)-C(6) | 1.386(3) | C(29)-H(29) | 0.95 |
| C(5)-C(25) | 1.503(3) | C(30)-C(31) | 1.406(5) |
| C(6)-C(7) | 1.424(3) | C(30)-H(30) | 0.95 |
| C(7)-C(8) | 1.358(3) | C(31)-C(32) | 1.389(3) |
| C(7)-H(7) | 0.95 | C(31)-H(31) | 0.95 |
| C(8)-C(9) | 1.425(3) | C(33)-C(38) | 1.383(3) |
| C(8)-H(8) | 0.95 | C(33)-C(34) | 1.384(3) |
| C(9)-C(10) | 1.513(3) | C(34)-C(35) | 1.368(4) |
| C(10)-C(11) | 1.507(3) | C(35)-C(36) | 1.363(5) |
| C(10)-C(32) | 1.537(3) | C(36)-C(37) | 1.387(3) |
| C(10)-C(26) | 1.552(3) | C(37)-C(38) | 1.387(3) |

| Bond | Angle | Bond | Angle |
|-----------------|-----------|-------------------|----------|
| N(1)-Pd(1)-N(2) | 89.39(7) | C(18)-C(17)-C(16) | 107.1(2) |
| N(1)-Pd(1)-N(4) | 91.49(7) | C(18)-C(17)-H(17) | 126.4 |
| N(2)-Pd(1)-N(4) | 167.06(7) | C(16)-C(17)-H(17) | 126.4 |
| N(1)-Pd(1)-N(3) | 169.24(7) | C(17)-C(18)-C(19) | 106.6(2) |

| | | | |
|-------------------|------------|---------------------|------------|
| N(2)-Pd(1)-N(3) | 91.30(6) | C(17)-C(18)-H(18) | 126.7 |
| N(4)-Pd(1)-N(3) | 90.23(7) | C(19)-C(18)-H(18) | 126.7 |
| C(1)-N(1)-C(4) | 107.10(17) | N(4)-C(19)-C(18) | 111.0(2) |
| C(1)-N(1)-Pd(1) | 125.72(15) | N(4)-C(19)-H(19) | 124.5 |
| C(4)-N(1)-Pd(1) | 127.15(14) | C(18)-C(19)-H(19) | 124.5 |
| C(9)-N(2)-C(6) | 106.49(15) | F(1)-C(20)-C(25) | 120.45(19) |
| C(9)-N(2)-Pd(1) | 126.82(13) | F(1)-C(20)-C(21) | 117.8(2) |
| C(6)-N(2)-Pd(1) | 123.97(12) | C(25)-C(20)-C(21) | 121.8(2) |
| C(11)-N(3)-C(14) | 107.05(16) | F(2)-C(21)-C(22) | 120.0(2) |
| C(11)-N(3)-Pd(1) | 126.79(13) | F(2)-C(21)-C(20) | 120.0(2) |
| C(14)-N(3)-Pd(1) | 123.98(13) | C(22)-C(21)-C(20) | 120.0(2) |
| C(19)-N(4)-C(16) | 106.65(17) | F(3)-C(22)-C(23) | 120.0(2) |
| C(19)-N(4)-Pd(1) | 125.74(14) | F(3)-C(22)-C(21) | 120.3(2) |
| C(16)-N(4)-Pd(1) | 126.92(13) | C(23)-C(22)-C(21) | 119.7(2) |
| N(1)-C(1)-C(2) | 110.5(2) | F(4)-C(23)-C(22) | 120.2(2) |
| N(1)-C(1)-H(1) | 124.7 | F(4)-C(23)-C(24) | 120.3(2) |
| C(2)-C(1)-H(1) | 124.7 | C(22)-C(23)-C(24) | 119.5(2) |
| C(3)-C(2)-C(1) | 106.7(2) | F(5)-C(24)-C(25) | 120.18(19) |
| C(3)-C(2)-H(2) | 126.6 | F(5)-C(24)-C(23) | 117.7(2) |
| C(1)-C(2)-H(2) | 126.6 | C(25)-C(24)-C(23) | 122.2(2) |
| C(2)-C(3)-C(4) | 107.1(2) | C(20)-C(25)-C(24) | 116.79(19) |
| C(2)-C(3)-H(3) | 126.4 | C(20)-C(25)-C(5) | 121.78(19) |
| C(4)-C(3)-H(3) | 126.4 | C(24)-C(25)-C(5) | 121.41(19) |
| N(1)-C(4)-C(5) | 122.94(17) | C(10)-C(26)-H(26A) | 109.5 |
| N(1)-C(4)-C(3) | 108.49(19) | C(10)-C(26)-H(26B) | 109.5 |
| C(5)-C(4)-C(3) | 127.8(2) | H(26A)-C(26)-H(26B) | 109.5 |
| C(6)-C(5)-C(4) | 126.15(18) | C(10)-C(26)-H(26C) | 109.5 |
| C(6)-C(5)-C(25) | 116.63(17) | H(26A)-C(26)-H(26C) | 109.5 |
| C(4)-C(5)-C(25) | 117.11(17) | H(26B)-C(26)-H(26C) | 109.5 |
| C(5)-C(6)-N(2) | 124.95(17) | C(28)-C(27)-C(32) | 121.0(3) |
| C(5)-C(6)-C(7) | 126.67(18) | C(28)-C(27)-H(27) | 119.5 |
| N(2)-C(6)-C(7) | 108.36(16) | C(32)-C(27)-H(27) | 119.5 |
| C(8)-C(7)-C(6) | 107.26(18) | C(29)-C(28)-C(27) | 120.0(4) |
| C(8)-C(7)-H(7) | 126.4 | C(29)-C(28)-H(28) | 120 |
| C(6)-C(7)-H(7) | 126.4 | C(27)-C(28)-H(28) | 120 |
| C(7)-C(8)-C(9) | 106.78(19) | C(28)-C(29)-C(30) | 120.1(3) |
| C(7)-C(8)-H(8) | 126.6 | C(28)-C(29)-H(29) | 119.9 |
| C(9)-C(8)-H(8) | 126.6 | C(30)-C(29)-H(29) | 119.9 |
| N(2)-C(9)-C(8) | 111.10(17) | C(29)-C(30)-C(31) | 121.1(3) |
| N(2)-C(9)-C(10) | 126.46(18) | C(29)-C(30)-H(30) | 119.5 |
| C(8)-C(9)-C(10) | 122.15(18) | C(31)-C(30)-H(30) | 119.5 |
| C(11)-C(10)-C(9) | 116.73(16) | C(32)-C(31)-C(30) | 119.0(3) |
| C(11)-C(10)-C(32) | 106.80(16) | C(32)-C(31)-H(31) | 120.5 |

| | | | |
|-------------------|------------|-------------------|------------|
| C(9)-C(10)-C(32) | 108.10(17) | C(30)-C(31)-H(31) | 120.5 |
| C(11)-C(10)-C(26) | 107.47(17) | C(31)-C(32)-C(27) | 118.8(2) |
| C(9)-C(10)-C(26) | 105.09(16) | C(31)-C(32)-C(10) | 122.4(2) |
| C(32)-C(10)-C(26) | 112.83(18) | C(27)-C(32)-C(10) | 118.78(19) |
| N(3)-C(11)-C(12) | 110.32(17) | F(6)-C(33)-C(38) | 120.06(19) |
| N(3)-C(11)-C(10) | 127.49(17) | F(6)-C(33)-C(34) | 117.2(2) |
| C(12)-C(11)-C(10) | 122.19(18) | C(38)-C(33)-C(34) | 122.8(2) |
| C(13)-C(12)-C(11) | 107.16(19) | F(7)-C(34)-C(35) | 120.8(2) |
| C(13)-C(12)-H(12) | 126.4 | F(7)-C(34)-C(33) | 120.0(3) |
| C(11)-C(12)-H(12) | 126.4 | C(35)-C(34)-C(33) | 119.2(3) |
| C(12)-C(13)-C(14) | 107.49(18) | F(8)-C(35)-C(36) | 120.1(3) |
| C(12)-C(13)-H(13) | 126.3 | F(8)-C(35)-C(34) | 119.7(3) |
| C(14)-C(13)-H(13) | 126.3 | C(36)-C(35)-C(34) | 120.2(2) |
| C(15)-C(14)-N(3) | 124.98(18) | F(9)-C(36)-C(35) | 120.3(3) |
| C(15)-C(14)-C(13) | 127.00(18) | F(9)-C(36)-C(37) | 119.9(3) |
| N(3)-C(14)-C(13) | 107.96(18) | C(35)-C(36)-C(37) | 119.9(3) |
| C(14)-C(15)-C(16) | 126.18(18) | F(10)-C(37)-C(36) | 117.9(2) |
| C(14)-C(15)-C(38) | 117.60(19) | F(10)-C(37)-C(38) | 120.2(2) |
| C(16)-C(15)-C(38) | 116.20(18) | C(36)-C(37)-C(38) | 121.9(3) |
| N(4)-C(16)-C(15) | 123.69(18) | C(33)-C(38)-C(37) | 116.0(2) |
| N(4)-C(16)-C(17) | 108.59(18) | C(33)-C(38)-C(15) | 122.99(19) |
| C(15)-C(16)-C(17) | 127.12(19) | C(37)-C(38)-C(15) | 121.0(2) |

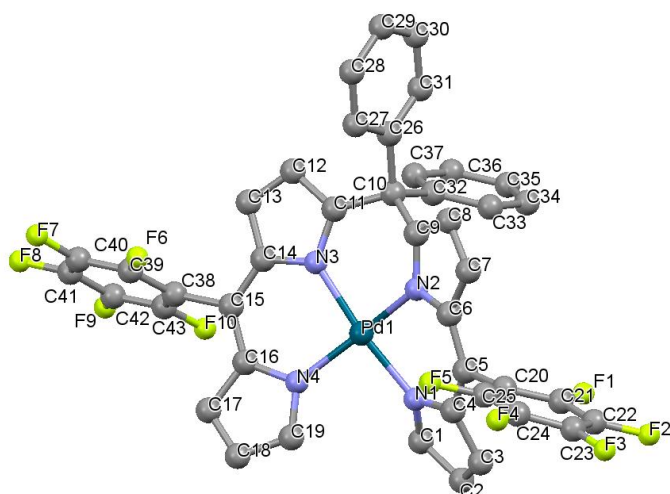


Figure A. 3 Fully labeled solid state structure of Pd[DPBil]. All non N-H hydrogens have been omitted for clarity.

Table A. 3 Bond Lengths (Å) and Bond angles (°) determined for Pd[DPBil]

| Bond | Length | Bond | Length |
|------------|----------|-------------|----------|
| Pd(1)-N(2) | 2.005(4) | C(13)-C(14) | 1.404(7) |

| | | | |
|-------------|----------|-------------|----------|
| Pd(1)-N(1) | 2.017(4) | C(13)-H(13) | 0.95 |
| Pd(1)-N(3) | 2.028(4) | C(14)-C(15) | 1.400(7) |
| Pd(1)-N(4) | 2.031(4) | C(15)-C(16) | 1.387(7) |
| F(1)-C(21) | 1.342(6) | C(15)-C(38) | 1.504(7) |
| F(2)-C(22) | 1.358(6) | C(16)-C(17) | 1.445(7) |
| F(3)-C(23) | 1.330(7) | C(17)-C(18) | 1.353(7) |
| F(4)-C(24) | 1.351(6) | C(17)-H(17) | 0.95 |
| F(5)-C(25) | 1.347(6) | C(18)-C(19) | 1.408(7) |
| F(6)-C(39) | 1.345(6) | C(18)-H(18) | 0.95 |
| F(7)-C(40) | 1.343(6) | C(19)-H(19) | 0.95 |
| F(8)-C(41) | 1.351(6) | C(20)-C(21) | 1.389(7) |
| F(9)-C(42) | 1.333(6) | C(20)-C(25) | 1.404(7) |
| F(10)-C(43) | 1.334(6) | C(21)-C(22) | 1.363(8) |
| N(1)-C(1) | 1.347(6) | C(22)-C(23) | 1.369(9) |
| N(1)-C(4) | 1.395(6) | C(23)-C(24) | 1.380(9) |
| N(2)-C(9) | 1.340(6) | C(24)-C(25) | 1.362(8) |
| N(2)-C(6) | 1.402(6) | C(26)-C(27) | 1.387(7) |
| N(3)-C(11) | 1.349(6) | C(26)-C(31) | 1.389(7) |
| N(3)-C(14) | 1.387(6) | C(27)-C(28) | 1.383(8) |
| N(4)-C(19) | 1.332(6) | C(27)-H(27) | 0.95 |
| N(4)-C(16) | 1.401(6) | C(28)-C(29) | 1.376(9) |
| C(1)-C(2) | 1.410(7) | C(28)-H(28) | 0.95 |
| C(1)-H(1) | 0.95 | C(29)-C(30) | 1.384(8) |
| C(2)-C(3) | 1.359(7) | C(29)-H(29) | 0.95 |
| C(2)-H(2) | 0.95 | C(30)-C(31) | 1.387(7) |
| C(3)-C(4) | 1.429(7) | C(30)-H(30) | 0.95 |
| C(3)-H(3) | 0.95 | C(31)-H(31) | 0.95 |
| C(4)-C(5) | 1.388(7) | C(32)-C(33) | 1.402(7) |
| C(5)-C(6) | 1.400(7) | C(32)-C(37) | 1.403(7) |
| C(5)-C(20) | 1.505(7) | C(33)-C(34) | 1.394(7) |
| C(6)-C(7) | 1.411(7) | C(33)-H(33) | 0.95 |
| C(7)-C(8) | 1.368(7) | C(34)-C(35) | 1.382(7) |
| C(7)-H(7) | 0.95 | C(34)-H(34) | 0.95 |
| C(8)-C(9) | 1.422(6) | C(35)-C(36) | 1.372(8) |
| C(8)-H(8) | 0.95 | C(35)-H(35) | 0.95 |
| C(9)-C(10) | 1.495(6) | C(36)-C(37) | 1.392(7) |
| C(10)-C(11) | 1.520(7) | C(36)-H(36) | 0.95 |
| C(10)-C(32) | 1.543(7) | C(37)-H(37) | 0.95 |
| C(10)-C(26) | 1.548(6) | C(38)-C(43) | 1.383(7) |
| C(11)-C(12) | 1.404(7) | C(38)-C(39) | 1.389(7) |
| C(12)-C(13) | 1.371(7) | C(39)-C(40) | 1.389(7) |
| C(12)-H(12) | 0.95 | C(40)-C(41) | 1.364(8) |
| C(41)-C(42) | 1.386(8) | C(42)-C(43) | 1.378(7) |

| Bond | Angle | Bond | Angle |
|------------------|------------|-------------------|----------|
| N(2)-Pd(1)-N(1) | 88.22(16) | C(19)-C(18)-H(18) | 126.4 |
| N(2)-Pd(1)-N(3) | 89.77(16) | N(4)-C(19)-C(18) | 111.6(5) |
| N(1)-Pd(1)-N(3) | 170.93(15) | N(4)-C(19)-H(19) | 124.2 |
| N(2)-Pd(1)-N(4) | 165.80(16) | C(18)-C(19)-H(19) | 124.2 |
| N(1)-Pd(1)-N(4) | 92.94(16) | C(21)-C(20)-C(25) | 115.6(5) |
| N(3)-Pd(1)-N(4) | 91.19(16) | C(21)-C(20)-C(5) | 123.7(4) |
| C(1)-N(1)-C(4) | 106.7(4) | C(25)-C(20)-C(5) | 120.6(4) |
| C(1)-N(1)-Pd(1) | 127.3(3) | F(1)-C(21)-C(22) | 118.7(5) |
| C(4)-N(1)-Pd(1) | 126.0(3) | F(1)-C(21)-C(20) | 118.9(5) |
| C(9)-N(2)-C(6) | 107.5(4) | C(22)-C(21)-C(20) | 122.4(5) |
| C(9)-N(2)-Pd(1) | 127.3(3) | F(2)-C(22)-C(21) | 120.4(6) |
| C(6)-N(2)-Pd(1) | 122.4(3) | F(2)-C(22)-C(23) | 119.1(5) |
| C(11)-N(3)-C(14) | 106.7(4) | C(21)-C(22)-C(23) | 120.4(5) |
| C(11)-N(3)-Pd(1) | 126.3(3) | F(3)-C(23)-C(22) | 121.0(6) |
| C(14)-N(3)-Pd(1) | 126.5(3) | F(3)-C(23)-C(24) | 119.9(6) |
| C(19)-N(4)-C(16) | 106.5(4) | C(22)-C(23)-C(24) | 119.1(5) |
| C(19)-N(4)-Pd(1) | 126.8(4) | F(4)-C(24)-C(25) | 120.7(5) |
| C(16)-N(4)-Pd(1) | 125.6(3) | F(4)-C(24)-C(23) | 119.1(5) |
| N(1)-C(1)-C(2) | 110.5(4) | C(25)-C(24)-C(23) | 120.1(5) |
| N(1)-C(1)-H(1) | 124.8 | F(5)-C(25)-C(24) | 118.8(5) |
| C(2)-C(1)-H(1) | 124.8 | F(5)-C(25)-C(20) | 119.1(5) |
| C(3)-C(2)-C(1) | 107.5(4) | C(24)-C(25)-C(20) | 122.1(5) |
| C(3)-C(2)-H(2) | 126.3 | C(27)-C(26)-C(31) | 117.8(5) |
| C(1)-C(2)-H(2) | 126.3 | C(27)-C(26)-C(10) | 119.6(4) |
| C(2)-C(3)-C(4) | 107.0(5) | C(31)-C(26)-C(10) | 122.5(4) |
| C(2)-C(3)-H(3) | 126.5 | C(28)-C(27)-C(26) | 120.9(5) |
| C(4)-C(3)-H(3) | 126.5 | C(28)-C(27)-H(27) | 119.5 |
| C(5)-C(4)-N(1) | 121.8(4) | C(26)-C(27)-H(27) | 119.5 |
| C(5)-C(4)-C(3) | 129.1(5) | C(29)-C(28)-C(27) | 120.8(5) |
| N(1)-C(4)-C(3) | 108.3(4) | C(29)-C(28)-H(28) | 119.6 |
| C(4)-C(5)-C(6) | 126.7(5) | C(27)-C(28)-H(28) | 119.6 |
| C(4)-C(5)-C(20) | 117.1(4) | C(28)-C(29)-C(30) | 119.2(5) |
| C(6)-C(5)-C(20) | 115.9(4) | C(28)-C(29)-H(29) | 120.4 |
| C(5)-C(6)-N(2) | 123.6(4) | C(30)-C(29)-H(29) | 120.4 |
| C(5)-C(6)-C(7) | 127.8(5) | C(29)-C(30)-C(31) | 119.8(5) |
| N(2)-C(6)-C(7) | 108.0(4) | C(29)-C(30)-H(30) | 120.1 |
| C(8)-C(7)-C(6) | 107.7(4) | C(31)-C(30)-H(30) | 120.1 |
| C(8)-C(7)-H(7) | 126.2 | C(30)-C(31)-C(26) | 121.4(5) |
| C(6)-C(7)-H(7) | 126.2 | C(30)-C(31)-H(31) | 119.3 |
| C(7)-C(8)-C(9) | 107.0(4) | C(26)-C(31)-H(31) | 119.3 |
| C(7)-C(8)-H(8) | 126.5 | C(33)-C(32)-C(37) | 117.3(5) |

| | | | |
|-------------------|----------|-------------------|----------|
| C(9)-C(8)-H(8) | 126.5 | C(33)-C(32)-C(10) | 121.1(4) |
| N(2)-C(9)-C(8) | 109.8(4) | C(37)-C(32)-C(10) | 121.5(4) |
| N(2)-C(9)-C(10) | 121.3(4) | C(34)-C(33)-C(32) | 120.9(5) |
| C(8)-C(9)-C(10) | 128.1(4) | C(34)-C(33)-H(33) | 119.5 |
| C(9)-C(10)-C(11) | 113.0(4) | C(32)-C(33)-H(33) | 119.5 |
| C(9)-C(10)-C(32) | 108.3(4) | C(35)-C(34)-C(33) | 120.5(5) |
| C(11)-C(10)-C(32) | 109.0(4) | C(35)-C(34)-H(34) | 119.7 |
| C(9)-C(10)-C(26) | 109.6(4) | C(33)-C(34)-H(34) | 119.7 |
| C(11)-C(10)-C(26) | 106.8(4) | C(36)-C(35)-C(34) | 119.4(5) |
| C(32)-C(10)-C(26) | 110.1(4) | C(36)-C(35)-H(35) | 120.3 |
| N(3)-C(11)-C(12) | 109.7(5) | C(34)-C(35)-H(35) | 120.3 |
| N(3)-C(11)-C(10) | 124.1(4) | C(35)-C(36)-C(37) | 120.8(5) |
| C(12)-C(11)-C(10) | 125.8(5) | C(35)-C(36)-H(36) | 119.6 |
| C(13)-C(12)-C(11) | 107.7(5) | C(37)-C(36)-H(36) | 119.6 |
| C(13)-C(12)-H(12) | 126.1 | C(36)-C(37)-C(32) | 121.0(5) |
| C(11)-C(12)-H(12) | 126.1 | C(36)-C(37)-H(37) | 119.5 |
| C(12)-C(13)-C(14) | 106.4(5) | C(32)-C(37)-H(37) | 119.5 |
| C(12)-C(13)-H(13) | 126.8 | C(43)-C(38)-C(39) | 116.5(5) |
| C(14)-C(13)-H(13) | 126.8 | C(43)-C(38)-C(15) | 121.0(4) |
| N(3)-C(14)-C(15) | 124.2(5) | C(39)-C(38)-C(15) | 122.6(5) |
| N(3)-C(14)-C(13) | 109.4(4) | F(6)-C(39)-C(40) | 118.2(5) |
| C(15)-C(14)-C(13) | 126.4(5) | F(6)-C(39)-C(38) | 119.7(5) |
| C(16)-C(15)-C(14) | 127.5(5) | C(40)-C(39)-C(38) | 122.1(5) |
| C(16)-C(15)-C(38) | 115.7(4) | F(7)-C(40)-C(41) | 120.5(5) |
| C(14)-C(15)-C(38) | 116.8(5) | F(7)-C(40)-C(39) | 120.1(5) |
| C(15)-C(16)-N(4) | 124.7(5) | C(41)-C(40)-C(39) | 119.3(5) |
| C(15)-C(16)-C(17) | 127.2(5) | F(8)-C(41)-C(40) | 119.5(5) |
| N(4)-C(16)-C(17) | 107.8(4) | F(8)-C(41)-C(42) | 119.9(5) |
| C(18)-C(17)-C(16) | 106.9(5) | C(40)-C(41)-C(42) | 120.5(5) |
| C(18)-C(17)-H(17) | 126.6 | F(9)-C(42)-C(43) | 121.1(5) |
| C(16)-C(17)-H(17) | 126.6 | F(9)-C(42)-C(41) | 120.0(5) |
| C(17)-C(18)-C(19) | 107.3(5) | C(43)-C(42)-C(41) | 118.9(5) |
| C(17)-C(18)-H(18) | 126.4 | F(10)-C(43)-C(42) | 117.6(4) |
| C(42)-C(43)-C(38) | 122.7(5) | F(10)-C(43)-C(38) | 119.7(5) |

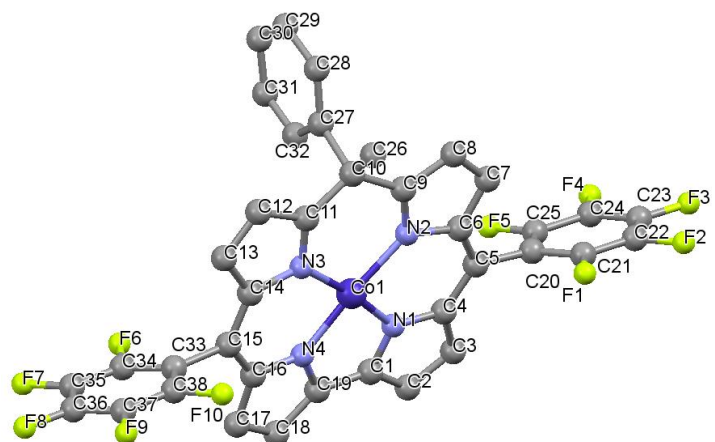


Figure A. 4 Fully labeled solid state structure of Co(10-MPIC). All non N-H hydrogens have been omitted for clarity.

Table A. 4 Bond Lengths (Å) and Bond angles (°) determined for Co(10-MPIC)

| Bond | Length | Bond | Length |
|-------------|-----------|--------------|-----------|
| Co(1)-N(1) | 1.860(6) | C(11)-C(12) | 1.394(12) |
| Co(1)-N(4) | 1.880(7) | C(12)-C(13) | 1.346(13) |
| Co(1)-N(3) | 1.880(7) | C(12)-H(12) | 0.95 |
| Co(1)-N(2) | 1.907(7) | C(13)-C(14) | 1.426(11) |
| F(1)-C(21) | 1.315(13) | C(13)-H(13) | 0.95 |
| F(2)-C(22) | 1.352(16) | C(14)-C(15) | 1.400(12) |
| F(3)-C(23) | 1.332(14) | C(15)-C(16) | 1.393(11) |
| F(4)-C(24) | 1.345(17) | C(15)-C(33) | 1.510(12) |
| F(5)-C(25) | 1.321(14) | C(16)-C(17) | 1.418(11) |
| F(6)-C(34) | 1.338(10) | C(17)-C(18) | 1.358(11) |
| F(7)-C(35) | 1.329(12) | C(17)-H(17) | 0.95 |
| F(8)-C(36) | 1.328(11) | C(18)-C(19) | 1.396(12) |
| F(9)-C(37) | 1.351(11) | C(18)-H(18) | 0.95 |
| F(10)-C(38) | 1.336(10) | C(20)-C(25) | 1.347(14) |
| N(1)-C(1) | 1.358(10) | C(20)-C(21) | 1.406(14) |
| N(1)-C(4) | 1.362(10) | C(21)-C(22) | 1.380(15) |
| N(2)-C(9) | 1.343(10) | C(22)-C(23) | 1.30(2) |
| N(2)-C(6) | 1.411(10) | C(23)-C(24) | 1.40(2) |
| N(3)-C(11) | 1.351(10) | C(24)-C(25) | 1.457(18) |
| N(3)-C(14) | 1.401(11) | C(26)-H(26A) | 0.98 |
| N(4)-C(16) | 1.356(10) | C(26)-H(26B) | 0.98 |
| N(4)-C(19) | 1.359(9) | C(26)-H(26C) | 0.98 |
| C(1)-C(2) | 1.410(11) | C(27)-C(28) | 1.377(11) |
| C(1)-C(19) | 1.442(12) | C(27)-C(32) | 1.390(12) |

| | | | |
|-------------|-----------|-------------|-----------|
| C(2)-C(3) | 1.353(13) | C(28)-C(29) | 1.400(12) |
| C(2)-H(2) | 0.95 | C(28)-H(28) | 0.95 |
| C(3)-C(4) | 1.420(12) | C(29)-C(30) | 1.371(13) |
| C(3)-H(3) | 0.95 | C(29)-H(29) | 0.95 |
| C(4)-C(5) | 1.414(12) | C(30)-C(31) | 1.385(13) |
| C(5)-C(6) | 1.388(12) | C(30)-H(30) | 0.95 |
| C(5)-C(20) | 1.492(12) | C(31)-C(32) | 1.374(12) |
| C(6)-C(7) | 1.402(12) | C(31)-H(31) | 0.95 |
| C(7)-C(8) | 1.353(13) | C(32)-H(32) | 0.95 |
| C(7)-H(7) | 0.95 | C(33)-C(34) | 1.370(12) |
| C(8)-C(9) | 1.422(12) | C(33)-C(38) | 1.374(11) |
| C(8)-H(8) | 0.95 | C(34)-C(35) | 1.370(13) |
| C(9)-C(10) | 1.502(11) | C(35)-C(36) | 1.390(16) |
| C(10)-C(11) | 1.499(12) | C(36)-C(37) | 1.340(14) |
| C(10)-C(26) | 1.526(12) | C(37)-C(38) | 1.392(13) |
| C(10)-C(27) | 1.569(11) | | |

| Bond | Angle | Bond | Angle |
|------------------|----------|-------------------|-----------|
| N(1)-Co(1)-N(4) | 81.6(3) | C(18)-C(17)-H(17) | 125.8 |
| N(1)-Co(1)-N(3) | 172.6(3) | C(16)-C(17)-H(17) | 125.8 |
| N(4)-Co(1)-N(3) | 91.2(3) | C(17)-C(18)-C(19) | 107.0(8) |
| N(1)-Co(1)-N(2) | 91.2(3) | C(17)-C(18)-H(18) | 126.5 |
| N(4)-Co(1)-N(2) | 172.7(3) | C(19)-C(18)-H(18) | 126.5 |
| N(3)-Co(1)-N(2) | 96.0(3) | N(4)-C(19)-C(18) | 108.6(7) |
| C(1)-N(1)-C(4) | 108.7(7) | N(4)-C(19)-C(1) | 111.5(7) |
| C(1)-N(1)-Co(1) | 117.8(5) | C(18)-C(19)-C(1) | 139.9(8) |
| C(4)-N(1)-Co(1) | 133.5(6) | C(25)-C(20)-C(21) | 117.8(10) |
| C(9)-N(2)-C(6) | 106.8(7) | C(25)-C(20)-C(5) | 121.6(10) |
| C(9)-N(2)-Co(1) | 126.2(6) | C(21)-C(20)-C(5) | 120.5(9) |
| C(6)-N(2)-Co(1) | 127.0(6) | F(1)-C(21)-C(22) | 116.2(12) |
| C(11)-N(3)-C(14) | 106.2(7) | F(1)-C(21)-C(20) | 122.6(9) |
| C(11)-N(3)-Co(1) | 127.6(6) | C(22)-C(21)-C(20) | 121.2(13) |
| C(14)-N(3)-Co(1) | 126.1(6) | C(23)-C(22)-F(2) | 117.5(14) |
| C(16)-N(4)-C(19) | 109.2(7) | C(23)-C(22)-C(21) | 122.3(16) |
| C(16)-N(4)-Co(1) | 133.5(5) | F(2)-C(22)-C(21) | 120.2(15) |
| C(19)-N(4)-Co(1) | 117.3(6) | C(22)-C(23)-F(3) | 123.6(19) |
| N(1)-C(1)-C(2) | 108.1(8) | C(22)-C(23)-C(24) | 119.7(13) |
| N(1)-C(1)-C(19) | 111.8(7) | F(3)-C(23)-C(24) | 116.7(17) |
| C(2)-C(1)-C(19) | 140.0(8) | F(4)-C(24)-C(23) | 124.2(14) |
| C(3)-C(2)-C(1) | 107.9(8) | F(4)-C(24)-C(25) | 116.9(16) |
| C(3)-C(2)-H(2) | 126 | C(23)-C(24)-C(25) | 118.8(14) |
| C(1)-C(2)-H(2) | 126 | F(5)-C(25)-C(20) | 121.6(11) |
| C(2)-C(3)-C(4) | 107.3(8) | F(5)-C(25)-C(24) | 118.2(12) |

| | | | |
|-------------------|----------|---------------------|-----------|
| C(2)-C(3)-H(3) | 126.4 | C(20)-C(25)-C(24) | 120.2(14) |
| C(4)-C(3)-H(3) | 126.4 | C(10)-C(26)-H(26A) | 109.5 |
| N(1)-C(4)-C(5) | 119.4(7) | C(10)-C(26)-H(26B) | 109.5 |
| N(1)-C(4)-C(3) | 107.9(8) | H(26A)-C(26)-H(26B) | 109.5 |
| C(5)-C(4)-C(3) | 132.7(9) | C(10)-C(26)-H(26C) | 109.5 |
| C(6)-C(5)-C(4) | 125.7(8) | H(26A)-C(26)-H(26C) | 109.5 |
| C(6)-C(5)-C(20) | 115.8(8) | H(26B)-C(26)-H(26C) | 109.5 |
| C(4)-C(5)-C(20) | 118.6(8) | C(28)-C(27)-C(32) | 118.4(8) |
| C(5)-C(6)-C(7) | 128.8(8) | C(28)-C(27)-C(10) | 123.2(8) |
| C(5)-C(6)-N(2) | 123.0(8) | C(32)-C(27)-C(10) | 118.4(7) |
| C(7)-C(6)-N(2) | 107.9(8) | C(27)-C(28)-C(29) | 120.9(9) |
| C(8)-C(7)-C(6) | 108.5(8) | C(27)-C(28)-H(28) | 119.6 |
| C(8)-C(7)-H(7) | 125.8 | C(29)-C(28)-H(28) | 119.6 |
| C(6)-C(7)-H(7) | 125.8 | C(30)-C(29)-C(28) | 119.8(8) |
| C(7)-C(8)-C(9) | 106.9(8) | C(30)-C(29)-H(29) | 120.1 |
| C(7)-C(8)-H(8) | 126.5 | C(28)-C(29)-H(29) | 120.1 |
| C(9)-C(8)-H(8) | 126.5 | C(29)-C(30)-C(31) | 119.6(9) |
| N(2)-C(9)-C(8) | 109.9(8) | C(29)-C(30)-H(30) | 120.2 |
| N(2)-C(9)-C(10) | 125.6(8) | C(31)-C(30)-H(30) | 120.2 |
| C(8)-C(9)-C(10) | 124.1(8) | C(32)-C(31)-C(30) | 120.4(9) |
| C(11)-C(10)-C(9) | 118.2(7) | C(32)-C(31)-H(31) | 119.8 |
| C(11)-C(10)-C(26) | 108.6(7) | C(30)-C(31)-H(31) | 119.8 |
| C(9)-C(10)-C(26) | 108.5(7) | C(31)-C(32)-C(27) | 120.9(8) |
| C(11)-C(10)-C(27) | 103.6(7) | C(31)-C(32)-H(32) | 119.5 |
| C(9)-C(10)-C(27) | 106.3(6) | C(27)-C(32)-H(32) | 119.5 |
| C(26)-C(10)-C(27) | 111.5(7) | C(34)-C(33)-C(38) | 116.3(8) |
| N(3)-C(11)-C(12) | 110.0(8) | C(34)-C(33)-C(15) | 122.7(8) |
| N(3)-C(11)-C(10) | 124.9(7) | C(38)-C(33)-C(15) | 121.0(8) |
| C(12)-C(11)-C(10) | 124.8(8) | F(6)-C(34)-C(33) | 119.2(8) |
| C(13)-C(12)-C(11) | 109.0(8) | F(6)-C(34)-C(35) | 117.0(9) |
| C(13)-C(12)-H(12) | 125.5 | C(33)-C(34)-C(35) | 123.8(9) |
| C(11)-C(12)-H(12) | 125.5 | F(7)-C(35)-C(34) | 121.6(11) |
| C(12)-C(13)-C(14) | 106.3(8) | F(7)-C(35)-C(36) | 119.8(10) |
| C(12)-C(13)-H(13) | 126.8 | C(34)-C(35)-C(36) | 118.6(10) |
| C(14)-C(13)-H(13) | 126.8 | F(8)-C(36)-C(37) | 122.0(11) |
| C(15)-C(14)-N(3) | 125.1(7) | F(8)-C(36)-C(35) | 119.1(11) |
| C(15)-C(14)-C(13) | 126.4(8) | C(37)-C(36)-C(35) | 118.9(10) |
| N(3)-C(14)-C(13) | 108.4(8) | C(36)-C(37)-F(9) | 120.4(10) |
| C(16)-C(15)-C(14) | 124.3(8) | C(36)-C(37)-C(38) | 121.7(10) |
| C(16)-C(15)-C(33) | 118.2(8) | F(9)-C(37)-C(38) | 117.9(10) |
| C(14)-C(15)-C(33) | 117.4(7) | F(10)-C(38)-C(33) | 120.8(8) |
| N(4)-C(16)-C(15) | 119.3(8) | F(10)-C(38)-C(37) | 118.4(8) |
| N(4)-C(16)-C(17) | 106.8(7) | C(33)-C(38)-C(37) | 120.8(9) |

C(15)-C(16)-C(17) 133.8(8) C(18)-C(17)-C(16) 108.3(8)

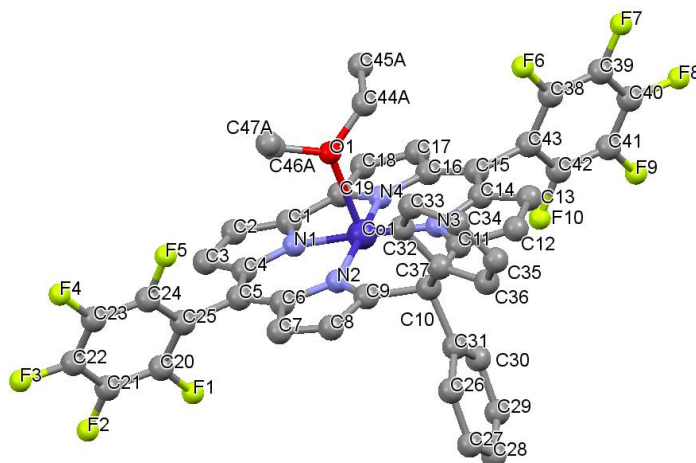


Figure A. 5 Fully labeled solid state structure of Co(10-DPIC) with a molecule of diethyl ether as an axial ligand. All non N-H hydrogens have been omitted for clarity.

Table A. 5 Bond Lengths (Å) and Bond angles (°) determined for Co(10-DPIC)

| Bond | Length | Bond | Length |
|-------------|----------|-------------|----------|
| Co(1)-N(4) | 1.867(2) | C(23)-C(24) | 1.382(4) |
| Co(1)-N(1) | 1.873(2) | C(24)-C(25) | 1.379(4) |
| Co(1)-N(2) | 1.902(2) | C(26)-C(27) | 1.393(5) |
| Co(1)-N(3) | 1.904(2) | C(26)-C(31) | 1.397(4) |
| Co(1)-O(1) | 2.312(3) | C(26)-H(26) | 0.95 |
| F(1)-C(20) | 1.348(4) | C(27)-C(28) | 1.380(6) |
| F(2)-C(21) | 1.335(4) | C(27)-H(27) | 0.95 |
| F(3)-C(22) | 1.338(4) | C(28)-C(29) | 1.379(5) |
| F(4)-C(23) | 1.344(4) | C(28)-H(28) | 0.95 |
| F(5)-C(24) | 1.338(4) | C(29)-C(30) | 1.383(5) |
| F(6)-C(38) | 1.345(4) | C(29)-H(29) | 0.95 |
| F(7)-C(39) | 1.334(4) | C(30)-C(31) | 1.392(4) |
| F(8)-C(40) | 1.332(4) | C(30)-H(30) | 0.95 |
| F(9)-C(41) | 1.345(4) | C(32)-C(37) | 1.391(4) |
| F(10)-C(42) | 1.337(4) | C(32)-C(33) | 1.391(5) |
| N(1)-C(1) | 1.354(4) | C(32)-H(32) | 0.95 |
| N(1)-C(4) | 1.369(4) | C(33)-C(34) | 1.382(6) |
| N(2)-C(9) | 1.344(4) | C(33)-H(33) | 0.95 |
| N(2)-C(6) | 1.407(4) | C(34)-C(35) | 1.381(5) |
| N(3)-C(11) | 1.334(4) | C(34)-H(34) | 0.95 |
| N(3)-C(14) | 1.409(3) | C(35)-C(36) | 1.388(5) |

| | | | |
|-------------|----------|---------------|-----------|
| N(4)-C(19) | 1.357(4) | C(35)-H(35) | 0.95 |
| N(4)-C(16) | 1.375(4) | C(36)-C(37) | 1.388(4) |
| C(1)-C(2) | 1.411(4) | C(36)-H(36) | 0.95 |
| C(1)-C(19) | 1.447(4) | C(38)-C(43) | 1.379(4) |
| C(2)-C(3) | 1.372(5) | C(38)-C(39) | 1.382(4) |
| C(2)-H(2) | 0.95 | C(39)-C(40) | 1.373(5) |
| C(3)-C(4) | 1.442(4) | C(40)-C(41) | 1.368(6) |
| C(3)-H(3) | 0.95 | C(41)-C(42) | 1.389(5) |
| C(4)-C(5) | 1.394(4) | C(42)-C(43) | 1.389(4) |
| C(5)-C(6) | 1.399(4) | O(1)-C(44B) | 1.393(9) |
| C(5)-C(25) | 1.493(4) | O(1)-C(44A) | 1.423(8) |
| C(6)-C(7) | 1.415(4) | O(1)-C(46A) | 1.435(9) |
| C(7)-C(8) | 1.363(4) | O(1)-C(46B) | 1.492(10) |
| C(7)-H(7) | 0.95 | C(44A)-C(45A) | 1.454(12) |
| C(8)-C(9) | 1.430(4) | C(44A)-H(44A) | 0.99 |
| C(8)-H(8) | 0.95 | C(44A)-H(44B) | 0.99 |
| C(9)-C(10) | 1.512(4) | C(45A)-H(45A) | 0.98 |
| C(10)-C(11) | 1.530(4) | C(45A)-H(45B) | 0.98 |
| C(10)-C(37) | 1.548(4) | C(45A)-H(45C) | 0.98 |
| C(10)-C(31) | 1.559(4) | C(46A)-C(47A) | 1.341(12) |
| C(11)-C(12) | 1.422(4) | C(46A)-H(46A) | 0.99 |
| C(12)-C(13) | 1.361(4) | C(46A)-H(46B) | 0.99 |
| C(12)-H(12) | 0.95 | C(47A)-H(47A) | 0.98 |
| C(13)-C(14) | 1.426(4) | C(47A)-H(47B) | 0.98 |
| C(13)-H(13) | 0.95 | C(47A)-H(47C) | 0.98 |
| C(14)-C(15) | 1.399(4) | C(44B)-C(45B) | 1.371(12) |
| C(15)-C(16) | 1.397(4) | C(44B)-H(44C) | 0.99 |
| C(15)-C(43) | 1.498(4) | C(44B)-H(44D) | 0.99 |
| C(16)-C(17) | 1.438(4) | C(45B)-H(45D) | 0.98 |
| C(17)-C(18) | 1.368(5) | C(45B)-H(45E) | 0.98 |
| C(17)-H(17) | 0.95 | C(45B)-H(45F) | 0.98 |
| C(18)-C(19) | 1.418(4) | C(46B)-C(47B) | 1.477(13) |
| C(18)-H(18) | 0.95 | C(46B)-H(46C) | 0.99 |
| C(20)-C(21) | 1.370(5) | C(46B)-H(46D) | 0.99 |
| C(20)-C(25) | 1.392(5) | C(47B)-H(47D) | 0.98 |
| C(21)-C(22) | 1.382(6) | C(47B)-H(47E) | 0.98 |
| C(22)-C(23) | 1.371(5) | C(47B)-H(47F) | 0.98 |

| Bond | Angle | Bond | Angle |
|-----------------|------------|-------------------|----------|
| N(4)-Co(1)-N(1) | 80.79(11) | C(28)-C(27)-H(27) | 119.8 |
| N(4)-Co(1)-N(2) | 170.13(11) | C(26)-C(27)-H(27) | 119.8 |
| N(1)-Co(1)-N(2) | 91.39(11) | C(29)-C(28)-C(27) | 119.8(4) |
| N(4)-Co(1)-N(3) | 91.71(10) | C(29)-C(28)-H(28) | 120.1 |

| | | | |
|------------------|------------|-------------------|----------|
| N(1)-Co(1)-N(3) | 170.49(11) | C(27)-C(28)-H(28) | 120.1 |
| N(2)-Co(1)-N(3) | 95.39(10) | C(28)-C(29)-C(30) | 120.1(4) |
| N(4)-Co(1)-O(1) | 93.44(11) | C(28)-C(29)-H(29) | 120 |
| N(1)-Co(1)-O(1) | 92.60(10) | C(30)-C(29)-H(29) | 120 |
| N(2)-Co(1)-O(1) | 92.93(11) | C(29)-C(30)-C(31) | 121.2(3) |
| N(3)-Co(1)-O(1) | 93.70(10) | C(29)-C(30)-H(30) | 119.4 |
| C(1)-N(1)-C(4) | 108.6(2) | C(31)-C(30)-H(30) | 119.4 |
| C(1)-N(1)-Co(1) | 118.3(2) | C(30)-C(31)-C(26) | 118.3(3) |
| C(4)-N(1)-Co(1) | 133.1(2) | C(30)-C(31)-C(10) | 120.4(3) |
| C(9)-N(2)-C(6) | 106.5(2) | C(26)-C(31)-C(10) | 121.1(3) |
| C(9)-N(2)-Co(1) | 127.6(2) | C(37)-C(32)-C(33) | 121.2(3) |
| C(6)-N(2)-Co(1) | 125.7(2) | C(37)-C(32)-H(32) | 119.4 |
| C(11)-N(3)-C(14) | 106.7(2) | C(33)-C(32)-H(32) | 119.4 |
| C(11)-N(3)-Co(1) | 127.8(2) | C(34)-C(33)-C(32) | 120.0(3) |
| C(14)-N(3)-Co(1) | 125.6(2) | C(34)-C(33)-H(33) | 120 |
| C(19)-N(4)-C(16) | 107.9(3) | C(32)-C(33)-H(33) | 120 |
| C(19)-N(4)-Co(1) | 118.6(2) | C(35)-C(34)-C(33) | 119.1(3) |
| C(16)-N(4)-Co(1) | 133.4(2) | C(35)-C(34)-H(34) | 120.5 |
| N(1)-C(1)-C(2) | 109.7(3) | C(33)-C(34)-H(34) | 120.5 |
| N(1)-C(1)-C(19) | 111.3(3) | C(34)-C(35)-C(36) | 120.9(4) |
| C(2)-C(1)-C(19) | 138.9(3) | C(34)-C(35)-H(35) | 119.5 |
| C(3)-C(2)-C(1) | 106.9(3) | C(36)-C(35)-H(35) | 119.5 |
| C(3)-C(2)-H(2) | 126.6 | C(35)-C(36)-C(37) | 120.6(3) |
| C(1)-C(2)-H(2) | 126.6 | C(35)-C(36)-H(36) | 119.7 |
| C(2)-C(3)-C(4) | 107.3(3) | C(37)-C(36)-H(36) | 119.7 |
| C(2)-C(3)-H(3) | 126.3 | C(36)-C(37)-C(32) | 118.1(3) |
| C(4)-C(3)-H(3) | 126.3 | C(36)-C(37)-C(10) | 122.8(3) |
| N(1)-C(4)-C(5) | 119.6(3) | C(32)-C(37)-C(10) | 119.0(3) |
| N(1)-C(4)-C(3) | 107.5(3) | F(6)-C(38)-C(43) | 119.7(3) |
| C(5)-C(4)-C(3) | 133.0(3) | F(6)-C(38)-C(39) | 117.7(3) |
| C(4)-C(5)-C(6) | 124.9(3) | C(43)-C(38)-C(39) | 122.6(3) |
| C(4)-C(5)-C(25) | 116.7(3) | F(7)-C(39)-C(40) | 120.2(3) |
| C(6)-C(5)-C(25) | 118.5(3) | F(7)-C(39)-C(38) | 120.7(4) |
| C(5)-C(6)-N(2) | 124.8(3) | C(40)-C(39)-C(38) | 119.1(3) |
| C(5)-C(6)-C(7) | 126.7(3) | F(8)-C(40)-C(41) | 119.9(4) |
| N(2)-C(6)-C(7) | 108.5(3) | F(8)-C(40)-C(39) | 119.9(4) |
| C(8)-C(7)-C(6) | 107.8(3) | C(41)-C(40)-C(39) | 120.2(3) |
| C(8)-C(7)-H(7) | 126.1 | F(9)-C(41)-C(40) | 120.5(3) |
| C(6)-C(7)-H(7) | 126.1 | F(9)-C(41)-C(42) | 119.6(4) |
| C(7)-C(8)-C(9) | 106.6(3) | C(40)-C(41)-C(42) | 119.9(3) |
| C(7)-C(8)-H(8) | 126.7 | F(10)-C(42)-C(41) | 118.3(3) |
| C(9)-C(8)-H(8) | 126.7 | F(10)-C(42)-C(43) | 120.3(3) |
| N(2)-C(9)-C(8) | 110.5(3) | C(41)-C(42)-C(43) | 121.4(3) |

| | | | |
|-------------------|----------|----------------------|-----------|
| N(2)-C(9)-C(10) | 124.9(3) | C(38)-C(43)-C(42) | 116.8(3) |
| C(8)-C(9)-C(10) | 124.4(3) | C(38)-C(43)-C(15) | 122.3(3) |
| C(9)-C(10)-C(11) | 117.6(2) | C(42)-C(43)-C(15) | 120.9(3) |
| C(9)-C(10)-C(37) | 109.0(2) | C(44A)-O(1)-C(46A) | 116.9(6) |
| C(11)-C(10)-C(37) | 106.4(2) | C(44B)-O(1)-C(46B) | 112.0(7) |
| C(9)-C(10)-C(31) | 103.6(2) | C(44B)-O(1)-Co(1) | 123.4(5) |
| C(11)-C(10)-C(31) | 106.9(2) | C(44A)-O(1)-Co(1) | 120.7(4) |
| C(37)-C(10)-C(31) | 113.4(2) | C(46A)-O(1)-Co(1) | 121.8(4) |
| N(3)-C(11)-C(12) | 111.0(3) | C(46B)-O(1)-Co(1) | 119.8(5) |
| N(3)-C(11)-C(10) | 124.7(3) | O(1)-C(44A)-C(45A) | 116.0(8) |
| C(12)-C(11)-C(10) | 123.6(3) | O(1)-C(44A)-H(44A) | 108.3 |
| C(13)-C(12)-C(11) | 106.7(3) | C(45A)-C(44A)-H(44A) | 108.3 |
| C(13)-C(12)-H(12) | 126.6 | O(1)-C(44A)-H(44B) | 108.3 |
| C(11)-C(12)-H(12) | 126.6 | C(45A)-C(44A)-H(44B) | 108.3 |
| C(12)-C(13)-C(14) | 107.6(3) | H(44A)-C(44A)-H(44B) | 107.4 |
| C(12)-C(13)-H(13) | 126.2 | C(44A)-C(45A)-H(45A) | 109.5 |
| C(14)-C(13)-H(13) | 126.2 | C(44A)-C(45A)-H(45B) | 109.5 |
| C(15)-C(14)-N(3) | 124.8(3) | H(45A)-C(45A)-H(45B) | 109.5 |
| C(15)-C(14)-C(13) | 127.1(3) | C(44A)-C(45A)-H(45C) | 109.5 |
| N(3)-C(14)-C(13) | 108.0(3) | H(45A)-C(45A)-H(45C) | 109.5 |
| C(16)-C(15)-C(14) | 125.2(3) | H(45B)-C(45A)-H(45C) | 109.5 |
| C(16)-C(15)-C(43) | 117.8(3) | C(47A)-C(46A)-O(1) | 112.8(9) |
| C(14)-C(15)-C(43) | 117.0(3) | C(47A)-C(46A)-H(46A) | 109 |
| N(4)-C(16)-C(15) | 119.1(3) | O(1)-C(46A)-H(46A) | 109 |
| N(4)-C(16)-C(17) | 108.2(3) | C(47A)-C(46A)-H(46B) | 109 |
| C(15)-C(16)-C(17) | 132.7(3) | O(1)-C(46A)-H(46B) | 109 |
| C(18)-C(17)-C(16) | 107.2(3) | H(46A)-C(46A)-H(46B) | 107.8 |
| C(18)-C(17)-H(17) | 126.4 | C(46A)-C(47A)-H(47A) | 109.5 |
| C(16)-C(17)-H(17) | 126.4 | C(46A)-C(47A)-H(47B) | 109.5 |
| C(17)-C(18)-C(19) | 107.1(3) | H(47A)-C(47A)-H(47B) | 109.5 |
| C(17)-C(18)-H(18) | 126.5 | C(46A)-C(47A)-H(47C) | 109.5 |
| C(19)-C(18)-H(18) | 126.5 | H(47A)-C(47A)-H(47C) | 109.5 |
| N(4)-C(19)-C(18) | 109.8(3) | H(47B)-C(47A)-H(47C) | 109.5 |
| N(4)-C(19)-C(1) | 110.9(3) | C(45B)-C(44B)-O(1) | 123.5(11) |
| C(18)-C(19)-C(1) | 139.3(3) | C(45B)-C(44B)-H(44C) | 106.4 |
| F(1)-C(20)-C(21) | 117.3(3) | O(1)-C(44B)-H(44C) | 106.4 |
| F(1)-C(20)-C(25) | 119.9(3) | C(45B)-C(44B)-H(44D) | 106.4 |
| C(21)-C(20)-C(25) | 122.8(3) | O(1)-C(44B)-H(44D) | 106.4 |
| F(2)-C(21)-C(20) | 120.7(4) | H(44C)-C(44B)-H(44D) | 106.5 |
| F(2)-C(21)-C(22) | 120.3(3) | C(44B)-C(45B)-H(45D) | 109.5 |
| C(20)-C(21)-C(22) | 119.0(3) | C(44B)-C(45B)-H(45E) | 109.5 |
| F(3)-C(22)-C(23) | 119.8(4) | H(45D)-C(45B)-H(45E) | 109.5 |
| F(3)-C(22)-C(21) | 120.2(4) | C(44B)-C(45B)-H(45F) | 109.5 |

| | | | |
|-------------------|----------|----------------------|-----------|
| C(23)-C(22)-C(21) | 120.0(3) | H(45D)-C(45B)-H(45F) | 109.5 |
| F(4)-C(23)-C(22) | 119.5(3) | H(45E)-C(45B)-H(45F) | 109.5 |
| F(4)-C(23)-C(24) | 120.7(3) | C(47B)-C(46B)-O(1) | 107.9(10) |
| C(22)-C(23)-C(24) | 119.8(3) | C(47B)-C(46B)-H(46C) | 110.1 |
| F(5)-C(24)-C(25) | 119.8(3) | O(1)-C(46B)-H(46C) | 110.1 |
| F(5)-C(24)-C(23) | 118.1(3) | C(47B)-C(46B)-H(46D) | 110.1 |
| C(25)-C(24)-C(23) | 122.1(3) | O(1)-C(46B)-H(46D) | 110.1 |
| C(24)-C(25)-C(20) | 116.3(3) | H(46C)-C(46B)-H(46D) | 108.4 |
| C(24)-C(25)-C(5) | 122.0(3) | C(46B)-C(47B)-H(47D) | 109.5 |
| C(20)-C(25)-C(5) | 121.5(3) | C(46B)-C(47B)-H(47E) | 109.5 |
| C(27)-C(26)-C(31) | 120.3(3) | H(47D)-C(47B)-H(47E) | 109.5 |
| C(27)-C(26)-H(26) | 119.9 | C(46B)-C(47B)-H(47F) | 109.5 |
| C(31)-C(26)-H(26) | 119.9 | H(47D)-C(47B)-H(47F) | 109.5 |
| C(28)-C(27)-C(26) | 120.4(4) | H(47E)-C(47B)-H(47F) | 109.5 |

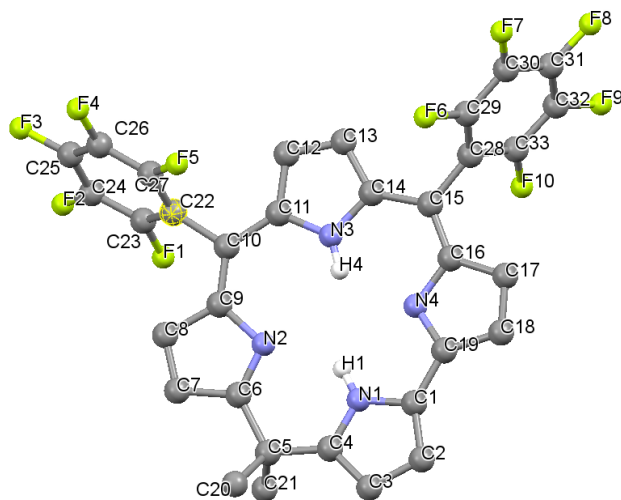


Figure A. 6 Fully labeled solid state structure of 5-DMIC. All non N-H hydrogens have been omitted for clarity.

Table A. 6 Bond Lengths (Å) and Bond angles (°) determined for 5-DMIC

| Bond | Length | Bond | Length |
|------------|----------|-------------|----------|
| F(1)-C(23) | 1.343(4) | C(9)-C(10) | 1.378(5) |
| F(2)-C(24) | 1.336(5) | C(10)-C(11) | 1.432(5) |
| F(3)-C(25) | 1.339(4) | C(10)-C(22) | 1.506(5) |
| F(4)-C(26) | 1.337(4) | C(11)-C(12) | 1.412(4) |
| F(5)-C(27) | 1.331(4) | C(12)-C(13) | 1.372(5) |
| F(6)-C(29) | 1.340(4) | C(12)-H(12) | 0.95 |
| F(7)-C(30) | 1.332(4) | C(13)-C(14) | 1.406(5) |
| F(8)-C(31) | 1.340(4) | C(13)-H(13) | 0.95 |
| F(9)-C(32) | 1.345(5) | C(14)-C(15) | 1.433(5) |

| | | | |
|-------------|----------|--------------|----------|
| F(10)-C(33) | 1.338(4) | C(15)-C(16) | 1.380(5) |
| N(1)-C(4) | 1.330(5) | C(15)-C(28) | 1.485(5) |
| N(1)-C(1) | 1.364(5) | C(16)-C(17) | 1.459(5) |
| N(1)-H(1) | 0.89(5) | C(17)-C(18) | 1.352(5) |
| N(2)-C(6) | 1.322(4) | C(17)-H(17) | 0.95 |
| N(2)-C(9) | 1.410(4) | C(18)-C(19) | 1.460(5) |
| N(3)-C(11) | 1.361(4) | C(18)-H(18) | 0.95 |
| N(3)-C(14) | 1.375(4) | C(20)-H(01D) | 0.98 |
| N(3)-H(4) | 0.85(4) | C(20)-H(01E) | 0.98 |
| N(4)-C(19) | 1.334(4) | C(20)-H(01F) | 0.98 |
| N(4)-C(16) | 1.378(5) | C(21)-H(21) | 0.98 |
| C(1)-C(2) | 1.400(5) | C(21)-H(01B) | 0.98 |
| C(1)-C(19) | 1.416(5) | C(21)-H(01C) | 0.98 |
| C(2)-C(3) | 1.394(6) | C(22)-C(23) | 1.388(5) |
| C(2)-H(2) | 0.95 | C(22)-C(27) | 1.389(5) |
| C(3)-C(4) | 1.401(5) | C(23)-C(24) | 1.385(5) |
| C(3)-H(3) | 0.95 | C(24)-C(25) | 1.378(6) |
| C(4)-C(5) | 1.501(5) | C(25)-C(26) | 1.386(6) |
| C(5)-C(6) | 1.536(5) | C(26)-C(27) | 1.385(5) |
| C(5)-C(20) | 1.546(5) | C(28)-C(29) | 1.384(5) |
| C(5)-C(21) | 1.559(5) | C(28)-C(33) | 1.396(5) |
| C(6)-C(7) | 1.446(5) | C(29)-C(30) | 1.384(5) |
| C(7)-C(8) | 1.345(5) | C(30)-C(31) | 1.382(6) |
| C(7)-H(7) | 0.95 | C(31)-C(32) | 1.363(6) |
| C(8)-C(9) | 1.455(5) | C(32)-C(33) | 1.387(5) |
| C(8)-H(8) | 0.95 | | |

| Bond | Angle | Bond | Angle |
|------------------|----------|---------------------|----------|
| C(4)-N(1)-C(1) | 112.3(3) | C(15)-C(16)-C(17) | 130.0(3) |
| C(4)-N(1)-H(1) | 123(3) | C(18)-C(17)-C(16) | 106.8(3) |
| C(1)-N(1)-H(1) | 125(3) | C(18)-C(17)-H(17) | 126.6 |
| C(6)-N(2)-C(9) | 106.5(3) | C(16)-C(17)-H(17) | 126.6 |
| C(11)-N(3)-C(14) | 110.2(3) | C(17)-C(18)-C(19) | 106.4(3) |
| C(11)-N(3)-H(4) | 129(2) | C(17)-C(18)-H(18) | 126.8 |
| C(14)-N(3)-H(4) | 121(2) | C(19)-C(18)-H(18) | 126.8 |
| C(19)-N(4)-C(16) | 107.5(3) | N(4)-C(19)-C(1) | 116.3(3) |
| N(1)-C(1)-C(2) | 105.9(3) | N(4)-C(19)-C(18) | 110.5(3) |
| N(1)-C(1)-C(19) | 114.1(3) | C(1)-C(19)-C(18) | 133.1(3) |
| C(2)-C(1)-C(19) | 139.6(4) | C(5)-C(20)-H(01D) | 109.5 |
| C(3)-C(2)-C(1) | 107.4(3) | C(5)-C(20)-H(01E) | 109.5 |
| C(3)-C(2)-H(2) | 126.3 | H(01D)-C(20)-H(01E) | 109.5 |
| C(1)-C(2)-H(2) | 126.3 | C(5)-C(20)-H(01F) | 109.5 |
| C(2)-C(3)-C(4) | 107.7(3) | H(01D)-C(20)-H(01F) | 109.5 |

| | | | |
|-------------------|----------|---------------------|----------|
| C(2)-C(3)-H(3) | 126.2 | H(01E)-C(20)-H(01F) | 109.5 |
| C(4)-C(3)-H(3) | 126.2 | C(5)-C(21)-H(21) | 109.5 |
| N(1)-C(4)-C(3) | 106.7(3) | C(5)-C(21)-H(01B) | 109.5 |
| N(1)-C(4)-C(5) | 119.6(3) | H(21)-C(21)-H(01B) | 109.5 |
| C(3)-C(4)-C(5) | 133.7(3) | C(5)-C(21)-H(01C) | 109.5 |
| C(4)-C(5)-C(6) | 115.1(3) | H(21)-C(21)-H(01C) | 109.5 |
| C(4)-C(5)-C(20) | 108.8(3) | H(01B)-C(21)-H(01C) | 109.5 |
| C(6)-C(5)-C(20) | 108.9(3) | C(23)-C(22)-C(27) | 117.0(3) |
| C(4)-C(5)-C(21) | 107.5(3) | C(23)-C(22)-C(10) | 121.0(3) |
| C(6)-C(5)-C(21) | 107.2(3) | C(27)-C(22)-C(10) | 121.9(3) |
| C(20)-C(5)-C(21) | 109.2(3) | F(1)-C(23)-C(24) | 117.8(3) |
| N(2)-C(6)-C(7) | 111.2(3) | F(1)-C(23)-C(22) | 119.9(3) |
| N(2)-C(6)-C(5) | 126.9(3) | C(24)-C(23)-C(22) | 122.4(3) |
| C(7)-C(6)-C(5) | 121.9(3) | F(2)-C(24)-C(25) | 120.4(4) |
| C(8)-C(7)-C(6) | 107.3(3) | F(2)-C(24)-C(23) | 120.4(4) |
| C(8)-C(7)-H(7) | 126.3 | C(25)-C(24)-C(23) | 119.2(4) |
| C(6)-C(7)-H(7) | 126.3 | F(3)-C(25)-C(24) | 119.4(4) |
| C(7)-C(8)-C(9) | 106.6(3) | F(3)-C(25)-C(26) | 120.5(4) |
| C(7)-C(8)-H(8) | 126.7 | C(24)-C(25)-C(26) | 120.0(3) |
| C(9)-C(8)-H(8) | 126.7 | F(4)-C(26)-C(27) | 120.4(4) |
| C(10)-C(9)-N(2) | 125.7(3) | F(4)-C(26)-C(25) | 119.9(3) |
| C(10)-C(9)-C(8) | 125.9(3) | C(27)-C(26)-C(25) | 119.6(3) |
| N(2)-C(9)-C(8) | 108.5(3) | F(5)-C(27)-C(26) | 117.9(3) |
| C(9)-C(10)-C(11) | 128.9(3) | F(5)-C(27)-C(22) | 120.4(3) |
| C(9)-C(10)-C(22) | 116.2(3) | C(26)-C(27)-C(22) | 121.7(3) |
| C(11)-C(10)-C(22) | 114.8(3) | C(29)-C(28)-C(33) | 116.4(3) |
| N(3)-C(11)-C(12) | 107.0(3) | C(29)-C(28)-C(15) | 122.5(3) |
| N(3)-C(11)-C(10) | 123.6(3) | C(33)-C(28)-C(15) | 121.0(3) |
| C(12)-C(11)-C(10) | 129.4(3) | F(6)-C(29)-C(30) | 117.4(3) |
| C(13)-C(12)-C(11) | 107.8(3) | F(6)-C(29)-C(28) | 119.8(3) |
| C(13)-C(12)-H(12) | 126.1 | C(30)-C(29)-C(28) | 122.8(4) |
| C(11)-C(12)-H(12) | 126.1 | F(7)-C(30)-C(31) | 120.5(3) |
| C(12)-C(13)-C(14) | 108.2(3) | F(7)-C(30)-C(29) | 120.5(4) |
| C(12)-C(13)-H(13) | 125.9 | C(31)-C(30)-C(29) | 118.9(4) |
| C(14)-C(13)-H(13) | 125.9 | F(8)-C(31)-C(32) | 120.1(4) |
| N(3)-C(14)-C(13) | 106.7(3) | F(8)-C(31)-C(30) | 119.8(4) |
| N(3)-C(14)-C(15) | 122.2(3) | C(32)-C(31)-C(30) | 120.1(3) |
| C(13)-C(14)-C(15) | 131.1(3) | F(9)-C(32)-C(31) | 120.5(4) |
| C(16)-C(15)-C(14) | 123.1(3) | F(9)-C(32)-C(33) | 119.1(4) |
| C(16)-C(15)-C(28) | 118.6(3) | C(31)-C(32)-C(33) | 120.3(4) |
| C(14)-C(15)-C(28) | 118.3(3) | F(10)-C(33)-C(32) | 118.5(4) |
| N(4)-C(16)-C(15) | 120.8(3) | F(10)-C(33)-C(28) | 120.1(3) |
| N(4)-C(16)-C(17) | 108.8(3) | C(32)-C(33)-C(28) | 121.4(4) |

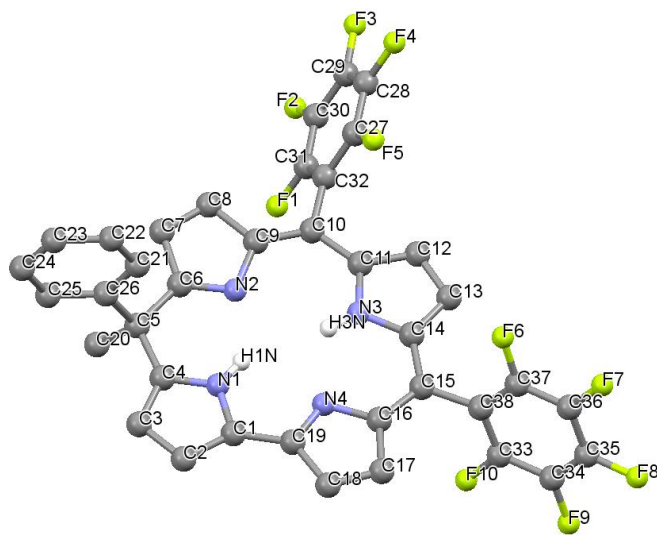


Figure A. 7 Fully labeled solid state structure of 5-MPIC. All non N-H hydrogens have been omitted for clarity.

Table A. 7 Bond Lengths (Å) and Bond angles (°) determined for 5-MPIC

| Bond | Length | Bond | Length |
|--------|----------|----------|----------|
| N1-C4 | 1.329(2) | C18-C19 | 1.459(3) |
| N1-C1 | 1.367(2) | C18-H18 | 0.93 |
| N1-H1N | 0.86 | C20-H20A | 0.96 |
| N2-C6 | 1.324(2) | C20-H20B | 0.96 |
| N2-C9 | 1.408(2) | C20-H20C | 0.96 |
| N3-C14 | 1.368(2) | C21-C26 | 1.388(3) |
| N3-C11 | 1.366(2) | C21-C22 | 1.387(3) |
| N3-H3N | 0.86 | C21-H21 | 0.93 |
| N4-C19 | 1.325(2) | C22-C23 | 1.372(3) |
| N4-C16 | 1.375(2) | C22-H22 | 0.93 |
| C1-C2 | 1.391(3) | C23-C24 | 1.375(3) |
| C1-C19 | 1.424(3) | C23-H23 | 0.93 |
| C2-C3 | 1.399(3) | C24-C25 | 1.394(3) |
| C2-H2 | 0.93 | C24-H24 | 0.93 |
| C3-C4 | 1.399(3) | C25-C26 | 1.381(3) |
| C3-H3 | 0.93 | C25-H25 | 0.93 |
| C4-C5 | 1.511(3) | C27-F5 | 1.341(2) |
| C5-C6 | 1.533(2) | C27-C28 | 1.378(3) |
| C5-C26 | 1.544(2) | C27-C32 | 1.388(2) |
| C5-C20 | 1.552(2) | C28-F4 | 1.337(2) |
| C6-C7 | 1.450(3) | C28-C29 | 1.378(3) |

| | | | |
|---------|----------|---------|----------|
| C7-C8 | 1.348(3) | C29-F3 | 1.328(2) |
| C7-H7 | 0.93 | C29-C30 | 1.379(3) |
| C8-C9 | 1.450(2) | C30-F2 | 1.340(2) |
| C8-H8 | 0.93 | C30-C31 | 1.377(3) |
| C9-C10 | 1.385(2) | C31-F1 | 1.338(2) |
| C10-C11 | 1.430(2) | C31-C32 | 1.389(3) |
| C10-C32 | 1.492(2) | C33-F10 | 1.341(2) |
| C11-C12 | 1.415(2) | C33-C38 | 1.387(3) |
| C12-C13 | 1.388(3) | C33-C34 | 1.381(3) |
| C12-H12 | 0.93 | C34-F9 | 1.340(2) |
| C13-C14 | 1.404(2) | C34-C35 | 1.376(3) |
| C13-H13 | 0.93 | C35-F8 | 1.332(2) |
| C14-C15 | 1.438(2) | C35-C36 | 1.383(3) |
| C15-C16 | 1.377(3) | C36-F7 | 1.334(2) |
| C15-C38 | 1.488(2) | C36-C37 | 1.379(3) |
| C16-C17 | 1.459(3) | C37-F6 | 1.336(2) |
| C17-C18 | 1.350(3) | C37-C38 | 1.383(2) |
| C17-H17 | 0.93 | C18-C19 | 1.459(3) |

| Bond | Angle | Bond | Angle |
|------------|------------|---------------|------------|
| C4-N1-C1 | 112.23(15) | C19-C18-H18 | 126.9 |
| C4-N1-H1N | 123.9 | N4-C19-C1 | 116.05(17) |
| C1-N1-H1N | 123.9 | N4-C19-C18 | 110.80(17) |
| C6-N2-C9 | 106.29(14) | C1-C19-C18 | 133.15(17) |
| C14-N3-C11 | 110.97(14) | C5-C20-H20A | 109.5 |
| C14-N3-H3N | 124.5 | C5-C20-H20B | 109.5 |
| C11-N3-H3N | 124.5 | H20A-C20-H20B | 109.5 |
| C19-N4-C16 | 107.31(16) | C5-C20-H20C | 109.5 |
| N1-C1-C2 | 106.03(17) | H20A-C20-H20C | 109.5 |
| N1-C1-C19 | 113.72(16) | H20B-C20-H20C | 109.5 |
| C2-C1-C19 | 140.25(19) | C26-C21-C22 | 120.82(19) |
| C1-C2-C3 | 107.51(17) | C26-C21-H21 | 119.6 |
| C1-C2-H2 | 126.2 | C22-C21-H21 | 119.6 |
| C3-C2-H2 | 126.2 | C23-C22-C21 | 120.3(2) |
| C4-C3-C2 | 107.52(16) | C23-C22-H22 | 119.8 |
| C4-C3-H3 | 126.2 | C21-C22-H22 | 119.8 |
| C2-C3-H3 | 126.2 | C22-C23-C24 | 119.49(19) |
| N1-C4-C3 | 106.71(17) | C22-C23-H23 | 120.3 |
| N1-C4-C5 | 120.03(16) | C24-C23-H23 | 120.3 |
| C3-C4-C5 | 133.23(16) | C23-C24-C25 | 120.5(2) |
| C4-C5-C6 | 115.01(14) | C23-C24-H24 | 119.8 |
| C4-C5-C26 | 107.09(14) | C25-C24-H24 | 119.8 |
| C6-C5-C26 | 107.16(14) | C26-C25-C24 | 120.4(2) |

| | | | |
|-------------|------------|-------------|------------|
| C4-C5-C20 | 107.97(15) | C26-C25-H25 | 119.8 |
| C6-C5-C20 | 107.56(14) | C24-C25-H25 | 119.8 |
| C26-C5-C20 | 112.16(14) | C25-C26-C21 | 118.47(17) |
| N2-C6-C7 | 111.41(15) | C25-C26-C5 | 122.83(17) |
| N2-C6-C5 | 127.53(16) | C21-C26-C5 | 118.62(16) |
| C7-C6-C5 | 121.05(15) | F5-C27-C28 | 117.79(16) |
| C8-C7-C6 | 106.73(16) | F5-C27-C32 | 119.71(17) |
| C8-C7-H7 | 126.6 | C28-C27-C32 | 122.48(18) |
| C6-C7-H7 | 126.6 | F4-C28-C29 | 119.97(18) |
| C7-C8-C9 | 106.90(16) | F4-C28-C27 | 120.11(19) |
| C7-C8-H8 | 126.6 | C29-C28-C27 | 119.91(17) |
| C9-C8-H8 | 126.6 | F3-C29-C28 | 120.55(19) |
| C10-C9-N2 | 125.05(16) | F3-C29-C30 | 120.3(2) |
| C10-C9-C8 | 126.28(16) | C28-C29-C30 | 119.14(18) |
| N2-C9-C8 | 108.67(15) | F2-C30-C31 | 119.78(18) |
| C9-C10-C11 | 128.70(16) | F2-C30-C29 | 120.13(18) |
| C9-C10-C32 | 116.57(15) | C31-C30-C29 | 120.08(18) |
| C11-C10-C32 | 114.73(14) | F1-C31-C30 | 118.06(17) |
| N3-C11-C12 | 106.31(15) | F1-C31-C32 | 119.64(16) |
| N3-C11-C10 | 124.80(15) | C30-C31-C32 | 122.30(17) |
| C12-C11-C10 | 128.89(16) | C27-C32-C31 | 116.09(16) |
| C13-C12-C11 | 108.02(16) | C27-C32-C10 | 121.97(16) |
| C13-C12-H12 | 126 | C31-C32-C10 | 121.92(15) |
| C11-C12-H12 | 126 | F10-C33-C38 | 120.06(16) |
| C12-C13-C14 | 107.70(15) | F10-C33-C34 | 117.93(17) |
| C12-C13-H13 | 126.2 | C38-C33-C34 | 122.01(18) |
| C14-C13-H13 | 126.2 | F9-C34-C35 | 120.01(19) |
| N3-C14-C13 | 107.00(15) | F9-C34-C33 | 120.0(2) |
| N3-C14-C15 | 122.37(15) | C35-C34-C33 | 119.94(19) |
| C13-C14-C15 | 130.60(16) | F8-C35-C34 | 120.2(2) |
| C16-C15-C14 | 122.63(16) | F8-C35-C36 | 120.4(2) |
| C16-C15-C38 | 117.76(16) | C34-C35-C36 | 119.42(18) |
| C14-C15-C38 | 119.62(15) | F7-C36-C37 | 120.47(19) |
| N4-C16-C15 | 120.84(17) | F7-C36-C35 | 120.03(18) |
| N4-C16-C17 | 109.01(16) | C37-C36-C35 | 119.50(18) |
| C15-C16-C17 | 130.13(17) | F6-C37-C36 | 117.92(17) |
| C18-C17-C16 | 106.64(17) | F6-C37-C38 | 119.62(16) |
| C18-C17-H17 | 126.7 | C36-C37-C38 | 122.46(18) |
| C16-C17-H17 | 126.7 | C33-C38-C37 | 116.58(16) |
| C17-C18-C19 | 106.25(17) | C33-C38-C15 | 120.79(16) |
| C17-C18-H18 | 126.9 | C37-C38-C15 | 122.41(16) |

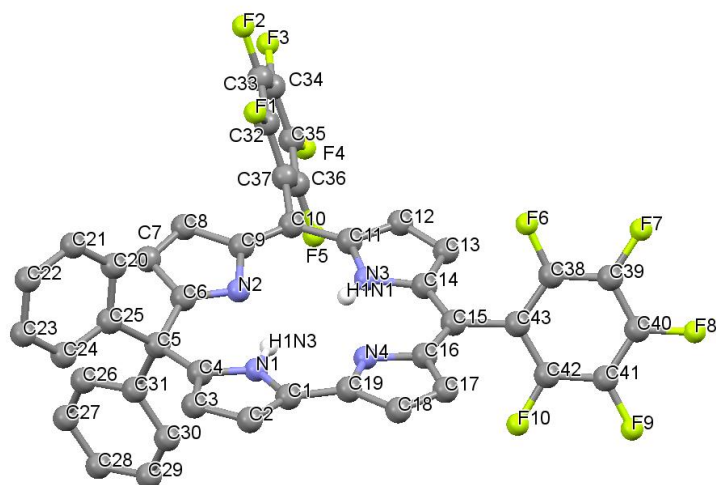


Figure A.8 Fully labeled solid state structure of 5-DPIC. All non N-H hydrogens have been omitted for clarity.

Table A. 8 Bond Lengths (Å) and Bond angles (°) determined for 5-DPIC

| Bond | Length | Bond | Length |
|-------------|----------|-------------|----------|
| F(1)-C(32) | 1.337(4) | C(14)-C(15) | 1.443(4) |
| F(2)-C(33) | 1.335(4) | C(15)-C(16) | 1.374(4) |
| F(3)-C(34) | 1.333(4) | C(15)-C(43) | 1.490(4) |
| F(4)-C(35) | 1.337(4) | C(16)-C(17) | 1.465(4) |
| F(5)-C(36) | 1.343(4) | C(17)-C(18) | 1.354(5) |
| F(6)-C(38) | 1.341(4) | C(17)-H(17) | 0.95 |
| F(7)-C(39) | 1.338(4) | C(18)-C(19) | 1.460(4) |
| F(8)-C(40) | 1.341(4) | C(18)-H(18) | 0.95 |
| F(9)-C(41) | 1.338(4) | C(20)-C(21) | 1.385(5) |
| F(10)-C(42) | 1.346(4) | C(20)-C(25) | 1.385(5) |
| N(1)-C(4) | 1.342(4) | C(20)-H(20) | 0.95 |
| N(1)-C(1) | 1.372(4) | C(21)-C(22) | 1.373(6) |
| N(1)-H(1N3) | 0.95(4) | C(21)-H(21) | 0.95 |
| N(2)-C(6) | 1.323(4) | C(22)-C(23) | 1.363(6) |
| N(2)-C(9) | 1.415(4) | C(22)-H(22) | 0.95 |
| N(3)-C(11) | 1.365(4) | C(23)-C(24) | 1.395(5) |
| N(3)-C(14) | 1.370(4) | C(23)-H(23) | 0.95 |
| N(3)-H(1N1) | 0.81(4) | C(24)-C(25) | 1.387(5) |
| N(4)-C(19) | 1.328(4) | C(24)-H(24) | 0.95 |
| N(4)-C(16) | 1.377(4) | C(26)-C(27) | 1.376(5) |
| C(1)-C(2) | 1.389(4) | C(26)-C(31) | 1.398(4) |
| C(1)-C(19) | 1.428(4) | C(26)-H(26) | 0.95 |

| | | | |
|-------------|----------|-------------|----------|
| C(2)-C(3) | 1.401(4) | C(27)-C(28) | 1.380(5) |
| C(2)-H(2) | 0.95 | C(27)-H(27) | 0.95 |
| C(3)-C(4) | 1.397(4) | C(28)-C(29) | 1.379(5) |
| C(3)-H(3) | 0.95 | C(28)-H(28) | 0.95 |
| C(4)-C(5) | 1.504(4) | C(29)-C(30) | 1.376(5) |
| C(5)-C(6) | 1.535(4) | C(29)-H(29) | 0.95 |
| C(5)-C(25) | 1.537(4) | C(30)-C(31) | 1.394(4) |
| C(5)-C(31) | 1.556(4) | C(30)-H(30) | 0.95 |
| C(6)-C(7) | 1.455(4) | C(32)-C(33) | 1.372(4) |
| C(7)-C(8) | 1.344(4) | C(32)-C(37) | 1.383(4) |
| C(7)-H(7) | 0.95 | C(33)-C(34) | 1.369(5) |
| C(8)-C(9) | 1.444(4) | C(34)-C(35) | 1.376(5) |
| C(8)-H(8) | 0.95 | C(35)-C(36) | 1.378(5) |
| C(9)-C(10) | 1.382(4) | C(36)-C(37) | 1.388(5) |
| C(10)-C(11) | 1.433(4) | C(38)-C(39) | 1.376(4) |
| C(10)-C(37) | 1.501(4) | C(38)-C(43) | 1.387(4) |
| C(11)-C(12) | 1.411(4) | C(39)-C(40) | 1.366(5) |
| C(12)-C(13) | 1.384(5) | C(40)-C(41) | 1.370(5) |
| C(12)-H(12) | 0.95 | C(41)-C(42) | 1.368(5) |
| C(13)-C(14) | 1.405(4) | C(42)-C(43) | 1.386(4) |
| C(13)-H(13) | 0.95 | | |

| Bond | Angle | Bond | Angle |
|-------------------|----------|-------------------|----------|
| C(4)-N(1)-C(1) | 111.8(2) | C(25)-C(20)-H(20) | 119.6 |
| C(4)-N(1)-H(1N3) | 119(3) | C(22)-C(21)-C(20) | 120.3(4) |
| C(1)-N(1)-H(1N3) | 129(3) | C(22)-C(21)-H(21) | 119.8 |
| C(6)-N(2)-C(9) | 106.1(2) | C(20)-C(21)-H(21) | 119.8 |
| C(11)-N(3)-C(14) | 110.9(3) | C(23)-C(22)-C(21) | 119.8(3) |
| C(11)-N(3)-H(1N1) | 129(3) | C(23)-C(22)-H(22) | 120.1 |
| C(14)-N(3)-H(1N1) | 120(3) | C(21)-C(22)-H(22) | 120.1 |
| C(19)-N(4)-C(16) | 107.6(3) | C(22)-C(23)-C(24) | 120.4(4) |
| N(1)-C(1)-C(2) | 106.3(3) | C(22)-C(23)-H(23) | 119.8 |
| N(1)-C(1)-C(19) | 113.8(3) | C(24)-C(23)-H(23) | 119.8 |
| C(2)-C(1)-C(19) | 139.7(3) | C(25)-C(24)-C(23) | 120.4(4) |
| C(1)-C(2)-C(3) | 107.5(3) | C(25)-C(24)-H(24) | 119.8 |
| C(1)-C(2)-H(2) | 126.2 | C(23)-C(24)-H(24) | 119.8 |
| C(3)-C(2)-H(2) | 126.2 | C(20)-C(25)-C(24) | 118.4(3) |
| C(4)-C(3)-C(2) | 107.8(3) | C(20)-C(25)-C(5) | 120.1(3) |
| C(4)-C(3)-H(3) | 126.1 | C(24)-C(25)-C(5) | 121.3(3) |
| C(2)-C(3)-H(3) | 126.1 | C(27)-C(26)-C(31) | 120.3(3) |
| N(1)-C(4)-C(3) | 106.6(3) | C(27)-C(26)-H(26) | 119.8 |
| N(1)-C(4)-C(5) | 119.7(2) | C(31)-C(26)-H(26) | 119.8 |
| C(3)-C(4)-C(5) | 133.8(3) | C(26)-C(27)-C(28) | 120.7(3) |

| | | | |
|-------------------|----------|-------------------|----------|
| C(4)-C(5)-C(6) | 114.2(2) | C(26)-C(27)-H(27) | 119.6 |
| C(4)-C(5)-C(25) | 106.1(2) | C(28)-C(27)-H(27) | 119.6 |
| C(6)-C(5)-C(25) | 111.1(2) | C(29)-C(28)-C(27) | 119.4(3) |
| C(4)-C(5)-C(31) | 110.4(2) | C(29)-C(28)-H(28) | 120.3 |
| C(6)-C(5)-C(31) | 103.0(2) | C(27)-C(28)-H(28) | 120.3 |
| C(25)-C(5)-C(31) | 112.2(2) | C(30)-C(29)-C(28) | 120.6(3) |
| N(2)-C(6)-C(7) | 111.2(2) | C(30)-C(29)-H(29) | 119.7 |
| N(2)-C(6)-C(5) | 126.0(3) | C(28)-C(29)-H(29) | 119.7 |
| C(7)-C(6)-C(5) | 122.5(2) | C(29)-C(30)-C(31) | 120.6(3) |
| C(8)-C(7)-C(6) | 106.9(3) | C(29)-C(30)-H(30) | 119.7 |
| C(8)-C(7)-H(7) | 126.5 | C(31)-C(30)-H(30) | 119.7 |
| C(6)-C(7)-H(7) | 126.5 | C(30)-C(31)-C(26) | 118.4(3) |
| C(7)-C(8)-C(9) | 106.9(3) | C(30)-C(31)-C(5) | 120.4(3) |
| C(7)-C(8)-H(8) | 126.5 | C(26)-C(31)-C(5) | 121.1(3) |
| C(9)-C(8)-H(8) | 126.5 | F(1)-C(32)-C(33) | 117.6(3) |
| C(10)-C(9)-N(2) | 125.1(3) | F(1)-C(32)-C(37) | 119.3(3) |
| C(10)-C(9)-C(8) | 126.0(3) | C(33)-C(32)-C(37) | 123.0(3) |
| N(2)-C(9)-C(8) | 108.9(2) | F(2)-C(33)-C(34) | 120.0(3) |
| C(9)-C(10)-C(11) | 128.9(3) | F(2)-C(33)-C(32) | 120.8(3) |
| C(9)-C(10)-C(37) | 116.3(3) | C(34)-C(33)-C(32) | 119.2(3) |
| C(11)-C(10)-C(37) | 114.8(2) | F(3)-C(34)-C(33) | 120.3(3) |
| N(3)-C(11)-C(12) | 106.6(3) | F(3)-C(34)-C(35) | 119.7(3) |
| N(3)-C(11)-C(10) | 124.7(3) | C(33)-C(34)-C(35) | 120.0(3) |
| C(12)-C(11)-C(10) | 128.8(3) | F(4)-C(35)-C(34) | 120.2(3) |
| C(13)-C(12)-C(11) | 107.9(3) | F(4)-C(35)-C(36) | 120.0(3) |
| C(13)-C(12)-H(12) | 126.1 | C(34)-C(35)-C(36) | 119.8(3) |
| C(11)-C(12)-H(12) | 126.1 | F(5)-C(36)-C(35) | 118.4(3) |
| C(12)-C(13)-C(14) | 108.1(3) | F(5)-C(36)-C(37) | 119.8(3) |
| C(12)-C(13)-H(13) | 126 | C(35)-C(36)-C(37) | 121.9(3) |
| C(14)-C(13)-H(13) | 126 | C(32)-C(37)-C(36) | 116.1(3) |
| N(3)-C(14)-C(13) | 106.6(3) | C(32)-C(37)-C(10) | 121.7(3) |
| N(3)-C(14)-C(15) | 122.8(3) | C(36)-C(37)-C(10) | 122.1(3) |
| C(13)-C(14)-C(15) | 130.6(3) | F(6)-C(38)-C(39) | 117.6(3) |
| C(16)-C(15)-C(14) | 122.5(3) | F(6)-C(38)-C(43) | 120.3(3) |
| C(16)-C(15)-C(43) | 119.3(3) | C(39)-C(38)-C(43) | 122.1(3) |
| C(14)-C(15)-C(43) | 118.2(3) | F(7)-C(39)-C(40) | 119.9(3) |
| C(15)-C(16)-N(4) | 120.1(3) | F(7)-C(39)-C(38) | 120.0(3) |
| C(15)-C(16)-C(17) | 131.0(3) | C(40)-C(39)-C(38) | 120.1(3) |
| N(4)-C(16)-C(17) | 108.8(3) | F(8)-C(40)-C(39) | 120.4(3) |
| C(18)-C(17)-C(16) | 106.5(3) | F(8)-C(40)-C(41) | 119.9(3) |
| C(18)-C(17)-H(17) | 126.7 | C(39)-C(40)-C(41) | 119.6(3) |
| C(16)-C(17)-H(17) | 126.7 | F(9)-C(41)-C(42) | 120.8(3) |
| C(17)-C(18)-C(19) | 106.4(3) | F(9)-C(41)-C(40) | 119.8(3) |

| | | | |
|-------------------|----------|-------------------|----------|
| C(17)-C(18)-H(18) | 126.8 | C(42)-C(41)-C(40) | 119.4(3) |
| C(19)-C(18)-H(18) | 126.8 | F(10)-C(42)-C(41) | 117.1(3) |
| N(4)-C(19)-C(1) | 116.4(3) | F(10)-C(42)-C(43) | 119.7(3) |
| N(4)-C(19)-C(18) | 110.6(3) | C(41)-C(42)-C(43) | 123.1(3) |
| C(1)-C(19)-C(18) | 132.9(3) | C(42)-C(43)-C(38) | 115.5(3) |
| C(21)-C(20)-C(25) | 120.7(3) | C(42)-C(43)-C(15) | 121.1(3) |
| C(21)-C(20)-H(20) | 119.6 | C(38)-C(43)-C(15) | 123.3(3) |

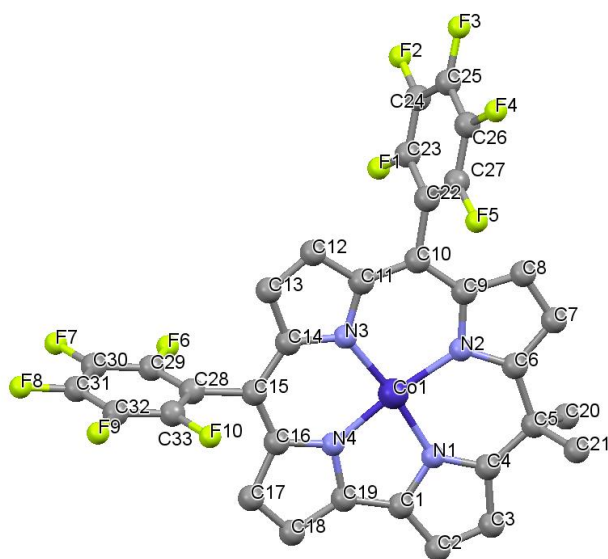


Figure A. 9 Fully labeled solid state structure of Co(5-DMIC). All non N-H hydrogens have been omitted for clarity.

Table A. 9 Bond Lengths (Å) and Bond angles (°) determined for Co(5-DMIC)

| Bond | Length | Bond | Length |
|------------|----------|-------------|----------|
| Co(1)-N(4) | 1.839(4) | C(8)-H(4) | 0.90(4) |
| Co(1)-N(1) | 1.863(3) | C(9)-C(10) | 1.385(5) |
| Co(1)-N(3) | 1.877(3) | C(10)-C(11) | 1.405(5) |
| Co(1)-N(2) | 1.880(3) | C(10)-C(22) | 1.495(5) |
| F(1)-C(23) | 1.338(5) | C(11)-C(12) | 1.432(5) |
| F(2)-C(24) | 1.343(5) | C(12)-C(13) | 1.349(6) |
| F(3)-C(25) | 1.337(5) | C(12)-H(5) | 0.89(6) |
| F(4)-C(26) | 1.343(5) | C(13)-C(14) | 1.423(5) |
| F(5)-C(27) | 1.338(4) | C(13)-H(6) | 0.87(4) |
| F(6)-C(29) | 1.346(5) | C(14)-C(15) | 1.426(5) |
| F(7)-C(30) | 1.339(5) | C(15)-C(16) | 1.374(5) |
| F(8)-C(31) | 1.349(5) | C(15)-C(28) | 1.497(5) |

| | | | |
|-------------|----------|-------------|----------|
| F(9)-C(32) | 1.337(5) | C(16)-C(17) | 1.456(6) |
| F(10)-C(33) | 1.347(5) | C(17)-C(18) | 1.352(6) |
| N(1)-C(4) | 1.325(5) | C(17)-H(7) | 1.00(5) |
| N(1)-C(1) | 1.397(5) | C(18)-C(19) | 1.446(6) |
| N(2)-C(6) | 1.345(5) | C(18)-H(8) | 0.92(5) |
| N(2)-C(9) | 1.416(5) | C(20)-H(9) | 0.91(4) |
| N(3)-C(14) | 1.378(5) | C(20)-H(10) | 1.03(5) |
| N(3)-C(11) | 1.385(5) | C(20)-H(11) | 0.96(5) |
| N(4)-C(16) | 1.373(5) | C(21)-H(12) | 0.97(6) |
| N(4)-C(19) | 1.378(5) | C(21)-H(13) | 1.03(6) |
| C(1)-C(19) | 1.394(6) | C(21)-H(14) | 0.98(5) |
| C(1)-C(2) | 1.417(6) | C(22)-C(27) | 1.390(6) |
| C(2)-C(3) | 1.364(7) | C(22)-C(23) | 1.391(5) |
| C(2)-H(1) | 0.95(5) | C(23)-C(24) | 1.373(6) |
| C(3)-C(4) | 1.444(6) | C(24)-C(25) | 1.377(6) |
| C(3)-H(2) | 0.92(6) | C(25)-C(26) | 1.380(6) |
| C(4)-C(5) | 1.486(6) | C(26)-C(27) | 1.379(6) |
| C(5)-C(6) | 1.531(5) | C(28)-C(29) | 1.378(6) |
| C(5)-C(20) | 1.544(6) | C(28)-C(33) | 1.381(6) |
| C(5)-C(21) | 1.561(5) | C(29)-C(30) | 1.374(7) |
| C(6)-C(7) | 1.418(6) | C(30)-C(31) | 1.368(7) |
| C(7)-C(8) | 1.377(6) | C(31)-C(32) | 1.376(7) |
| C(7)-H(3) | 0.91(5) | C(32)-C(33) | 1.369(6) |
| C(8)-C(9) | 1.435(5) | | |

| Bond | Angle | Bond | Angle |
|------------------|------------|-------------------|----------|
| N(4)-Co(1)-N(1) | 81.97(15) | C(16)-C(15)-C(14) | 122.2(4) |
| N(4)-Co(1)-N(3) | 90.64(14) | C(16)-C(15)-C(28) | 118.9(4) |
| N(1)-Co(1)-N(3) | 172.56(15) | C(14)-C(15)-C(28) | 118.9(3) |
| N(4)-Co(1)-N(2) | 173.20(14) | N(4)-C(16)-C(15) | 120.5(4) |
| N(1)-Co(1)-N(2) | 91.33(15) | N(4)-C(16)-C(17) | 107.8(4) |
| N(3)-Co(1)-N(2) | 96.03(14) | C(15)-C(16)-C(17) | 131.7(4) |
| C(4)-N(1)-C(1) | 108.7(3) | C(18)-C(17)-C(16) | 108.3(4) |
| C(4)-N(1)-Co(1) | 134.8(3) | C(18)-C(17)-H(7) | 128(3) |
| C(1)-N(1)-Co(1) | 116.5(3) | C(16)-C(17)-H(7) | 124(3) |
| C(6)-N(2)-C(9) | 106.7(3) | C(17)-C(18)-C(19) | 106.7(4) |
| C(6)-N(2)-Co(1) | 128.4(3) | C(17)-C(18)-H(8) | 130(3) |
| C(9)-N(2)-Co(1) | 124.9(3) | C(19)-C(18)-H(8) | 123(3) |
| C(14)-N(3)-C(11) | 106.5(3) | N(4)-C(19)-C(1) | 112.2(4) |
| C(14)-N(3)-Co(1) | 127.2(3) | N(4)-C(19)-C(18) | 109.1(4) |
| C(11)-N(3)-Co(1) | 126.2(3) | C(1)-C(19)-C(18) | 138.6(4) |
| C(16)-N(4)-C(19) | 108.0(4) | C(5)-C(20)-H(9) | 108(3) |
| C(16)-N(4)-Co(1) | 134.0(3) | C(5)-C(20)-H(10) | 108(3) |

| | | | |
|-------------------|----------|-------------------|----------|
| C(19)-N(4)-Co(1) | 117.7(3) | H(9)-C(20)-H(10) | 111(4) |
| C(19)-C(1)-N(1) | 111.5(3) | C(5)-C(20)-H(11) | 112(3) |
| C(19)-C(1)-C(2) | 140.0(4) | H(9)-C(20)-H(11) | 106(4) |
| N(1)-C(1)-C(2) | 108.4(4) | H(10)-C(20)-H(11) | 112(4) |
| C(3)-C(2)-C(1) | 106.5(4) | C(5)-C(21)-H(12) | 109(3) |
| C(3)-C(2)-H(1) | 131(3) | C(5)-C(21)-H(13) | 107(3) |
| C(1)-C(2)-H(1) | 122(3) | H(12)-C(21)-H(13) | 110(4) |
| C(2)-C(3)-C(4) | 108.0(4) | C(5)-C(21)-H(14) | 108(3) |
| C(2)-C(3)-H(2) | 126(4) | H(12)-C(21)-H(14) | 111(4) |
| C(4)-C(3)-H(2) | 126(4) | H(13)-C(21)-H(14) | 112(4) |
| N(1)-C(4)-C(3) | 108.3(4) | C(27)-C(22)-C(23) | 116.0(4) |
| N(1)-C(4)-C(5) | 122.7(4) | C(27)-C(22)-C(10) | 122.9(4) |
| C(3)-C(4)-C(5) | 128.9(4) | C(23)-C(22)-C(10) | 121.1(4) |
| C(4)-C(5)-C(6) | 115.5(3) | F(1)-C(23)-C(24) | 118.7(4) |
| C(4)-C(5)-C(20) | 107.4(4) | F(1)-C(23)-C(22) | 118.8(4) |
| C(6)-C(5)-C(20) | 108.7(3) | C(24)-C(23)-C(22) | 122.4(4) |
| C(4)-C(5)-C(21) | 108.4(3) | F(2)-C(24)-C(23) | 120.7(4) |
| C(6)-C(5)-C(21) | 107.4(3) | F(2)-C(24)-C(25) | 119.1(4) |
| C(20)-C(5)-C(21) | 109.2(4) | C(23)-C(24)-C(25) | 120.2(4) |
| N(2)-C(6)-C(7) | 110.7(3) | F(3)-C(25)-C(24) | 119.8(4) |
| N(2)-C(6)-C(5) | 127.0(4) | F(3)-C(25)-C(26) | 121.0(4) |
| C(7)-C(6)-C(5) | 122.3(3) | C(24)-C(25)-C(26) | 119.1(4) |
| C(8)-C(7)-C(6) | 107.7(4) | F(4)-C(26)-C(27) | 119.9(4) |
| C(8)-C(7)-H(3) | 123(3) | F(4)-C(26)-C(25) | 120.1(4) |
| C(6)-C(7)-H(3) | 128(3) | C(27)-C(26)-C(25) | 120.0(4) |
| C(7)-C(8)-C(9) | 106.5(4) | F(5)-C(27)-C(26) | 117.8(4) |
| C(7)-C(8)-H(4) | 127(3) | F(5)-C(27)-C(22) | 120.0(4) |
| C(9)-C(8)-H(4) | 126(3) | C(26)-C(27)-C(22) | 122.3(4) |
| C(10)-C(9)-N(2) | 123.9(4) | C(29)-C(28)-C(33) | 116.4(4) |
| C(10)-C(9)-C(8) | 127.6(4) | C(29)-C(28)-C(15) | 121.7(4) |
| N(2)-C(9)-C(8) | 108.4(3) | C(33)-C(28)-C(15) | 121.9(4) |
| C(9)-C(10)-C(11) | 125.4(4) | F(6)-C(29)-C(30) | 118.3(4) |
| C(9)-C(10)-C(22) | 117.5(4) | F(6)-C(29)-C(28) | 119.0(4) |
| C(11)-C(10)-C(22) | 117.1(3) | C(30)-C(29)-C(28) | 122.7(5) |
| N(3)-C(11)-C(10) | 123.4(3) | F(7)-C(30)-C(31) | 120.6(5) |
| N(3)-C(11)-C(12) | 109.0(3) | F(7)-C(30)-C(29) | 120.6(5) |
| C(10)-C(11)-C(12) | 127.5(4) | C(31)-C(30)-C(29) | 118.7(4) |
| C(13)-C(12)-C(11) | 107.1(4) | F(8)-C(31)-C(30) | 120.1(5) |
| C(13)-C(12)-H(5) | 133(4) | F(8)-C(31)-C(32) | 119.2(5) |
| C(11)-C(12)-H(5) | 119(4) | C(30)-C(31)-C(32) | 120.7(4) |
| C(12)-C(13)-C(14) | 108.1(4) | F(9)-C(32)-C(33) | 121.0(4) |
| C(12)-C(13)-H(6) | 127(3) | F(9)-C(32)-C(31) | 120.0(4) |
| C(14)-C(13)-H(6) | 125(3) | C(33)-C(32)-C(31) | 119.0(4) |

| | | | |
|-------------------|----------|-------------------|----------|
| N(3)-C(14)-C(13) | 109.1(4) | F(10)-C(33)-C(32) | 118.0(4) |
| N(3)-C(14)-C(15) | 125.3(3) | F(10)-C(33)-C(28) | 119.6(4) |
| C(13)-C(14)-C(15) | 125.6(4) | C(32)-C(33)-C(28) | 122.4(4) |

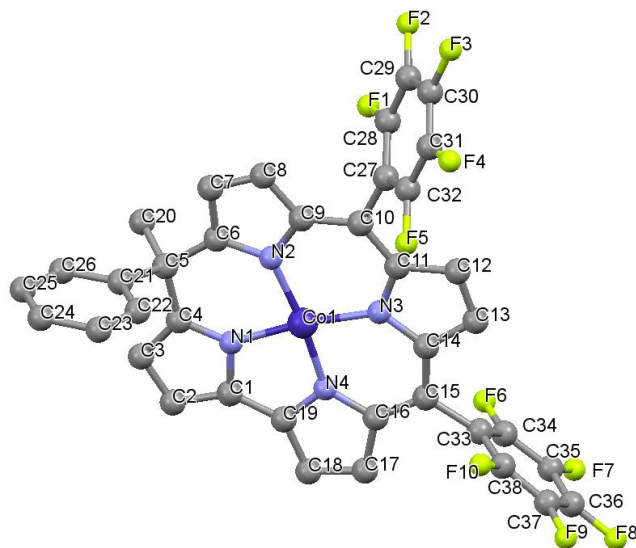


Figure A. 10 Fully labeled solid state structure of Co(5-MPIC). All non N-H hydrogens have been omitted for clarity.

Table A. 10 Bond Lengths (Å) and Bond angles (°) determined for Co(5-MPIC)

| Bond | Length | Bond | Length |
|-------------|----------|--------------|-----------|
| Co(1)-N(4) | 1.821(5) | C(11)-C(12) | 1.422(8) |
| Co(1)-N(2) | 1.867(5) | C(12)-C(13) | 1.371(8) |
| Co(1)-N(1) | 1.875(5) | C(12)-H(12) | 0.95 |
| Co(1)-N(3) | 1.909(5) | C(13)-C(14) | 1.431(8) |
| F(1)-C(28) | 1.349(7) | C(13)-H(13) | 0.95 |
| F(2)-C(29) | 1.333(8) | C(14)-C(15) | 1.424(7) |
| F(3)-C(30) | 1.343(7) | C(15)-C(16) | 1.381(9) |
| F(4)-C(31) | 1.346(7) | C(15)-C(33) | 1.499(8) |
| F(5)-C(32) | 1.346(8) | C(16)-C(17) | 1.467(8) |
| F(6)-C(34) | 1.352(8) | C(17)-C(18) | 1.353(10) |
| F(7)-C(35) | 1.321(8) | C(17)-H(17) | 0.95 |
| F(8)-C(36) | 1.330(7) | C(18)-C(19) | 1.450(9) |
| F(9)-C(37) | 1.346(8) | C(18)-H(18) | 0.95 |
| F(10)-C(38) | 1.323(7) | C(20)-H(20A) | 0.98 |
| N(1)-C(4) | 1.319(7) | C(20)-H(20B) | 0.98 |
| N(1)-C(1) | 1.388(7) | C(20)-H(20C) | 0.98 |

| | | | |
|-------------|----------|-------------|-----------|
| N(2)-C(6) | 1.347(7) | C(21)-C(22) | 1.382(9) |
| N(2)-C(9) | 1.406(7) | C(21)-C(26) | 1.390(9) |
| N(3)-C(14) | 1.372(7) | C(22)-C(23) | 1.395(10) |
| N(3)-C(11) | 1.375(7) | C(22)-H(22) | 0.95 |
| N(4)-C(16) | 1.358(7) | C(23)-C(24) | 1.390(11) |
| N(4)-C(19) | 1.363(8) | C(23)-H(23) | 0.95 |
| C(1)-C(19) | 1.394(9) | C(24)-C(25) | 1.338(12) |
| C(1)-C(2) | 1.420(9) | C(24)-H(24) | 0.95 |
| C(2)-C(3) | 1.376(9) | C(25)-C(26) | 1.409(10) |
| C(2)-H(2) | 0.95 | C(25)-H(25) | 0.95 |
| C(3)-C(4) | 1.431(8) | C(26)-H(26) | 0.95 |
| C(3)-H(3) | 0.95 | C(27)-C(28) | 1.378(8) |
| C(4)-C(5) | 1.499(8) | C(27)-C(32) | 1.390(8) |
| C(5)-C(6) | 1.526(8) | C(28)-C(29) | 1.371(9) |
| C(5)-C(21) | 1.542(8) | C(29)-C(30) | 1.390(10) |
| C(5)-C(20) | 1.549(9) | C(30)-C(31) | 1.343(11) |
| C(6)-C(7) | 1.432(8) | C(31)-C(32) | 1.374(9) |
| C(7)-C(8) | 1.354(9) | C(33)-C(34) | 1.370(8) |
| C(7)-H(7) | 0.95 | C(33)-C(38) | 1.384(9) |
| C(8)-C(9) | 1.419(8) | C(34)-C(35) | 1.372(9) |
| C(8)-H(8) | 0.95 | C(35)-C(36) | 1.394(11) |
| C(9)-C(10) | 1.398(8) | C(36)-C(37) | 1.361(10) |
| C(10)-C(11) | 1.398(7) | C(37)-C(38) | 1.376(9) |
| C(10)-C(27) | 1.494(8) | | |

| Bond | Angle | Bond | Angle |
|------------------|----------|---------------------|----------|
| N(4)-Co(1)-N(2) | 173.3(2) | C(18)-C(17)-C(16) | 107.3(5) |
| N(4)-Co(1)-N(1) | 82.9(2) | C(18)-C(17)-H(17) | 126.4 |
| N(2)-Co(1)-N(1) | 90.3(2) | C(16)-C(17)-H(17) | 126.4 |
| N(4)-Co(1)-N(3) | 89.8(2) | C(17)-C(18)-C(19) | 106.7(5) |
| N(2)-Co(1)-N(3) | 96.9(2) | C(17)-C(18)-H(18) | 126.6 |
| N(1)-Co(1)-N(3) | 172.8(2) | C(19)-C(18)-H(18) | 126.6 |
| C(4)-N(1)-C(1) | 108.9(5) | N(4)-C(19)-C(1) | 113.4(5) |
| C(4)-N(1)-Co(1) | 136.1(4) | N(4)-C(19)-C(18) | 109.4(6) |
| C(1)-N(1)-Co(1) | 115.0(4) | C(1)-C(19)-C(18) | 137.2(6) |
| C(6)-N(2)-C(9) | 106.1(5) | C(5)-C(20)-H(20A) | 109.5 |
| C(6)-N(2)-Co(1) | 129.0(4) | C(5)-C(20)-H(20B) | 109.5 |
| C(9)-N(2)-Co(1) | 124.9(4) | H(20A)-C(20)-H(20B) | 109.5 |
| C(14)-N(3)-C(11) | 107.6(5) | C(5)-C(20)-H(20C) | 109.5 |
| C(14)-N(3)-Co(1) | 127.5(4) | H(20A)-C(20)-H(20C) | 109.5 |
| C(11)-N(3)-Co(1) | 124.9(4) | H(20B)-C(20)-H(20C) | 109.5 |
| C(16)-N(4)-C(19) | 108.3(5) | C(22)-C(21)-C(26) | 118.3(6) |
| C(16)-N(4)-Co(1) | 134.7(4) | C(22)-C(21)-C(5) | 118.9(5) |

| | | | |
|-------------------|----------|-------------------|----------|
| C(19)-N(4)-Co(1) | 116.9(4) | C(26)-C(21)-C(5) | 122.6(6) |
| N(1)-C(1)-C(19) | 111.6(5) | C(21)-C(22)-C(23) | 121.7(7) |
| N(1)-C(1)-C(2) | 108.3(5) | C(21)-C(22)-H(22) | 119.1 |
| C(19)-C(1)-C(2) | 140.1(6) | C(23)-C(22)-H(22) | 119.1 |
| C(3)-C(2)-C(1) | 106.3(6) | C(24)-C(23)-C(22) | 118.7(7) |
| C(3)-C(2)-H(2) | 126.8 | C(24)-C(23)-H(23) | 120.6 |
| C(1)-C(2)-H(2) | 126.8 | C(22)-C(23)-H(23) | 120.6 |
| C(2)-C(3)-C(4) | 107.3(6) | C(25)-C(24)-C(23) | 120.4(7) |
| C(2)-C(3)-H(3) | 126.3 | C(25)-C(24)-H(24) | 119.8 |
| C(4)-C(3)-H(3) | 126.3 | C(23)-C(24)-H(24) | 119.8 |
| N(1)-C(4)-C(3) | 109.2(5) | C(24)-C(25)-C(26) | 121.3(8) |
| N(1)-C(4)-C(5) | 122.1(5) | C(24)-C(25)-H(25) | 119.3 |
| C(3)-C(4)-C(5) | 128.7(5) | C(26)-C(25)-H(25) | 119.3 |
| C(4)-C(5)-C(6) | 114.6(5) | C(21)-C(26)-C(25) | 119.4(7) |
| C(4)-C(5)-C(21) | 106.8(5) | C(21)-C(26)-H(26) | 120.3 |
| C(6)-C(5)-C(21) | 108.3(5) | C(25)-C(26)-H(26) | 120.3 |
| C(4)-C(5)-C(20) | 107.8(5) | C(28)-C(27)-C(32) | 115.8(5) |
| C(6)-C(5)-C(20) | 107.3(5) | C(28)-C(27)-C(10) | 121.8(5) |
| C(21)-C(5)-C(20) | 112.2(5) | C(32)-C(27)-C(10) | 122.4(5) |
| N(2)-C(6)-C(7) | 110.3(5) | F(1)-C(28)-C(29) | 117.0(6) |
| N(2)-C(6)-C(5) | 127.9(5) | F(1)-C(28)-C(27) | 119.9(5) |
| C(7)-C(6)-C(5) | 121.6(5) | C(29)-C(28)-C(27) | 123.1(6) |
| C(8)-C(7)-C(6) | 107.2(5) | F(2)-C(29)-C(28) | 120.6(6) |
| C(8)-C(7)-H(7) | 126.4 | F(2)-C(29)-C(30) | 120.8(6) |
| C(6)-C(7)-H(7) | 126.4 | C(28)-C(29)-C(30) | 118.6(6) |
| C(7)-C(8)-C(9) | 107.3(5) | C(31)-C(30)-F(3) | 121.4(7) |
| C(7)-C(8)-H(8) | 126.3 | C(31)-C(30)-C(29) | 120.1(6) |
| C(9)-C(8)-H(8) | 126.3 | F(3)-C(30)-C(29) | 118.5(7) |
| C(10)-C(9)-N(2) | 122.9(5) | C(30)-C(31)-F(4) | 120.7(6) |
| C(10)-C(9)-C(8) | 128.1(6) | C(30)-C(31)-C(32) | 120.3(6) |
| N(2)-C(9)-C(8) | 109.0(5) | F(4)-C(31)-C(32) | 119.0(7) |
| C(9)-C(10)-C(11) | 127.3(5) | F(5)-C(32)-C(31) | 118.8(6) |
| C(9)-C(10)-C(27) | 116.1(5) | F(5)-C(32)-C(27) | 119.2(6) |
| C(11)-C(10)-C(27) | 116.6(5) | C(31)-C(32)-C(27) | 122.1(6) |
| N(3)-C(11)-C(10) | 123.1(5) | C(34)-C(33)-C(38) | 117.7(6) |
| N(3)-C(11)-C(12) | 109.1(5) | C(34)-C(33)-C(15) | 119.5(6) |
| C(10)-C(11)-C(12) | 127.9(5) | C(38)-C(33)-C(15) | 122.4(6) |
| C(13)-C(12)-C(11) | 107.4(5) | F(6)-C(34)-C(33) | 120.9(6) |
| C(13)-C(12)-H(12) | 126.3 | F(6)-C(34)-C(35) | 116.4(6) |
| C(11)-C(12)-H(12) | 126.3 | C(33)-C(34)-C(35) | 122.7(7) |
| C(12)-C(13)-C(14) | 107.1(5) | F(7)-C(35)-C(34) | 121.7(7) |
| C(12)-C(13)-H(13) | 126.4 | F(7)-C(35)-C(36) | 119.9(6) |
| C(14)-C(13)-H(13) | 126.4 | C(34)-C(35)-C(36) | 118.4(7) |

| | | | |
|-------------------|----------|-------------------|----------|
| N(3)-C(14)-C(15) | 124.8(5) | F(8)-C(36)-C(37) | 120.5(7) |
| N(3)-C(14)-C(13) | 108.8(5) | F(8)-C(36)-C(35) | 119.8(7) |
| C(15)-C(14)-C(13) | 126.3(5) | C(37)-C(36)-C(35) | 119.6(6) |
| C(16)-C(15)-C(14) | 121.4(5) | F(9)-C(37)-C(36) | 120.5(6) |
| C(16)-C(15)-C(33) | 118.3(5) | F(9)-C(37)-C(38) | 118.7(7) |
| C(14)-C(15)-C(33) | 120.2(5) | C(36)-C(37)-C(38) | 120.8(6) |
| N(4)-C(16)-C(15) | 121.6(5) | F(10)-C(38)-C(37) | 119.3(6) |
| N(4)-C(16)-C(17) | 108.4(5) | F(10)-C(38)-C(33) | 120.1(6) |
| C(15)-C(16)-C(17) | 130.0(5) | C(37)-C(38)-C(33) | 120.6(6) |

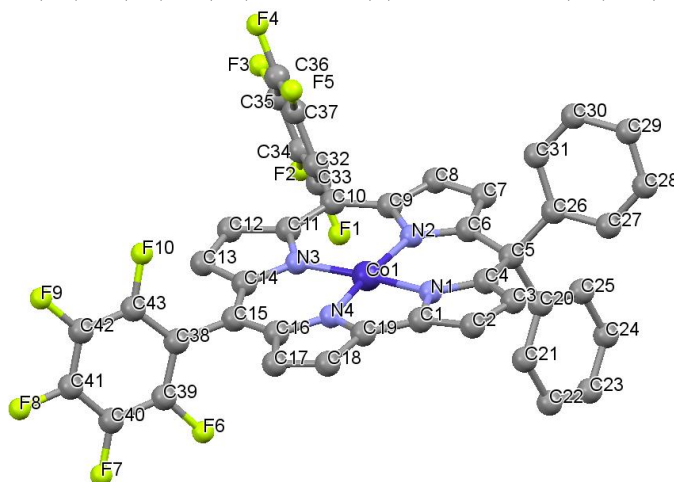


Figure A. 11 Fully labeled solid state structure of Co(5-DPIC). All non N-H hydrogens have been omitted for clarity.

Table A. 11 Bond Lengths (Å) and Bond angles (°) determined for Co(5-DPIC)

| Bond | Length | Bond | Length |
|------------|----------|-------------|----------|
| Co(1)-N(4) | 1.858(3) | C(13)-H(13) | 0.95 |
| Co(1)-N(1) | 1.869(3) | C(14)-C(15) | 1.442(5) |
| Co(1)-N(2) | 1.889(3) | C(15)-C(16) | 1.378(5) |
| Co(1)-N(3) | 1.893(3) | C(15)-C(38) | 1.492(5) |
| F(1)-C(33) | 1.351(4) | C(16)-C(17) | 1.467(4) |
| F(2)-C(34) | 1.346(4) | C(17)-C(18) | 1.362(5) |
| F(3)-C(35) | 1.345(4) | C(17)-H(17) | 0.95 |
| F(4)-C(36) | 1.346(4) | C(18)-C(19) | 1.462(4) |
| F(5)-C(37) | 1.358(4) | C(18)-H(18) | 0.95 |
| F(6)-C(39) | 1.347(5) | C(20)-C(21) | 1.389(5) |
| F(7)-C(40) | 1.348(6) | C(20)-C(25) | 1.400(6) |
| F(8)-C(41) | 1.354(5) | C(21)-C(22) | 1.396(6) |
| F(9)-C(42) | 1.352(5) | C(21)-H(21) | 0.95 |

| | | | |
|-------------|----------|-------------|----------|
| F(10)-C(43) | 1.350(5) | C(22)-C(23) | 1.357(8) |
| N(1)-C(4) | 1.340(4) | C(22)-H(22) | 0.95 |
| N(1)-C(1) | 1.400(4) | C(23)-C(24) | 1.390(8) |
| N(2)-C(6) | 1.359(4) | C(23)-H(23) | 0.95 |
| N(2)-C(9) | 1.412(4) | C(24)-C(25) | 1.407(7) |
| N(3)-C(14) | 1.381(4) | C(24)-H(24) | 0.95 |
| N(3)-C(11) | 1.384(4) | C(25)-H(25) | 0.95 |
| N(4)-C(19) | 1.361(4) | C(26)-C(27) | 1.399(5) |
| N(4)-C(16) | 1.372(4) | C(26)-C(31) | 1.400(5) |
| C(1)-C(19) | 1.403(5) | C(27)-C(28) | 1.389(6) |
| C(1)-C(2) | 1.423(5) | C(27)-H(27) | 0.95 |
| C(2)-C(3) | 1.392(5) | C(28)-C(29) | 1.364(7) |
| C(2)-H(2) | 0.95 | C(28)-H(28) | 0.95 |
| C(3)-C(4) | 1.427(5) | C(29)-C(30) | 1.399(7) |
| C(3)-H(3) | 0.95 | C(29)-H(29) | 0.95 |
| C(4)-C(5) | 1.513(5) | C(30)-C(31) | 1.392(6) |
| C(5)-C(6) | 1.541(4) | C(30)-H(30) | 0.95 |
| C(5)-C(26) | 1.548(5) | C(31)-H(31) | 0.95 |
| C(5)-C(20) | 1.562(5) | C(32)-C(37) | 1.380(5) |
| C(6)-C(7) | 1.432(5) | C(32)-C(33) | 1.386(5) |
| C(7)-C(8) | 1.373(5) | C(33)-C(34) | 1.385(5) |
| C(7)-H(7) | 0.95 | C(34)-C(35) | 1.370(5) |
| C(8)-C(9) | 1.429(5) | C(35)-C(36) | 1.390(5) |
| C(8)-H(8) | 0.95 | C(36)-C(37) | 1.383(5) |
| C(9)-C(10) | 1.392(5) | C(38)-C(39) | 1.388(5) |
| C(10)-C(11) | 1.416(5) | C(38)-C(43) | 1.395(5) |
| C(10)-C(32) | 1.500(4) | C(39)-C(40) | 1.395(5) |
| C(11)-C(12) | 1.435(5) | C(40)-C(41) | 1.381(7) |
| C(12)-C(13) | 1.365(5) | C(41)-C(42) | 1.369(7) |
| C(12)-H(12) | 0.95 | C(42)-C(43) | 1.382(6) |
| C(13)-C(14) | 1.425(4) | | |

| Bond | Angle | Bond | Angle |
|-----------------|------------|-------------------|----------|
| N(4)-Co(1)-N(1) | 82.47(12) | N(4)-C(19)-C(1) | 113.5(3) |
| N(4)-Co(1)-N(2) | 173.05(11) | N(4)-C(19)-C(18) | 108.7(3) |
| N(1)-Co(1)-N(2) | 90.59(12) | C(1)-C(19)-C(18) | 137.8(3) |
| N(4)-Co(1)-N(3) | 89.96(12) | C(21)-C(20)-C(25) | 118.6(4) |
| N(1)-Co(1)-N(3) | 172.26(12) | C(21)-C(20)-C(5) | 120.4(3) |
| N(2)-Co(1)-N(3) | 96.97(12) | C(25)-C(20)-C(5) | 121.1(4) |
| C(4)-N(1)-C(1) | 108.6(3) | C(20)-C(21)-C(22) | 121.1(5) |
| C(4)-N(1)-Co(1) | 135.6(2) | C(20)-C(21)-H(21) | 119.4 |
| C(1)-N(1)-Co(1) | 115.7(2) | C(22)-C(21)-H(21) | 119.4 |
| C(6)-N(2)-C(9) | 106.6(3) | C(23)-C(22)-C(21) | 120.4(5) |

| | | | |
|-------------------|----------|-------------------|----------|
| C(6)-N(2)-Co(1) | 129.2(2) | C(23)-C(22)-H(22) | 119.8 |
| C(9)-N(2)-Co(1) | 124.2(2) | C(21)-C(22)-H(22) | 119.8 |
| C(14)-N(3)-C(11) | 106.3(3) | C(22)-C(23)-C(24) | 119.9(5) |
| C(14)-N(3)-Co(1) | 128.4(2) | C(22)-C(23)-H(23) | 120.1 |
| C(11)-N(3)-Co(1) | 125.4(2) | C(24)-C(23)-H(23) | 120.1 |
| C(19)-N(4)-C(16) | 109.6(3) | C(23)-C(24)-C(25) | 120.5(5) |
| C(19)-N(4)-Co(1) | 116.6(2) | C(23)-C(24)-H(24) | 119.7 |
| C(16)-N(4)-Co(1) | 133.8(2) | C(25)-C(24)-H(24) | 119.7 |
| N(1)-C(1)-C(19) | 111.4(3) | C(20)-C(25)-C(24) | 119.5(5) |
| N(1)-C(1)-C(2) | 108.2(3) | C(20)-C(25)-H(25) | 120.2 |
| C(19)-C(1)-C(2) | 140.4(3) | C(24)-C(25)-H(25) | 120.2 |
| C(3)-C(2)-C(1) | 106.5(3) | C(27)-C(26)-C(31) | 118.2(3) |
| C(3)-C(2)-H(2) | 126.8 | C(27)-C(26)-C(5) | 121.1(3) |
| C(1)-C(2)-H(2) | 126.8 | C(31)-C(26)-C(5) | 120.4(3) |
| C(2)-C(3)-C(4) | 107.5(3) | C(28)-C(27)-C(26) | 120.8(4) |
| C(2)-C(3)-H(3) | 126.2 | C(28)-C(27)-H(27) | 119.6 |
| C(4)-C(3)-H(3) | 126.2 | C(26)-C(27)-H(27) | 119.6 |
| N(1)-C(4)-C(3) | 109.2(3) | C(29)-C(28)-C(27) | 121.2(5) |
| N(1)-C(4)-C(5) | 121.8(3) | C(29)-C(28)-H(28) | 119.4 |
| C(3)-C(4)-C(5) | 128.8(3) | C(27)-C(28)-H(28) | 119.4 |
| C(4)-C(5)-C(6) | 114.3(3) | C(28)-C(29)-C(30) | 118.7(4) |
| C(4)-C(5)-C(26) | 106.1(3) | C(28)-C(29)-H(29) | 120.6 |
| C(6)-C(5)-C(26) | 109.9(3) | C(30)-C(29)-H(29) | 120.6 |
| C(4)-C(5)-C(20) | 109.2(3) | C(31)-C(30)-C(29) | 121.0(4) |
| C(6)-C(5)-C(20) | 105.2(3) | C(31)-C(30)-H(30) | 119.5 |
| C(26)-C(5)-C(20) | 112.2(3) | C(29)-C(30)-H(30) | 119.5 |
| N(2)-C(6)-C(7) | 109.9(3) | C(30)-C(31)-C(26) | 120.0(4) |
| N(2)-C(6)-C(5) | 126.6(3) | C(30)-C(31)-H(31) | 120 |
| C(7)-C(6)-C(5) | 123.5(3) | C(26)-C(31)-H(31) | 120 |
| C(8)-C(7)-C(6) | 107.7(3) | C(37)-C(32)-C(33) | 116.2(3) |
| C(8)-C(7)-H(7) | 126.1 | C(37)-C(32)-C(10) | 121.7(3) |
| C(6)-C(7)-H(7) | 126.1 | C(33)-C(32)-C(10) | 122.1(3) |
| C(7)-C(8)-C(9) | 106.8(3) | F(1)-C(33)-C(34) | 117.6(3) |
| C(7)-C(8)-H(8) | 126.6 | F(1)-C(33)-C(32) | 119.9(3) |
| C(9)-C(8)-H(8) | 126.6 | C(34)-C(33)-C(32) | 122.5(3) |
| C(10)-C(9)-N(2) | 123.8(3) | F(2)-C(34)-C(35) | 119.7(3) |
| C(10)-C(9)-C(8) | 127.2(3) | F(2)-C(34)-C(33) | 120.8(3) |
| N(2)-C(9)-C(8) | 109.0(3) | C(35)-C(34)-C(33) | 119.5(3) |
| C(9)-C(10)-C(11) | 126.5(3) | F(3)-C(35)-C(34) | 120.4(3) |
| C(9)-C(10)-C(32) | 117.3(3) | F(3)-C(35)-C(36) | 119.6(3) |
| C(11)-C(10)-C(32) | 116.2(3) | C(34)-C(35)-C(36) | 120.0(3) |
| N(3)-C(11)-C(10) | 123.0(3) | F(4)-C(36)-C(37) | 121.6(3) |
| N(3)-C(11)-C(12) | 109.6(3) | F(4)-C(36)-C(35) | 119.7(3) |

| | | | |
|-------------------|----------|-------------------|----------|
| C(10)-C(11)-C(12) | 127.4(3) | C(37)-C(36)-C(35) | 118.7(3) |
| C(13)-C(12)-C(11) | 106.9(3) | F(5)-C(37)-C(32) | 119.8(3) |
| C(13)-C(12)-H(12) | 126.6 | F(5)-C(37)-C(36) | 117.1(3) |
| C(11)-C(12)-H(12) | 126.6 | C(32)-C(37)-C(36) | 123.1(3) |
| C(12)-C(13)-C(14) | 107.6(3) | C(39)-C(38)-C(43) | 116.5(3) |
| C(12)-C(13)-H(13) | 126.2 | C(39)-C(38)-C(15) | 120.9(3) |
| C(14)-C(13)-H(13) | 126.2 | C(43)-C(38)-C(15) | 122.6(3) |
| N(3)-C(14)-C(13) | 109.7(3) | F(6)-C(39)-C(38) | 120.5(3) |
| N(3)-C(14)-C(15) | 124.2(3) | F(6)-C(39)-C(40) | 117.0(4) |
| C(13)-C(14)-C(15) | 126.1(3) | C(38)-C(39)-C(40) | 122.5(4) |
| C(16)-C(15)-C(14) | 122.1(3) | F(7)-C(40)-C(41) | 121.9(4) |
| C(16)-C(15)-C(38) | 118.5(3) | F(7)-C(40)-C(39) | 119.8(5) |
| C(14)-C(15)-C(38) | 119.3(3) | C(41)-C(40)-C(39) | 118.3(4) |
| N(4)-C(16)-C(15) | 121.3(3) | F(8)-C(41)-C(42) | 119.8(5) |
| N(4)-C(16)-C(17) | 107.2(3) | F(8)-C(41)-C(40) | 119.1(5) |
| C(15)-C(16)-C(17) | 131.4(3) | C(42)-C(41)-C(40) | 121.1(4) |
| C(18)-C(17)-C(16) | 108.0(3) | F(9)-C(42)-C(41) | 120.5(4) |
| C(18)-C(17)-H(17) | 126 | F(9)-C(42)-C(43) | 120.1(5) |
| C(16)-C(17)-H(17) | 126 | C(41)-C(42)-C(43) | 119.4(4) |
| C(17)-C(18)-C(19) | 106.6(3) | F(10)-C(43)-C(42) | 118.1(4) |
| C(17)-C(18)-H(18) | 126.7 | F(10)-C(43)-C(38) | 119.7(3) |
| C(19)-C(18)-H(18) | 126.7 | C(42)-C(43)-C(38) | 122.1(4) |

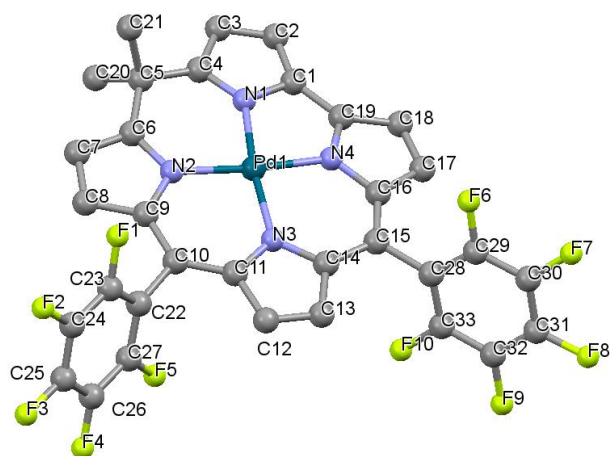


Figure A. 12 Fully labeled solid state structure of Pd(5-DMIC). All non N-H hydrogens have been omitted for clarity.

Table A. 12 Bond Lengths (Å) and Bond angles (°) determined for Pd(5-DMIC)

| Bond | Length | Bond | Length |
|-------------|----------|--------------|----------|
| Pd(1)-N(4) | 1.920(3) | C(8)-H(8) | 0.95 |
| Pd(1)-N(1) | 1.936(4) | C(9)-C(10) | 1.414(6) |
| Pd(1)-N(2) | 1.947(4) | C(10)-C(11) | 1.414(6) |
| Pd(1)-N(3) | 1.967(3) | C(10)-C(22) | 1.493(6) |
| F(1)-C(23) | 1.343(5) | C(11)-C(12) | 1.434(5) |
| F(2)-C(24) | 1.345(6) | C(12)-C(13) | 1.352(6) |
| F(3)-C(25) | 1.344(5) | C(12)-H(12) | 0.95 |
| F(4)-C(26) | 1.334(6) | C(13)-C(14) | 1.437(6) |
| F(5)-C(27) | 1.345(5) | C(13)-H(13) | 0.95 |
| F(6)-C(29) | 1.343(6) | C(14)-C(15) | 1.441(6) |
| F(7)-C(30) | 1.349(6) | C(15)-C(16) | 1.387(6) |
| F(8)-C(31) | 1.349(6) | C(15)-C(28) | 1.496(6) |
| F(9)-C(32) | 1.337(6) | C(16)-C(17) | 1.461(6) |
| F(10)-C(33) | 1.339(5) | C(17)-C(18) | 1.351(7) |
| N(1)-C(4) | 1.320(6) | C(17)-H(17) | 0.95 |
| N(1)-C(1) | 1.409(6) | C(18)-C(19) | 1.452(6) |
| N(2)-C(6) | 1.350(5) | C(18)-H(18) | 0.95 |
| N(2)-C(9) | 1.384(5) | C(20)-H(20A) | 0.98 |
| N(3)-C(14) | 1.363(5) | C(20)-H(20B) | 0.98 |
| N(3)-C(11) | 1.363(5) | C(20)-H(20C) | 0.98 |
| N(4)-C(16) | 1.359(5) | C(21)-H(21A) | 0.98 |
| N(4)-C(19) | 1.363(5) | C(21)-H(21B) | 0.98 |
| C(1)-C(2) | 1.407(6) | C(21)-H(21C) | 0.98 |
| C(1)-C(19) | 1.414(6) | C(22)-C(27) | 1.386(6) |
| C(2)-C(3) | 1.368(7) | C(22)-C(23) | 1.394(6) |
| C(2)-H(2) | 0.95 | C(23)-C(24) | 1.377(6) |
| C(3)-C(4) | 1.428(6) | C(24)-C(25) | 1.363(8) |
| C(3)-H(3) | 0.95 | C(25)-C(26) | 1.385(7) |
| C(4)-C(5) | 1.511(6) | C(26)-C(27) | 1.381(6) |
| C(5)-C(6) | 1.525(6) | C(28)-C(33) | 1.385(6) |
| C(5)-C(20) | 1.540(6) | C(28)-C(29) | 1.383(7) |
| C(5)-C(21) | 1.555(6) | C(29)-C(30) | 1.381(7) |
| C(6)-C(7) | 1.434(6) | C(30)-C(31) | 1.370(8) |
| C(7)-C(8) | 1.373(6) | C(31)-C(32) | 1.368(8) |
| C(7)-H(7) | 0.95 | C(32)-C(33) | 1.375(6) |
| C(8)-C(9) | 1.433(6) | | |

| Bond | Angle | Bond | Angle |
|-----------------|------------|-------------------|----------|
| N(4)-Pd(1)-N(1) | 80.69(15) | C(16)-C(15)-C(14) | 125.3(4) |
| N(4)-Pd(1)-N(2) | 172.71(14) | C(16)-C(15)-C(28) | 117.1(4) |
| N(1)-Pd(1)-N(2) | 92.27(15) | C(14)-C(15)-C(28) | 117.6(4) |
| N(4)-Pd(1)-N(3) | 91.57(14) | N(4)-C(16)-C(15) | 121.4(4) |

| | | | |
|------------------|------------|---------------------|----------|
| N(1)-Pd(1)-N(3) | 171.72(14) | N(4)-C(16)-C(17) | 106.1(4) |
| N(2)-Pd(1)-N(3) | 95.35(14) | C(15)-C(16)-C(17) | 132.3(4) |
| C(4)-N(1)-C(1) | 110.3(4) | C(18)-C(17)-C(16) | 108.4(4) |
| C(4)-N(1)-Pd(1) | 132.9(3) | C(18)-C(17)-H(17) | 125.8 |
| C(1)-N(1)-Pd(1) | 116.1(3) | C(16)-C(17)-H(17) | 125.8 |
| C(6)-N(2)-C(9) | 109.5(4) | C(17)-C(18)-C(19) | 107.3(4) |
| C(6)-N(2)-Pd(1) | 125.8(3) | C(17)-C(18)-H(18) | 126.4 |
| C(9)-N(2)-Pd(1) | 124.6(3) | C(19)-C(18)-H(18) | 126.4 |
| C(14)-N(3)-C(11) | 109.2(3) | N(4)-C(19)-C(1) | 114.7(4) |
| C(14)-N(3)-Pd(1) | 125.7(3) | N(4)-C(19)-C(18) | 107.1(4) |
| C(11)-N(3)-Pd(1) | 125.2(3) | C(1)-C(19)-C(18) | 138.1(4) |
| C(16)-N(4)-C(19) | 111.0(4) | C(5)-C(20)-H(20A) | 109.5 |
| C(16)-N(4)-Pd(1) | 131.0(3) | C(5)-C(20)-H(20B) | 109.5 |
| C(19)-N(4)-Pd(1) | 116.6(3) | H(20A)-C(20)-H(20B) | 109.5 |
| C(2)-C(1)-N(1) | 106.4(4) | C(5)-C(20)-H(20C) | 109.5 |
| C(2)-C(1)-C(19) | 142.1(5) | H(20A)-C(20)-H(20C) | 109.5 |
| N(1)-C(1)-C(19) | 111.3(4) | H(20B)-C(20)-H(20C) | 109.5 |
| C(3)-C(2)-C(1) | 107.5(4) | C(5)-C(21)-H(21A) | 109.5 |
| C(3)-C(2)-H(2) | 126.2 | C(5)-C(21)-H(21B) | 109.5 |
| C(1)-C(2)-H(2) | 126.2 | H(21A)-C(21)-H(21B) | 109.5 |
| C(2)-C(3)-C(4) | 108.3(4) | C(5)-C(21)-H(21C) | 109.5 |
| C(2)-C(3)-H(3) | 125.8 | H(21A)-C(21)-H(21C) | 109.5 |
| C(4)-C(3)-H(3) | 125.8 | H(21B)-C(21)-H(21C) | 109.5 |
| N(1)-C(4)-C(3) | 107.5(4) | C(27)-C(22)-C(23) | 116.2(4) |
| N(1)-C(4)-C(5) | 122.2(4) | C(27)-C(22)-C(10) | 122.6(4) |
| C(3)-C(4)-C(5) | 130.3(4) | C(23)-C(22)-C(10) | 121.1(4) |
| C(4)-C(5)-C(6) | 117.2(4) | F(1)-C(23)-C(24) | 118.0(4) |
| C(4)-C(5)-C(20) | 108.6(4) | F(1)-C(23)-C(22) | 120.2(4) |
| C(6)-C(5)-C(20) | 108.3(4) | C(24)-C(23)-C(22) | 121.8(4) |
| C(4)-C(5)-C(21) | 106.9(4) | F(2)-C(24)-C(25) | 119.4(4) |
| C(6)-C(5)-C(21) | 106.6(4) | F(2)-C(24)-C(23) | 120.4(5) |
| C(20)-C(5)-C(21) | 109.1(4) | C(25)-C(24)-C(23) | 120.2(4) |
| N(2)-C(6)-C(7) | 107.7(4) | F(3)-C(25)-C(24) | 120.4(5) |
| N(2)-C(6)-C(5) | 128.3(4) | F(3)-C(25)-C(26) | 119.5(5) |
| C(7)-C(6)-C(5) | 124.0(4) | C(24)-C(25)-C(26) | 120.1(4) |
| C(8)-C(7)-C(6) | 108.4(4) | F(4)-C(26)-C(27) | 120.3(4) |
| C(8)-C(7)-H(7) | 125.8 | F(4)-C(26)-C(25) | 120.9(4) |
| C(6)-C(7)-H(7) | 125.8 | C(27)-C(26)-C(25) | 118.8(5) |
| C(7)-C(8)-C(9) | 106.5(4) | F(5)-C(27)-C(26) | 118.0(4) |
| C(7)-C(8)-H(8) | 126.8 | F(5)-C(27)-C(22) | 119.2(4) |
| C(9)-C(8)-H(8) | 126.8 | C(26)-C(27)-C(22) | 122.8(4) |
| N(2)-C(9)-C(10) | 123.7(4) | C(33)-C(28)-C(29) | 116.2(4) |
| N(2)-C(9)-C(8) | 107.9(4) | C(33)-C(28)-C(15) | 122.5(4) |

| | | | |
|-------------------|----------|-------------------|----------|
| C(10)-C(9)-C(8) | 128.4(4) | C(29)-C(28)-C(15) | 121.2(4) |
| C(9)-C(10)-C(11) | 127.8(4) | F(6)-C(29)-C(30) | 118.5(5) |
| C(9)-C(10)-C(22) | 115.0(4) | F(6)-C(29)-C(28) | 119.6(4) |
| C(11)-C(10)-C(22) | 117.2(4) | C(30)-C(29)-C(28) | 122.0(5) |
| N(3)-C(11)-C(10) | 123.4(4) | F(7)-C(30)-C(31) | 120.8(5) |
| N(3)-C(11)-C(12) | 108.0(4) | F(7)-C(30)-C(29) | 119.4(5) |
| C(10)-C(11)-C(12) | 128.7(4) | C(31)-C(30)-C(29) | 119.8(5) |
| C(13)-C(12)-C(11) | 107.4(4) | F(8)-C(31)-C(32) | 120.7(5) |
| C(13)-C(12)-H(12) | 126.3 | F(8)-C(31)-C(30) | 119.4(5) |
| C(11)-C(12)-H(12) | 126.3 | C(32)-C(31)-C(30) | 119.9(5) |
| C(12)-C(13)-C(14) | 107.8(4) | F(9)-C(32)-C(31) | 119.7(5) |
| C(12)-C(13)-H(13) | 126.1 | F(9)-C(32)-C(33) | 120.8(5) |
| C(14)-C(13)-H(13) | 126.1 | C(31)-C(32)-C(33) | 119.4(5) |
| N(3)-C(14)-C(13) | 107.6(4) | F(10)-C(33)-C(32) | 117.5(4) |
| N(3)-C(14)-C(15) | 124.6(4) | F(10)-C(33)-C(28) | 119.9(4) |
| C(13)-C(14)-C(15) | 127.7(4) | C(32)-C(33)-C(28) | 122.6(5) |

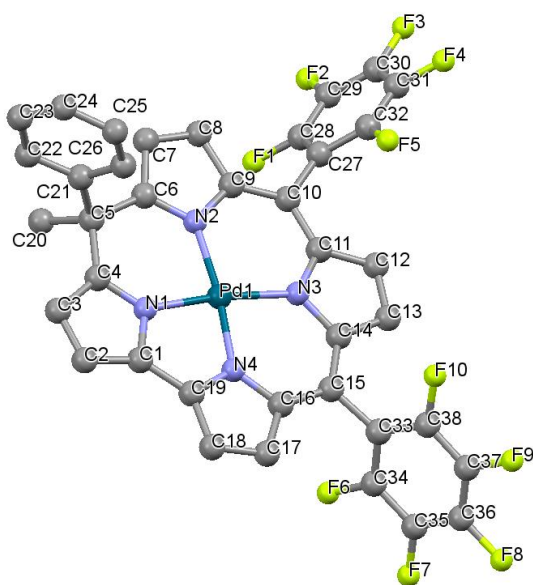


Figure A. 13 Fully labeled solid state structure of Pd(5-MPIC). All non N-H hydrogens have been omitted for clarity.

Table A. 13 Bond Lengths (Å) and Bond angles (°) determined for Pd(5-MPIC)

| Bond | Length | Bond | Length |
|------------|----------|-------------|----------|
| Pd(1)-N(4) | 1.910(4) | C(11)-C(12) | 1.426(7) |
| Pd(1)-N(1) | 1.934(4) | C(12)-C(13) | 1.357(7) |
| Pd(1)-N(2) | 1.952(4) | C(12)-H(12) | 0.95 |
| Pd(1)-N(3) | 1.967(4) | C(13)-C(14) | 1.424(6) |

| | | | |
|-------------|----------|--------------|-----------|
| F(1)-C(28) | 1.354(6) | C(13)-H(13) | 0.95 |
| F(2)-C(29) | 1.349(6) | C(14)-C(15) | 1.440(7) |
| F(3)-C(30) | 1.338(6) | C(15)-C(16) | 1.405(7) |
| F(4)-C(31) | 1.346(6) | C(15)-C(33) | 1.489(7) |
| F(5)-C(32) | 1.352(6) | C(16)-C(17) | 1.442(7) |
| F(6)-C(34) | 1.346(6) | C(17)-C(18) | 1.360(8) |
| F(7)-C(35) | 1.327(6) | C(17)-H(17) | 0.95 |
| F(8)-C(36) | 1.357(6) | C(18)-C(19) | 1.437(8) |
| F(9)-C(37) | 1.364(6) | C(18)-H(18) | 0.95 |
| F(10)-C(38) | 1.331(6) | C(20)-H(20A) | 0.98 |
| N(1)-C(4) | 1.323(6) | C(20)-H(20B) | 0.98 |
| N(1)-C(1) | 1.407(6) | C(20)-H(20C) | 0.98 |
| N(2)-C(6) | 1.342(6) | C(21)-C(26) | 1.354(7) |
| N(2)-C(9) | 1.410(6) | C(21)-C(22) | 1.358(8) |
| N(3)-C(11) | 1.357(6) | C(22)-C(23) | 1.398(10) |
| N(3)-C(14) | 1.383(6) | C(22)-H(22) | 0.95 |
| N(4)-C(19) | 1.338(6) | C(23)-C(24) | 1.361(10) |
| N(4)-C(16) | 1.360(6) | C(23)-H(23) | 0.95 |
| C(1)-C(2) | 1.401(7) | C(24)-C(25) | 1.333(9) |
| C(1)-C(19) | 1.429(8) | C(24)-H(24) | 0.95 |
| C(2)-C(3) | 1.367(7) | C(25)-C(26) | 1.373(8) |
| C(2)-H(2) | 0.95 | C(25)-H(25) | 0.95 |
| C(3)-C(4) | 1.443(7) | C(26)-H(26) | 0.95 |
| C(3)-H(3) | 0.95 | C(27)-C(28) | 1.374(7) |
| C(4)-C(5) | 1.518(7) | C(27)-C(32) | 1.378(7) |
| C(5)-C(20) | 1.545(7) | C(28)-C(29) | 1.380(7) |
| C(5)-C(21) | 1.549(7) | C(29)-C(30) | 1.366(8) |
| C(5)-C(6) | 1.549(7) | C(30)-C(31) | 1.365(8) |
| C(6)-C(7) | 1.412(7) | C(31)-C(32) | 1.378(7) |
| C(7)-C(8) | 1.363(7) | C(33)-C(34) | 1.382(7) |
| C(7)-H(7) | 0.95 | C(33)-C(38) | 1.391(7) |
| C(8)-C(9) | 1.433(7) | C(34)-C(35) | 1.381(8) |
| C(8)-H(8) | 0.95 | C(35)-C(36) | 1.375(8) |
| C(9)-C(10) | 1.397(7) | C(36)-C(37) | 1.363(8) |
| C(10)-C(11) | 1.424(6) | C(37)-C(38) | 1.363(7) |
| C(10)-C(27) | 1.495(6) | | |

| Bond | Angle | Bond | Angle |
|-----------------|------------|-------------------|----------|
| N(4)-Pd(1)-N(1) | 80.93(17) | C(18)-C(17)-C(16) | 108.1(5) |
| N(4)-Pd(1)-N(2) | 172.46(16) | C(18)-C(17)-H(17) | 125.9 |
| N(1)-Pd(1)-N(2) | 91.55(17) | C(16)-C(17)-H(17) | 125.9 |
| N(4)-Pd(1)-N(3) | 91.76(16) | C(17)-C(18)-C(19) | 106.4(4) |
| N(1)-Pd(1)-N(3) | 172.69(17) | C(17)-C(18)-H(18) | 126.8 |

| | | | |
|------------------|-----------|---------------------|----------|
| N(2)-Pd(1)-N(3) | 95.76(16) | C(19)-C(18)-H(18) | 126.8 |
| C(4)-N(1)-C(1) | 110.7(4) | N(4)-C(19)-C(1) | 114.0(5) |
| C(4)-N(1)-Pd(1) | 133.8(4) | N(4)-C(19)-C(18) | 108.6(5) |
| C(1)-N(1)-Pd(1) | 115.5(3) | C(1)-C(19)-C(18) | 137.4(5) |
| C(6)-N(2)-C(9) | 109.1(4) | C(5)-C(20)-H(20A) | 109.5 |
| C(6)-N(2)-Pd(1) | 127.5(3) | C(5)-C(20)-H(20B) | 109.5 |
| C(9)-N(2)-Pd(1) | 123.4(3) | H(20A)-C(20)-H(20B) | 109.5 |
| C(11)-N(3)-C(14) | 109.2(4) | C(5)-C(20)-H(20C) | 109.5 |
| C(11)-N(3)-Pd(1) | 125.3(3) | H(20A)-C(20)-H(20C) | 109.5 |
| C(14)-N(3)-Pd(1) | 125.5(3) | H(20B)-C(20)-H(20C) | 109.5 |
| C(19)-N(4)-C(16) | 110.3(4) | C(26)-C(21)-C(22) | 117.4(5) |
| C(19)-N(4)-Pd(1) | 117.8(4) | C(26)-C(21)-C(5) | 120.2(5) |
| C(16)-N(4)-Pd(1) | 131.8(3) | C(22)-C(21)-C(5) | 122.2(5) |
| C(2)-C(1)-N(1) | 106.8(5) | C(21)-C(22)-C(23) | 120.2(7) |
| C(2)-C(1)-C(19) | 141.6(5) | C(21)-C(22)-H(22) | 119.9 |
| N(1)-C(1)-C(19) | 111.7(4) | C(23)-C(22)-H(22) | 119.9 |
| C(3)-C(2)-C(1) | 107.5(5) | C(24)-C(23)-C(22) | 120.6(7) |
| C(3)-C(2)-H(2) | 126.3 | C(24)-C(23)-H(23) | 119.7 |
| C(1)-C(2)-H(2) | 126.3 | C(22)-C(23)-H(23) | 119.7 |
| C(2)-C(3)-C(4) | 108.5(5) | C(25)-C(24)-C(23) | 118.7(6) |
| C(2)-C(3)-H(3) | 125.7 | C(25)-C(24)-H(24) | 120.6 |
| C(4)-C(3)-H(3) | 125.7 | C(23)-C(24)-H(24) | 120.6 |
| N(1)-C(4)-C(3) | 106.5(5) | C(24)-C(25)-C(26) | 120.5(6) |
| N(1)-C(4)-C(5) | 122.7(4) | C(24)-C(25)-H(25) | 119.7 |
| C(3)-C(4)-C(5) | 130.8(5) | C(26)-C(25)-H(25) | 119.7 |
| C(4)-C(5)-C(20) | 108.6(4) | C(21)-C(26)-C(25) | 122.3(6) |
| C(4)-C(5)-C(21) | 105.0(4) | C(21)-C(26)-H(26) | 118.8 |
| C(20)-C(5)-C(21) | 113.1(4) | C(25)-C(26)-H(26) | 118.8 |
| C(4)-C(5)-C(6) | 117.2(4) | C(28)-C(27)-C(32) | 116.3(5) |
| C(20)-C(5)-C(6) | 106.7(4) | C(28)-C(27)-C(10) | 121.2(4) |
| C(21)-C(5)-C(6) | 106.4(4) | C(32)-C(27)-C(10) | 122.4(4) |
| N(2)-C(6)-C(7) | 109.2(4) | F(1)-C(28)-C(27) | 120.7(4) |
| N(2)-C(6)-C(5) | 127.3(5) | F(1)-C(28)-C(29) | 116.8(4) |
| C(7)-C(6)-C(5) | 123.5(4) | C(27)-C(28)-C(29) | 122.5(5) |
| C(8)-C(7)-C(6) | 107.7(5) | F(2)-C(29)-C(30) | 120.2(5) |
| C(8)-C(7)-H(7) | 126.2 | F(2)-C(29)-C(28) | 120.3(5) |
| C(6)-C(7)-H(7) | 126.2 | C(30)-C(29)-C(28) | 119.5(5) |
| C(7)-C(8)-C(9) | 108.3(5) | F(3)-C(30)-C(31) | 119.3(5) |
| C(7)-C(8)-H(8) | 125.8 | F(3)-C(30)-C(29) | 121.0(5) |
| C(9)-C(8)-H(8) | 125.8 | C(31)-C(30)-C(29) | 119.7(5) |
| C(10)-C(9)-N(2) | 124.4(4) | F(4)-C(31)-C(30) | 121.1(5) |
| C(10)-C(9)-C(8) | 129.8(5) | F(4)-C(31)-C(32) | 119.0(5) |
| N(2)-C(9)-C(8) | 105.7(4) | C(30)-C(31)-C(32) | 119.9(5) |

| | | | |
|-------------------|----------|-------------------|----------|
| C(9)-C(10)-C(11) | 127.6(4) | F(5)-C(32)-C(31) | 118.2(4) |
| C(9)-C(10)-C(27) | 116.2(4) | F(5)-C(32)-C(27) | 119.6(4) |
| C(11)-C(10)-C(27) | 116.1(4) | C(31)-C(32)-C(27) | 122.1(5) |
| N(3)-C(11)-C(10) | 123.5(4) | C(34)-C(33)-C(38) | 116.3(4) |
| N(3)-C(11)-C(12) | 107.5(4) | C(34)-C(33)-C(15) | 121.1(4) |
| C(10)-C(11)-C(12) | 128.9(4) | C(38)-C(33)-C(15) | 122.3(4) |
| C(13)-C(12)-C(11) | 108.4(4) | F(6)-C(34)-C(35) | 117.5(5) |
| C(13)-C(12)-H(12) | 125.8 | F(6)-C(34)-C(33) | 119.5(5) |
| C(11)-C(12)-H(12) | 125.8 | C(35)-C(34)-C(33) | 123.0(5) |
| C(12)-C(13)-C(14) | 107.5(4) | F(7)-C(35)-C(36) | 120.6(5) |
| C(12)-C(13)-H(13) | 126.3 | F(7)-C(35)-C(34) | 121.2(5) |
| C(14)-C(13)-H(13) | 126.3 | C(36)-C(35)-C(34) | 118.2(5) |
| N(3)-C(14)-C(13) | 107.4(4) | F(8)-C(36)-C(37) | 120.7(5) |
| N(3)-C(14)-C(15) | 124.7(4) | F(8)-C(36)-C(35) | 119.0(6) |
| C(13)-C(14)-C(15) | 127.9(5) | C(37)-C(36)-C(35) | 120.3(5) |
| C(16)-C(15)-C(14) | 124.8(4) | C(38)-C(37)-C(36) | 120.6(5) |
| C(16)-C(15)-C(33) | 116.1(4) | C(38)-C(37)-F(9) | 119.7(5) |
| C(14)-C(15)-C(33) | 119.1(4) | C(36)-C(37)-F(9) | 119.7(5) |
| N(4)-C(16)-C(15) | 121.4(4) | F(10)-C(38)-C(37) | 119.2(5) |
| N(4)-C(16)-C(17) | 106.6(4) | F(10)-C(38)-C(33) | 119.4(4) |
| C(15)-C(16)-C(17) | 132.0(5) | C(37)-C(38)-C(33) | 121.4(5) |

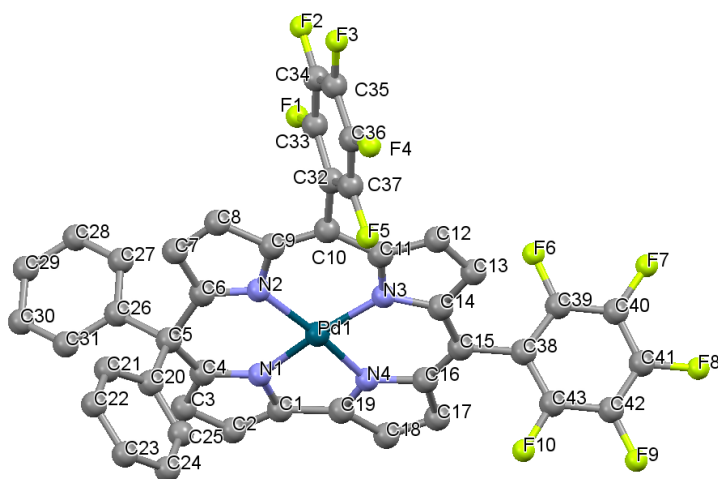


Figure A. 14 Fully labeled solid state structure of Pd(5-DPIC). All non N-H hydrogens have been omitted for clarity.

Table A. 14 Bond Lengths (Å) and Bond angles (°) determined for Pd(5-DPIC)

| Bond | Length | Bond | Length |
|------------|----------|-------------|--------|
| Pd(1)-N(4) | 1.928(4) | C(13)-H(13) | 0.95 |

| | | | |
|-------------|----------|-------------|-----------|
| Pd(1)-N(1) | 1.932(4) | C(14)-C(15) | 1.458(8) |
| Pd(1)-N(2) | 1.956(4) | C(15)-C(16) | 1.386(8) |
| Pd(1)-N(3) | 1.963(4) | C(15)-C(38) | 1.488(7) |
| F(1)-C(33) | 1.348(7) | C(16)-C(17) | 1.468(8) |
| F(2)-C(34) | 1.332(6) | C(17)-C(18) | 1.351(8) |
| F(3)-C(35) | 1.330(7) | C(17)-H(17) | 0.95 |
| F(4)-C(36) | 1.325(7) | C(18)-C(19) | 1.451(7) |
| F(5)-C(37) | 1.336(6) | C(18)-H(18) | 0.95 |
| F(6)-C(39) | 1.353(6) | C(20)-C(25) | 1.388(8) |
| F(7)-C(40) | 1.350(6) | C(20)-C(21) | 1.394(8) |
| F(8)-C(41) | 1.340(7) | C(21)-C(22) | 1.362(9) |
| F(9)-C(42) | 1.325(7) | C(21)-H(21) | 0.95 |
| F(10)-C(43) | 1.342(7) | C(22)-C(23) | 1.374(9) |
| N(1)-C(4) | 1.329(6) | C(22)-H(22) | 0.95 |
| N(1)-C(1) | 1.393(6) | C(23)-C(24) | 1.360(9) |
| N(2)-C(6) | 1.328(6) | C(23)-H(23) | 0.95 |
| N(2)-C(9) | 1.396(7) | C(24)-C(25) | 1.383(8) |
| N(3)-C(11) | 1.360(7) | C(24)-H(24) | 0.95 |
| N(3)-C(14) | 1.372(6) | C(25)-H(25) | 0.95 |
| N(4)-C(16) | 1.360(6) | C(26)-C(27) | 1.373(8) |
| N(4)-C(19) | 1.354(7) | C(26)-C(31) | 1.405(8) |
| C(1)-C(2) | 1.379(7) | C(27)-C(28) | 1.394(8) |
| C(1)-C(19) | 1.428(7) | C(27)-H(27) | 0.95 |
| C(2)-C(3) | 1.399(8) | C(28)-C(29) | 1.377(10) |
| C(2)-H(2) | 0.95 | C(28)-H(28) | 0.95 |
| C(3)-C(4) | 1.406(8) | C(29)-C(30) | 1.361(11) |
| C(3)-H(3) | 0.95 | C(29)-H(29) | 0.95 |
| C(4)-C(5) | 1.530(7) | C(30)-C(31) | 1.388(9) |
| C(5)-C(26) | 1.529(7) | C(30)-H(30) | 0.95 |
| C(5)-C(6) | 1.549(7) | C(31)-H(31) | 0.95 |
| C(5)-C(20) | 1.560(8) | C(32)-C(37) | 1.386(8) |
| C(6)-C(7) | 1.433(7) | C(32)-C(33) | 1.401(7) |
| C(7)-C(8) | 1.345(8) | C(33)-C(34) | 1.375(8) |
| C(7)-H(7) | 0.95 | C(34)-C(35) | 1.365(9) |
| C(8)-C(9) | 1.438(7) | C(35)-C(36) | 1.381(8) |
| C(8)-H(8) | 0.95 | C(36)-C(37) | 1.396(8) |
| C(9)-C(10) | 1.394(7) | C(38)-C(43) | 1.386(8) |
| C(10)-C(11) | 1.436(7) | C(38)-C(39) | 1.399(7) |
| C(10)-C(32) | 1.481(8) | C(39)-C(40) | 1.365(8) |
| C(11)-C(12) | 1.422(7) | C(40)-C(41) | 1.361(8) |
| C(12)-C(13) | 1.354(8) | C(41)-C(42) | 1.358(9) |
| C(12)-H(12) | 0.95 | C(42)-C(43) | 1.390(8) |
| C(13)-C(14) | 1.414(8) | | |

| Bond | Angle | Bond | Angle |
|------------------|------------|-------------------|----------|
| N(4)-Pd(1)-N(1) | 80.82(18) | N(4)-C(19)-C(1) | 114.4(5) |
| N(4)-Pd(1)-N(2) | 172.13(18) | N(4)-C(19)-C(18) | 107.1(5) |
| N(1)-Pd(1)-N(2) | 91.72(17) | C(1)-C(19)-C(18) | 138.5(5) |
| N(4)-Pd(1)-N(3) | 91.32(18) | C(25)-C(20)-C(21) | 117.0(5) |
| N(1)-Pd(1)-N(3) | 171.77(18) | C(25)-C(20)-C(5) | 121.1(5) |
| N(2)-Pd(1)-N(3) | 96.03(18) | C(21)-C(20)-C(5) | 121.7(5) |
| C(4)-N(1)-C(1) | 109.6(4) | C(22)-C(21)-C(20) | 121.9(6) |
| C(4)-N(1)-Pd(1) | 133.7(4) | C(22)-C(21)-H(21) | 119 |
| C(1)-N(1)-Pd(1) | 116.2(3) | C(20)-C(21)-H(21) | 119 |
| C(6)-N(2)-C(9) | 109.5(4) | C(21)-C(22)-C(23) | 120.0(6) |
| C(6)-N(2)-Pd(1) | 127.1(4) | C(21)-C(22)-H(22) | 120 |
| C(9)-N(2)-Pd(1) | 123.2(3) | C(23)-C(22)-H(22) | 120 |
| C(11)-N(3)-C(14) | 108.5(4) | C(24)-C(23)-C(22) | 119.8(6) |
| C(11)-N(3)-Pd(1) | 125.0(4) | C(24)-C(23)-H(23) | 120.1 |
| C(14)-N(3)-Pd(1) | 126.5(4) | C(22)-C(23)-H(23) | 120.1 |
| C(16)-N(4)-C(19) | 111.5(5) | C(23)-C(24)-C(25) | 120.4(6) |
| C(16)-N(4)-Pd(1) | 131.3(4) | C(23)-C(24)-H(24) | 119.8 |
| C(19)-N(4)-Pd(1) | 116.4(3) | C(25)-C(24)-H(24) | 119.8 |
| C(2)-C(1)-N(1) | 107.6(5) | C(24)-C(25)-C(20) | 120.9(6) |
| C(2)-C(1)-C(19) | 140.7(5) | C(24)-C(25)-H(25) | 119.6 |
| N(1)-C(1)-C(19) | 111.7(5) | C(20)-C(25)-H(25) | 119.6 |
| C(1)-C(2)-C(3) | 107.4(5) | C(27)-C(26)-C(31) | 116.6(5) |
| C(1)-C(2)-H(2) | 126.3 | C(27)-C(26)-C(5) | 121.4(5) |
| C(3)-C(2)-H(2) | 126.3 | C(31)-C(26)-C(5) | 121.8(5) |
| C(2)-C(3)-C(4) | 107.1(5) | C(26)-C(27)-C(28) | 122.4(6) |
| C(2)-C(3)-H(3) | 126.5 | C(26)-C(27)-H(27) | 118.8 |
| C(4)-C(3)-H(3) | 126.5 | C(28)-C(27)-H(27) | 118.8 |
| N(1)-C(4)-C(3) | 108.3(5) | C(29)-C(28)-C(27) | 119.6(6) |
| N(1)-C(4)-C(5) | 120.8(5) | C(29)-C(28)-H(28) | 120.2 |
| C(3)-C(4)-C(5) | 130.7(5) | C(27)-C(28)-H(28) | 120.2 |
| C(26)-C(5)-C(4) | 106.3(5) | C(30)-C(29)-C(28) | 119.7(6) |
| C(26)-C(5)-C(6) | 110.2(4) | C(30)-C(29)-H(29) | 120.1 |
| C(4)-C(5)-C(6) | 116.6(4) | C(28)-C(29)-H(29) | 120.1 |
| C(26)-C(5)-C(20) | 112.4(4) | C(29)-C(30)-C(31) | 120.5(7) |
| C(4)-C(5)-C(20) | 109.4(4) | C(29)-C(30)-H(30) | 119.7 |
| C(6)-C(5)-C(20) | 102.0(4) | C(31)-C(30)-H(30) | 119.7 |
| N(2)-C(6)-C(7) | 109.0(5) | C(30)-C(31)-C(26) | 121.3(7) |
| N(2)-C(6)-C(5) | 126.6(4) | C(30)-C(31)-H(31) | 119.4 |
| C(7)-C(6)-C(5) | 123.9(4) | C(26)-C(31)-H(31) | 119.4 |
| C(8)-C(7)-C(6) | 107.0(5) | C(37)-C(32)-C(33) | 115.7(5) |
| C(8)-C(7)-H(7) | 126.5 | C(37)-C(32)-C(10) | 123.1(5) |

| | | | |
|-------------------|----------|-------------------|----------|
| C(6)-C(7)-H(7) | 126.5 | C(33)-C(32)-C(10) | 121.1(5) |
| C(7)-C(8)-C(9) | 108.7(5) | F(1)-C(33)-C(34) | 117.7(5) |
| C(7)-C(8)-H(8) | 125.6 | F(1)-C(33)-C(32) | 119.4(5) |
| C(9)-C(8)-H(8) | 125.6 | C(34)-C(33)-C(32) | 123.0(6) |
| N(2)-C(9)-C(10) | 124.9(5) | F(2)-C(34)-C(33) | 119.8(6) |
| N(2)-C(9)-C(8) | 105.7(4) | F(2)-C(34)-C(35) | 120.6(6) |
| C(10)-C(9)-C(8) | 129.3(5) | C(33)-C(34)-C(35) | 119.6(5) |
| C(9)-C(10)-C(11) | 127.3(5) | F(3)-C(35)-C(34) | 120.7(6) |
| C(9)-C(10)-C(32) | 116.0(5) | F(3)-C(35)-C(36) | 119.1(6) |
| C(11)-C(10)-C(32) | 116.6(5) | C(34)-C(35)-C(36) | 120.1(6) |
| N(3)-C(11)-C(12) | 108.4(5) | F(4)-C(36)-C(35) | 120.4(6) |
| N(3)-C(11)-C(10) | 123.3(5) | F(4)-C(36)-C(37) | 120.1(6) |
| C(12)-C(11)-C(10) | 128.2(5) | C(35)-C(36)-C(37) | 119.4(6) |
| C(13)-C(12)-C(11) | 107.2(5) | F(5)-C(37)-C(32) | 119.5(5) |
| C(13)-C(12)-H(12) | 126.4 | F(5)-C(37)-C(36) | 118.4(5) |
| C(11)-C(12)-H(12) | 126.4 | C(32)-C(37)-C(36) | 122.1(5) |
| C(12)-C(13)-C(14) | 108.2(5) | C(43)-C(38)-C(39) | 115.0(5) |
| C(12)-C(13)-H(13) | 125.9 | C(43)-C(38)-C(15) | 121.6(5) |
| C(14)-C(13)-H(13) | 125.9 | C(39)-C(38)-C(15) | 123.4(5) |
| N(3)-C(14)-C(13) | 107.8(5) | F(6)-C(39)-C(40) | 118.1(5) |
| N(3)-C(14)-C(15) | 123.6(5) | F(6)-C(39)-C(38) | 119.2(5) |
| C(13)-C(14)-C(15) | 128.6(5) | C(40)-C(39)-C(38) | 122.7(5) |
| C(16)-C(15)-C(14) | 125.4(5) | F(7)-C(40)-C(39) | 120.2(5) |
| C(16)-C(15)-C(38) | 118.1(5) | F(7)-C(40)-C(41) | 119.8(5) |
| C(14)-C(15)-C(38) | 116.6(5) | C(39)-C(40)-C(41) | 120.0(6) |
| N(4)-C(16)-C(15) | 121.6(5) | F(8)-C(41)-C(42) | 120.1(6) |
| N(4)-C(16)-C(17) | 105.8(5) | F(8)-C(41)-C(40) | 119.5(6) |
| C(15)-C(16)-C(17) | 132.6(5) | C(42)-C(41)-C(40) | 120.4(6) |
| C(18)-C(17)-C(16) | 108.1(5) | F(9)-C(42)-C(41) | 120.3(6) |
| C(18)-C(17)-H(17) | 126 | F(9)-C(42)-C(43) | 120.6(6) |
| C(16)-C(17)-H(17) | 126 | C(41)-C(42)-C(43) | 119.1(6) |
| C(17)-C(18)-C(19) | 107.5(5) | F(10)-C(43)-C(38) | 119.9(5) |
| C(17)-C(18)-H(18) | 126.2 | F(10)-C(43)-C(42) | 117.3(5) |
| C(19)-C(18)-H(18) | 126.2 | C(38)-C(43)-C(42) | 122.8(6) |

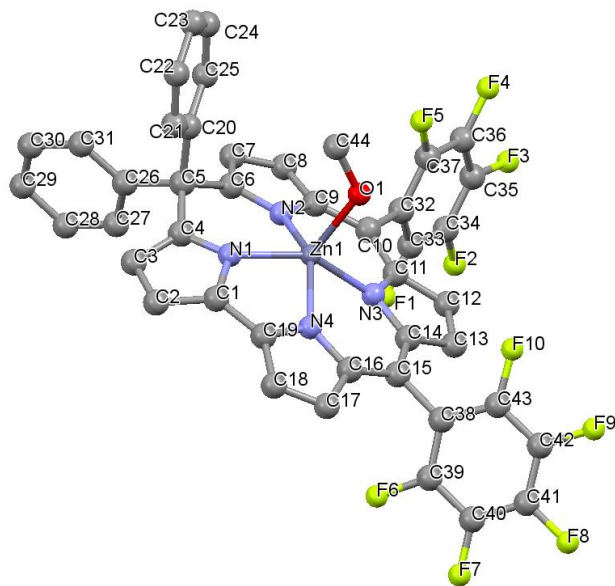


Figure A. 15 Fully labeled solid state structure of Zn(5-DPIC) with a molecule of methanol as the fifth coordination ligand. All non N-H hydrogens have been omitted for clarity.

Table A. 15 Bond Lengths (Å) and Bond angles (°) determined for Zn(5-DPIC)

| Bond | Length | Bond | Length |
|-------------|----------|-------------|----------|
| Zn(1)-N(2) | 2.007(3) | C(13)-H(13) | 0.95 |
| Zn(1)-N(1) | 2.012(2) | C(14)-C(15) | 1.458(4) |
| Zn(1)-N(3) | 2.013(3) | C(15)-C(16) | 1.387(4) |
| Zn(1)-N(4) | 2.031(2) | C(15)-C(38) | 1.492(4) |
| Zn(1)-O(1) | 2.066(3) | C(16)-C(17) | 1.472(4) |
| F(1)-C(33) | 1.337(4) | C(17)-C(18) | 1.352(4) |
| F(2)-C(34) | 1.340(4) | C(17)-H(17) | 0.95 |
| F(3)-C(35) | 1.334(4) | C(18)-C(19) | 1.462(4) |
| F(4)-C(36) | 1.339(4) | C(18)-H(18) | 0.95 |
| F(5)-C(37) | 1.340(3) | C(20)-C(21) | 1.380(5) |
| F(6)-C(39) | 1.334(4) | C(20)-C(25) | 1.396(4) |
| F(7)-C(40) | 1.335(4) | C(21)-C(22) | 1.396(5) |
| F(8)-C(41) | 1.340(4) | C(21)-H(21) | 0.95 |
| F(9)-C(42) | 1.347(4) | C(22)-C(23) | 1.390(6) |
| F(10)-C(43) | 1.344(4) | C(22)-H(22) | 0.95 |
| O(1)-C(44) | 1.425(5) | C(23)-C(24) | 1.369(5) |
| O(1)-H(1) | 0.70(4) | C(23)-H(23) | 0.95 |
| O(2)-C(45) | 1.411(5) | C(24)-C(25) | 1.382(5) |
| O(2)-H(4) | 1.08(9) | C(24)-H(24) | 0.95 |

| | | | |
|-------------|----------|--------------|----------|
| N(1)-C(4) | 1.338(4) | C(25)-H(25) | 0.95 |
| N(1)-C(1) | 1.390(4) | C(26)-C(31) | 1.387(4) |
| N(2)-C(6) | 1.337(4) | C(26)-C(27) | 1.401(5) |
| N(2)-C(9) | 1.395(4) | C(27)-C(28) | 1.386(5) |
| N(3)-C(14) | 1.360(4) | C(27)-H(27) | 0.95 |
| N(3)-C(11) | 1.375(4) | C(28)-C(29) | 1.389(5) |
| N(4)-C(19) | 1.333(4) | C(28)-H(28) | 0.95 |
| N(4)-C(16) | 1.370(4) | C(29)-C(30) | 1.373(6) |
| C(1)-C(2) | 1.407(4) | C(29)-H(29) | 0.95 |
| C(1)-C(19) | 1.428(4) | C(30)-C(31) | 1.389(5) |
| C(2)-C(3) | 1.381(5) | C(30)-H(30) | 0.95 |
| C(2)-H(2) | 0.95 | C(31)-H(31) | 0.95 |
| C(3)-C(4) | 1.422(4) | C(32)-C(33) | 1.385(4) |
| C(3)-H(3) | 0.95 | C(32)-C(37) | 1.388(4) |
| C(4)-C(5) | 1.531(4) | C(33)-C(34) | 1.384(4) |
| C(5)-C(6) | 1.546(4) | C(34)-C(35) | 1.368(5) |
| C(5)-C(26) | 1.548(4) | C(35)-C(36) | 1.382(5) |
| C(5)-C(20) | 1.561(4) | C(36)-C(37) | 1.387(4) |
| C(6)-C(7) | 1.430(4) | C(38)-C(39) | 1.385(5) |
| C(7)-C(8) | 1.362(4) | C(38)-C(43) | 1.389(4) |
| C(7)-H(7) | 0.95 | C(39)-C(40) | 1.395(5) |
| C(8)-C(9) | 1.426(4) | C(40)-C(41) | 1.360(6) |
| C(8)-H(8) | 0.95 | C(41)-C(42) | 1.372(6) |
| C(9)-C(10) | 1.399(4) | C(42)-C(43) | 1.378(4) |
| C(10)-C(11) | 1.423(4) | C(44)-H(44A) | 0.98 |
| C(10)-C(32) | 1.498(4) | C(44)-H(44B) | 0.98 |
| C(11)-C(12) | 1.426(4) | C(44)-H(44C) | 0.98 |
| C(12)-C(13) | 1.366(4) | C(45)-H(45A) | 0.98 |
| C(12)-H(12) | 0.95 | C(45)-H(45B) | 0.98 |
| C(13)-C(14) | 1.435(4) | C(45)-H(45C) | 0.98 |

| Bond | Angle | Bond | Angle |
|------------------|--------------|-------------------|--------------|
| N(2)-Zn(1)-N(1) | 88.07(10) | C(1)-C(19)-C(18) | 136.2(3) |
| N(2)-Zn(1)-N(3) | 93.34(10) | C(21)-C(20)-C(25) | 117.5(3) |
| N(1)-Zn(1)-N(3) | 149.43(10) | C(21)-C(20)-C(5) | 121.0(3) |
| N(2)-Zn(1)-N(4) | 148.20(11) | C(25)-C(20)-C(5) | 121.4(3) |
| N(1)-Zn(1)-N(4) | 78.42(10) | C(20)-C(21)-C(22) | 121.5(4) |
| N(3)-Zn(1)-N(4) | 84.65(10) | C(20)-C(21)-H(21) | 119.3 |
| N(2)-Zn(1)-O(1) | 103.96(12) | C(22)-C(21)-H(21) | 119.3 |
| N(1)-Zn(1)-O(1) | 110.19(11) | C(23)-C(22)-C(21) | 119.9(4) |
| N(3)-Zn(1)-O(1) | 99.10(11) | C(23)-C(22)-H(22) | 120.1 |
| N(4)-Zn(1)-O(1) | 107.70(11) | C(21)-C(22)-H(22) | 120.1 |
| C(44)-O(1)-Zn(1) | 124.5(2) | C(24)-C(23)-C(22) | 119.0(3) |

| | | | |
|------------------|------------|-------------------|----------|
| C(44)-O(1)-H(1) | 119(3) | C(24)-C(23)-H(23) | 120.5 |
| Zn(1)-O(1)-H(1) | 101(3) | C(22)-C(23)-H(23) | 120.5 |
| C(45)-O(2)-H(4) | 110(4) | C(23)-C(24)-C(25) | 120.9(3) |
| C(4)-N(1)-C(1) | 108.4(2) | C(23)-C(24)-H(24) | 119.6 |
| C(4)-N(1)-Zn(1) | 131.7(2) | C(25)-C(24)-H(24) | 119.6 |
| C(1)-N(1)-Zn(1) | 115.96(19) | C(24)-C(25)-C(20) | 121.3(3) |
| C(6)-N(2)-C(9) | 107.8(2) | C(24)-C(25)-H(25) | 119.4 |
| C(6)-N(2)-Zn(1) | 129.4(2) | C(20)-C(25)-H(25) | 119.4 |
| C(9)-N(2)-Zn(1) | 122.5(2) | C(31)-C(26)-C(27) | 118.2(3) |
| C(14)-N(3)-C(11) | 107.7(2) | C(31)-C(26)-C(5) | 122.9(3) |
| C(14)-N(3)-Zn(1) | 128.2(2) | C(27)-C(26)-C(5) | 118.9(3) |
| C(11)-N(3)-Zn(1) | 122.97(19) | C(28)-C(27)-C(26) | 120.9(3) |
| C(19)-N(4)-C(16) | 110.1(2) | C(28)-C(27)-H(27) | 119.5 |
| C(19)-N(4)-Zn(1) | 116.12(19) | C(26)-C(27)-H(27) | 119.5 |
| C(16)-N(4)-Zn(1) | 133.7(2) | C(27)-C(28)-C(29) | 119.9(4) |
| N(1)-C(1)-C(2) | 108.3(3) | C(27)-C(28)-H(28) | 120.1 |
| N(1)-C(1)-C(19) | 113.3(3) | C(29)-C(28)-H(28) | 120.1 |
| C(2)-C(1)-C(19) | 135.7(3) | C(30)-C(29)-C(28) | 119.6(3) |
| C(3)-C(2)-C(1) | 107.0(3) | C(30)-C(29)-H(29) | 120.2 |
| C(3)-C(2)-H(2) | 126.5 | C(28)-C(29)-H(29) | 120.2 |
| C(1)-C(2)-H(2) | 126.5 | C(29)-C(30)-C(31) | 120.8(3) |
| C(2)-C(3)-C(4) | 107.2(3) | C(29)-C(30)-H(30) | 119.6 |
| C(2)-C(3)-H(3) | 126.4 | C(31)-C(30)-H(30) | 119.6 |
| C(4)-C(3)-H(3) | 126.4 | C(26)-C(31)-C(30) | 120.6(3) |
| N(1)-C(4)-C(3) | 109.0(3) | C(26)-C(31)-H(31) | 119.7 |
| N(1)-C(4)-C(5) | 120.3(2) | C(30)-C(31)-H(31) | 119.7 |
| C(3)-C(4)-C(5) | 130.5(3) | C(33)-C(32)-C(37) | 116.8(3) |
| C(4)-C(5)-C(6) | 114.2(2) | C(33)-C(32)-C(10) | 122.7(3) |
| C(4)-C(5)-C(26) | 108.0(2) | C(37)-C(32)-C(10) | 120.4(3) |
| C(6)-C(5)-C(26) | 107.6(2) | F(1)-C(33)-C(34) | 118.2(3) |
| C(4)-C(5)-C(20) | 108.3(2) | F(1)-C(33)-C(32) | 120.0(3) |
| C(6)-C(5)-C(20) | 108.6(2) | C(34)-C(33)-C(32) | 121.7(3) |
| C(26)-C(5)-C(20) | 110.1(2) | F(2)-C(34)-C(35) | 119.6(3) |
| N(2)-C(6)-C(7) | 109.6(3) | F(2)-C(34)-C(33) | 120.2(3) |
| N(2)-C(6)-C(5) | 125.1(3) | C(35)-C(34)-C(33) | 120.2(3) |
| C(7)-C(6)-C(5) | 125.2(3) | F(3)-C(35)-C(34) | 120.0(3) |
| C(8)-C(7)-C(6) | 107.3(3) | F(3)-C(35)-C(36) | 120.2(3) |
| C(8)-C(7)-H(7) | 126.3 | C(34)-C(35)-C(36) | 119.7(3) |
| C(6)-C(7)-H(7) | 126.3 | F(4)-C(36)-C(35) | 120.5(3) |
| C(7)-C(8)-C(9) | 107.1(3) | F(4)-C(36)-C(37) | 120.2(3) |
| C(7)-C(8)-H(8) | 126.5 | C(35)-C(36)-C(37) | 119.3(3) |
| C(9)-C(8)-H(8) | 126.5 | F(5)-C(37)-C(36) | 117.6(3) |
| N(2)-C(9)-C(10) | 123.7(3) | F(5)-C(37)-C(32) | 120.2(3) |

| | | | |
|-------------------|----------|---------------------|----------|
| N(2)-C(9)-C(8) | 108.2(3) | C(36)-C(37)-C(32) | 122.2(3) |
| C(10)-C(9)-C(8) | 127.9(3) | C(39)-C(38)-C(43) | 116.2(3) |
| C(9)-C(10)-C(11) | 128.7(3) | C(39)-C(38)-C(15) | 123.4(3) |
| C(9)-C(10)-C(32) | 116.7(2) | C(43)-C(38)-C(15) | 120.3(3) |
| C(11)-C(10)-C(32) | 114.6(2) | F(6)-C(39)-C(38) | 120.4(3) |
| N(3)-C(11)-C(10) | 123.1(3) | F(6)-C(39)-C(40) | 117.6(3) |
| N(3)-C(11)-C(12) | 109.2(2) | C(38)-C(39)-C(40) | 122.1(3) |
| C(10)-C(11)-C(12) | 127.6(3) | F(7)-C(40)-C(41) | 119.8(3) |
| C(13)-C(12)-C(11) | 106.8(3) | F(7)-C(40)-C(39) | 120.5(4) |
| C(13)-C(12)-H(12) | 126.6 | C(41)-C(40)-C(39) | 119.7(3) |
| C(11)-C(12)-H(12) | 126.6 | F(8)-C(41)-C(40) | 120.3(4) |
| C(12)-C(13)-C(14) | 107.4(3) | F(8)-C(41)-C(42) | 119.7(4) |
| C(12)-C(13)-H(13) | 126.3 | C(40)-C(41)-C(42) | 119.9(3) |
| C(14)-C(13)-H(13) | 126.3 | F(9)-C(42)-C(41) | 120.2(3) |
| N(3)-C(14)-C(13) | 108.8(3) | F(9)-C(42)-C(43) | 119.8(3) |
| N(3)-C(14)-C(15) | 125.1(3) | C(41)-C(42)-C(43) | 120.0(3) |
| C(13)-C(14)-C(15) | 125.9(3) | F(10)-C(43)-C(42) | 118.0(3) |
| C(16)-C(15)-C(14) | 123.8(3) | F(10)-C(43)-C(38) | 119.8(3) |
| C(16)-C(15)-C(38) | 119.9(3) | C(42)-C(43)-C(38) | 122.1(3) |
| C(14)-C(15)-C(38) | 116.2(3) | O(1)-C(44)-H(44A) | 109.5 |
| N(4)-C(16)-C(15) | 119.9(3) | O(1)-C(44)-H(44B) | 109.5 |
| N(4)-C(16)-C(17) | 107.2(3) | H(44A)-C(44)-H(44B) | 109.5 |
| C(15)-C(16)-C(17) | 132.8(3) | O(1)-C(44)-H(44C) | 109.5 |
| C(18)-C(17)-C(16) | 106.7(3) | H(44A)-C(44)-H(44C) | 109.5 |
| C(18)-C(17)-H(17) | 126.7 | H(44B)-C(44)-H(44C) | 109.5 |
| C(16)-C(17)-H(17) | 126.7 | O(2)-C(45)-H(45A) | 109.5 |
| C(17)-C(18)-C(19) | 107.6(3) | O(2)-C(45)-H(45B) | 109.5 |
| C(17)-C(18)-H(18) | 126.2 | H(45A)-C(45)-H(45B) | 109.5 |
| C(19)-C(18)-H(18) | 126.2 | O(2)-C(45)-H(45C) | 109.5 |
| N(4)-C(19)-C(1) | 115.4(3) | H(45A)-C(45)-H(45C) | 109.5 |
| N(4)-C(19)-C(18) | 108.2(3) | H(45B)-C(45)-H(45C) | 109.5 |